



THE UNIVERSITY OF QUEENSLAND
A U S T R A L I A

**Colour Vision in Mantis Shrimps: Understanding One of the Most Complex
Visual Systems in the World**

Hanne Halkinrud Thoen

BSc, MSc

*A thesis submitted for the degree of Doctor of Philosophy at
The University of Queensland in 2014
Queensland Brain Institute*

Abstract

Stomatopods (commonly known as mantis shrimps) have one of the most complex visual systems in the animal kingdom with up to 20 different photoreceptor types and the ability to see both linear and circular polarized light. The eye of a stomatopod is divided into three different parts; a dorsal and a ventral hemisphere divided up by 6 distinct rows of specialised ommatidia (visual units) termed the midband. The midband contains a complex array of up to 12 spectral receptors with maximum sensitivities ranging from the ultraviolet (UV) to the far-red (300-700 nm), in addition to achromatic receptors of which several are sensitive to different forms of polarized light. The abundance of spectral receptors has puzzled researchers, as it seemed excessive even for an animal living in a spectrally rich environment such as the coral reef. Furthermore, theoretical analyses suggest that there is really no need to have more than 4-7 receptors to have satisfactory colour vision in the 300-400 nm spectral range. Our increasing knowledge of polarization sensitivity is rapidly expanding the theme of photoreceptor proliferation with up to six channels of polarization information from a combination of midband and hemisphere receptors.

The aim of this thesis was to investigate how stomatopods process and analyse chromatic and polarization information using a complementary approach of behavioural, electrophysiological and neuroanatomical techniques. A comparison of spectral sensitivities across species in the superfamily Gonodactyloidea was carried out in Chapter 2. This study showed that their spectral sensitivities remain very similar between species, with narrow, steeply shaped sensitivity curves spread evenly throughout the spectrum, suggesting there is a benefit of having uniform sampling of all wavelengths. Behavioural experiments were performed to test stomatopod spectral discrimination in Chapter 3, and this was found to be surprisingly poor, both compared to other animals and to theoretical modelling. To investigate if the poor discrimination was due to the spectral shape of the stimuli, more natural-shaped stimuli (with step-shaped spectra instead of the conventional peak-shaped spectra) were tested in similar experiments (Chapter 4). However, these experiments yielded similar results to the ones obtained in Chapter 3. The electrophysiological and behavioural results suggest that the stomatopod visual system may use a simpler, serial processing system unlike the "conventional" opponency system known from other animals and may be the reason for why the spectral and polarization space must be covered by several channels.

While such a system may appear exceptional, there are similarities between this system and they way primates process colour, only at different steps in the processing pathway (Chapter 5). Using an interval-decoding scheme coupled with the narrow, binned spectral sensitivities of stomatopods could allow quick and precise colour judgements but at the cost of very fine discrimination.

As very little was known about the neural architecture of the stomatopods visual system, and to investigate possible answers to questions posed in Chapter 2-5, a range of methods was employed to examine the various neuronal structures. These included: immunohistochemistry experiments and 3D-reconstructions to visualise the gross morphology of the optic lobes, Bodian staining and fluorescent tracer injections to investigate the neuronal pathways, and Golgi impregnations to identify single neuronal types (Chapter 6). First, observations from previous studies were confirmed, in that the midband information pathway remains visible throughout the three first optic lobes as a distinct swelling (Kleinlogel et al., 2003). Chapter 6.2 describes the cell types found in the first optic neuropil, the lamina, where despite size and shape differences between some cells, no clear specializations were observed in the midband region compared to the hemispherical regions of the lamina.

The stomatopod medulla was described in Chapter 6.3 and was shown to be clearly stratified having at least 12 main layers, with the midband pathway distinctly visible as a swelling on the distal side of the medulla. The chromatic information appears to be integrated with the achromatic information in the lobula (the third optic lobe, Chapter 6.4) with lateral collaterals forming in the midband pathway and projecting into the hemispherical regions of the lobula. Further projections from the lobula terminate in optic glomeruli in the lateral protocerebrum, which may be involved in refining and sharpening the signals from the lobula columnar neurons. Finally, the stomatopod central complex in the cephalic brain was described in Chapter 6.5, revealing that stomatopods have a central complex more similar to that of an insect than to other crustaceans, possibly shedding new light of to the evolutionary relationship between crustaceans and insects.

Overall, this study has given new insights into how stomatopods process chromatic and polarization information. It has revealed a system that at the photoreceptor level appears very complex, but that not necessarily requires high levels of complex processing. These findings may provide inspiration to the development of new optic and camera technologies, and propose a sparse signal-processing scheme, which could provide useful in artificial imaging technologies that require fast and low-power processing speeds.

Declaration by author

This thesis is composed of my original work, and contains no material previously published or written by another person except where due reference has been made in the text. I have clearly stated the contribution by others to jointly-authored works that I have included in my thesis.

I have clearly stated the contribution of others to my thesis as a whole, including statistical assistance, survey design, data analysis, significant technical procedures, professional editorial advice, and any other original research work used or reported in my thesis. The content of my thesis is the result of work I have carried out since the commencement of my research higher degree candidature and does not include a substantial part of work that has been submitted to qualify for the award of any other degree or diploma in any university or other tertiary institution. I have clearly stated which parts of my thesis, if any, have been submitted to qualify for another award.

I acknowledge that an electronic copy of my thesis must be lodged with the University Library and, subject to the General Award Rules of The University of Queensland, immediately made available for research and study in accordance with the *Copyright Act 1968*.

I acknowledge that copyright of all material contained in my thesis resides with the copyright holder(s) of that material. Where appropriate I have obtained copyright permission from the copyright holder to reproduce material in this thesis.

Publications during candidature

Peer-reviewed papers:

- **Thoen, H. H.**, How, M. J., Chiou, T. H., & Marshall, J. (2014). A Different Form of Color Vision in Mantis Shrimp. *Science*, 343(6169), 411-413.
- Zaidi, Q., Marshall, J., **Thoen, H.**, & Conway, B. R. (2014). Evolution of neural computations: Mantis shrimp and human color decoding. *i-Perception*, 5(6), 492-496.

Conference abstracts:

- **Thoen, H.H.**, Strausfeld, N.J., Marshall, N.J. Colour and polarisation processing in Stomatopods. (2014) *International Congress of Neuroethology*
- **Thoen, H.H.**, How, M. Chiou, T-H. and Marshall, J (2013) A new form of colour vision in mantis shrimp? *International Conference on Invertebrate Vision*. doi: 10.3389/conf.fphys.2013.25.00074
- **Thoen, H.H.**, How, M. Chiou, T-H. and Marshall, J. (2012) Understanding the complex visual system of Mantis shrimps, a new form of colour processing? *International Congress of Neuroethology* doi: 10.3389 conf.fnbeh.2012.27.00226

Publications included in this thesis

Thoen, H. H., How, M. J., Chiou, T. H., & Marshall, J. (2014). A Different Form of Color Vision in Mantis Shrimp. *Science*, 343(6169), 411-413.

Incorporated as Chapter 3.

Contributor	Statement of contribution
Author Thoen, H. H. (Candidate)	Designed experiments (40%) Wrote the paper (60%) Data collection (80%)
Author How, M. J.	Designed experiments (20%) Wrote and edited paper (20%)
Author Chiou, T-H.	Designed experiments (10%) Data collection (20%)
Author Marshall, J.	Designed experiments (30%) Wrote and edited the paper (30%)

Zaidi, Q., Marshall, J., **Thoen, H.H.**, & Conway, B. R. (2014). Evolution of neural computations: Mantis shrimp and human color decoding. *i-Perception*, 5(6), 492-496.
Incorporated as Chapter 5.

Contributor	Statement of contribution
Author Zaidi, Q.	Designed experiments (70%) Wrote the paper (60%) Data collection (80%)
Author Marshall, J.	Wrote and edited paper (20%)
Author Thoen, H. H. (Candidate)	Data collection (10%) Edited paper (10%)
Author Conway, B. R.	Data collection (10%) Designed experiments (30%) Wrote and edited the paper (30%)

Contributions by others to the thesis

- Chapter 2. Electrophysiological recordings of the spectral sensitivities of *G. chiragra* and *H. glyptocerus* and some of the recordings of *H. trispinosa* and *G. smithii* were performed by Prof. Tsyr-Huei Chiou (National Cheng Kung University), while he was working in Prof. Justin Marshalls lab at the University of Queensland.
- Chapter 3 and 4. Dr. Martin How (University of Bristol) contributed significantly to the modelling of spectral discrimination curves in these chapters. Professor Justin Marshall contributed to the ideas, modelling and writing of the manuscript.
- Chapter 5. Prof. Qasim Zaidi (State University of New York) and Prof. Bevil Conway (Wesley College) carried out most of the data acquisition, analysis and writing of the manuscript.
- Chapter 6. Prof. Nick Strausfeld (University of Arizona) assisted significantly in method development of the Golgi impregnations and the Bodian staining in this chapter. He has also been of great help with ideas and suggestions regarding the neuroanatomical work.

Statement of parts of the thesis submitted to qualify for the award of another degree

None

Acknowledgements

First of all I have to thank my wonderful supervisors Professor Justin Marshall and Dr. Martin How for their help and support throughout my PhD. Your ideas, encouragements and enthusiasm have been invaluable.

I have to thank Professor Tsyr-Huei (Short) Chiou for teaching me the art of intracellular electrophysiology, and for repairing our rig after the devastating lab flood. Wen-Sung Chung has also been a great support and was always eager to help if anything electrical needed fixing. Alan Goldizen deserves a big thank you for answering endless questions about administration and paperwork and anything else you can think of. Thank you to Luke Hammond for teaching me how to use the many microscopes in QBI and for his enthusiasm regarding microscopy. Professor Nicholas Strausfeld has been an inspiration when it comes to anything to do with arthropod neuroanatomy, and being able to work with him in Tucson was such a pleasure. Much of the neuroanatomical work presented in this thesis would not have been possible without him. Thank you to Rachel Templin and The Centre for Microscopy and Microanalysis (CMM) for your help with embedding samples. Also thank you to Martin Berón de Astrada for your tips for doing the fluorescent tracer insertions.

Thank you to the staff at Lizard Island for all your help and support during my field trips, and to the Lizard Island Reef Research Foundation for providing me with funding to carry out much of the fieldwork. Thank you to the University of Queensland for the University of Queensland International Scholarship (UQI) tuition fee and living allowance awards, which has funded this work.

A very big thank you goes through the rest of the Marshall lab for your endless support and for making it such a good lab to work in. Genevieve, Rachel, Yakir, Fabio, Wen-Sung, Yi-Hsin, Martin, Sara, Qamar and the CoralWatch crew, you make going to work a joy! I also want to thank Professor Tom Cronin and Professor Nicholas Roberts and the members of their labs who have made the annual field trips to Lizard Island both educational and fun.

Another big thank you goes to my family back home in Norway, I know it has been hard to have us living so far away, but your endless support and love has meant the world to me. Most of all I have to thank my wonderful husband Eivind who has supported me through the rollercoaster of doing a PhD, always being positive, encouraging and interested. I would not have made it without you.

Keywords

*Stomatopod, vision, colour, polarization, photoreceptors, opponent processing, optic pathways
electrophysiology, behaviour, neuroanatomy*

Australian and New Zealand Standard Research Classifications (ANZSRC)

ANZSRC code: 060805 Animal Neurobiology (50%)

ANZSRC code: 060201 Behavioural Ecology (30%)

ANZSRC code: 060602 Animal Physiology - Cell (20%)

Fields of Research (FoR) Classification

FoR code: 0608 Zoology (50%)

FoR code: 0602 Ecology (30%)

FoR code: 0606 Physiology (20%)

Table of Contents

1 CHAPTER 1. GENERAL INTRODUCTION.....	16
1.1.1 <i>Ecology</i>	16
1.1.2 <i>Behaviour and communication</i>	17
1.1.3 <i>Eye structure</i>	18
1.1.4 <i>Spectral and polarization processing in stomatopods</i>	20
1.2 SIGNIFICANCE OF PROJECT	22
1.3 AIMS AND QUESTIONS	22
1.4 THESIS ORGANISATION:.....	23
2 CHAPTER 2. INTRACELLULAR RECORDINGS OF SPECTRAL SENSITIVITIES IN STOMATOPODS: A COMPARISON ACROSS SPECIES.....	25
2.1 ABSTRACT:	25
2.2 INTRODUCTION	25
2.2.1 <i>Stomatopod colour vision</i>	25
2.2.2 <i>Function</i>	26
2.2.3 <i>Opsins and filters</i>	26
2.3 MATERIALS AND METHODS.....	28
2.3.1 <i>Animals</i>	28
2.3.2 <i>Intracellular electrophysiology</i>	28
2.3.3 <i>Dye injections</i>	28
2.4 RESULTS	29
2.4.1 <i>Spectral sensitivities</i>	29
2.4.2 <i>Secondary peaks</i>	35
2.5 DISCUSSION.....	35
2.5.1 <i>Comparisons of spectral sensitivities</i>	35
2.5.2 <i>Tuning of sensitivities</i>	36
2.5.3 <i>Secondary UV-peaks</i>	36
2.5.4 <i>Conclusion</i>	37
3 CHAPTER 3. A DIFFERENT FORM OF COLOUR VISION IN MANTIS SHRIMP	40
4 CHAPTER 4. USING STEP-SHAPED VS. PEAK SHAPED STIMULI IN SPECTRAL DISCRIMINATION TESTING	44
4.1 INTRODUCTION	44
4.1.1 <i>Colour vision testing</i>	45
4.1.2 <i>Stomatopod colour vision</i>	46
4.2 MATERIALS AND METHODS.....	47
4.2.1 <i>Spectral measurements</i>	47
4.2.2 <i>Modelling</i>	47
4.2.3 <i>Behavioural experiments</i>	48
4.3 RESULTS	49
4.3.1 <i>Spectral measurements</i>	49
4.3.2 <i>Modelling</i>	49
4.3.3 <i>Behavioural experiments</i>	50
4.4 DISCUSSION.....	51
4.4.1 <i>Modelling of step- vs. peak-shaped stimuli</i>	51
4.4.2 <i>Broad vs. narrowbanded sensitivities</i>	51
4.4.3 <i>Stomatopod discrimination</i>	52
4.4.4 <i>Summary and conclusions</i>	53
5 CHAPTER 5. EVOLUTION OF NEURAL COMPUTATIONS: MANTIS SHRIMP AND HUMAN COLOUR DECODING	55
6 CHAPTER 6. STOMATOPOD VISUAL NEUROANATOMY	60
6.1 MATERIALS AND METHODS - NEUROANATOMY	63
6.1.1 <i>Immunohistochemistry</i>	63
6.1.2 <i>Silver stains</i>	64

6.1.3	<i>Fluorescent dye insertions</i>	66
6.1.4	<i>Imaging and reconstructions</i>	66
6.1.5	<i>Methods that have been tested but still needs improvement</i>	68
6.2	THE NEURAL ORGANISATION OF THE STOMATOPOD LAMINA.....	73
6.2.1	<i>Introduction</i>	73
6.2.2	<i>Results</i>	74
6.2.3	<i>Discussion</i>	85
6.2.4	<i>Summary and conclusion</i>	88
6.3	ANATOMICALLY SEGREGATED VISUAL PATHWAYS IN THE MEDULLA OF STOMATOPODS.....	90
6.3.1	<i>Introduction</i>	90
6.3.2	<i>Results</i>	91
6.3.3	<i>Discussion</i>	99
6.4	INTEGRATION AND PROCESSING OF CHROMATIC AND ACHROMATIC INFORMATION IN THE STOMATOPOD LOBULA AND LATERAL PROTOCEREBRUM.....	104
6.4.1	<i>Introduction</i>	104
6.4.2	<i>Results</i>	106
6.4.3	<i>Discussion</i>	114
6.4.4	<i>Summary and future questions</i>	116
6.5	THE STOMATOPOD CENTRAL BRAIN	119
6.5.1	<i>Introduction</i>	119
6.5.2	<i>Results</i>	120
6.5.3	<i>Discussion</i>	125
6.5.4	<i>Summary and conclusion</i>	126
7	CHAPTER 7. SUMMARY AND FUTURE DIRECTIONS.....	129
7.1.1	<i>Major findings:</i>	129
7.1.2	<i>Summary of new neuroanatomical findings:</i>	130
7.1.3	<i>Use of stomatopods as study animal</i>	132
7.1.4	<i>Future directions:</i>	133
8	REFERENCES	135
9	APPENDIX I.....	148

List of figure and tables

Figure 1.1 Stomatopod eye structure.....	17
Figure 1.2 Diversity of signals.....	18
Figure 1.3 Photoreceptor structure and axon projections.....	20
Figure 2.1 Comparison of spectral sensitivities across species of stomatopods.....	30
Figure 2.2 Comparison of spectral sensitivities across each photoreceptor.....	31
Figure 2.3 Spectral sensitivities of <i>G. smithii</i>	33
Figure 2.4 Examples of cells recorded using the scan and the flash method.....	34
Figure 2.5 Computed spectral sensitivities.....	34
Figure 2.6 Secondary UV-peaks.....	35
Figure 3.1 Spectral sensitivities of <i>H. trispinosa</i>	40
Figure 3.2 Examples of correct choice data from a two-way choice test of <i>H. trispinosa</i>	41
Figure 3.3 Spectral discrimination curves ($\Delta\lambda/\lambda$).....	41
Figure 3.4 Proposed processing mechanism.....	41
Figure 4.1 Examples of natural reflectance spectra on a coral reef and artificial spectra...	46
Figure 4.2 Model input.....	48
Figure 4.3 Examples of peak-shaped and step-shaped spectra used in this experiment.....	49
Figure 4.4 Peak-shaped vs. step-shaped stimuli with narrow or broad sensitivities.....	50
Figure 4.5 Discrimination testing of step-shaped stimuli.....	51
Figure 5.1 Colour tuning of mantis shrimp photoreceptors and a few neurons in macaque inferior temporal cortex.....	56
Figure 5.2 Poisson responses of IT neurons.....	57
Figure 6.1.1 Methods that need improvement.....	69
Figure 6.2.1 Lamina overview.....	75
Figure 6.2.2 Lamina photoreceptor terminals.....	76
Figure 6.2.3 Lamina monopolar cell types 1 and 2.....	78
Figure 6.2.4 Stratified lamina monopolar cell types 3 and 4.....	79
Figure 6.2.5 Examples of monopolar cells.....	80
Figure 6.2.6 Possible monopolar cell type 5.....	81
Figure 6.2.7 Tangential cells.....	82
Figure 6.2.8 Amacrine cells.....	83
Figure 6.2.9 Centrifugal cells.....	83
Figure 6.2.10 Cells in the midband lamina cartridges.....	84
Figure 6.2.11 Summary of types and function of monopolar cells.....	87
Figure 6.3.1 Overview of the optic neuropils and the medulla.....	92
Figure 6.3.2 Medulla layers.....	93
Figure 6.3.3 Termination patterns in the outer medulla layers.....	94
Figure 6.3.4 Termination patterns in the medulla midband lobe.....	95
Figure 6.3.5 Neuron types within the medulla midband lobe.....	96
Figure 6.3.6 Medulla midband lobe.....	97
Figure 6.3.7 Serotonin and synapsin-like staining in the medulla.....	98
Figure 6.4.1 Lobula overview.....	106
Figure 6.4.2 Lobula layers.....	107
Figure 6.4.3 Midband projections through lobula.....	108
Figure 6.4.4 Lobula projections.....	109
Figure 6.4.5 T-shaped and Y-shaped cells in the lobula of <i>N. oerstedii</i>	110
Figure 6.4.6 Hemiellipsoid bodies.....	111
Figure 6.4.7 Glomerular complex.....	112
Figure 6.4.8 Model of major neuronal types and arrangements in the lobula.....	113
Figure 6.5.1 Overview of the stomatopod brain.....	121
Figure 6.5.2 Stomatopod central complex.....	122

Figure 6.5.3 Immunofluorescence in the stomatopod brain.....	123
Figure 6.5.4 Mass fillings of dextran conjugated with Texas red or Fluorescein into the protocerebrum.	124
Figure 6.5.5 Olfactory lobes.....	125
Figure S1 Test setup.....	152
Figure S2 Brightness control.....	153
Table 2.1 Sensitivity maxima (λ) of photoreceptors for each species.....	32
Table 2.2 Number of recorded cells and number of recordings per cell from each photoreceptor.....	32
Table 2.3 Species ecology and physiology.....	34
Table 6.3.1 Similarities and differences between the stomatopod and crab medulla.....	99
Table S 1 Electrophysiological recordings.....	154
Table S 2 Choice numbers.....	155
Table S 3 P-values.....	156

Abbreviations list:

AL	antennal lobe	Lvfs	long visual fibres
AMPN	anterior median protocerebral neuropil	MAN	median antennular neuropil
AnN	antennal sensory neuropil	MB	midband
ATP	anterior posterior tangential processes	MBL	midband lobe
CA	corpo allungato	Me	medulla
CC	central complex	M-MDN	monostratified motion detection neuron
CN	cornea	M1-M6	monopolar cell 1 to 6
B-MDN	bistratified motion detection neuron	nm	nanometer
CB	central body	No	noduli
DH	dorsal hemisphere	Och₁ or ₂	optic chiasmata 1 and 2
DLT	distal tangential layer	OGT	olfactory globular tract
DML	distal monopolar cell layer	OGTN	olfactory globular tract
DVT	dorsoventral tangential layer	OL	neuropil
EB	ellipsoid body	PB	olfactory lobe
Epl₁ or ₂	lamina plexiform layer 1 or 2	PLT	protocerebral bridge
FB	fanshaped body	PMPN	proximal tangential layer
FT	fibre tracts	PML	posterior median protocerebral neuropil
FWHM	full-width at half-maximum	RCA	proximal monopolar cell layer
GC	glomerular complex	Re	retinula cell axon
HB	hemiellipsoid body	R1-8	retina
IT	inferior temporal cortex	Row 1-6	retinula cell 1 - 8
La	lamina	Svfs	midband row 1 to 6
LAN	lateral antennular lobes	Tan 1-3	short visual fibres
LCN	lobula columnar neurons	Tm	tangential cell 1 to 3
LC	lateral cluster	UV	transmedullary
LGN	lateral geniculate nucleus	VH	ultraviolet
LPC	lateral protocerebrum	WL	ventral hemisphere
LMT	lateromedial tangential processes		wavelength
Lo	lobula		

Chapter 1.

General introduction

1 Chapter 1. General introduction

1.1.1 Ecology

Stomatopods, commonly known as mantis shrimps, are benthic crustaceans found in tropical and temperate waters worldwide (Manning, 1977). They normally live in burrows made of sand or coral rubble and inhabit depths between 0 to 1500 m (Schram et al., 2013). Stomatopods separated from other crustacean lineages over 400 million years ago (Schram, 1969) and are divided into around 450 species within the following superfamilies; *Squilloidea*, *Parasquilloidea*, *Eurysquilloidea*, *Bathysquilloidea*, *Lysiosquilloidea*, *Erythrosquilloidea* and *Gonodactyloidea*, *Hemisquilloidea* and *Pseudosquilloidea* (Ahyong, 2001, Ahyong and Jarman, 2009, Porter et al., 2010). Despite previous investigations into the stomatopod visual system (Schönenberger, 1977, Manning et al., 1984, Schiff et al., 1986) it was not until 1988 that researchers discovered exactly how intricate their eyes are (Marshall, 1988, Cronin and Marshall, 1989a, Cronin and Marshall, 1989b, Marshall et al., 2007 provides a recent review)

Stomatopods have the most complex visual system found in any animal at least at photoreceptor level, possessing a total of 16 anatomically distinct photoreceptor types of which 12 are used for detecting colour, with spectral sensitivities ranging from the ultraviolet to the far-red (Fig. 1.1). In addition to this multitude of spectral receptors they also have the ability to detect the polarization of light in both linear and circular forms (Fig. 1.1) (Kleinlogel and Marshall, 2006, Marshall et al., 2007, Chiou et al., 2008). When the functional categories are added, the final count for photoreceptor diversity expands to 20. Compared to the human visual system, with its three spectral receptors (De Valois and Jacobs, 1968, Dartnall et al., 1983) and no ability to detect different forms of polarised light, the stomatopod visual system appears quite baffling. In fact the only animals that come close to this kind of photoreceptor diversity are the butterflies. The genus *Papilio xuthus* for example can have up to 9 photoreceptor types (Arikawa, 2003, Koshitaka et al., 2008). It is, however, only shallow-water species in the stomatopod superfamilies *Gonodactyloidea*, *Lysiosquilloidea*, *Hemisquilloidea* and *Pseudosquilloidea* that have this photoreceptor diversity, with deeper-living species thought to have had an evolved loss of complexity (Manning et al., 1984, Ahyong and Harling, 2000, Porter et al., 2010), likely due to the restricted light environment. All further referrals to stomatopods will therefore only be from the four superfamilies mentioned above.

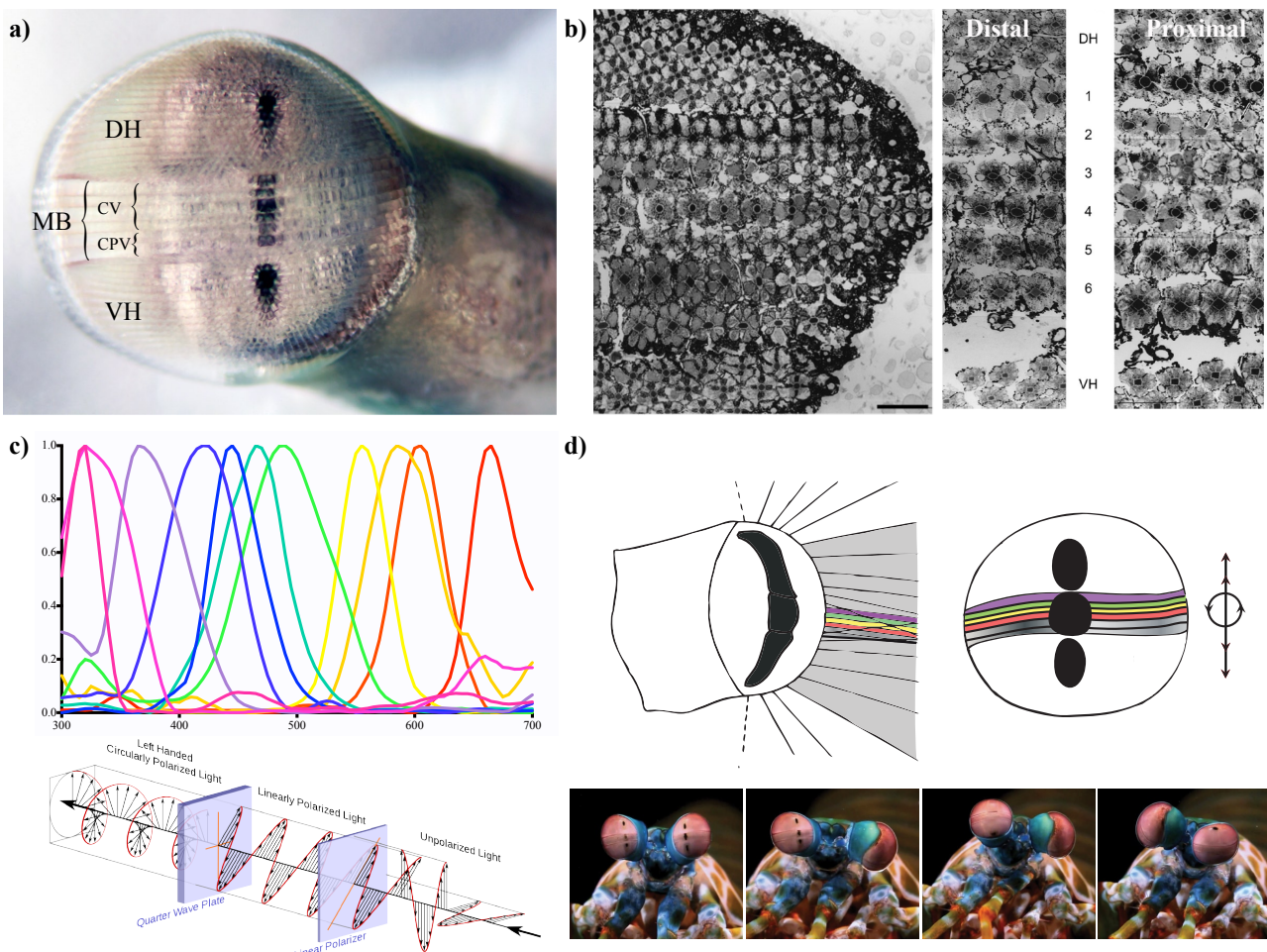


Figure 1.1. Stomatopod eye structure. a) Frontal view of the eye of *Haptosquilla trispinosa* showing the midband (MB), dorsal (DH) and ventral hemisphere (VH), colour vision (CV) row 1-4 and circular polarisation vision (CPV) rows 5 and 6. Note the three pseudopupils. b) Coronal section of the retina of a stomatopod eye, showing the six midband rows and the dorsal and ventral hemisphere. Right side shows the distal and the proximal photoreceptors (from Marshall et al. 2007). c) Top. Spectral sensitivities of *H. trispinosa*. Bottom: Illustration of unpolarised, linear and circular polarised light (source:Wikimedia commons). d) Left: Illustration of a sagittal section of the stomatopod eye showing the anatomical visual axis. Right: Frontal diagram of eye showing midband and three pseudopupils (adapted from Marshall and Land 1993). Arrows indicate eye movements. Bottom: Images showing the scanning eye movements in stomatopods (Photo: Mike Bok).

1.1.2 Behaviour and communication

Stomatopods are known to be fierce and territorial predators (Dingle and Caldwell, 1969). There are two main types; the smashers which hunt or fight using hammer-like raptorial appendages, ideal for crushing the hard exoskeleton of crabs, snails and mussels (Patek et al., 2004, Patek and Caldwell, 2005); and the speakers, which typically ambush soft-bodied prey such as fish from camouflaged sandy burrows (Caldwell and Dingle, 1976) (Fig. 1.2). They live in a colourful world typically surrounded by coral and fish with bright colourful displays. As an aggressive predator it is important to have the ability to quickly and reliably identify other animals and objects as potential prey or threat (Fig. 1.2). Stomatopods are known for using colour (Cheroske et al., 1999, Chiao et al., 2000), polarization (Marshall et al., 1999) and fluorescence (Mazel et al., 2003) to produce and enhance displays on various body parts. It is likely that the main use of these displays is for intraspecific communication and species recognition (Hazlett, 1979). Particularly well known is the “meral spot”, an eyespot on the surface of the meral segments of the second maxilliped (Fig. 1.2).

The meral spot display gives a very conspicuous signal and is often revealed during interactions with other stomatopods. The purpose of the display may be to inform about sexual receptivity or health, or about strength during conflicts over territory or mates (Caldwell and Dingle, 1976, Cheroske and Cronin, 2005, Chiou et al., 2011). The display may also be used as a bluff signal to avoid conflict during moulting (Steger and Caldwell, 1983, Adams and Caldwell, 1990). Stomatopods also have the ability to reflect highly polarised light from various body parts (Fig. 1.2) (Chiou et al., 2005, Cronin et al., 2009, Chiou et al., 2011). Chiou et al. (2005) found that these polarized parts can be divided into two major types; a red/pink type located within the animal's cuticle and an iridescent blue type which is located in the soft tissue underneath the exoskeleton, and is therefore unaffected by the moulting cycle. In addition to reflecting linearly polarised light, a few stomatopod species can also produce circularly polarized signals (Fig. 1.2c) (Cronin et al., 2009), a property which is only known to exist in few other animal groups, including the scarab beetles (Neville and Caveney, 1969, Jewell et al., 2007) and lobsters (Neville and Luke, 1971).

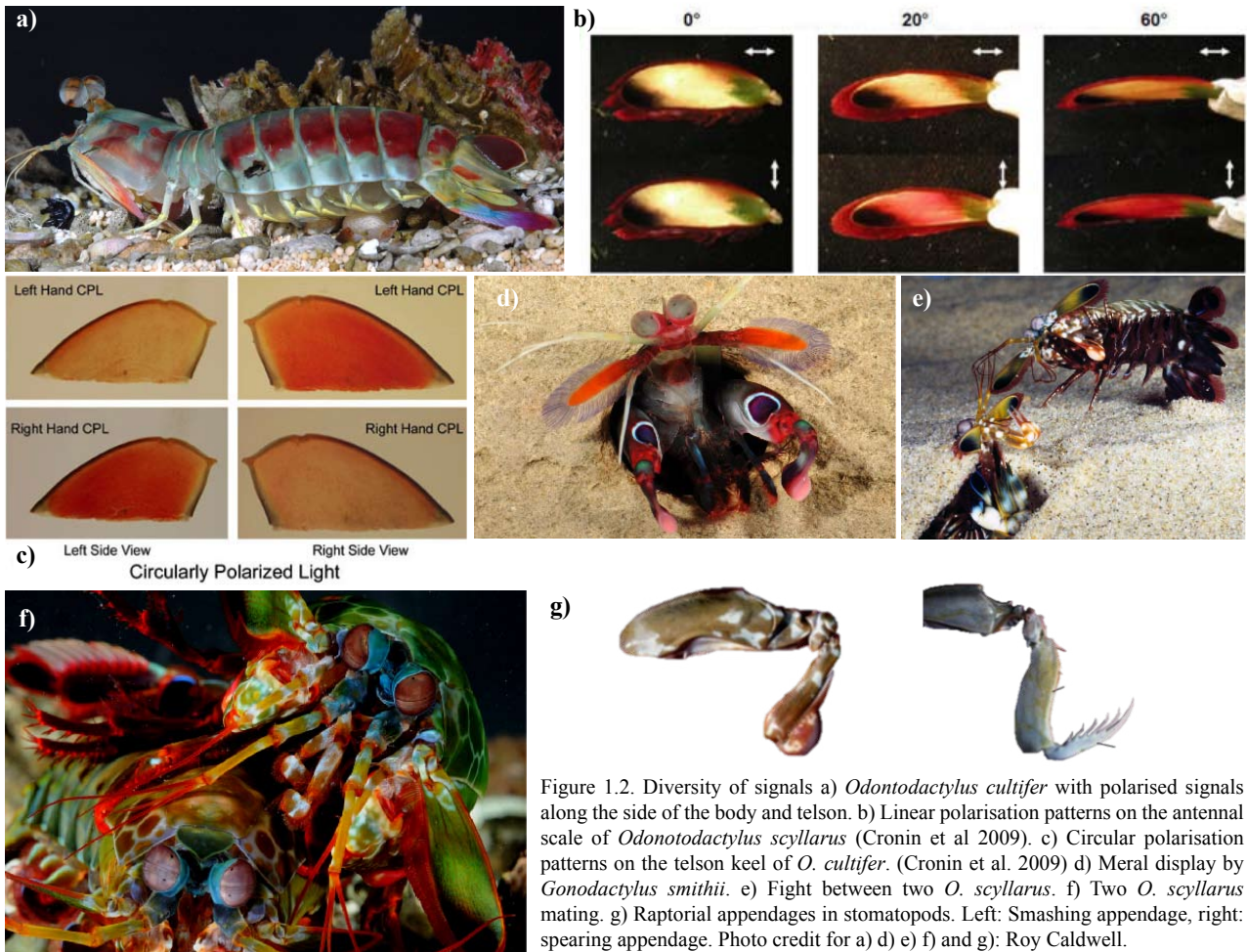


Figure 1.2. Diversity of signals a) *Odontodactylus cultifer* with polarised signals along the side of the body and telson. b) Linear polarisation patterns on the antennal scale of *Odontodactylus scyllarus* (Cronin et al 2009). c) Circular polarisation patterns on the telson keel of *O. cultifer*. (Cronin et al. 2009) d) Meral display by *Gonodactylus smithii*. e) Fight between two *O. scyllarus*. f) Two *O. scyllarus* mating. g) Raptorial appendages in stomatopods. Left: Smashing appendage, right: spearing appendage. Photo credit for a) d) e) f) and g): Roy Caldwell.

1.1.3 Eye structure

Stomatopod eyes are mounted on stalks, and the eyes move independently of each other, giving them a curious, attentive appearance. This is one of the reasons why they are often thought to be

more aware of their surroundings than other crustaceans (Land et al., 1990) (Fig. 1.1). They use their eyes in discrete, spontaneous movements, essentially scanning the environment around them (Horridge, 1978, Land et al., 1990, Marshall et al., 2014). The eye is an apposition compound eye made up of a dorsal and a ventral hemisphere, divided by a distinct region of specialised ommatidia (optical units) termed the midband (Fig. 1.1 a). At certain angles, three dark pseudopupils are visible. These pseudopupils occur when the local ommatidia are orthogonal to the viewer. The occurrence of three simultaneous pseudopupils at certain viewing angles implies that the animal can make use of trinocular vision within each eye, allowing it to sample colour and circular polarization (see below) information with the midband while simultaneously receiving depth, linear polarization and light intensity information from the hemispheres (Fig. 1.1) (Marshall et al., 1991a, Marshall et al., 2007).

The midband consists of 6 separate rows of ommatidia each with different functionalities (Fig. 1.3 a and b); Row 1-4 being involved in colour processing while Row 5 and 6 are involved in detecting polarized light (Marshall et al., 1991a, Marshall et al., 1991b). Each ommatidia is composed of a cornea and a crystalline cone that focuses light into the rhabdom (photoreceptor) (Land and Nilsson, 2002). The rhabdom is fused with interdigitating bands of orthogonal microvilli and is built up of one small retinula cell termed R8 and seven retinular cells termed R1-7. The UV-sensitive R8 cells are located distally in the retina on top of the R 1-7 cells (Fig. 1.3 a). In Row 1-4 the R1-7 cells are divided into two tiers; Row 1,3 and 4 having three cells (1,4,5) over four cells (2,3,6 and 7). Row 2 has a reversed arrangement with four cells over three cells (Marshall et al., 1989, Marshall et al., 1991a). The purpose of this reversal of cell number in Row 2 is not well understood but it may be linked to the additional polarization sensitivity of this row (Kleinlogel and Marshall, 2006, Marshall et al., 2007).

Three types of ommatidia can be classified from the midband (Fig. 1.1a); Type I is found in Row 5 and 6 (as well as in the hemispheres) and is the simplest type with one main rhabdom. This type is specialised for polarization vision. The rhabdom in Type II ommatidia is divided into three tiers; R8, distal and proximal, each containing different visual pigments. This type is found in Row 1 and Row 4. Type III ommatidia which is found in Row 2 and 3 and is similar to Type II, except that they may have coloured filters placed between the tiers (Cronin and Marshall, 2001). These filters function by shifting and narrowing the spectral sensitivity of the underlying photoreceptor (Cronin et al., 2014). The hemispheres function more like a “normal” crustacean eye containing only two populations of cells; R8 cells most often involved in UV vision and the underlying R1-7 cells with a

broadband, achromatic spectral sensitivity and likely polarization sensitivity equivalent to other crustaceans (Marshall and Cronin, 2014)

Previous work on the neural architecture underlying this complex retina has focused on the retina to lamina photoreceptor projections (Strausfeld and Nässel, 1981, Kleinlogel et al., 2003, Kleinlogel and Marshall, 2005). These studies determined that the axons from each ommatidia project to the lamina in a retinotopic fashion, with no connections between axons of different ommatidia. Furthermore, the axons from the R1-7 cells terminate in two different strata in the lamina (Fig 1.3 d), while the axon from the small R8 cell project through the lamina and terminate in the distal medulla (Fig 1.3 e).

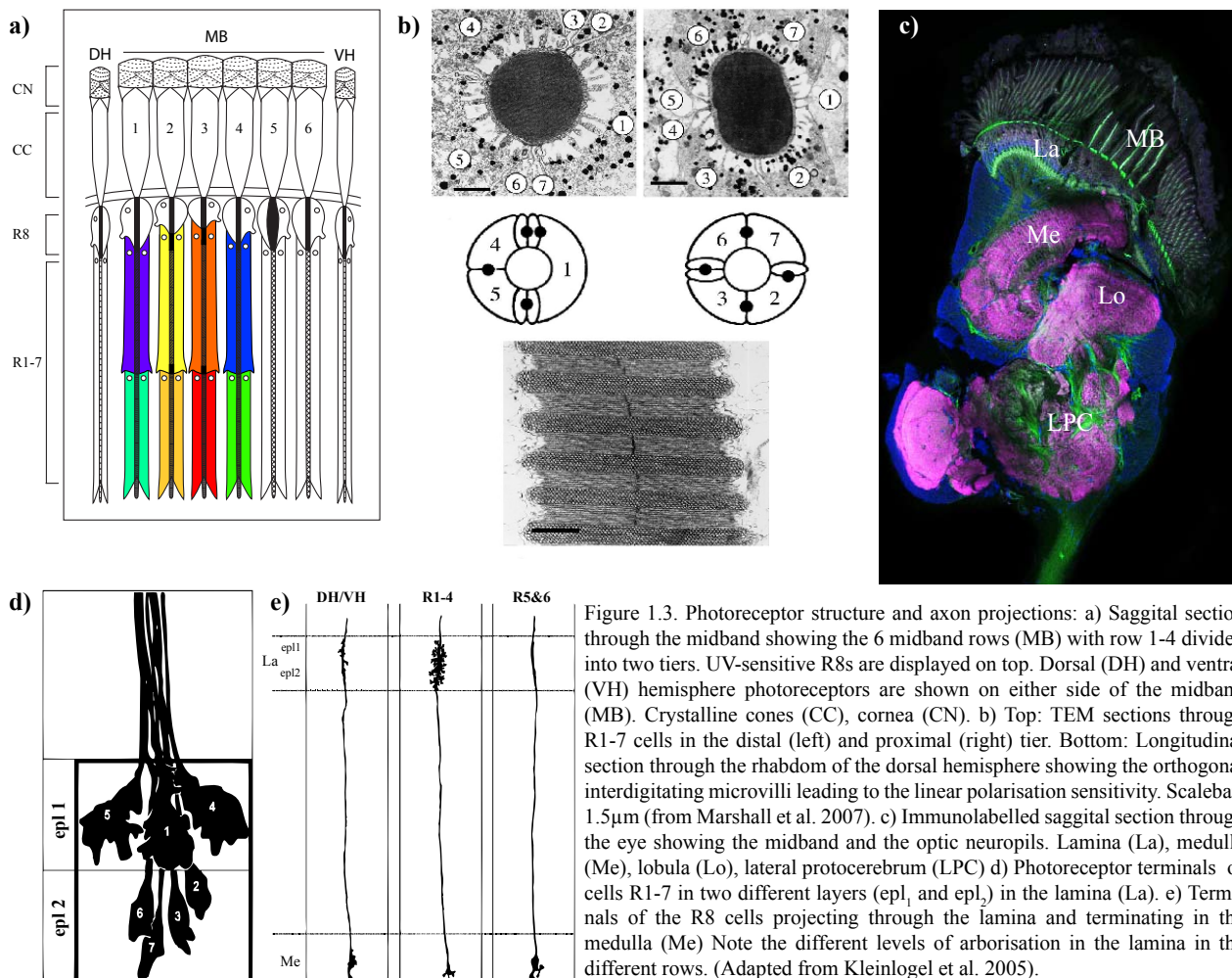


Figure 1.3. Photoreceptor structure and axon projections: a) Saggital section through the midband showing the 6 midband rows (MB) with row 1-4 divided into two tiers. UV-sensitive R8s are displayed on top. Dorsal (DH) and ventral (VH) hemisphere photoreceptors are shown on either side of the midband (MB). Crystalline cones (CC), cornea (CN). b) Top: TEM sections through R1-7 cells in the distal (left) and proximal (right) tier. Bottom: Longitudinal section through the rhabdom of the dorsal hemisphere showing the orthogonal interdigitating microvilli leading to the linear polarisation sensitivity. Scalebar: 1.5 μ m (from Marshall et al. 2007). c) Immunolabelled saggital section through the eye showing the midband and the optic neuropils. Lamina (La), medulla (Me), lobula (Lo), lateral protocerebrum (LPC) d) Photoreceptor terminals of cells R1-7 in two different layers (epil₁ and epil₂) in the lamina (La). e) Terminals of the R8 cells projecting through the lamina and terminating in the medulla (Me) Note the different levels of arborisation in the lamina in the different rows. (Adapted from Kleinlogel et al. 2005).

1.1.4 Spectral and polarization processing in stomatopods

How colour is processed in the brain of animals has been a much debated issue since the three-colour theory of Young-Helmholtz (Young, 1802, Helmholtz, 1859, Hurvich and Jameson, 1949) and the opponency theory of Hering (Hurvich and Jameson, 1957). Young-Helmholtz suggested that colour was interpreted by the receptor input of three different colour sensitive photoreceptors while Hering argued that colour was perceived through antagonistic pairs of receptors recording the

differences in activity from three opponent channels; red vs. green, blue vs. yellow and black vs. white (the latter type is achromatic and detects luminance). Although there are many unsolved puzzles regarding how human colour vision is actually processed through the areas of such as the lateral geniculate nucleus (LGN) and the visual cortex (Conway, 2014) we do know now that we likely use a combination of mechanisms from the two ideas. We have three colour receptors (short (S), medium (M) and long (L)) in the retina and opponent cells in the LGN, which send chromatic information to the V1 and the inferior temporal cortex areas of the brain for further processing. We also know that our three receptors are sufficient to encode many colours between 400-700 nm very well and that we are able to discriminate between colours from 1-5 nm apart, at least in some areas of the spectrum (De Valois and Jacobs, 1968, Pokorny and Smith, 1970).

One of the main questions researchers therefore asked when the stomatopods abundance of spectral receptors was revealed was; how do they process all this chromatic information? It is hard to imagine how the world would look if we used 12 classes of spectral receptors instead of only 3. The stomatopods sensitivity curves have a very steep and narrow function (shape). If they were to use an opponent processing system similar to that of humans (and other animals), it should provide them with extremely fine discrimination due to the large change in activity ratio that even a very small difference in wavelength would give them. But having an opponent processing system between 12 spectral receptors necessarily require a very intricate web of neuronal wiring and would likely be very costly in terms of energy demand. In addition, theoretical modelling of visual systems suggests that having more receptors is not necessarily better for colour discrimination. The optimal number of receptors to sample the visual world effectively and efficiently from the ultraviolet (UV) to the far-red would likely be between 4-7 (Barlow, 1982, Maloney, 1986). Trichromacy (three receptors) is found in almost all animals that lack UV sensitivity while those that do extend the range possess four receptors (tetrachromacy). This parsimony of information flow suggests another explanation is needed for stomatopods.

Previous studies (Marshall et al., 1996, 2007) have suggested that, instead of using an opponent processing system like that of humans, stomatopods have opted for a much simpler design, relying on parallel processing and binning of colour signals. This implies that, instead of taking the spectral output from each channel and comparing them, the information is rather being processed in parallel streams, essentially “binned” into separate compartments where colour information is sent directly and linearly from the retina to the brain. An analogue to this system could be the cochlea in the inner ear where sound is encoded on the basis of frequency. Another possibility, which is not necessarily mutually exclusive is that the colour is encoded on the basis of serial dichromacy

(Marshall et al., 1996, Cronin and Marshall, 2001). In this organisation, each midband row would function as a dichromatic colour channel, comparing the input from the distal and proximal main retinular cells. Such a system would require much less processing power than a fully opponent organisation, and would leave each channel (row) with a narrow spectral window to analyse. Previous work on stomatopod neural wiring beneath the retina (Fig. 1.3 a) (Kleinlogel et al., 2003, Kleinlogel and Marshall, 2005), and visual modelling (Chiao et al., 2000) gives support to the hypothesis of a simpler colour processing system.

1.2 Significance of project

In addition to the value of increased knowledge about the visual capabilities of these fascinating crustaceans, gaining a better understanding of one of the most complex visual systems known could potentially aid in the development of novel optical technologies. Biomimicry is an emerging field with increased interest as the technical, economical and environmental value of such findings are gaining recognition. New findings on the physiological structures in the stomatopod eyes used for manipulation of polarized light (quarter-wave retarders) show that they have superior performance to currently produced artificial filters (Roberts et al., 2009). This has further led to the development of a novel material that could lead to better digital data storage (Jen et al., 2011). In addition comes other innovative designs for a variety of optics-dependent technologies including hyperspectral imagers used in remote sensing, an imaging technique frequently employed in areas such as marine monitoring (Roberts et al., 2014, York et al., 2014).

1.3 Aims and questions

This thesis attempts to answer some of the questions regarding how and where the stomatopod processes colour and polarization information. Using methods including behavioural experiments, intracellular electrophysiological recordings and neural tracing experiments the following hypothesis are examined:

- Do the intracellularly recorded spectral sensitivity maxima remain similar across species of stomatopods living within the same depth? (Chapter 2)
- How well do stomatopods discriminate between different wavelengths of light, and what can this tell us about their colour processing system? (Chapter 3)
- Would it be more appropriate to test spectral discrimination using natural spectra, and can stomatopods discriminate between these? (Chapter 4)
- How would a proposed parallel colour processing system work? (Chapter 5)

- What is the general layout of the colour and polarization pathways in the stomatopod neural architecture? (Chapter 6)
- What do the various stages of processing (lamina, medulla, lobula, lateral protocerebrum and central brain) tell us about how stomatopods see colour and polarised light? (Chapter 6)

1.4 Thesis organisation:

Chapter 1: Gives a general description of the stomatopod visual system and behavioural ecology

Chapter 2: Describes the similarities of the spectral sensitivities across species of *Gonodactyloid* stomatopods.

Chapter 3: Investigates the spectral discrimination abilities of stomatopods and suggests a new colour processing system

Chapter 4: Discusses the benefits of using step-shaped stimuli in spectral discrimination experiments

Chapter 5: Proposes a colour vision system based on interval decoding and a "winner-takes-it-all" system.

Chapter 6: This chapter is divided into subchapters going through the neural architecture of the stomatopod visual system:

Chapter 6.1: Gives an overview of the neuroanatomical methods used for the following chapters.

Chapter 6.2: Investigates the layout of the first optic neuropil, the lamina

Chapter 6.3: Examines the second optic lobe (the medulla) in regards to the structural organisation and communication between the information contained in the midband pathway and the hemispherical regions.

Chapter 6.4: Goes through the third optic neuropil (the lobula) in addition to the lateral protocerebrum to investigate the mixing of the chromatic and achromatic channels and projection pathways.

Chapter 6.5: Gives a description of the major features of the stomatopod central brain.

Chapter 7: Summarizes the thesis and provides the concluding remarks

Chapter 2.

Intracellular recordings of spectral sensitivities in stomatopods: a comparison across species

2 Chapter 2. Intracellular recordings of spectral sensitivities in stomatopods: a comparison across species

2.1 Abstract:

The complex eyes of stomatopods have been studied for a quarter of a century and while we have a thorough knowledge of the anatomical structures of the retina there are still unanswered questions regarding the function of these structures. These species possess one of the most complex eyes in the natural world, with up to 20 different classes of photoreceptors of 16 anatomically separate types, 12 of which are used in colour vision. It is not yet understood why stomatopods use almost 4 times more receptors than other animals, although some suggest it could provide a mechanism for colour constancy (Osorio et al., 1997) Here we investigate the spectral sensitivities of 5 species of stomatopods within the superfamily Gonodactyloidea using intracellular electrophysiological recordings. The results show that the spectral sensitivities across species of stomatopod are qualitatively remarkably similar indicating that animals living in similar environments retain very similar spectral sensitivities across species. A colour vision system based on parallel processing of each separate sensitivity, as suggested by Thoen et al. (2014, Chapter 3) would necessitate broad coverage throughout the spectrum and narrow sensitivity curves within each photoreceptor to be able to sample the environment efficiently. The observed similarity of spectral sensitivities across species therefore lends support to the hypothesis of an unconventional colour vision system.

2.2 Introduction

2.2.1 Stomatopod colour vision

Living in a spectrally rich environment, such as shallow coral reefs, may or may not lead to good colour vision. Stomatopods, commonly known as mantis shrimp have one of the most complex visual systems known in the animal kingdom, with 16 different classes of photoreceptors and the capacity to see linear, circular and elliptical polarised light (Marshall, 1988, Cronin and Marshall, 1989b, Kleinlogel and Marshall, 2006, Marshall et al., 2007, Chiou et al., 2008). As colour attenuates quickly with increasing depth it is only the shallow water species within the four superfamilies *Pseudosquilloidea*, *Hemisquilloidea*, *Gonodactyloidea* and *Lysiosquilloidea* (Marshall et al., 2007, Porter et al., 2010) that appear to take advantage of the spectral range available to them, with species living in deeper water most likely having lost these specialisations (Cronin and Porter, 2008, Porter et al., 2010). The eye of the stomatopod is divided by a band of specialised ommatidia, termed the midband, which separates the rest of the eye into dorsal and a ventral hemispheres (Fig 2.1). The midband consists of 6 rows of ommatidia; row 1-4 contains 12 narrowbanded spectral receptors while row 5 and 6 are achromatic but with receptors that are

sensitive to circular polarised light, a visual modality that no other animal is known to have (Chiou et al., 2008). The ommatidia in the stomatopod eye are composed of 8 retinula cells (R1-R8). Retinula cells 1-7 (R1-R7) make up the main rhabdom, while R8 is a small, four-lobed UV-sensitive cell placed on top of the other seven. In rows 1-4 of the midband the R1-7 cells are divided into two different tiers, R1, 4 and 5 making up one tier and R 2,3,6 and 7 making up the other. These two tiers have different spectral sensitivities, giving each ommatidium in row 1-4 a total of three spectral sensitivities, one UV sensitive R8 cell, and 2 in the "visual" part of the spectrum (Fig. 1.3 introduction). Rows 1-4 therefore have a total of 12 different spectral sensitivities. In row 5 and 6 the R1-7 are not divided into different tiers and have an achromatic broadband spectral sensitivity centred around 500 nm in addition to their ability to detect circular polarization.

2.2.2 *Function*

The reason for the stomatopods many spectral sensitivities have been puzzling scientist ever since they were discovered in 1988 (Marshall, 1988). Most other animals have between 2-3 spectral sensitivities. This enables them to discriminate colours well within most of the visual part of the spectrum. Some animals have one or two extra sensitivities increasing their discrimination abilities into the ultraviolet (UV) range of the spectrum. Theoretical modelling show that the ideal number of spectral sensitivities for sampling the whole spectrum (from UV to far-red) range between 4-7 but any more than that will not be beneficial due to an increased signal-to-noise ratio (Barlow, 1982, Maloney, 1986). Osorio et al. (1997) suggested that the stomatopods multiple spectral sensitivities gives them better colour constancy (ability to perceive colours under varying illumination) under water. Stomatopods are known for using different coloured signals on their body parts for communication, especially during territorial fights (Dingle and Caldwell, 1969, Adams and Caldwell, 1990) or during sexual interactions (Chiou et al., 2011), and having good colour constancy may therefore be of benefit as it allows them to achieve fast and reliable colour identification.

2.2.3 *Opsins and filters*

With 16 different classes of photoreceptor it was hypothesised that stomatopods could have up to 16 different visual pigments, where each photoreceptor to express a different opsin gene. But Porter et al. (2009, 2010) and Cronin et al. (2010) found that this is not the case. Surprisingly, the number of opsins identified in the stomatopod retina greatly exceeds the number of spectral sensitivities (a total of 54 unique retinal opsins were isolated from 5 species), suggesting that several opsins are co-expressed within single photoreceptor cells or used at different times. This implies that there have been extensive gene duplication events, both in recent time, but also within the stem crustacean

lineage, forming distinct clades separating opsins into colour or polarization vision specialists (Cronin et al., 2010). Although the stomatopods have such a diversity of opsins, their spectral maxima only have a range from between 300 nm to 550 nm (Bok et al., 2014, Cronin et al., 2014). One of the reasons that stomatopods may have so many spectral sensitivities ranging from 300 to 700 nm is because of the filtering of light through the rhabdom. Row 2 and 3 have intra-rhabdomal filters (Marshall, 1988, Cronin et al., 1994b) consisting of segmented photostable pigments located between the two photoreceptor tiers. The number of filters varies between species but can be up to four. These filters functions as long-pass filters that successively narrow the spectrum of light passing through the rhabdom, thus increasing the long wavelength sensitivity at each step. Row 1 and 4 does not have these intra-rhabdomal filters, but instead the actual placement of the visual pigments within the tiers (using a short wavelength pigment in the distal tier and a longer wavelength pigment in the proximal tier) helps shift the light to a narrower and sharper spectral sensitivity in the proximal tier. In addition to filtering in the rhabdom itself, the stomatopods also seem to use specialized ultraviolet long- and short-pass optical filters which are located in the crystalline cones (Bok et al., 2014, Cronin et al., 2014) to tune the UV-sensitivities further and diversifying them into as many as six distinct UV receptor types in some species (Marshall and Oberwinkler, 1999).

With all these specialisations and diversity of opsins and filters one could assume that there would be a high degree of variability in the spectral sensitivities within species of stomatopods. Previous studies have investigated the spectral sensitivities using microspectrophotometry (MSP) (Cronin and Marshall, 1989b, Cronin and Marshall, 1989a, Cronin et al., 1993, Cronin et al., 1994e, Cronin et al., 1996, Chiao et al., 2000) which records the absorption spectra of the visual pigments and intra-rhabdomal filters in a tissue section, but does not take any other modifications in the optic pathway into account. The final photoreceptor sensitivities have then been modelled using the various filtering mechanisms and physiological measurements from each ommatidium. Intracellular electrophysiological recordings of the photoreceptors is a much more accurate method, as it is able to take all of the previously mentioned specialisations into account. The information recorded using this method is what is finally encoded and transferred down to the optic processing system for further computations, and so represents a more precise estimate of the spectral sensitivity within each photoreceptor.

The objective of this study was to use intracellular electrophysiology to investigate the spectral sensitivities in several species of stomatopods, and relate these to previous models of sensitivities obtained using MSP. We also wanted to compare spectral sensitivities across species to determine

whether the diverse arsenal of visual modifications does generate variability. Findings were discussed in relation to the retinal anatomy, proposed processing systems and ecology of the different species.

2.3 Materials and methods

2.3.1 Animals

Species used were *Haplosquilla trispinosa*, *H. glyptocercus*, *Gonodactylus smithii*, *G. chiragra*, and *Neogonodactylus oerstedi*. The first four are all Australian species collected from Lizard island research station on the northern Great Barrier Reef (GBRMPA Permit no. G12/35005.1, Fisheries Act no.140763), while *N. oerstedi* was collected on the reef flats in Florida Keys, USA. All animals were collected from waters of 0-5m depth. Animals were shipped back to the lab and kept in saltwater aquaria in a 12h/12h-dark/light cycle with UV-enhanced full-spectrum lighting.

2.3.2 Intracellular electrophysiology

Spectral sensitivity was recorded using a setup described elsewhere (Kleinlogel and Marshall, 2006) and are therefore only briefly described here: At least half an hour before each experiment the animal was placed in total darkness to dark-adapt, and all following steps were performed in dim red light. The animal was anaesthetised by cooling before decapitation, and the eyestalk was removed from the body. The eyestalk was attached to a plastic rod using cyano-acrylate glue and placed in a petri dish containing stomatopod saline (Watanabe et al., 1967). A small hole was cut through the cornea in the dorsal or ventral hemisphere using a sharp razorblade, taking care not to disturb the underlying photoreceptor cells. The eye was then placed in a spherical glass vial filled with saline and placed on a cardan arm device mounted on a pneumatic table inside a Faraday-cage. Microelectrodes (Borosilicate, O.D. 1.2 mm x I.D. 0.69mm) filled with 1 M KCL and with a resistance between 50-100 M Ω were inserted into the eye. A drop in resting potential to between -20 to -50 mV and response to a brief flash of white light identified photoreceptor cells. Spectral sensitivities were recorded either the spectral scan procedure or the flash method according to Menzel et al. (1986) and DeVoe et al. (1997) and the data were recorded as an excel file.

2.3.3 Dye injections

Injections of the fluorescent dye Alexa Fluor 568 (Molecular probes, Invitrogen) into the cell after the recording were used to determine the position of the cell in the midband and the distal/proximal position in the rhabdom. The tip of the microelectrode was filled with dye and then backfilled with 1 M KCL. The dye was injected into the cell using a hyperpolarizing current between 0.1 - 0.2 nA in a 1 HZ duty regime using between 20-30 min injection times. After injection the cell condition was checked by flashing a brief white light making sure the resting potential of the cell were similar

to the resting potential before the injection. The eye was then fixed in 4% paraformaldehyde for 1 h and sectioned on a cryomictrotome (Leica CM 1100) in 8-10 μm thick sections. A Zeiss Axioskop Microscope with fluorescent filters was used to visualise the filled cells. In recordings from cells that were not injected with dye the cell identity was assumed based on previously filled cells and data from MSP recordings.

2.4 Results

2.4.1 Spectral sensitivities

Recordings of photoreceptor sensitivities were obtained from all five species. Only sensitivities obtained from the photoreceptor cells within rows 1-4 and the UV-sensitive R8 cells were included in this study (the broadband sensitivities from row 5 and 6 and the hemispheres were omitted). A total of 13 sensitivities were identified within *N. oerstedii*, 11 in *H. trispinosa*, 8 in *G. chiragra*, 10 in *H. glyptocercus* and 11 in *G. smithii* (Fig. 2.1 to 2.4, Table 2.1 and 2.2). Some of the recordings shown here have been published previously: the recordings from the ultraviolet receptors in *N. oerstedii* were published in Marshall and Oberwinkler (1999) and the remaining sensitivities were published in Marshall et al. (2007). The spectral sensitivities of *H. trispinosa* were performed by H. H. Thoen and Prof. Tsyr-Huei Chiou and were published in Thoen et al. (2014, Chapter 3). The sensitivities of *G. chiragra* and *H. glyptocercus* were recorded by Prof. Tsyr-Huei Chiou, while the *G. smithii* recordings were performed by H. H. Thoen and Prof. Tsyr-Huei Chiou. Neither of the *G. chiragra*, *H. glyptocerus* or *G. smithii* recordings have been published before. Kleinlogel and Marshall (2006) published some recordings of the sensitivities of row 2D and rows 5&6 in *G. chiragra*, but the recordings presented here are not the same as these. An overview of the spectral sensitivities of each species is shown in figure 2.1. Cell identities according to midband row and distal/proximal position were determined either by injections into the cell using a fluorescent dye or by comparisons to similar sensitivities determined by injections or MSP recordings. The spectral sensitivity curves have been smoothed and normalised (Fig. 2.3) as it is believed that, due to distal filtering, all mid-band sensitivities have approximately the same shape (Marshall et al., 1996).

The spectral scan procedure produces the spectral sensitivity immediately. The flash method recordings on other hand, needs to be corrected to the response-log stimulus intensity (V/log I) curve using the Naka-Rushton equation (Naka and Rushton, 1966b, 1966a). Due to time restrictions, this work has not yet been carried out for the species *G. chiragra*, *H. glyptocerus* and *G. smithii*, but will be performed as soon as possible. We nevertheless chose to include the flash recordings here, as the shift in λ -max between the scan recorded and flash recorded cells were relatively small (Fig. 2.4) and we wanted to illustrate the range of recorded cells.

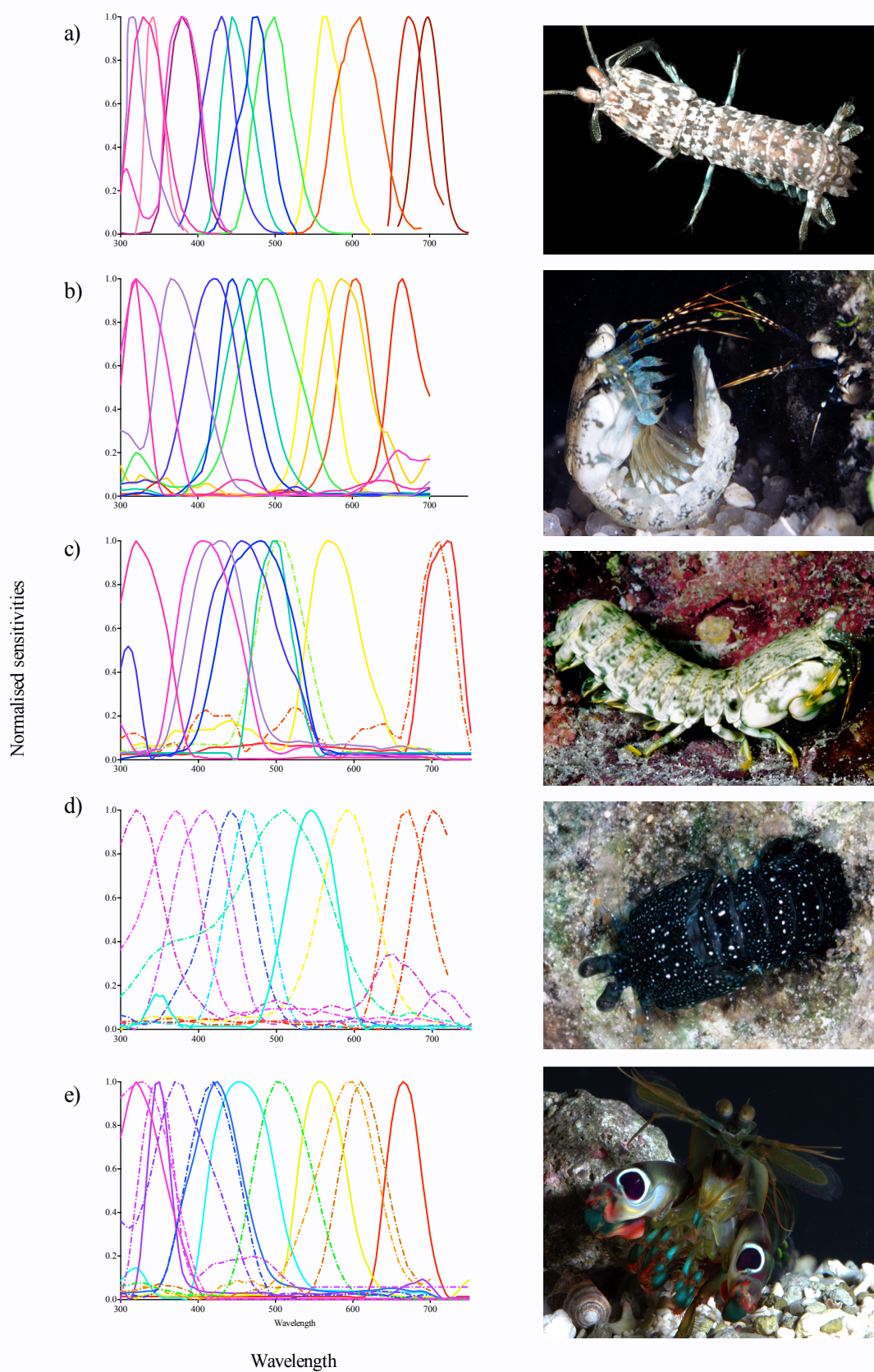


Figure 2.1. Comparison of spectral sensitivities across species of stomatopods. Spectral sensitivities measured with the SCAN method are shown in solid lines while sensitivities measured with the FLASH method are shown in dash-dotted lines. a) *N. oerstedii*, b) *H. trispinosa*, c) *G. chiragra*, d) *H. glyptocercus* and e) *G. smithii*. All photos: Roy Caldwell

When comparing the spectral sensitivities from each species by photoreceptor identities their similarity becomes apparent (Fig. 2.2). Some variability does exist, in particular within rows 2 and 3. In *H. trispinosa* row 3P were identified as having a maximum sensitivity (λ -max) around 665 nm

and row 3D had a λ -max around 610 nm, which is shifted towards shorter wavelengths compared to the other species. *G. smithii* also have shifted sensitivities towards shorter wavelengths, with row 3P λ -max around 670 nm.

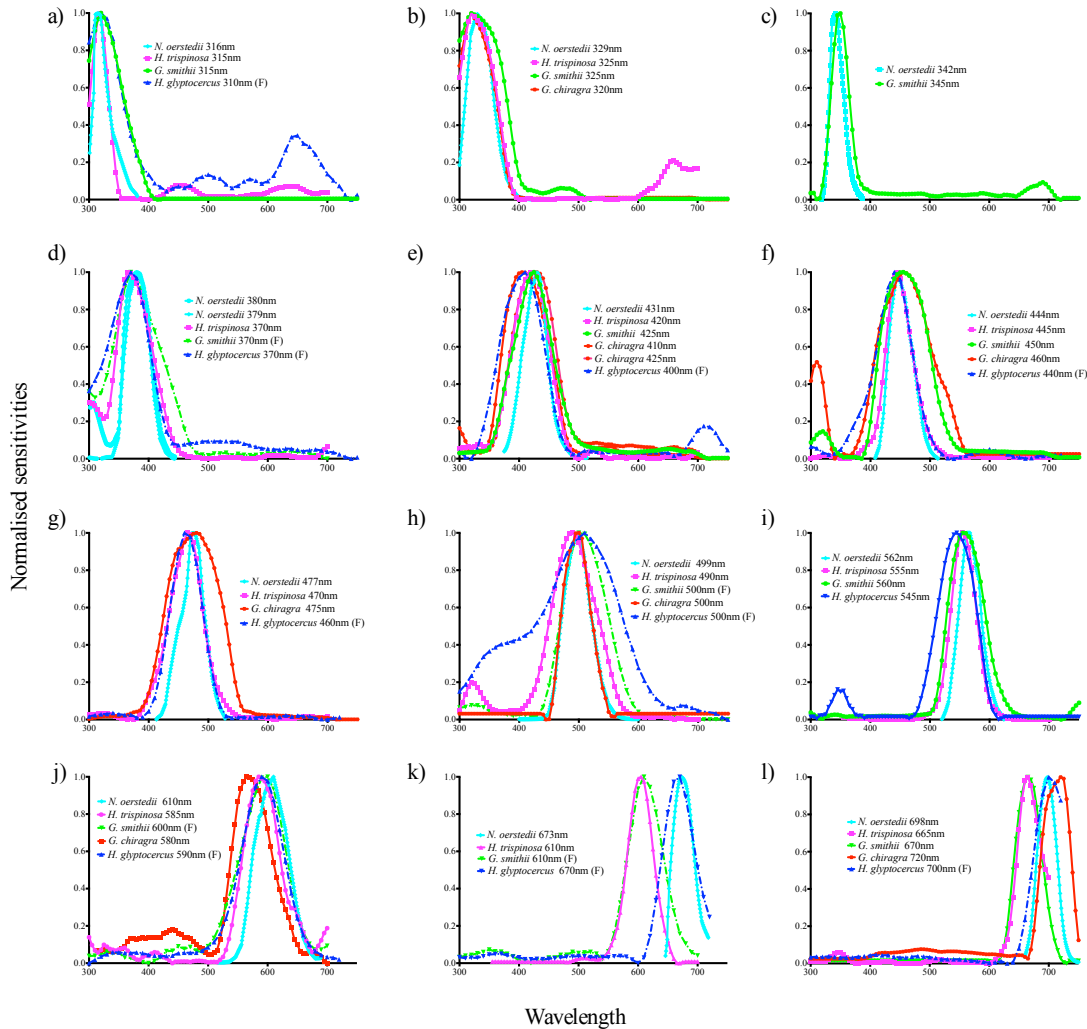


Figure 2.2. Comparison of sensitivities across each photoreceptor. a) to d) belongs to the UV sensitive R8 cells, e) Row 1 distal, f) Row 4 distal, g) Row 1 proximal, h) Row 4 proximal, i) Row 2 distal, j) Row 2 proximal, k) Row 3 distal, l) Row 3 proximal. Recordings performed with the Scan methods are shown in solid line while recordings performed with the Flash (F) method are shown in dash-dotted lines.

Several studies have been performed where it was shown that stomatopods are able to tune their colour vision according to habitat depth, (Chiao et al., 2000, Cronin and Caldwell, 2002, Cheroske and Cronin, 2005, Cheroske et al., 2006) (Fig. 2.5). *H. trispinosa* and *G. smithii* have been shown to shift their long wavelength sensitivities towards shorter wavelengths in Row 2 and 3 (Fig. 2.5 a, b) when inhabiting restricted light environments, while *N. oerstedii* did not display any spectral tuning (Fig. 2.5 c)(Cheroske et al., 2006). Comparing the results in this study to the calculated sensitivities from MSP data of deep and shallow tuned sensitivities, the long wavelength sensitivities of row 3D are more similar to the deep-water tuned than the shallow-water tuned sensitivities. On the other hand, the row 3P sensitivity of *N. oerstedii* is shifted slightly towards longer wavelengths when

compared to the computed sensitivities from MSP data (Cronin et al., 1994a, Marshall et al., 2007) (Fig. 2.5).

Table 2.1. Sensitivity maxima (λ) of photoreceptors for each species.

Sensitivities	<i>Neogonodactylus oerstedii</i>	<i>Haptosquilla trispinosa</i>	<i>Gonodactylus smithii</i>	<i>Gonodactylus chiragra</i>	<i>Haptosquilla glyptocercus</i>
R8	316	315	315	-	310 (F)
R8	329	325	325	320	-
R8	342	-	345	-	-
R8	379	370	370 (F)	-	370 (F)
R8	380	-	-	410	-
R1D	431	420	425	425	400(F)
R4D	444	445	450	460	440(F)
R1P	477	470	-	475	460 (F)
R4P	499	490	500 (F)	500	500(F)
R2D	562	555	560	-	545
R2P	610	585	600(F)	580	590(F)
R3D	673	610	610(F)	-	670 (F)
R3P	698	665	670	720	700 (F)

R1-4 indicates row number, distal (D) or proximal (P) position, retinula cell number 8 (R8), scan (S) or flash (F) method.

Table 2.2. Number of recorded cells and number of recordings per cell from each photoreceptor

<i>Neogonodactylus oerstedii</i>			<i>Haptosquilla trispinosa</i>			<i>Gonodactylus smithii</i>			<i>Gonodactylus chiragra</i>			<i>Haptosquilla glyptocercus</i>			
	#Cells	#Rec		#Cells	#Rec		#Cells	#Rec		#Cells	#Rec		#Cells	#Rec	
	S	F		S	F		S	F		S	F		S	F	
R8	3	3	3	1	4	-	4	14	-	-	-	-	2	-	2
R8	3	-	3	3	9	-	3	2	4	3	3	4	-	-	-
R8	3	3	3	-	-	-	3	4	1	-	-	-	-	-	-
R8	3	-	3	5	15	-	3	6	3	-	-	-	4	1	7
R8	3	3	-	-	-	-	-	-	-	3	8	-	-	-	-
R1D	3	2	3	6	20	-	8	17	4	3	5	3	2	1	1
R4D	3	3	1	7	21	-	17	37	9	3	7	-	4	2	6
R1P	3	3	-	4	12	-	-	-	-	2	4	3	5	-	9
R4P	1	-	3	5	16	-	1	1	1	1	2	1	2	-	5
R2D	3	3	3	5	18	-	5	24	2	-	-	-	2	3	3
R2P	1	-	3	2	6	-	2	2	1	2	7	2	3	6	7
R3D	3	3	3	2	6	-	1	2	-	-	-	-	5	4	9
R3P	1	-	3	5	21	-	5	12	2	1	2	1	1	-	3

Number of cells recorded from in total (#Cells), number of recordings in total (#Rec), scan method (S), flash method (F).

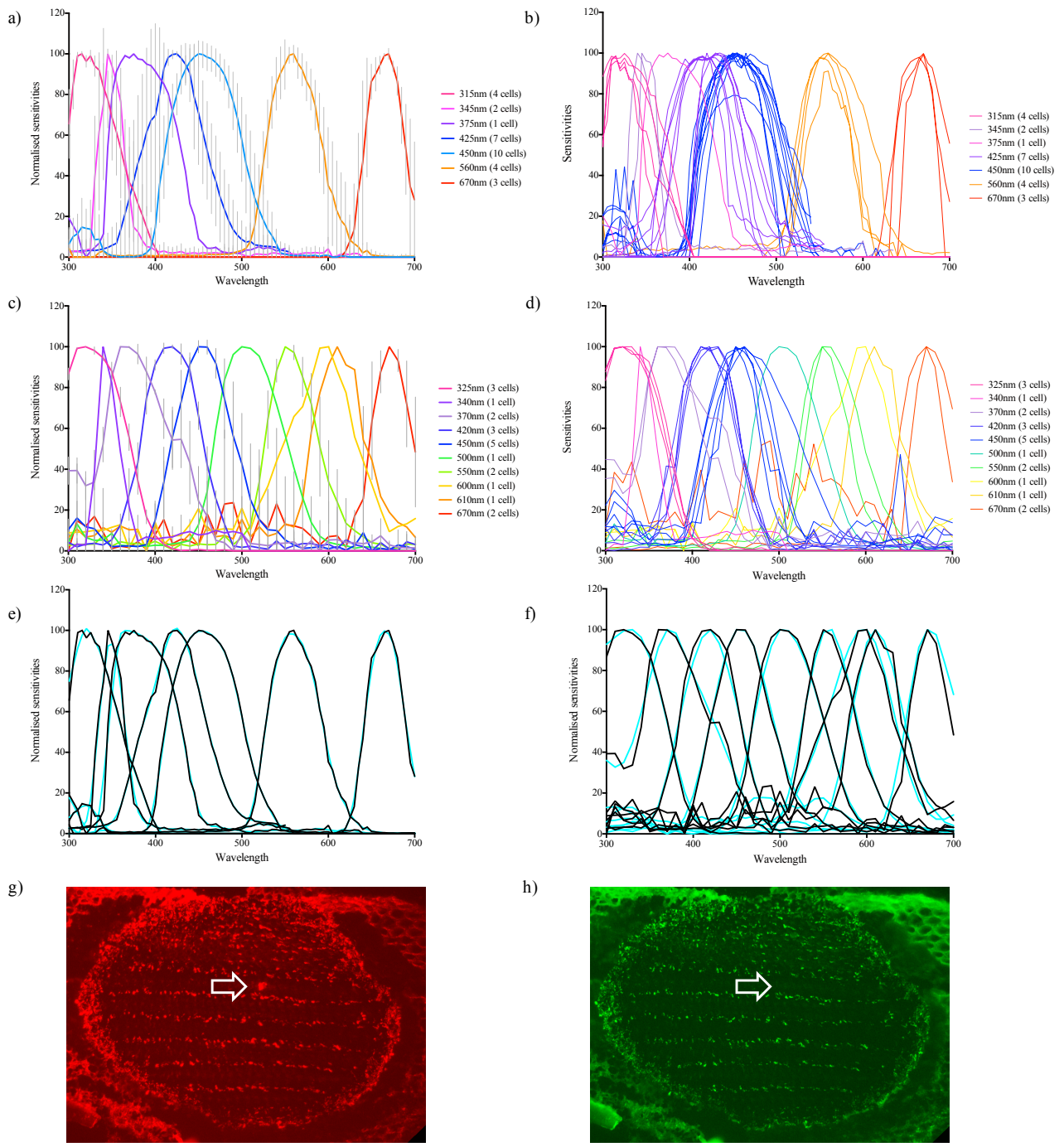


Figure 2.3. Spectral sensitivities of *G. smithii*. a) Scan recorded spectral sensitivities (mean \pm SD). b) Scan recorded sensitivities (raw recording traces). c) Flash recorded spectral sensitivities (mean \pm SD). d) Flash recorded sensitivities (raw recording traces). e) Scan recorded spectral sensitivities showing unsmoothed (black lines) and smoothed (turquoise lines) data. f) Flash recorded spectral sensitivities showing unsmoothed (black lines) and smoothed (turquoise lines) data. g) and h) showing injected photoreceptor in row 1D with the filled cell visible (arrow) in the red channel in g) while not in the green channel in h).

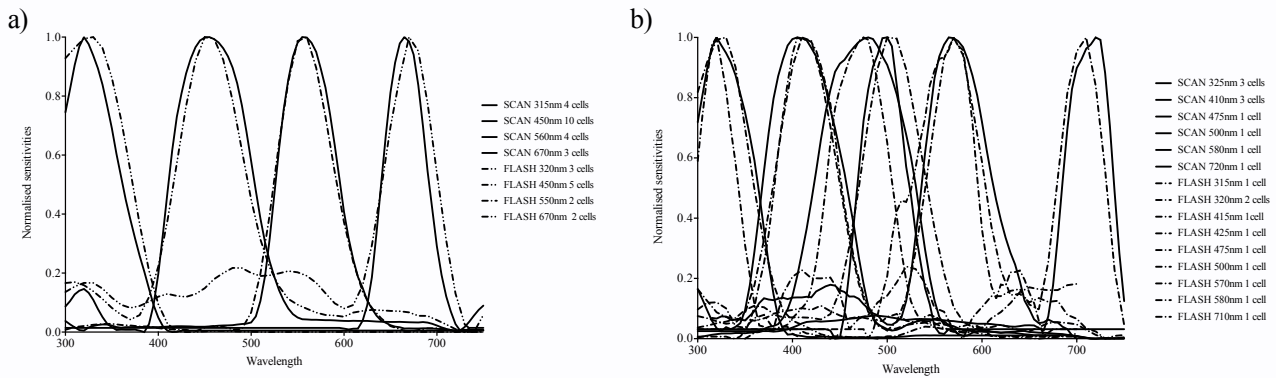


Figure 2.4. Examples of cells recorded using the scan and the flash method. Scan recordings are shown in solid lines while flash recordings are shown in dash-dot lines. a) *G. smithii*. b) *G. chiragra*.

Table 2.3. Species ecology and physiology. Overview of species, collections sites, depth range, the number of rhabdomal filters in row 1 to 4 and the habitat they occupy.

Species	Location	Depth	Rhabdomal filters	Ecology/habitat
<i>Neogonodactylus oerstedi</i>	Florida Keys	0-5m	4	Reef flats
<i>Haptosquilla trispinosa</i>	Lizard island	0-30m	4	In burrows in coral rubble
<i>Gonodactylus smithii</i>	Lizard island	0-20m	4	Reef flats
<i>Gonodactylus chiragra</i>	Lizard island	0-5m	4	Reef flats
<i>Haptosquilla glyptocercus</i>	Lizard island	0-10m	4	In burrows in coral rubble

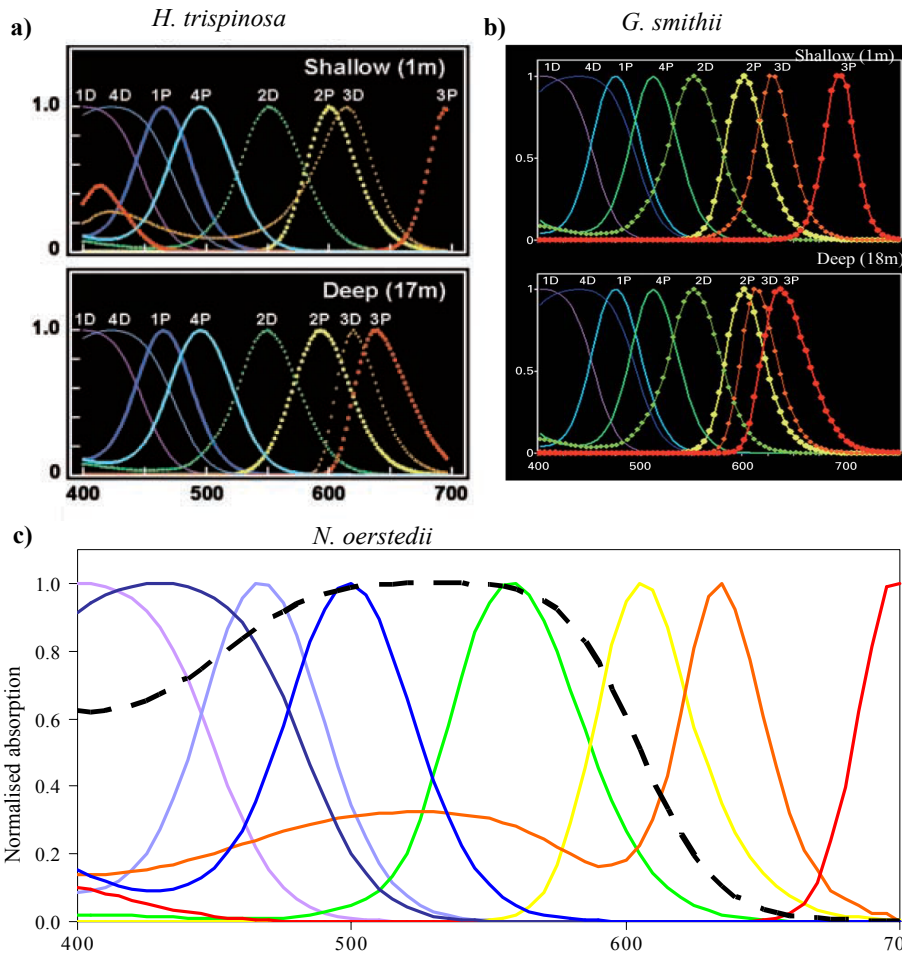


Figure 2.5. Computed spectral sensitivities: a) Sensitivities for *H. trispinosa* computed from MSP data for shallow and deep populations. From Cronin and Caldwell (2002). b) Sensitivities for *G. smithii* computed from MSP data for shallow and deep populations. From Chiao et al. (2000) and Cheroske and Cronin (2005). c) Computed sensitivities for *N. oerstedi* from MSP data. From: Cronin et al. (1994a) and Marshall et al. (2007)

2.4.2 Secondary peaks

In some recordings a smaller, secondary peak in the ultraviolet region appears (Fig. 2.6). So far these peaks have mostly been observed in the shorter wavelength sensitivities between 370 nm to 550 nm. Similar peaks were observed in all the investigated species, although the λ -max of the original sensitivity varied. Kleinlogel and Marshall (2005) found that the UV-sensitive R8 axons demonstrated varying degrees of arborisations in the lamina with row 1-4 having extensive arborisation compared to the smooth axons of row 5 and 6 (Fig. 2.6b).

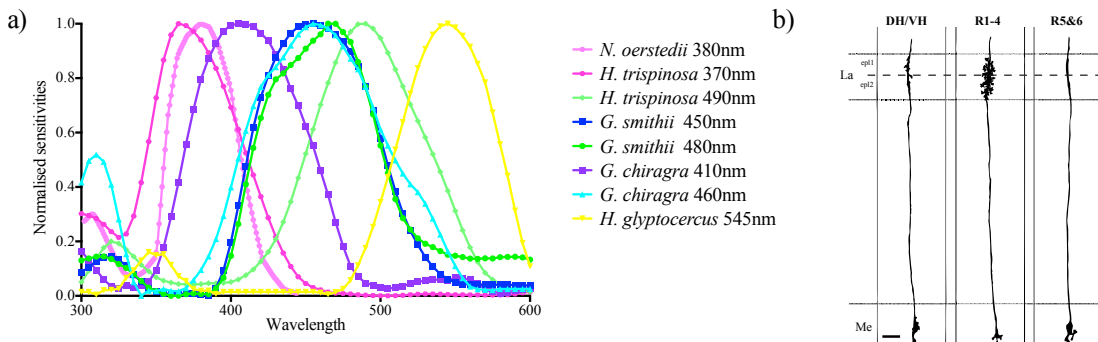


Figure 2.6. Secondary UV peaks. a) Showing the main spectral sensitivities of *N. oerstedii*, *H. trispinosa*, *G. smithii*, *G. chiragra* and *H. glyptocercus* with their smaller secondary peaks in the UV. The secondary maxima range between 305nm to 345nm. All measurements are carried out using the SCAN method. b) Illustration of the R8 axons from the dorsal/ventral hemisphere (DH/VH), Rows 1-4 and Rows 5 & 6 (Adapted from Kleinlogel and Marshall, 2005).

2.5 Discussion

2.5.1 Comparisons of spectral sensitivities

The results found in this study are in good agreement with microspectrophotometric recordings from other stomatopod species (Cronin and Marshall, 1989b, Cronin et al., 1993, Cronin et al., 1994a, Cronin et al., 1994c, Cronin et al., 1994e, Chiao et al., 2000, Marshall et al., 2007) (Fig. 2.3). Previous studies (Cronin et al., 2001, Cronin and Caldwell, 2002, Cronin et al., 2002) have shown that stomatopods are able to tune their spectral sensitivities according to their habitat. This tuning is performed using the intra-rhabdomal filters, where the optical density and spectral shape of the filter is adjusted according to the dominating light environment (Cronin and Caldwell, 2002). The visual pigments themselves do not appear to be tuneable (Cronin et al., 2002), and as it is only midband row 2 and 3 that contains filters, row 1 and 4 remain the same under different light conditions. Differences among the filters themselves are also evident, with those in row 2 using a different filter pigment in each major stomatopod lineage while row 3 filters use flexible interconversion and mixing of pigments, making these filters tuneable within an individual (Cheroske et al., 2006, Porter et al., 2010). As red light attenuates quicker than blue light with increasing depth this system is logical, as it enables the stomatopods to tune the maximum sensitivity of their colour vision system according to their environmental depth.

2.5.2 Tuning of sensitivities

Looking at the results from this study, the largest variability of λ -max is found in the sensitivities in row 2 and 3. The recordings from *H. trispinosa* and *G. smithii* indicate that the row 3 proximal photoreceptor sensitivities have shifted towards shorter wavelengths, though not as much as the calculated MSP sensitivities from 18m depth (Cronin and Caldwell, 2002, Cheroske and Cronin, 2005). The species included in this study were all collected in shallow water (0 - 5m) (2.3), but despite recording from the animals as quickly as possible after bringing them to the lab and keeping them in a light environment as close as possible to natural, some changes to their spectral sensitivities may have occurred. Both Cronin et al. (2001) and Cheroske et al. (2006) found that individuals of *H. trispinosa*, *Neogonodactylus wennerae* and *Neogonodactylus bredini* kept in restricted light environment (lacking wavelengths longer than 550 nm) for about 3 months changed their filters to resemble filters of deep-water living animals, indicating that their colour vision encompass a significant level of phenotypic plasticity. *G. smithii* have also been shown to be able to tune their colour vision (Cheroske and Cronin, 2005), as well as being able to change their body colouration according to depth. *N. oerstedii* on the other hand did not change its filters significantly, suggesting a more limited ecological variation in habitat depth. This is in agreement with our results, which showed no shifting towards shorter wavelengths in *N. oerstedii*. *H. trispinosa* and *G. smithii* are known to inhabit depths from 0 to ~30m, and hence may exhibit a larger amount of tuning ability in their colour vision, while *N. oerstedii* and *G. chiragra* only live in very shallow waters (0-5 m) and therefore have no need for this tuning ability. Kleinlogel and Marshall (2006) published the sensitivities of *G. chiragra* row 2 and row 5 and 6 as having very similar sensitivities around 565 nm. As the sensitivities of row 5 and 6 are normally found to be broadbanded this was quite surprising. We did not have any recording of sensitivities around 565 nm (the closest had a λ -max of 580 nm) so we cannot confirm this, but it may just be the case that we have not yet been able to record from these cells.

2.5.3 Secondary UV-peaks

In some recordings of sensitivities between 350-550 nm a secondary peak in the UV was observed. These results suggest that there could be communication between the UV sensitive R8 cells and the R1-7 cells in row 1-4. Morphological descriptions of the axons of the UV sensitive R8 cells (long visual fibres, lvfs) in Kleinlogel and Marshall (2005) (Fig. 2.4) give some support to this theory. While the axons of photoreceptor cells 1-7 (short visual fibres, svfs) terminate in the first optic neuropil (the lamina), the lvfs project through the lamina and terminate in the second optic neuropil (the medulla). Kleinlogel and Marshall found that the lvfs in row 1 to 4 have extensive arborisations in the lamina (in both lamina plexiform layers, epl₁ and epl₂), while in row 5 & 6 the lvfs are

smooth and with no arborisations. In the hemispherical parts the lvfs have some arborisations but not as much as in row 1-4. Kleinlogel et al. (2003) found that the lvfs in row 1-4 do form triad synapses with the terminals of the svfs and the monopolar cells, but were unable to determine the directionality in their ultrastructural observations (though the lvf were assumed to be presynaptic). No dye coupling was observed so it was assumed that there were no electrical contacts between the lvfs and the svfs or monopolar cells. Kleinlogel et al. (2003) also suggested that the screening pigments of the R8 cells in stomatopods (Cronin et al., 1994e), which are not found in other crustaceans, indicate that the R8s of row 1-4 are used as spectral receptors. All the species investigated exhibited secondary peaks in the UV, but there were differences regarding the type of cell from which they were obtained. The majority had sensitivities between 400-500 nm, indicating that they belonged to row 1 or 4 photoreceptors, but one recording had a λ -max at 545 nm suggesting that other rows also have some UV communication. Other reasons for this secondary UV-peak could be that there has been a cross-recording between the R8 cell and the R1-7 cells, or that the secondary peak is in fact a β -band of the original spectral sensitivity.

2.5.4 Conclusion

The work on identifying specific opsins contained within each midband row/photoreceptor type is still being carried out. However, we do know that stomatopod retinae contain an extreme diversity of opsin sequences. Porter et al. (2009) found for example that *G. smithii* and *N. oerstedii* possessed 10 and 15 unique opsin sequences respectively. Despite this diversity of opsins, the spectral sensitivities remain remarkably stable (at least within species of the same light environment), as shown both in MSP measurements and in this study. Proposed explanations (Schram et al., 2013) for this are; that either some of the transcripts are not translated/integrated in with a chromophore in the membrane; or that multiple spectrally indistinct opsins are expressed within single photoreceptors, possibly due to involvement in the cells polarization sensitivity (Roberts et al., 2011). It is interesting to note that, despite such variability in opsins and filters, there is still a strong trend towards maintaining similar spectral sensitivities between species. Recent studies (Thoen et al., 2014, Chapter 3) on the colour vision system of stomatopods have found that, despite the large number of photoreceptors, stomatopods have quite poor spectral discrimination. This has led to the hypothesis that the stomatopods may process colour differently to other animals, possibly using a system based on a "winner takes it all" principle coupled with interval decoding, as proposed in Zaidi et al. (2014, Chapter 5). Such a system would necessitate photoreceptor sensitivities that are evenly spread through the spectrum to enable sufficient sampling of the colours encountered in their environment. This is exactly what was found in all the shallow-water stomatopod species examined. The similarities and distribution of sensitivities across species would

then be determined by the type of colour vision they employ rather than the ecological constraints that they encounter and could be the explanation for the surplus of spectral sensitivities in stomatopods.

Chapter 3.

A different form of colour vision in Mantis shrimp

References and Notes

- K. Takahashi, K. Hayashi, T. Kinoshita, *Plant Physiol.* **159**, 632–641 (2012).
- T. Kinoshita, K. Shimazaki, *EMBO J.* **18**, 5548 (1999).
- G. Pearce, D. S. Moura, J. Stratmann, C. A. Ryan Jr., *Proc. Natl. Acad. Sci. U.S.A.* **98**, 12843–12847 (2001).
- M. Haruta, C. P. Constabel, *Plant Physiol.* **131**, 814–823 (2003).
- M. Haruta, G. Monshausen, S. Gilroy, M. R. Sussman, *Biochemistry* **47**, 6311–6321 (2008).
- J. L. Matos, C. S. Fiori, M. C. Silva-Filho, D. S. Moura, *FEBS Lett.* **582**, 3343–3347 (2008).
- J. Wu *et al.*, *Plant J.* **52**, 877–890 (2007).
- J. V. Olsen *et al.*, *Cell* **127**, 635–648 (2006).
- G. Pearce, Y. Yamaguchi, G. Munske, C. A. Ryan, *Peptides* **31**, 1973–1977 (2010).
- K. G. Kline-Jonakin, G. A. Barrett-Wilt, M. R. Sussman, *Curr. Opin. Plant Biol.* **14**, 507–511 (2011).
- J. J. Sanchez-Serrano, *Arabidopsis Protocols* (Springer, New York, 2013).
- P. J. Bertics *et al.*, *J. Biol. Chem.* **263**, 3610–3617 (1988).
- J.-M. Escobar-Restrepo *et al.*, *Science* **317**, 656–660 (2007).
- H. Lindner, L. M. Müller, A. Boisson-Dernier, U. Grossniklaus, *Curr. Opin. Plant Biol.* **15**, 659–669 (2012).
- K. Chae *et al.*, *Plant J.* **71**, 684–697 (2012).
- D. J. Cosgrove, Z. C. Li, *Plant Physiol.* **103**, 1321–1328 (1993).
- T. Nomura *et al.*, *J. Biol. Chem.* **280**, 17873–17879 (2005).
- J. Hu *et al.*, *Plant Cell* **20**, 320–336 (2008).
- D. Lee, D. H. Polisensky, J. Braam, *New Phytol.* **165**, 429–444 (2005).
- G. Felix, J. D. Duran, S. Volko, T. Boller, *Plant J.* **18**, 265–276 (1999).
- T. S. Nühse, A. R. Bottrell, A. M. E. Jones, S. C. Peck, *Plant J.* **51**, 931–940 (2007).
- E. L. Rudashevskaya, J. Ye, O. N. Jensen, A. T. Fuglsang, M. G. Palmgren, *J. Biol. Chem.* **287**, 4904–4913 (2012).
- M. Haruta *et al.*, *J. Biol. Chem.* **285**, 17918–17929 (2010).
- A. Goossens, N. de La Fuente, J. Forment, R. Serrano, F. Portillo, *Mol. Cell. Biol.* **20**, 7654–7661 (2000).
- G. Wu, E. P. Spalding, *Proc. Natl. Acad. Sci. U.S.A.* **104**, 18813–18818 (2007).

Acknowledgments: We thank H. Burch for technical assistance; M. Ivancic for advice on mass spectrometry data analyses; R. Wrobel, B. Fox (National Institute of General Medical Sciences Protein Structure Initiative, US4 GM074901), and S. Litscher for assistance with *E. coli* expression experiments; G. Barrett-Wilt for mass spectrometric

instrumentation; M. A. Beg, M. Hoffman, and O. Ginther for assistance with the iodination experiments; F. Li for advice on *Nicotiana* expression; S.-H. Su and the Plant Imaging Center for assistance with microscopy; and W. Aylward for advice on Etruscan mythology. Supported by NSF grant MCB-0929395 and U.S. Department of Energy Office of Basic Energy Sciences grant DEFG02-88ER13938 (M.R.S.), NSF grant DGE-1256259 (K.S.), and the National Human Genome Research Institute–University of Wisconsin Genomic Sciences Training Program (NIH grant 5T32HG002760, B.B.M.). Phosphoproteome data are deposited in PRIDE (Proteomics Identification Database) with accession numbers 31655 to 31656 and ProteomeXchange accession number PXD000515. Microarray data are deposited in ArrayExpress (E-MEXP-3994).

Supplementary Materials

www.science.org/content/343/6169/408/suppl/DC1
Materials and Methods
Figs. S1 to S14
Tables S1 and S2
References (26–44)

9 August 2013; accepted 17 December 2013
10.1126/science.1244454

A Different Form of Color Vision in Mantis Shrimp

Hanne H. Thoen,^{1*} Martin J. How,¹ Tsyr-Huei Chiou,² Justin Marshall¹

One of the most complex eyes in the animal kingdom can be found in species of stomatopod crustaceans (mantis shrimp), some of which have 12 different photoreceptor types, each sampling a narrow set of wavelengths ranging from deep ultraviolet to far red (300 to 720 nanometers) (1–3). Functionally, this chromatic complexity has presented a mystery (3–5). Why use 12 color channels when three or four are sufficient for fine color discrimination? Behavioral wavelength discrimination tests ($\Delta\lambda$ functions) in stomatopods revealed a surprisingly poor performance, ruling out color vision that makes use of the conventional color-opponent coding system (6–8). Instead, our experiments suggest that stomatopods use a previously unknown color vision system based on temporal signaling combined with scanning eye movements, enabling a type of color recognition rather than discrimination.

Stomatopods are benthic marine crustaceans that are generally found in tropical and temperate waters. Their compound eyes possess the largest number of photoreceptor types known in any animal [between 16 and 21 different receptors in some species (1, 3, 9)], allowing them to discriminate color (5) as well as both linear and circular polarized light (3, 10). Such retinal complexity is unrivaled in the animal kingdom, although papilionid butterflies may have up to eight spectral sensitivities (11). Theoretical approaches have predicted that between four and seven photoreceptor types are all that is needed to accurately encode the colors of the visible spectrum (12–14). The four-channel (tetrachromatic) solution that birds and reptiles use to sample a spectral range from 300 to 700 nm is optimally arranged to encode the known colors within this range. Where the spectrum examined loses the ultraviolet (UV) or red end, three photoreceptors

suffice, and trichromacy is the solution that many animals exhibit (12).

Our question was therefore, why do the stomatopods use 12 different photoreceptors to encode color? Before the experiments described here, Marshall *et al.* (5) demonstrated that stomatopods are capable of simple color discriminations based on color-card tests, similar to those devised by Carl von Frisch for bees and now used widely for

a number of animals (15). We hypothesized two alternative mechanisms for color information processing in stomatopods: (i) a multiple dichromatic color-opponent system (as described below), or (ii) the binning of colors into 12 separate channels, without any between-channel comparisons (4, 16).

Like butterflies, stomatopods have a variety of colorful body patterns, even using fluorescence to enhance color display (17). Furthermore, many of these species inhabit shallow coral reefs, one of the most colorful environments on Earth. The stomatopod's colors are thought to be involved in particularly complex communication systems, both between and within species (18), but little of this complexity requires a 12-dimensional color space to distinguish the colors available. Osorio *et al.* (19) speculated that stomatopods use their color sense to make reliable and quick judgements of color signals from conspecifics under changing light conditions, their steep-sided spectral sensitivities allowing particularly good color constancy. This would require comparison of the spectrally adjacent sharply tuned spectral sensitivities, and there is some anatomical evidence supporting this idea (6).

Stomatopod eyes are made up of a dorsal and ventral hemisphere, divided by a region of distinct

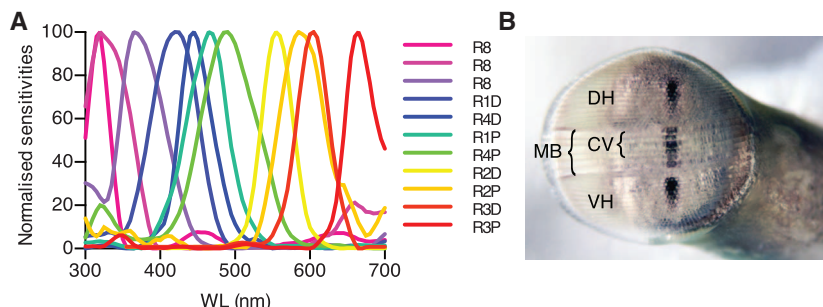


Fig. 1. (A) Spectral sensitivities of *H. trispinosa*. Spectral sensitivity curves obtained from intracellular electrophysiological recordings. The figure shows smoothed data (four neighbors on each side, second-order polynomial), normalized to 100% (see table S1). **(B)** Eye of *H. trispinosa*. Showing the dorsal hemisphere (DH) and ventral hemisphere (VH), divided by the midband (MB) containing the color receptors in the four top rows (CV).

¹Queensland Brain Institute, University of Queensland, Brisbane, Queensland 4072, Australia. ²Department of Life Sciences, National Cheng Kung University, Tainan City 70101, Taiwan, Republic of China.

*Corresponding author. E-mail: h.thoen@uq.edu.au

ommatidia (optical units) termed the midband (Fig. 1). Within two superfamilies of stomatopods (Gonodactyloidea and Lysiosquilloidea), this midband consists of six separate rows of ommatidia, each with different functionalities (2). Rows 1 to 4 are involved in color processing; rows 5 and 6 mediate the detection of circular or linear polarized light (3). A total of 12 cell types, each with different spectral sensitivities, are found within rows 1 to 4, with four UV-sensitive retinular cells located distally in the retina and by convention termed R8 cells (3). Beneath the R8 cells, the remaining seven retinular cells (R1 to R7) are further divided into two tiers (2). Comparison of the secondary R1 to R7 cell tiers would yield a set of highly tuned dichromatic mechanisms, sampling the 400- to 700-nm part of the spectrum in four bins as per hypothesis (i) above (3, 6, 19) (Fig. 1). Hypothesis (ii) would require a recognition of the pattern of excitation over the entire spectrum.

To distinguish between the two proposed hypotheses, we tested the ability of stomatopods to distinguish between different hues [spectral discrimination ($\Delta\lambda$) functions] using the Gonodactyloid stomatopod species *Haptosquilla trispinosa*. When two narrow-band spectral stimuli are presented simultaneously, they can only be discriminated when the difference between them is over a certain threshold, giving the minimum discriminable difference. Spectral discrimination curves obtained from other animals usually exhibit certain minima

in areas between the spectral sensitivity curves (20). Therefore, dichromats usually exhibit one such minimum, trichromats have two minima, tetrachromats have three, and so on. Our goal was therefore to test the color discrimination abilities of mantis shrimp by using a two-way choice test (Fig. 2 and fig. S1) in which the animal is trained to a specific wavelength by means of food rewards. The wavelength stimuli were presented to the animal with a pair of optical fibers, and a choice was recorded when the animal grabbed or tapped the end of the fiber. Test colors were presented together with the trained colors at varying wavelength intervals to determine at what point the animal could no longer discriminate between the two stimuli (i.e., when the success rate dropped to 50%).

Animals were trained successfully to 10 different color wavelengths: 400, 425, 450, 470, 500, 525, 570, 578, 628, and 650 nm. When the test wavelength was 50 to 100 nm from the trained wavelength, the success rates were between 70 and 80%, indicating that they discriminated well between the two stimuli. However, when the interval between the trained and test wavelengths was reduced to between 25 and 12 nm, the success rates dropped to around 50%, and it was clear that the stomatopods could no longer distinguish test from trained stimuli. An example of success rates is given in Fig. 2, and further results are shown in tables S2 and S3. The discrimination threshold was chosen to be at a 60% success rate, in accordance

with previous studies on animal discrimination thresholds (20). Using the interpolated points at 60%, we determined a relative spectral discrimination curve of $\Delta\lambda/\lambda$ (Fig. 3). The resulting values of $\Delta\lambda$ were all in the region between 12 and 25 nm, and the prominent dips, or minima, usually associated with the points between spectral sensitivity maxima in other studies were not clearly defined by spectral overlap regions (Fig. 3).

The potential spectral discrimination ability, based on previously known color vision systems, was also modeled to allow us to make predictions about the stomatopod color processing system. The

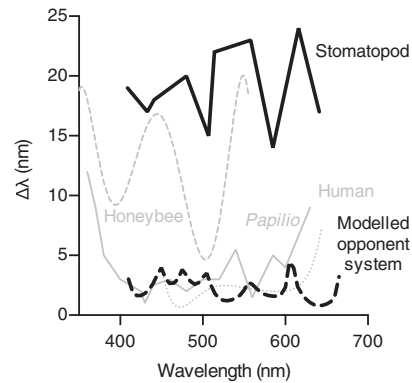


Fig. 3. Spectral discrimination curves ($\Delta\lambda/\lambda$). The spectral discrimination curve from behavioral testing of *H. trispinosa* is shown by a thick black line, and the modeled spectral discrimination curve is shown by a thick dashed line. [The figure is modified from Koshitaka *et al.* (20).]

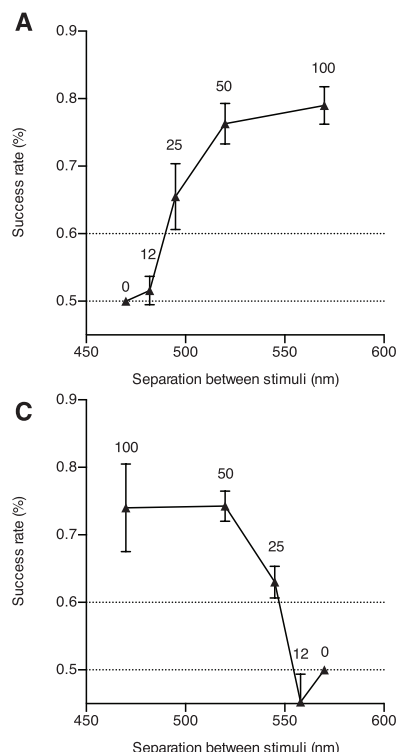


Fig. 2. Examples of correct choice data from a two-way choice test of *H. trispinosa*. Curves are plotted as mean \pm SEM. The horizontal dashed lines indicate the 50% (chance) and 60% (discrimination) criteria. (A) Choices of animals trained to 470 nm ($n = 7$) and tested toward longer wavelengths. (C) Choices of animals trained to 570 nm ($n = 4$) and tested toward shorter wavelengths. The number above each point indicates the tested wavelength interval. (B and D) Examples of animals making a choice.

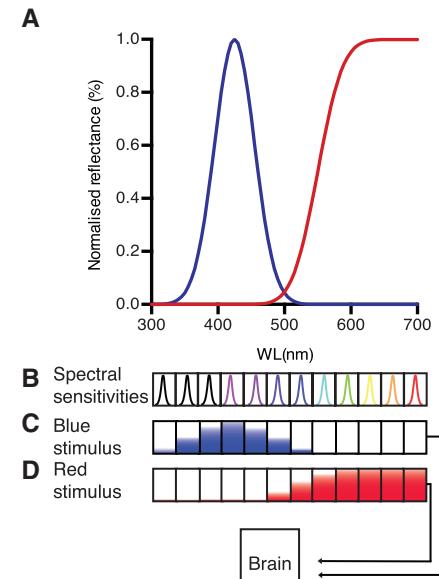


Fig. 4. Proposed processing mechanism. (A) Idealized spectral reflectance from stomatopod body parts. WL, wavelength. (B) Spectral sensitivities throughout the spectrum divided into separate bins. (C and D) Excitation patterns of each spectral sensitivity when looking at the blue (C) and red (D) reflectance spectra. (E) Brain receiving input from the spectral sensitivities.

sensitivities of the photoreceptors in *H. trispinosa* were measured using intracellular electrophysiology (9) (table S1). Eight sensitivity maxima were found in the visible part of the spectrum, and another three were found in the UV {the fourth UV cell often proving hard to locate and record from [(9), Fig. 1]}. We modeled the stomatopod spectral discrimination curve using the Vorobyev/Osorio noise-limited model (21) (which determines color thresholds using photoreceptor noise levels) for a serial dichromatic system with comparison between each adjacent spectral sensitivity [mechanism (i) above (note S1)]. This system predicts very fine discrimination between 1 to 5 nm throughout the spectrum, with few peaks of coarser discrimination as seen in other animals. Such fine spectral discrimination would be expected in a color vision system that made analog comparisons between adjacent spectral sensitivities. The behavioral results presented here (Fig. 2) suggest that such analog comparisons are not made. Instead, stomatopod color vision is remarkably coarse (Fig. 3).

The results from our experiments suggest that the stomatopods do not use a processing system of multiple dichromatic comparisons as previously hypothesized based on assumed neural connections (16). Instead, we provide evidence that scanning eye movements (22) may generate a temporal signal for each spectral sensitivity, enabling them to recognize colors instead of discriminating them. (Fig. 4) (3, 4). In such a system, the 12 sensitivities (including the UV, not analyzed here but with its multiple sensitivities a good fit to the system envisaged) would be converted into a temporal pattern when scanned across an object, which the animal could recognize as color. This system is comparable to the spectral linear analyzers (termed "push-broom" analyzers because of the arrangement of the sensors and the flight direction) used in remote sensing systems (23) and is a unique way for animals to encode color. Although this system does not have the ability to discriminate between closely positioned wavelengths (and results in spectral "discrimination" defined by the distances between sensitivity peaks, seen when comparing Fig. 1 and 3), it would enable the stomatopod to make quick and reliable determinations of color, without the processing delay required for a multidimensional color space. Without the comparison of spectral channels, color constancy would not function in the way we currently understand it in other animals. Instead, identification of a color pattern by the mid-band and luminance by the hemispheres might function as a "panchromatic" method to discount illuminance (23). The eye is optically skewed so that both midband and hemispheres examine the same areas in space, which lends support to this idea (3). However, the details of the neural processing from the receptors remain unknown.

Stomatopods live a rapid-fire lifestyle of combat and territoriality, so possessing a simple, temporally efficient color recognition ability may be critical for survival (24, 25). As with many invertebrate information-encoding solutions, the actual processing of the problem is dealt with at

the periphery, in this case by an array of detectors seen in animals and unconsciously duplicated by remote-sensing engineers. What remains for us to discover is the nature of the information and its importance in the biological decisions these engaging crustaceans make.

References and Notes

- N. J. Marshall, *Nature* **333**, 557–560 (1988).
- T. Cronin, N. J. Marshall, *J. Comp. Physiol. A Neuroethol. Sens. Neural Behav. Physiol.* **166**, 261 (1989).
- J. Marshall, T. W. Cronin, S. Kleinlogel, *Arthropod Struct. Dev.* **36**, 420–448 (2007).
- C. Neumeyer, in *Evolution of the Eye and Visual System*, J. R. Cronly-Dillon, Ed. (Macmillian, London, 1991), vol. 2, pp. 284–305.
- N. J. Marshall, J. P. Jones, T. W. Cronin, *J. Comp. Physiol. A Neuroethol. Sens. Neural Behav. Physiol.* **179**, 473 (1996).
- S. Kleinlogel, N. J. Marshall, J. M. Horwood, M. F. Land, *J. Comp. Neurol.* **467**, 326–342 (2003).
- K. R. Gegenfurtner, D. C. Kiper, *Annu. Rev. Neurosci.* **26**, 181–206 (2003).
- J. Molton, C. Cavonius, in *Colour Vision Deficiencies VIII*, G. Verriest, Ed. (Springer, Netherlands, 1986), pp. 473–483.
- J. Marshall, J. Oberwinkler, *Nature* **401**, 873–874 (1999).
- T.-H. Chion *et al.*, *Curr. Biol.* **18**, 429–434 (2008).
- K. Arikawa, *J. Comp. Physiol. A Neuroethol. Sens. Neural Behav. Physiol.* **189**, 791–800 (2003).
- H. B. Barlow, *Vision Res.* **22**, 635–643 (1982).
- L. T. Maloney, *J. Opt. Soc. Am. A* **3**, 1673–1683 (1986).
- M. Vorobyev, in *Biophysics of Photoreception: Molecular and Phototransductive Events*, C. Tadei-Ferretti, Ed. (World Scientific, Singapore, 1997), pp. 263–272.
- A. Kelber, M. Vorobyev, D. Osorio, *Biol. Rev. Camb. Philos. Soc.* **78**, 81–118 (2003).

- N. J. Marshall, M. F. Land, C. A. King, T. W. Cronin, *Philos. Trans. R. Soc. London Ser. B* **334**, 57–84 (1991).
- C. H. Mazel, T. W. Cronin, R. L. Caldwell, N. J. Marshall, *Science* **303**, 51 (2004).
- E. Adams, R. Caldwell, *Anim. Behav.* **39**, 706–716 (1990).
- D. Osorio, N. J. Marshall, T. W. Cronin, *Vision Res.* **37**, 3299–3309 (1997).
- H. Koshitaka, M. Kinoshita, M. Vorobyev, K. Arikawa, *Proc. R. Soc. B Biol. Sci.* **275**, 947–954 (2008).
- M. Vorobyev, D. Osorio, *Proc. R. Soc. B Biol. Sci.* **265**, 351–358 (1998).
- M. F. Land, J. N. Marshall, D. Brownless, T. W. Cronin, *J. Comp. Physiol. A Neuroethol. Sens. Neural Behav. Physiol.* **167**, 155 (1990).
- H. D. Wolpert, *Opt. Photon.* **22**, 16–19 (2011).
- H. Dingle, R. L. Caldwell, *Behaviour* **33**, 115–136 (1969).
- R. L. Caldwell, H. Dingle, *Naturwissenschaften* **62**, 214–222 (1975).

Acknowledgments: This work was supported by grants from the Asian Office of Aerospace Research and Development, the Air Force Office of Scientific Research, the Australian Research Council, the Lizard Island Research Foundation, and a Doctoral Fellowship (2013) from the Lizard Island Research Station, a facility of the Australian Museum. We thank the reviewers for their great comments and W.-S. Chung, M. Bue, and R. Bedford for technical help. All data described in this manuscript are presented in either the main manuscript or the supplementary materials.

Supplementary Materials

www.sciencemag.org/content/343/6169/411/suppl/DC1
Materials and Methods
Figs. S1 and S2
Tables S1 to S3
References (26–29)

11 September 2013; accepted 19 November 2013
10.1126/science.1245824

Risky Ripples Allow Bats and Frogs to Eavesdrop on a Multisensory Sexual Display

W. Halfwerk,^{1, 2*} P.L. Jones,^{1, 3} R. C. Taylor,⁴ M. J. Ryan,^{1, 3} R. A. Page¹

Animal displays are often perceived by intended and unintended receivers in more than one sensory system. In addition, cues that are an incidental consequence of signal production can also be perceived by different receivers, even when the receivers use different sensory systems to perceive them. Here we show that the vocal responses of male túngara frogs (*Physalaemus pustulosus*) increase twofold when call-induced water ripples are added to the acoustic component of a rival's call. Hunting bats (*Trachops cirrhosus*) can echolocate this signal by-product and prefer to attack model frogs when ripples are added to the acoustic component of the call. This study illustrates how the perception of a signal by-product by intended and unintended receivers through different sensory systems generates both costs and benefits for the signaller.

Elaborate courtship displays are favored by sexual selection but are often opposed by predation (1, 2). Animals can produce complex signals that are detected and processed through multiple sensory systems [commonly referred to as multimodal or multisensory signals (3, 4)]. Many communication systems once thought to operate primarily in a single sensory mode actually include secondary components that stimulate additional

senses (5–7). For instance, lip movements are necessary to produce human speech, but the associated visual cue of moving lips can also have a dramatic impact on speech perception (7). Such secondary signal components can be beneficial when they enhance the detection and perception of signals (3, 4). However, communication between the sender and intended receiver rarely occurs in private channels (8), and signalers are prone to costs imposed by eavesdroppers, such as predators and parasites who also attend to their displays (9–11).

Many male frogs possess conspicuous vocal sacs that evolved to recycle air during the production of their advertisement calls (6). The inflation and deflation of the vocal sac additionally act as

¹Smithsonian Tropical Research Institute, Apartado 0843-03092, Balboa, Ancón, Republic of Panama. ²Institute of Biology, Leiden University, 2300 RA Leiden, Netherlands. ³Department of Integrative Biology, University of Texas, Austin, TX 78712, USA. ⁴Department of Biology, Salisbury University, Salisbury, MD 21801, USA.

*Corresponding author. E-mail: w.halfwerk@biology.leidenuniv.nl

Chapter 4.

Using step-shaped vs. peak-shaped spectra in spectral discrimination testing

4 Chapter 4. Using step-shaped vs. peak shaped stimuli in spectral discrimination testing

Abstract

Investigations into how other animals see colour can give us a better understanding of the fundamental principles underlying colour vision. It is, however, hard to ask the animal exactly what it sees, requiring the use of behavioural experiments and electrophysiological recordings to disentangle which visual cues are being used for what purpose. Behavioural testing of colour vision ranges from the simple discrimination of coloured stimuli from shades of grey (von Frisch, 1914) to spectral threshold testing (Kelber et al., 2003). Threshold tests of spectral discrimination typically involve presenting peak-shaped stimuli to an animal, which are trained to perform a specific task in relation to the stimuli. Here we argue that using these peak-shaped stimuli is not biologically relevant, in particular in the long-wavelength part of the spectrum (i.e. yellow-red colours). Instead we investigate the possibility of using step-shaped spectra to test discrimination of stimuli that are closer in shape to many natural reflectance spectra. Modelling of the discrimination curve for peak-shaped and step-shaped spectra shows that a simple dichromatic system using an opponent processing system should be able to discriminate both types of stimuli equally well with only minor variations.

Stomatopods, which have one of the most complex colour vision systems in the world, have been shown to have relatively poor spectral discrimination compared to both theoretical modelling and other animals (Thoen et al., 2014). We tested whether using step-shaped stimuli would improve their spectral discrimination, but found that the results were very similar to ones obtained using peak-shaped stimuli. These results support the hypothesis that stomatopods use a different form of colour vision, and demonstrate the need to test step-shaped discriminatory behaviour on animals with more conventional colour vision, and such differences are modelled here.

4.1 Introduction

The natural world is filled with a multitude of colours, which we humans perceive without much consideration. Investigations into the colour vision abilities of other animals often reveal that the way we see the world does not necessarily match how other animals see it. Understanding how other animals perceive colour could give us vital clues into to the principles of colour decoding and processing. True colour vision requires the ability to detect changes in the spectral composition of light independently of its intensity. A basic requisite to having true colour vision is therefore to possess at least two photoreceptor types with different spectral sensitivities, and one type of opponent cell that can compare the signals from the two (Maxwell, 1860, Hering, 1878, Helmholtz,

1896). Only having one sensitivity would confound the input of wavelength and intensity, as the same sensitivity could be equally excited by a low-intensity wavelength near its peak sensitivity and a high intensity wavelength further away from this peak. This is termed the principle of univariance, and was first described by Naka and Rushton (1966a). There is a great range of what can be considered colour vision, from simple organisms that can detect and be guided towards favourable light environments, to higher levels of colour perception such as colour categorisation and distinguishing between hue and saturation (Kelber and Osorio, 2010). The latter are largely based on studies of human colour perception, and it is relatively unknown how other animals detect these types of colour phenomena.

4.1.1 Colour vision testing

To investigate if an animal has "true" colour vision, i.e. the ability to discriminate two stimuli based on wavelength regardless of illumination, it is necessary to study the animal's behavioural response to colour stimuli. The type of experiment used depends on the animal in question due to their varying cognitive abilities and natural behaviour, but usually it involves one of the following: *i*) Grey card tests in which colours are discriminated against different levels of grey, first introduced by Von Frisch (1914) to investigate colour vision in bees; *ii*) discrimination of relatively monochromatic stimuli that can be varied in intensity; and *iii*) discrimination of broadband stimuli, which can be adjusted so that one emits more photons across the spectrum than the other (Kelber et al., 2003). When true colour vision has been established using one of the methods described above, the next level of testing would usually involve examination of colour discrimination thresholds. In these tests the animal's ability to discriminate between two wavelengths across the spectrum is assessed, which provides the animal's spectral discrimination curve ($\Delta\lambda/\lambda$) (Kelber et al., 2003). Such experiments tend to be carried out using intervals of peak-shaped relatively monochromatic stimuli, in which the stimulus intensity is adjusted to remove achromatic signals. By narrowing the interval between the tested wavelengths, the point of no discrimination is determined. The resulting spectral discrimination curve can then be compared to visual models of spectral discrimination and inferences can be made regarding which spectral sensitivities are being used and how they are being compared. These types of threshold studies require precise stimulus spectra, and typically use narrowbanded, peak-shaped light for testing, either delivered through an interference filter or, more recently, with light emitting diodes (LEDs) (Fig. 4.1 a). On investigating natural reflectance spectra it becomes clear that these can take on a variety of forms, most of which are not narrowbanded (Marshall, 2000). While some have a peak shape (Fig. 4.1 a), they are usually broadband, with a full-width at half-maximum (FWHM) of 100–200 nm. Many natural spectra are, in fact, rather wide and have a step-shaped curve, especially

colours in the longer wavelength end of the spectrum (i.e. yellow and red colours) (Fig. 4.1 b). One can therefore question whether the use of narrowbanded peak-shaped stimuli in such experiments with FWHMs at 20 nm or less is biologically relevant, and if using a different type of stimuli would produce different spectral discrimination results.

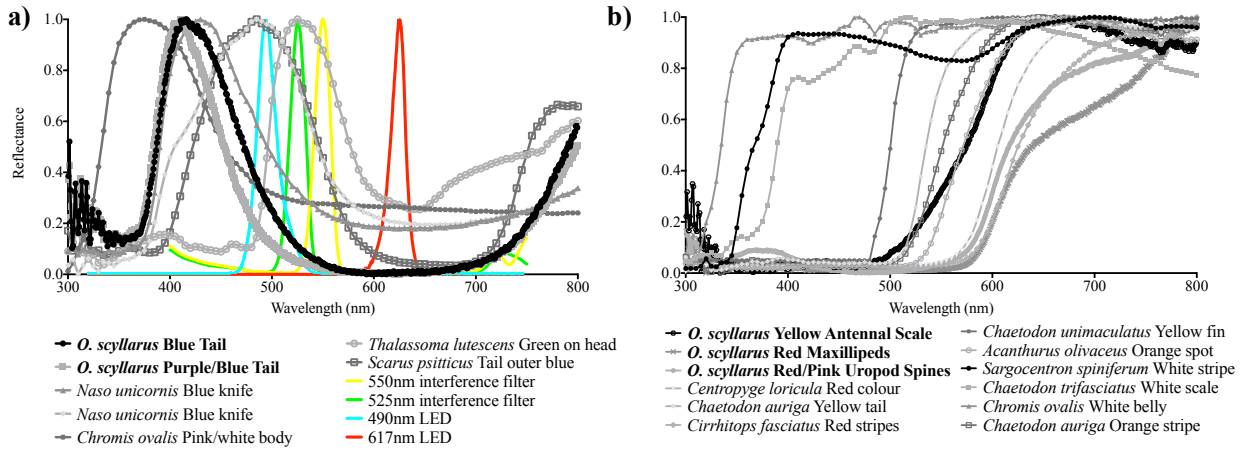


Figure 4.1. Examples of natural reflectance spectra on a coral reef and artificial spectra. Peak- (a) and step- (b) shaped natural spectra. Species in bold text are spectra from various body parts of the stomatopod species *Odontodactylus scyllarus*. The other spectra are from various body parts of fish found on the reef. The fish spectra are from Marshall (2000) while the *O. scyllarus* spectra are from Osorio et al. (1997) The coloured lines represent peak-shaped artificial spectra obtained using either LED's or interference filters.

4.1.2 Stomatopod colour vision

One animal that is well known for its colour vision is the stomatopod (commonly known as mantis shrimp) (See also Chapter 1 and 3). With 12 different types of spectral receptors (Marshall, 1988, Cronin and Marshall, 1989b, b, Marshall et al., 1991b, Cronin et al., 1994e, Marshall et al., 2007) stomatopods suggested the potential for a dodecachromatic colour space, although it was not clear how such a system would be processed on a neurological level. Marshall et al. (1996) carried out behavioural experiments using a variant of the grey-card experiments mentioned above, and showed that stomatopods indeed do have true colour vision. A recent study using behavioural experiments to test the spectral discrimination of stomatopods have come one step closer to understanding their colour vision system (Thoen et al. 2014, Chapter 3). This study revealed that the stomatopods have relatively poor spectral discrimination, perhaps unexpected due to the narrow and steep shapes of their spectral sensitivities, which by normal conventions (Vorobyev and Osorio, 1998) should impart very fine colour discrimination. Such poor discrimination suggests that stomatopods use a different form of colour vision, one that is not based on opponency between all receptors. While it is not known exactly how such a colour vision system would work, Zaidi et al. (2014, Chapter 5) proposed a possible solution that relies on a principle of interval decoding coupled with a winner-takes-all scheme. To further investigate how the stomatopod's colour vision works more behavioural, electrophysiological and neuroanatomical experiments are required.

The aim of this chapter was to test whether stimuli that are more biologically relevant, such as step-shaped spectra, could be used in behavioural experiments instead of, or together with narrowbanded peak-shaped stimuli. As stomatopods have been shown able to discriminate peak-shaped stimuli, but with poor ability compared to other animals, we wanted to determine whether using more natural spectra would increase, or in other ways change, their discrimination capabilities. We also wanted to explore the potential benefits and drawbacks of having steep and narrowbanded vs. broadband spectral sensitivities when it comes to detecting these two types of stimuli.

4.2 Materials and methods

4.2.1 Spectral measurements

The natural reflectance spectra of various fish body parts were obtained from Marshall (2000), while the reflectance spectra from the stomatopod *O. scyllarus* were obtained from Osorio et al. (1997). Spectral measurements of stimuli used in behavioural experiments were obtained using a USB 4000 spectrometer (Ocean Optics).

4.2.2 Modelling

To understand how step- and peak-shaped colours are discriminated in a hypothetical system, we created idealised curves as stimuli and spectral sensitivities to make the results as clear as possible. Two sets of spectral sensitivities with normal distribution curves were generated: 1) a dichromatic set of narrowbanded sensitivities (St. dev. 20 nm); and 2) a set of broadband sensitivities (St. dev. 50 nm) (Fig. 4.2 a and b). Spectral discrimination modelling (Vorobyev and Osorio, 1998, Kelber et al., 2003) typically finds the point of best discrimination to be at the midpoint between two sensitivities, we therefore chose to adjust the λ -max of the sensitivities so that they cross at the same point, enabling us to compare the discrimination abilities directly (Fig. 4.2 c). We then created idealised peak-shaped and step-shaped stimuli with a normal distribution and St. dev. of 5 nm (Fig. 4.2d and e). Both sensitivities and stimuli were normalised to a maximum of 1. Using the Vorobyev-Osorio receptor noise-limited colour model (Vorobyev and Osorio, 1998) and the idealised sensitivities and stimuli described above, we modelled the discrimination curve of a simplified dichromatic system coupled to an opponent processing system. This provides us with the ΔS^1 , which is an estimated perceptual distance between two stimuli. Using this distance and by setting a threshold distance for ΔS (in this case we set the distance to be 1), we can predict the $\Delta\lambda$ -function (Koshitaka et al., 2008, Thoen et al., 2014). The equations used were the same as the equations in Chapter 3 (equations 3.1 to 3.5, supplementary material). This modelling was performed in 5 nm incremental steps from 300 nm to 650 nm, thereby obtaining a full spectral

discrimination curve between the λ -max of each sensitivity. Information obtained "outside" of the λ -max of each sensitivity was disregarded.

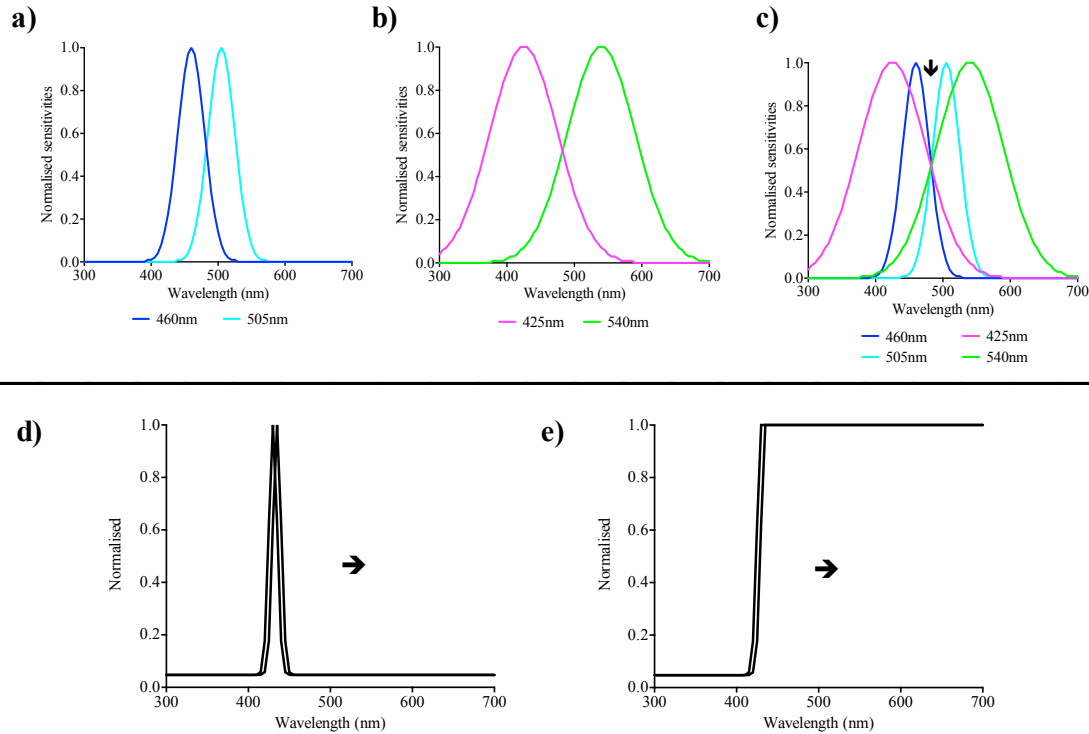


Figure 4.2. a) Idealised narrowbanded spectral sensitivities (St. Dev. 20nm). b) Idealised broadband spectral sensitivities (St. Dev. 50nm). c) The idealised spectral sensitivities in a) and b) shown in the same graph showing the sensitivities crossing at the same point (50%) (arrow). d) Examples of idealised narrowbanded peakshaped stimuli (St. Dev. 5nm) positioned 5nm apart. Arrow indicate further stimuli at longer wavelengths. e) Examples of idealised step shaped stimuli (St. Dev. 5nm) positioned 5nm apart. Arrow indicated further stimuli at longer wavelengths.

4.2.3 Behavioural experiments

A similar behavioural setup was used to that described in Chapter 3 (Thoen et al., 2014), and so will only been described briefly here; The stomatopod species used was *Haplosquilla trispinosa*, a small (2-4cm) animal whose natural behavior involves smashing or grabbing objects in front of the burrow. Animals were placed in small artificial burrows constructed from 25ml plastic screw-top vials covered with black electrical tape, and positioned into shallow individual aquaria filled with sand. Step-shaped stimuli were created using long-pass linear variable filters (Ocean optics FHS-LVF) and a halogen light source (Olympus, LG-PS2) (Fig. 4.3). Stimuli were presented to the animal using 1000 μ m optical fibres, with one trained cut-off wavelength and one test cut-off wavelength of varying intervals away from the trained wavelength (50 nm, 25 nm or 12 nm). For the 578 nm trained cut-off wavelength the intervals were shifted towards longer wavelengths (i.e. 578 nm vs. 628 nm, 578 nm vs. 603 nm etc.) while for the 628 nm-trained wavelength the intervals were towards shorter cut-off wavelengths. We defined the step-shaped stimuli to be at a specific wavelength, i.e. 578nm when the edge of the step aligned with the peak-shaped stimuli of this wavelength (Fig 4.3). Small pieces of prawn placed on the end of a feeding stick were used as food

rewards for correct choice. The stimuli were positioned close together and the animal chose between the stimuli by swimming out and grabbed/smashed the end of one or other of the optical fibres.

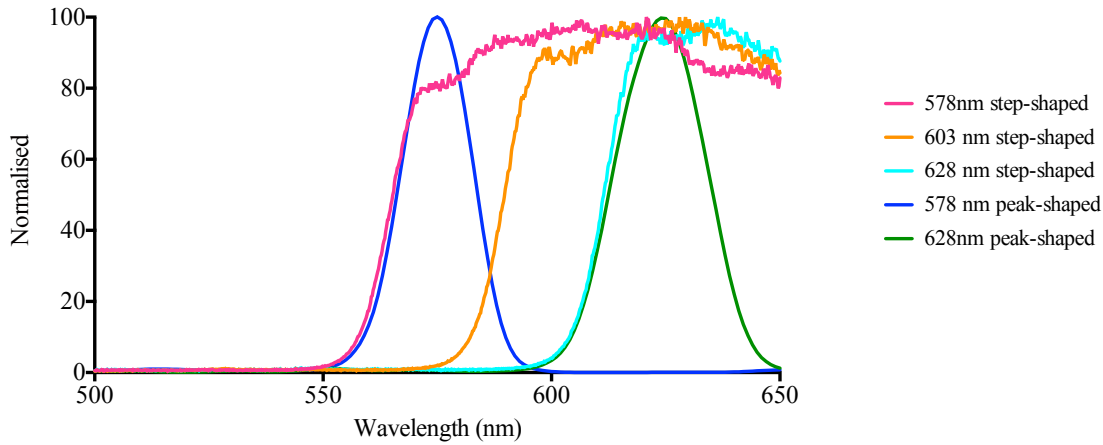


Figure 4.3. Examples peak-shaped and step-shaped stimuli used in this experiment. Step-shaped stimuli were defined to be at a certain wavelength when the edge of the step aligned with the edge of the peak-shaped stimuli.

4.3 Results

4.3.1 Spectral measurements

Reflectance spectra were obtained from various body parts of fish and stomatopods. Some body parts, such as the blue tail of *O. scyllarus* and green on the head of *Thalassoma lutescens* had peak-shaped spectra, as shown in Figure 4.1a. Other body parts, such as the uropods of *O. scyllarus* and the yellow tail of *Chaetodon auriga* had distinct step-shaped spectra (Fig. 4.1b) (Osorio et al., 1997, Marshall, 2000).

4.3.2 Modelling

For the comparison of the spectral discrimination of peak-shaped vs. step-shaped stimuli we found that the spectral discrimination curves were qualitatively similar (Fig. 4.4). This was true for both narrowbanded sensitivities (Fig. 4.4 a) and broadband sensitivities (Fig. 4.4 b). While the peak-shaped stimuli gave slightly (1-1.5 nm) better discrimination in the region between the two spectral sensitivities, step-shaped stimuli gave somewhat better discrimination in the shorter wavelength region. For the comparison between narrow and broadband sensitivities, we found that narrowbanded sensitivities gave better discrimination in the region between the two sensitivities than the broadband, while broadband sensitivities produced better discrimination over a broader range than the narrowbanded ones. This was true for both peak-shaped and step-shaped stimuli (Fig. 4.4 c and d).

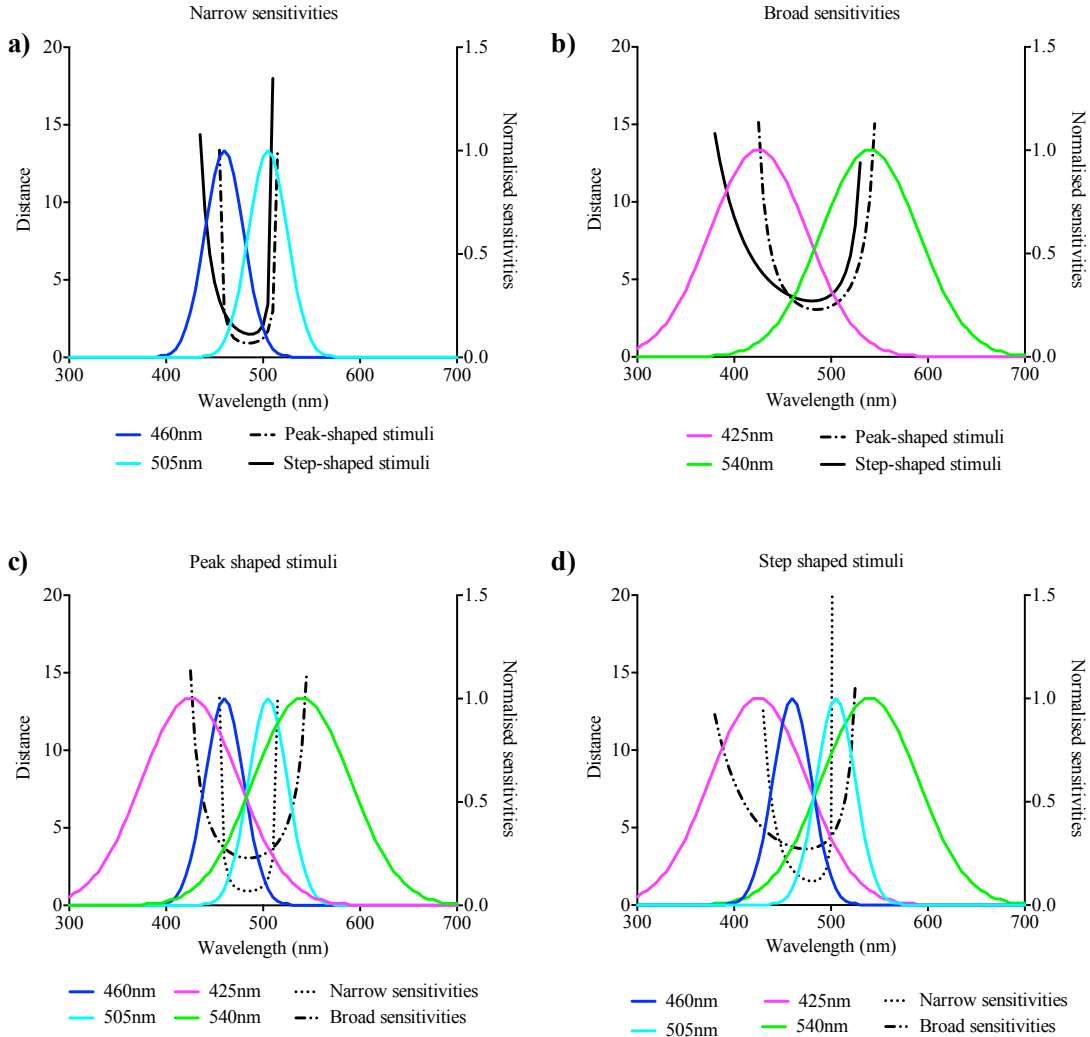


Figure 4.4. Peak-shaped vs. step-shaped stimuli with narrow or broad sensitivities. a) Modelled spectral discrimination of peak- and step-shaped stimuli seen by narrowbanded sensitivities. b) Modelled spectral discrimination of peak- and step-shaped stimuli seen by broadband sensitivities. c) Same results as in a) and b) but plotted to show the difference between narrow and broad sensitivities. This difference is shown for peak-shaped stimuli in c) and for step-shaped stimuli in d).

4.3.3 Behavioural experiments

Behavioural experiments carried out using training wavelengths of 578 nm and 628 nm showed that the stomatopods were able to discriminate stimuli that were 50 nm and 25 nm apart, but failed to discriminate stimuli close to 12 nm apart (Fig. 4.5). A generalized linear mixed model with Laplace approximation was used to test whether the success rates were significantly different from chance (0.5). For animals trained to 578 nm the results were as follows: 50 nm interval, N=9, n=209, p<0.001. 25 nm interval, N=9, n= 312, p<0.001. 12 nm interval: N=9, n=352, p=0.594. For animals trained to 628 nm: 50 nm interval, N=7, n=142, p<0.001. 25 nm interval, N=7, n= 254, p <0.01. 12 nm interval: N=7, n= 304, p= 0.422.

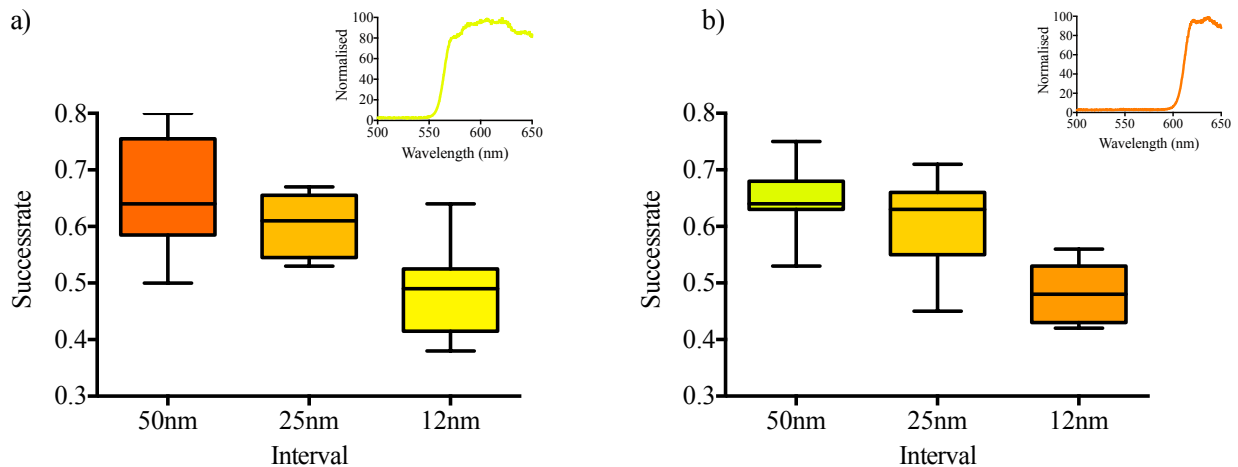


Figure 4.5: Discrimination testing of step-shaped stimuli. a) Animals trained to the cut-off wavelength of 578nm and tested against wavelengths 50nm, 25nm and 12nm away (against longer wavelengths) from trained wavelength. The spectral profile of the trained stimulus is inserted top right. b) Animals trained to a cut-off wavelength of 628nm and tested against wavelengths 50nm, 25nm and 12nm away (against shorter wavelengths) from trained wavelength. The spectral profile of the trained stimulus is inserted top right. Colours of boxes refer to the tested colour in the way they appear to the human eye.

4.4 Discussion

4.4.1 Modelling of step- vs. peak-shaped stimuli

The results from the modelling demonstrate that using step-shaped colour stimuli in behavioural experiments could produce similar discrimination curves to those obtained with peak-shaped stimuli, but with some deviations. The importance of these deviations would likely depend on biological significance of the specific colours for the animal. Step-shaped stimuli generate curves with slightly poorer discrimination in areas between sensitivities but with slightly better discrimination in shorter wavelength areas than peak-shaped stimuli. The increased discrimination in shorter wavelengths is likely due to using a long-pass filter in these experiments, using a short-pass filter would presumably produce inverted results with better discrimination in areas of longer wavelengths. Step-shaped stimuli could therefore be used as effectively as peak-shaped stimuli in spectral discrimination testing. It can also be argued that step-shaped stimuli are more biologically relevant than peak-shaped, in particular in the longer wavelength part of the spectrum, which could again influence an animal's discrimination abilities in this region (Menzel and Shmida, 1993, Chittka et al., 1994, Vorobyev, 1997).

4.4.2 Broad vs. narrowbanded sensitivities

Most animals have 2-4 broadband sensitivities (Menzel, 1979) and modelling has demonstrated that this number is fairly close to optimal for discriminating colours in the range between 400-700 nm, while still maintaining good spatial resolution (Barlow, 1982, Maloney, 1986). Increasing this with one or two sensitivities can spread the visible range into the ultraviolet (UV), but many more than this could potentially generate problems regarding the signal-to-noise ratio (Van Hateren,

1993, Osorio and Vorobyev, 2008) and would therefore not be beneficial for increasing discrimination. Here we showed that having narrow sensitivities theoretically increases wavelength discrimination in a small area between the λ -max of the sensitivities. This may be beneficial if there is an ecological importance for detecting small differences in reflectance at specific wavelengths, or if there is a lot of variation in the reflectance (Osorio and Vorobyev, 2005). The adaptive advantage conveyed by the stomatopod's multiple narrowbanded spectral sensitivities is therefore somewhat paradoxical. Osorio et al. (1997) suggested that the stomatopods sensitivities may be beneficial to improve colour constancy (i.e. the ability to keep the perceived colour relatively constant under varying illumination) in the underwater environment. Colour constancy (without von Kries transformation) is dependent on the ability to separate the spectra of the illuminant and the reflectance to be interpreted (Maloney, 1986, Osorio et al., 1997). The processing system proposed by Thoen et al. (2014, Chapter 3) and Zaidi et al. (2014, Chapter 5) would likely support such colour constancy, using the hemispheres as achromatic illuminant detectors, while the midband deals with the chromatic reflectance spectra. This information would then have to be combined at a later stage, and there are early indications that this may occur in the third optic neuropil, the lobula (see Chapter 6. 4).

4.4.3 *Stomatopod discrimination*

Stomatopods in this study were trained to discriminate between step-shaped stimuli in the long wavelength region (578 nm to 628 nm). We found that they were able to discriminate step-shaped stimuli that were positioned 50 nm and 25 nm away from the trained cut-off wavelength, but when the interval between test and trained wavelength was reduced to 12 nm they were no longer able to discriminate between the two stimuli. This is in accordance with previous experiments (Thoen et al., 2014, Chapter 3) where stomatopods were found to have surprisingly poor discrimination compared to other animals and modelled discrimination curves. As they demonstrate a similarly poor discrimination when presented with step-shaped stimuli, this study supports the idea that the stomatopod uses a different form of colour vision compared to other animals (Thoen et al., 2014, Chapter 3, Zaidi et al., 2014, Chapter 5). As the stomatopod colour vision appears to be so different to other animals, it would be of interest to use step-shaped stimuli to test discriminatory behaviour in animals with more conventional colour vision. These experiments could then be compared with discrimination curves previously obtained using peak-shaped stimuli.

Despite their poor discrimination ability, the stomatopods were still able to discriminate between two step-shaped stimuli, and further experiments in other parts of the spectrum could yield valuable results. Due to the restricted timeline of this thesis, further experiments were not conducted. It

would, however, be of interest to test the stomatopods spectral discrimination using step-shaped stimuli around 400 nm to 450 nm. For the human eye, long-pass step-shaped spectra in this region appear white, as all our photoreceptors have λ -max at longer wavelengths (Smith and Pokorny, 1972, Stockman et al., 1993), and are therefore all excited at the same time. We are therefore not able to easily discriminate stimuli of say 400 nm and 420 nm, as they would both appear or at least pale yellow/white. Stomatopods, with several narrow spectral sensitivities in the range between ~310 nm to 450 nm (see example in figure 1.1, chapter 1), should be able to discriminate these types of stimuli with equal ease as those at longer wavelengths. Experiments in this range would hopefully help to determine whether stomatopods use their whole range of narrowbanded spectral sensitivities to discriminate chromatic signals.

4.4.4 *Summary and conclusions*

Using step-shaped spectra in spectral discrimination experiments produces a similar theoretical spectral discrimination curve to one obtained with peak-shaped spectra, with only slightly poorer discrimination (1-1.5 nm). Stimuli that are more similar to natural spectra may provide different results than peak-shaped stimuli and should therefore be used to compliment peak-shaped stimuli when testing spectral discrimination. Stomatopods were able to discriminate step-shaped stimuli at a similar level to peak-shaped stimuli, but showed poor discrimination in both, likely due to their use of a different form of colour vision.

Chapter 5.

Evolution of neural computations: Mantis shrimp and human colour decoding

SHORT AND SWEET

Evolution of neural computations: Mantis shrimp and human color decoding

Qasim Zaidi

Graduate Center for Vision Research, State University of New York, New York; e-mail: gz@sunyopt.edu

Justin Marshall

Queensland Brain Institute, The University of Queensland, Brisbane, Queensland 4072, Australia; e-mail: h.thoen@uq.edu.au

Hanne Thoen

Queensland Brain Institute, The University of Queensland, Brisbane, Queensland 4072, Australia;
e-mail: justin_marshall@uq.edu.au

Bevil R. Conway

Neuroscience Program, Wellesley College, Wellesley, Massachusetts; e-mail: bconway@wellesley.edu

Received 25 April 2014, in revised form 14 August 2014; published 17 September 2014

Abstract. Mantis shrimp and primates both possess good color vision, but the neural implementation in the two species is very different, a reflection of the largely unrelated evolutionary lineages of these creatures. Mantis shrimp have scanning compound eyes with 12 classes of photoreceptors, and have evolved a system to decode color information at the front-end of the sensory stream. Primates have image-focusing eyes with three classes of cones, and decode color further along the visual-processing hierarchy. Despite these differences, we report a fascinating parallel between the computational strategies at the color-decoding stage in the brains of stomatopods and primates. Both species appear to use narrowly tuned cells that support interval decoding color identification.

Keywords: mantis shrimp, primate color vision, color decoding, tuning curves, winner-take-all, photoreceptors, IT cortex.

In the second half of the 19th century, James Clerk Maxwell showed that people make color matches by equating light absorbed in each of three photoreceptor classes. Maxwell's results supported the idea that color is represented in the human brain by a linear three-dimensional (3-D) space in which distinct points correspond to different colors, while each point (color) within this space corresponds to an almost infinite number of physically distinct lights (metamers). For example, the single-wavelength yellow of the rainbow is indistinguishable from an appropriate mixture of wavelengths that separately appear red and green—both stimuli cause the same relative activation of the three cone types. Maxwell's discovery pointed to the critical role that neural comparison of photoreceptor outputs plays in determining what colors we see.

When Cronin and Marshall (1989) reported that mantis shrimp, a predatory stomatopod crustacean, has 12 classes of narrowly tuned photoreceptors (Figure 1A), three in the ultra-violet range and nine covering the 400–700-nm spectrum, the scientific imagination ran wild: do they have a 12-dimensional (12-D) color space, so that they distinguish colors we confuse, and see colors we cannot even imagine? Such conjectures were restrained by the concern that their small brains could be overloaded by color computations in a 12-D space. Behavioral experiments by Thoen, How, Chiou, and Marshall (2014) have since shown that mantis shrimp are in fact poor at discriminating colors that humans see as distinct. The results suggested that the 12 classes of photoreceptors function independently, and their outputs are not compared by later neurons. So it has been concluded that mantis shrimp have a color system unlike humans, or possibly any other creature. The requirements of rapid hunting decisions and a small brain, could have led mantis shrimp to evolve 12 narrow-tuned color receptors at the front end of the visual system: presumably the photoreceptors feed a fast, hard-wired, interval-decoding computation, where perceived color corresponds to the peak sensitivity of the most responsive photoreceptor. Such hard-wiring is typical of many invertebrate sensory systems where behavioral tasks are “matched” to the environmental parameters that drive the task.

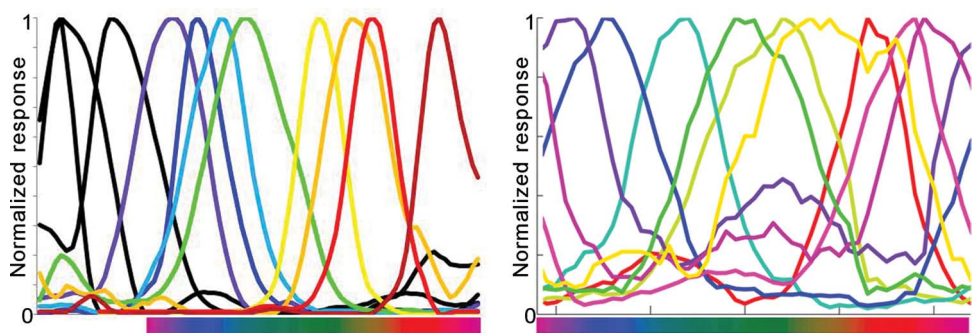


Figure 1. Color tuning of (A) mantis shrimp photoreceptors, and (B) of a few neurons in macaque inferior temporal cortex.

The eyes and photoreceptors of mantis shrimp and humans are clearly different, but are the neural strategies used to compute color that different? On the basis of physiological and anatomical research in macaque monkeys, a trichromat with color vision very similar to humans (Stoughton, Lafer-Sousa, Gagin, & Conway, 2012), we have reason to believe that the computations carried out by the color-vision systems in humans and mantis shrimp are more similar than they first appear. Although color in trichromatic primates is encoded using three (not 12) classes of broadly tuned photoreceptors, primates have much larger brains than shrimp: neural circuits compare cone responses within the retina (Sun, Smithson, Zaidi, & Lee 2006), and the neural circuits responsible for color perception are linked across several different cortical regions (Conway, 2014). In inferior temporal cortex (IT), several steps downstream of the cones, the cells are remarkably color specific (Komatsu, Ideura, Kaji, & Yamane, 1992), as shown for a sample of IT neurons in Figure 1B (Conway, Moeller, & Tsao, 2007). Some cells respond only to red, others to reddish blue, bluish red, violet, and so on. In their specificity, the color preferences of these cells are strikingly similar to the color specificity of the mantis shrimp photoreceptors, suggesting that the 400 million year old color processing system in stomatopods and the 40 million year old primate system could ultimately use a similar strategy at the decoding stage.

To test this idea, we used simulations to determine the extent to which primates could use narrowly tuned IT cells for an interval-color-decoding strategy similar to the one that is postulated to operate in the mantis shrimp. The strategy hypothesizes that the decoded color of a stimulus corresponds to the color preference of the IT neuron that produced the highest firing to the stimulus. In formal terms, this approach couples interval coding with a winner-take-all decision rule. For each of 279 posterior IT “glob” cells, based on responses to brief presentations of 45 colors measured with single-unit recording (Conway et al., 2007), we simulated a model cell with the same color-tuning. Firing rates for each stimulus color were generated by a Poisson distribution with mean and variance equal to the mean firing rate of the measured cell. So in every trial, the simulated response varied around the color-tuning by an amount chosen at random from the Poisson distribution. Each frame of the movie in Figure 2 (left—movie can be found at <http://i-perception.perceptionweb.com/journal/I/volume/5/article/i0662sas>) shows the simulated responses of the whole population to each color stimulus. The cells have been sorted along the x-axis according to their color preferences: cells tuned to red are on the left, followed rightwards by cells tuned to orange, yellow and so on around the color circle. The stimulus is depicted by the red symbol, and the decoded color is simply the color preference of the cell with the maximum firing rate. For the first trial, the cell with the maximum firing is tuned to the stimulus color, showing that the simple decoding strategy worked. As the simulated stimulus changes from 1 to 45, even with this meager number of cells and stimuli, the population supports fairly accurate interval decoding of color. Since each cortical neuron receives thousands of synapses, and color cells are organized into local columns of similarly color-tuned cells, it may be unrealistic to restrict the decision to a single neuron’s response. So we used the average of the responses of all cells with the same preferred color, and found that the decoding accuracy improved markedly (Figure 2—right). The success of interval decoding presents a physiologically realistic and computationally efficient alternative to color theories based on unique hues (De Valois & De Valois, 1993) that have no physiological support. Interval decoding is also compatible with the results of the only color micro-stimulation experiment done on humans (Murphy, Yoshor, & Beauchamp, 2008).

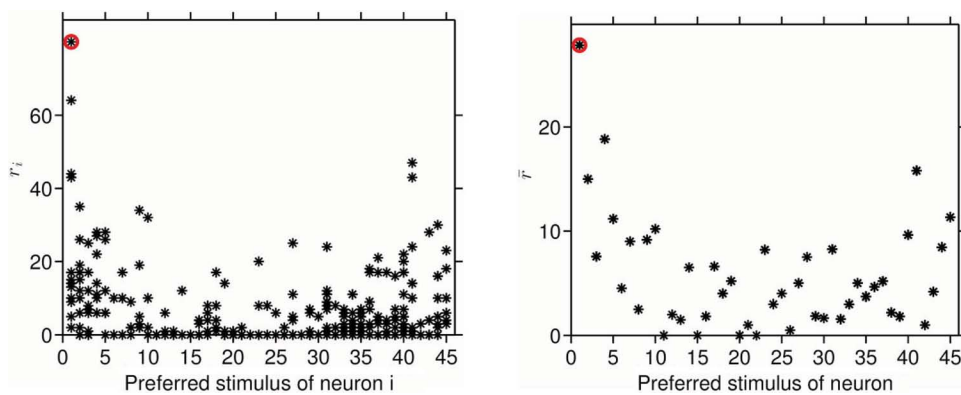


Figure 2. Stills of movies that can be found at <http://i-perception.perceptionweb.com/journal/I/volume/5/article/i0662sas>. (Left) In the movie each frame shows Poisson responses of 279 IT neurons (black stars) elicited by a stimulus color (red circle) on one trial, plotted versus the mode of the tuning curve of each cell. The stimulus color progresses on each frame representing an independent trial. At the end of the 45-color cycle, blue circles plot the decoded color (the preferred color of the cell that fired maximally on that trial) against the stimulus color. The simulations are repeated five times to demonstrate the variability in probabilistic decoding. (Right) In the movie the black stars now give the average response of all the cells preferentially tuned to the color on the x-axis. The decoding is considerably more accurate.

It is intriguing to consider whether winner-take-all with IT cells represents a hard-wired approximation of optimal Bayesian decoding of the population of responses. If the neurons in the population have independent variability, then the population response probability will be the product of the Poisson probability of all the neurons. Applying Bayes' rule to get the probability of decoding a stimulus color given a pattern of population responses, leads to an expression for decoding that contains a term that represents multiplication of tuning curves raised by the number of spikes, and is the only term that depends on the pattern of responses on a trial. A cell that only fires if it gets spikes from two cells within a short time interval, will only fire for stimuli for which the tuning curves of the earlier cells overlap, i.e. the output tuning curve will look like a multiplication of the input tuning curves. Similarly, a cell that only fires if it receives a defined number of input spikes in a short interval, will have a tuning curve that looks like the input tuning curve raised to the power of the number of spikes (Sanger, 1998). These operations will approximate the response-dependent term in Bayesian decoding, and performed on broadly tuned outputs from antecedent stages of processing will generate narrower tuning, consistent with empirical observations in IT. Interval decoding would therefore provide rapid color identification because no further computations would be required on the outputs of IT neurons. Since IT cortex has millions of color-tuned cells, they can sample the spectrum much more finely than the 12 mantis shrimp photoreceptors, so interval decoding could simultaneously provide much better color identification and discrimination compared to mantis shrimp, resolving the paradox that mantis shrimp have poorer color vision than humans despite having more photoreceptor classes.

In mantis shrimp, the cost of early functional specialization in the compound eye, and the subdivision of tasks to different eye areas (Cronin & Marshall, 1989), requires that the animal scan the scene to generate a representation of its visual world (Land, Marshall, Brownless, & Cronin, 1990). The primate eye is fundamentally different from the shrimp, like a digital camera it possesses a single focusing apparatus for a dense array of photoreceptors. Using just three classes of broadly tuned cone photoreceptors, the primate visual system is able to distinguish the spectra of natural lights and objects sufficiently (Barlow, 1982), while maintaining good spatial resolution, and providing the means to identify objects by their colors despite variations in ambient lights and surrounding scenes (Zaidi, 1998, 2001). More classes of photoreceptors would improve the sampling of natural spectra (Nascimento, Foster, & Amano, 2005), but would seriously compromise spatial resolution. Generating narrow color tuning in functionally specialized cortical regions affords rapid interval decoding without losing these features.

Despite tremendous differences in human versus mantis shrimp eye structure and brain circuitry, the striking similarity between the color sensitivities of primate IT neurons and stomatopod photoreceptors provides evidence of a common computational strategy across largely unrelated species. Interval decoding of color is an interesting example of independent evolutionary histories converging on

the same robust computational principle, and may thus be worth emulating by machine vision systems designed to function in the real world.

Acknowledgments. We would like to thank Daniel Osorio for discussions, Galina Gagin and Kaitlin Bohon for spike sorting, and Romain Bachy for movies. This work was supported by NIH grants EY007556 and EY013312 to QZ, EY023322 to BC, and grants from Asian Office of Aerospace Research and Development, Air Force Office of Scientific Research, and Australian Research Council to JN.

References

- Barlow, H. B. (1982). What causes trichromacy? A theoretical analysis using comb-filtered spectra. *Vision Research*, 22(6), 635–643. [doi:10.1016/0042-6989\(82\)90099-2](https://doi.org/10.1016/0042-6989(82)90099-2)
- Conway, B. R. (2014). Color signals through dorsal and ventral visual pathways. *Visual Neuroscience*, 31(2), 197–209. [doi:10.1017/S0952523813000382](https://doi.org/10.1017/S0952523813000382)
- Conway, B. R., Moeller, S., & Tsao, D. Y. (2007). Specialized color modules in macaque extrastriate cortex. *Neuron*, 56(3), 560–573. [doi:10.1016/j.neuron.2007.10.008](https://doi.org/10.1016/j.neuron.2007.10.008)
- Cronin, T. W., & Marshall, N. J. (1989). A retina with at least ten spectral types of photoreceptors in a mantis shrimp. *Nature*, 339(6220), 137–140. [doi:10.1038/339137a0](https://doi.org/10.1038/339137a0)
- De Valois, R. L., & De Valois, K. K. (1993). A multi-stage color model. *Vision Research*, 33(8), 1053–1065. [doi:10.1016/0042-6989\(93\)00163-8](https://doi.org/10.1016/0042-6989(93)00163-8)
- Komatsu, H., Ideura, Y., Kaji, S., & Yamane, S. (1992). Color selectivity of neurons in the inferior temporal cortex of the awake macaque monkey. *Journal of Neuroscience*, 12(2), 408–424.
- Land, M., Marshall, J., Brownless, D., & Cronin, T. (1990). The eye-movements of the mantis shrimp *Odontodactylus scyllarus* (Crustacea: Stomatopoda). *Journal of Comparative Physiology A*, 167, 155–166. [doi:10.1007/BF00188107](https://doi.org/10.1007/BF00188107)
- Murphrey, D. K., Yoshor, D., & Beauchamp, M. S. (2008). Perception matches selectivity in the human anterior color center. *Current Biology*, 18(3), 216–220. [doi:10.1016/j.cub.2008.01.013](https://doi.org/10.1016/j.cub.2008.01.013)
- Nascimento, S. M., Foster, D. H., & Amano, K. (2005). Psychophysical estimates of the number of spectral-reflectance basis functions needed to reproduce natural scenes. *Journal of the Optical Society of America*, A22(6), 1017–1022. [doi:10.1364/JOSAA.22.001017](https://doi.org/10.1364/JOSAA.22.001017)
- Sanger, T. D. (1998). Probability density methods for smooth function approximation and learning in populations of tuned spiking neurons. *Neural Computation*, 10(6), 1567–1586. [doi:10.1162/089976698300017313](https://doi.org/10.1162/089976698300017313)
- Stoughton, C. M., Lafer-Sousa, R., Gagin, G., & Conway, B. R. (2012). Psychophysical chromatic mechanisms in macaque monkey. *Journal of Neuroscience*, 32(43), 15216–15226. [doi:10.1523/JNEUROSCI.2048-12.2012](https://doi.org/10.1523/JNEUROSCI.2048-12.2012)
- Sun, H., Smithson, H. E., Zaidi, Q., & Lee, B. B. (2006). Specificity of cone inputs to macaque retinal ganglion cells. *Journal of Neurophysiology*, 95(2), 837. [doi:10.1152/jn.00714.2005](https://doi.org/10.1152/jn.00714.2005)
- Thoen, H. H., How, M. J., Chiou, T. H., & Marshall, J. (2014). A different form of color vision in mantis shrimp. *Science*, 343(6169), 411–413. [doi:10.1126/science.1245824](https://doi.org/10.1126/science.1245824)
- Zaidi, Q. (1998). Identification of illuminant and object colors: heuristic-based algorithms. *Journal of the Optical Society of America*, A15, 1767–1776. [doi:10.1364/JOSAA.15.001767](https://doi.org/10.1364/JOSAA.15.001767)
- Zaidi, Q. (2001). Color constancy in a rough world. *Color Research and Application*, 26, S192–S200. [doi:10.1002/1520-6378](https://doi.org/10.1002/1520-6378)

Chapter 6.

Stomatopod visual neuroanatomy

6 Chapter 6. Stomatopod visual neuroanatomy

Abstract:

While the stomatopods complex retinal structures have been studied intensively in the last two decades, few studies have investigated the visual neural architecture that process the abundance of visual information obtained by the retina. Previously Schiff, Strausfeld and Nässel have described some of the general features of stomatopod optic neuropils and made some comparisons to other arthropods (Strausfeld and Nässel, 1981, Schiff et al., 1986, 1987). A few studies have described properties of the photoreceptor projections to the first optic neuropil, the lamina (Kleinlogel et al., 2003, 2005), but detailed investigations of the other optic lobes (the medulla and lobula) have not been carried out. This study examines the general morphology of the optic lobes, the optic pathways from the midband and the hemispheres through the optic lobes and detailed structures of single neuronal types within these lobes. The lamina appears similar in organisation to other crustaceans investigated, and no particular specializations have been found in the cells of the lamina midband region. The stomatopod medulla on the other hand is highly stratified compared to other crustaceans, divided into a total of 12 main layers, while the midband projections are visible as a distinct swelling on the distal side of the medulla. Neurons in this medulla midband lobe appear to stay segregated from the hemispherical parts of the medulla, and contain distinct Y-shaped neurons. Midband projections are still visible in the lobula, where they appear to form lateral collaterals that project into the hemispherical parts of the lobula, possibly establishing a form of chromatic and achromatic channel mixing? Optic glomeruli of different sizes are found in the lateral protocerebrum, with a large number of these clustered in a distinct region termed the glomeruli complex, which receives projections from the lobula. The hemiellipsoid body is another neuropil in the lateral protocerebrum which is involved in processing olfactory input, but which possibly receive lobula projections as well. Finally, the stomatopod central complex appears elaborate with a prominent protocerebral bridge, a central body divided into two parts and two possible noduli, giving it a close resemblance to the insect central complex.

General introduction neuroanatomy:

The previous chapters have outlined the intricate retinal structures of the stomatopod eye, evaluated the stomatopods spectral discrimination and proposed hypotheses on how the stomatopod may process the array of visual information it receives. But as we know very little about the actual neural architecture underlying the complex stomatopod retina, it is difficult to make any exact predictions of how and where this processing would take place. Previous studies have determined that the optic lobes of the stomatopods follow the general crustacean outline of three main visual neuropils termed the lamina, medulla and lobula (Strausfeld and Nässel, 1981, Schiff et al., 1986, 1987,

Kleinlogel et al., 2003, Kleinlogel and Marshall, 2005). Kleinlogel et al. (2003) found that the division of the retina into a midband and two hemispheres is visible through the three first optic lobes, with the midband areas discernable as distinct equatorial swellings. Kleinlogel and Marshall (2005) established that the photoreceptor axons in stomatopods follow the same general retinotopic projection pattern as in other crustaceans with axons from the seven short visual fibres (svfs) formed by retinula cells 1-7 (R1-R7) terminating in two distinct strata in the lamina. This means that in the midband region axons from R1, R4 and R 5 (forming the distal photoreceptor) terminates in the distal lamina stratum (epl_1) while the proximal photoreceptor tier consisting of R2, R3, R6 and R7 terminate in the proximal lamina stratum (epl_2). Axons from retinula cell number 8, the R8 (termed the long visual fibres, lvfs) project through both lamina strata and terminate in the distal layers of the medulla. Schiff et al. (1986, 1987) together with Strausfeld and Nässel (Strausfeld and Nässel, 1981) carried out some investigations into visual neural architecture of the *Squilla mantis*, which have a reduced midband, but no further investigations have been performed on the visual neural architecture of stomatopods with a 6-row midband. In addition, a few studies have been carried out investigating the neuroanatomy of the olfactory pathways in stomatopods. Derby et al. (2003) described the peripheral and central antennular pathway in *Neogonodactylus oerstedii* and presented some general descriptions of the central brain of this species. Sullivan and Beltz (2004) investigated the hemiellipsoid bodies and olfactory pathways of *Gonodactylus bredini* using injections of fluorescent dyes into the olfactory lobes.

This study was carried out to increase our knowledge about the layout of the optic neuropils and the central brain of stomatopods, and also to investigate the various optic pathways through the neuropils. Furthermore we wanted to examine the neuronal types found in the different neuropils to investigate potential chromatic and polarization processing cells and any connections of these to the hemispherical neuropil regions.

The following chapter describes our findings of the stomatopod neuronal architecture from the first visual neuropil (the lamina) to the central brain. For simplification, the chapter has been divided into four subchapters (Chapters 6.2 to 6.4) based on each of the three first neuropils (the lamina, the medulla and lobula/ lateral protocerebrum) and the central brain (Chapter 6.5). As the techniques used to investigate these structures were similar, a separate materials and methods chapter (Chapter 6.1) was added to avoid repetition.

Subchapter 6.1.

Materials and methods - neuroanatomy

6.1 Materials and methods - neuroanatomy

For the following four sub-chapters on the neuroanatomy of the stomatopod visual systems a variety of methods were employed to visualise the numerous structures and neuronal types. As similar extensive procedures were used in the four neuroanatomy chapters, the materials and methods are presented here as a separate sub-chapter. Methods that were tested but which did not produce any useful results have also been included at the end of the chapter, with some comments on possible reasons why they were not successful.

Terminology:

Traditionally the first three optic lobes in decapod crustaceans have been called *lamina*, *medulla externa* and *medulla interna*. Here we use the terms *lamina*, *medulla* and *lobula* to conform with the homologues structures in insects (Strausfeld and Nässel, 1981, Harzsch, 2002, Sinakevitch et al., 2003). Another term we have adopted is the naming of the elevated equatorial region of the midband projections, which is evident in the lamina, medulla and lobula. Previously these structures have been termed *accessory lobes* (i.e. *lamina accessory lobe* etc.) but to avoid confusion with the unrelated structures lateral accessory lobes in the brain of insects (Strausfeld, 2009b) and the accessory medulla in the locust (El Jundi et al., 2009) we have chosen to call these distinct regions for midband lobes (i.e. *lamina midband lobe*, *medulla midband lobe* etc.).

Animals:

Stomatopods used in this study were collected either at Lizard Island research station, Australia (GBRMPA Permit no. G12/35005.1, Fisheries Act no. 140763) or in the Florida Keys, USA. Species used included: *Neogonodactylus oerstedii*, *Haptosquilla trispinosa*, *Haptosquilla glyptocerus*, *Gonodactylus smithii* and *Pseudosquilla ciliata*. Animals were either processed in the field or brought back to our aquarium at the University of Queensland where they were kept in artificial seawater (Aquasonic, Wauchope, Australia), in a 12h dark-light cycle using artificial lighting enhanced with UV to make it as close to natural as possible.

6.1.1 Immunohistochemistry

Labelling of synapsin, f-actin and cell nuclei

Three types of antibodies were used to visualise structures in the stomatopod brain and optical neuropils. A monoclonal antibody against synapsin I, a protein associated with synaptic vesicles in *Drosophila*, was used to label the visual neuropils. F-actin in dendritic spines and muscle tissue was visualised using fluorescently labelled phalloidin. Finally, cell nuclei were labelled using a blue-

fluorescent DNA stain (DAPI, Molecular Probes D1306). *Procedure:* Animals were killed by decapitation and small slits were cut along the cornea to allow fixative (4% paraformaldehyde in 0.1M PBS, pH 7.4) to penetrate. The eyes were left in fixative in 4°C for 2 hours before the eyestalk (containing the optical neuropils) and retina were dissected from the cuticle and left in fix overnight at 4°C. The eyes were then washed in 0.1M PBS for 3 x 10 min before they were embedded in 5% LMP agarose (LMP, A9414, Sigma Aldrich) and sectioned at 150 µm in 0.1M PBS using a Leica vibrating microtome. Sections were then washed in 0.1M PBS with 0.2% Triton X-100 for 2 x 10 min before they were pre - incubated in 0.1M PBS with 0.2% Triton X-100 and 2% Normal Goat Serum (NGS, Life-Technologies, 50-062Z) for one hour at room temperature. To label neuronal f-actin sections were incubated in 0.2 units of Alexa Fluor Phalloidin (Molecular probes, A12379), in 500µl 0.1M PBS with 0.2% Triton X-100 and 2% NGS together with SYNORF1, a monoclonal antibody against synapsin (1:100, kindly provided by E. Buchner, University of Wurzburg, Germany), for 3 days at 4°C. The sections were then rinsed 5x10min in 0.1M PBS before they were incubated in Alexa Fluor 647 goat anti-mouse (1-250, Molecular Probes, A21236) in 0.1M PBS with 1% NGS for 2 hours at room temperature. After another 2x10 min rinses with 0.1M PBS the sections were incubated in 300 µM DAPI (Molecular probes, D1306) in 500µl PBS for 5 minutes. The tissue was washed in 0.1M PBS for 10 min before being cleared in Scaleview clearing agent (Olympus, Scaleview A2 (Hama et al., 2011)) or in 80% glycerol overnight. Sections were then mounted on slides in either a fluorescent mounting medium (DAKO, S3023) or 80% glycerol.

Labelling of serotonin

To locate serotonin-like immunoreactive neurons in the stomatopods neuropil dissections, fixation and sectioning was carried out according to the same procedure as the synapsin/phalloidin/DAPI labelling. Sections were then treated with 0.2% Triton X-100 in 0.1M PBS for 2 x 10 min before being incubated with a primary antibody against serotonin (5-HT, Immunostar) in a 1:1000 dilution with 0.1M PBS, 0.2% Triton X-100 and 2% NGS. The sections were incubated for 2 days at 4°C before being rinsed with 0.2% Triton X-100 in 0.1M PBS (3x10min) and incubated in Alexa Fluor 568 anti-rabbit with 0.2% Triton X-100 and 2% NGS in 0.1M PBS overnight at 4°C. The sections were then rinsed in PBS (3x10min), before being counterstained with DAPI.

6.1.2 Silver stains

Bodian staining

Reduced silver staining were performed using Bodian's original method (Bodian, 1936). Briefly, brains and optic lobes were fixed in AAF fixative (80mL 96% ethanol, 5mL glacial acetic acid, 15mL 37% formaldehyde), dehydrated using an ascending ethanol series, cleared in terpineol and

embedded in Paraplast Plus (Sherwood Medical, St Louis, MO). Sections were cut at 12 µm using a rotary microtome and mounted on slides using albumin before being deparaffinised, rehydrated and incubated in Protargol (Roques, Paris, France) solution (2.5g Protargol in 250mL of double-distilled water with 5 g copper) overnight at 60°C. Sections were then briefly washed in distilled water and processed through 1% hydroquinone and 5% sodium sulphite solution for 5 minutes, 1 % gold chloride solution for 9 minutes, 2% oxalic acid for 5 minutes and sodium thiosulfate for 5 minutes, before being dehydrated and coverslipped using Entellan (Merck, Darmstadt, Germany).

Golgi impregnations

Golgi impregnations were carried out using a variation of the mixed Colonnier-rapid technique (Li and Strausfeld, 1997). Stomatopods were anaesthetised on ice and their raptorial appendages, antennas and antennal scales were removed. Slits were cut along the edge of the cornea, down the side of the eyestalk and along the scales covering the brain before the animal was decapitated and the head and eyes were placed in cold (4°C) chromation solution containing 2.5% potassium dichromate with 12% sucrose for 30 minutes. The retina, optic lobes and brain were then dissected out from the cornea, cuticle and muscle tissue and placed in fresh cold chromation solution containing 5 parts 2.5% potassium dichromate, 1 part 25% glutaraldehyde and 12% sucrose for 4 days. After this the tissue were swirled several times in fresh 2.5% potassium dichromate before being placed in a solution of 99 parts 2.5% potassium dichromate to 1 part 1% osmium tetroxide (in 4°C). After 3 days the tissue were rinsed briefly in distilled water and immersed in 0.75% silver nitrate for another 3 days. Double impregnations were performed by repeating the osmium and silver nitrate steps, but at only 24 hours for each step. After the final impregnation of silver, the tissue were dehydrated, embedded in Durcupan (Sigma 44610 Fluka) and sectioned at 40 µm using a sliding microtome.

Double staining of Golgi impregnated tissue using immunofluorescence

To better visualise where in the tissue the Golgi impregnated neurons were positioned, counterstaining with anti-synapsin and DAPI were attempted. Golgi impregnations were performed according to the method described above up until the dehydration steps. After the final silver impregnations, the tissue was rinsed briefly in distilled water before being embedded into 5% LMP agarose. Sections were made at 150 µm and rinsed in 0.1M PBS. They were then incubated with an antibody against synapsin (SYNORF1 1:100) in 500µl 0.1M PBS with 0.2% Triton X-100 and 2% NGS for 3 days at 4°C. After the incubation the sections were washed in 0.1M PBS for 2 x 10 min before being incubated with Alexa Fluor 647 goat anti-mouse in 0.1M PBS with 1% NGS for 2

hours in room temperature. Sections were then washed for 2 x 10 min with 0.1M PBS before being incubated in DAPI for 10 minutes, washed, and mounted on slides in 80% glycerol.

6.1.3 Fluorescent dye insertions

Mass fills using fluorescent dye-dextran conjugates

Anterograde tract tracing (Ehmer and Gronenberg, 2002) was used to investigate the optic pathway from the retina through the lamina, the medulla and the lobula. They were also used to visualise the connections between the lateral protocerebrum and the central brain. Due to the rapid solubility of the dextran conjugated crystals and the haemolymph leaking from the stomatopod tissue, it was necessary to use a method similar to the one described in Utting et al. (2000). Briefly, a small amount of crystals of dextran conjugated with Texas red (D-3328) or Fluorescein (D-3306 Molecular probes, Life Technologies) were placed on a glass slide. The glass slide was then placed on top of a cube of ice to allow for some condensation to build up on the slide and the dextran to dissolve giving it a paste-like consistency. Using the tip of glass microelectrode the dextran paste was twisted around until it made a small droplet on the tip of the electrode, which was then allowed to dry. Animals were anaesthetised on ice and a small piece of either the eyestalk or the cornea was removed. Glass electrodes with the droplet of dextran were then inserted into either the retina or the optic lobes and kept in place for about 30 seconds to allow it to slowly dissolve. The area was then covered using superglue and the animal was placed back in saltwater for 3-6 hours. After this the animal was anaesthetised on ice and decapitated, the eyes and brain were opened up and placed in cold fixative (4% paraformaldehyde) overnight. The next day the tissue was dissected out of the remaining cuticle, rinsed several times in 0.1M PBS and embedded in 5% agarose (LMP, A9414, Sigma Aldrich). Sections were cut at 100- 150 μm using a vibrating microtome, mounted and coverslipped using 80% glycerol.

6.1.4 Imaging and reconstructions

Imaging of silver stains:

The Bodian stained and Golgi impregnated tissue were imaged using an Axio Imager microscope (Zeiss), using a 10x (0.3) air objective, a 20x (0.8) air objective a 63x (1.4) oil immersion objective or a 100x (1.3) oil immersion objective. Image tiles were captured and stitched using the Zeiss blue software at 1388 x 1040 pixel resolution at 1 μm increments. Image stacks were then automatically reconstructed in the z-plane using Helicon Focus software (Helicon Soft, Kharkov, Ukraine). Finally, brightness and contrast of the images were adjusted using Adobe Photoshop CS3.

Laser scanning confocal microscopy:

Sections treated with antibodies against synapsin, f-actin, DAPI and serotonin were imaged using a LSM 510 Meta upright scanning laser confocal microscope (Leica, Leica Microsystems, Wetzlar, Germany) with a 10x (0.3) and a 20x (0.8) objective using a HeNe 633 nm laser to detect Alexa 647, an argon laser (488 nm) for the 488 phalloidin and a blue laser diode (405 nm) for detecting DAPI. Sections were scanned with 1024x1024 pixels per stack in x-y direction and in 2- μ m step size in z-direction. Image stacks of the visual neuropils were processed using the open source software Fiji(Schindelin et al., 2012), using the Stitching plugin to stich the tiles and the brightness tool to adjust the brightness and contrast. Maximum projection images were made using the z-project plugin.

Sections containing mass filled neurons were imaged using either the LSM 510 confocal microscope mentioned above or the LSM 710 inverted point-scanning laser confocal microscope (ARC LIEF grant no. LE130100078) with the 20x (0.8) air objective or 63x (1.4) oil immersion objective at 1024x1024 resolution and 0.5-1 μ m depth.

3D-reconstructions

Image stacks of the various brain structures were aligned and segmented using the TrakEM-2 plugin in Fiji (Schindelin et al., 2012). Each structure was manually traced and visualised using the 3D-viewer. These reconstructions were performed both on Bodian stained tissue (at 12um z-depth) and on synapsin stained tissue imaged with the confocal microscope (at 10um z-depth).

Camera Lucida

Camera Lucida-like drawings were made of the Golgi impregnated single neurons to visualise and categorise the different neuronal types. This was carried out in a few ways, either by using the curves tool in Adobe Photoshop CS3 to increase the contrast in the images that had previously been reconstructed in the Helicon software. The images were then opened in Adobe Illustrator CS3 and using the Live Trace tool a black and white drawing of the imaged neuron was obtained. If there were too many artefacts or confounding articles in the images the neurons were traced manually using the brush tool in Adobe Illustrator while also checking the image stack to confirm connections. Standard Camera Lucida drawings using a drawing tube and manually outlining the neurons were also used.

Confocal imaging of Golgi impregnated neurons

Confocal reconstructions of the Golgi impregnated neurons were made according to the method of Spiga et al (2011) using an upright Zeiss LSM 510 confocal microscope with a 20x (0.8) air or 63x (1.4) oil immersion objective. By replacing the dichroic filter with a 30/70-beam splitter and using the reflected light from the Argon 488 laser, confocal image stacks could be obtained. Z- stacks were made using images of 2048 x 2048 pixel resolution at 8-bit colour depth at 1- μm increments. For sections counterstained with anti-synapsin and DAPI the Golgi impregnated neurons were imaged as a separate channel. Maximum projection images and depth correlated colour images were made using respectively the z-project function and the temporal colour code function plugin in Fiji (Schindelin et al., 2012).

6.1.5 Methods that have been tested but still needs improvement

Photopermeabilisation and photodegeneration experiments

Attempts were made to employ the method of using photodynamic damage by extrinsic fluorescent dyes to trigger neuronal degeneration and cell permeabilisation, suggested by Picaud et al.(1988, 1990). This could then be used to induce uptake in only a few or specific types of photoreceptors. Experimental procedure: Stomatopods were anaesthetised on ice, decapitated and the eyes and eyestalks were cut off. The cuticle surrounding the optic nerve and the bottom part of the eye stalk was carefully dissected off and each eye was placed in a small droplet of 0.5% of the fluorescent dye Sulforhodamine 101 (SR101) (S-359 Molecular Probes, Life Technologies) in the bottom of a 0.5 ml Eppendorf tube so the optic nerve was exposed to the dye. Two different techniques were then used:

i) Using a halogen light source, and a 10- μm optic fibre, white light was positioned in front of the eye using a small amount of blue tack so that only a small part of the retina was illuminated. The illumination was continued for ~30 minutes before the eye was removed from the SR101, briefly washed in 0.1M PBS and placed in a solution of 1% Lucifer Yellow (L-453, Molecular Probes, Life Technologies) for 10 minutes. The eye was then briefly washed in 0.1M PBS before being fixed overnight in 4% paraformaldehyde. After fixation the eye was embedded in 5% agarose, sectioned at 150 μm and mounted on slides in 80% glycerol.

ii) Using a halogen light source and monochromatic filters, monochromatic light of 20 nm half width was produced. Due to the sharp spectral sensitivities in the stomatopod retina, a monochromatic light should allow uptake in only one or a few of the midband photoreceptors, while the other chromatic and achromatic photoreceptors should remain unpermeabilised. The eye with the eyestalk immersed in 0.5% SR101 was then illuminated with the monochromatic stimulus for ~

30 minutes before being washed in 0.1M PBS, placed in 1% solution of Lucifer Yellow and processed in the same way as described above.

Unfortunately neither of the two methods gave satisfactory results. In method *i*) there appeared to only be uptake of the SR101 in parts of the retina when inspecting the whole eye (Fig. 6.1.1) but there were no signs of uptake in the nervous tissue or the retina. The dye had penetrated into the extracellular space, as there were a lot of background staining and uptake in the haemolymph circulatory system, but there did not appear to be any penetration into specific photoreceptors or neurons. Modifications in illumination time and dye concentration were attempted but without any change in the final result. One reason the experiment did not work could be that in Picaud (1988, 1990) they inserted a very small amount (100nl) of SR101 into a slit in the retina, meaning that the dye was very close to the actual photoreceptors when they were illuminated. This was attempted, but the right tools were not available at the time to produce such a small amount, so we instead tried uptake through the stalk. Future attempts may include cutting off more of the stalk and/or injecting into the retina itself.

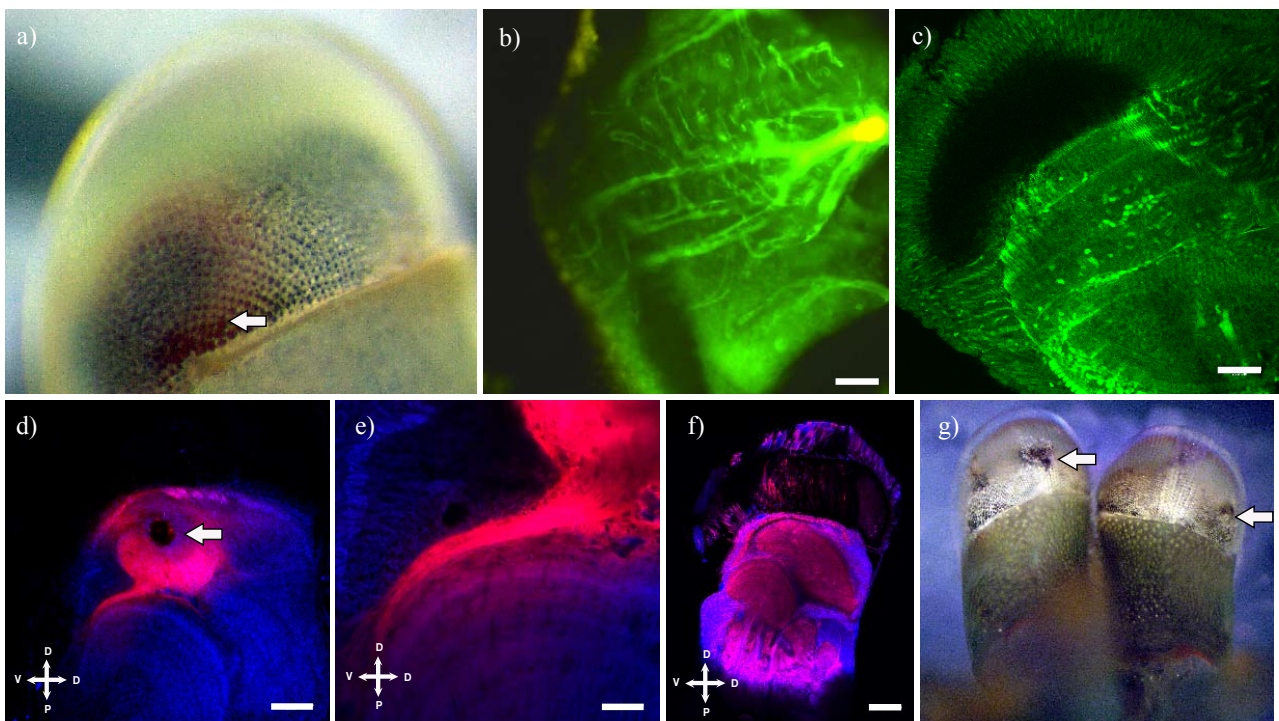


Figure 6.1.1 Methods that need improvement. a) Photodegeneration experiment: SR101 dye uptake in a small region of the eye (arrow). b) and c) examples of photodegeneration experiments where the Lucifer Yellow have filled the circulatory system and a few cell bodies, but no axonal fillings were observed. d) Insertion of a DIL crystal (arrow) into the medulla in a tissue section and spreading from the medulla into the lobula. e) Higher magnification view of the spreading from d) into the lobula. f) DIL crystal inserted into retina in a whole fixed eye which has spread through all the optic lobes. f) Examples of insertion sites into the midband and the hemisphere. Scale bars: e) 50 μ m, b) and c) 100 μ m, d) and f) 200 μ m

Activation of the mitochondrial dye DASPEI

Similar activity experiments to the ones described above were also attempted using DASPEI (2-(4-dimethylaminostyryl)-N-ethylpyridinium iodide (D-426 Molecular probes, Life Technologies), a

mitochondrial styryl dye that has been used as a selective vital marker of sensory terminals and cells in both vertebrates and invertebrates (Leise, 1996, Boudko et al., 1999, Grant et al., 2005). Using the same two setups as described above the dye was tested with varying concentrations and illumination periods. There appeared to be uptake in the nervous tissue and photoreceptors, but one issue was that this uptake appeared everywhere, not only in the areas which has been illuminated, or in the photoreceptors with the appropriate sensitivities to the monochromatic light stimulus. As discussed above, smaller amounts of dye and injection into the retina may alleviate some of these problems.

Iontophoresis of Lucifer yellow into nervous tissue

Another way of visualising single or a few neurons is to inject a fluorescent dye using a weak electric current in a process called iontophoresis. *Procedure:* Animals were anaesthetised on ice and decapitated, small slits were cut in the cornea and the eyes were placed in a light fix (2% paraformaldehyde) for 2-3 hours. Lucifer Yellow (CH) (Molecular probes, Life Technologies) dissolved in 2% lithium chloride were injected into a small opening in the retina or into the optic lobe using a hyperpolarising current (20nA) for 10 minutes to 60 minutes. The eye were then dissected out and fixed overnight in 4% paraformaldehyde at 4C. The eyes were then dehydrated and embedded in Spurr's resin before being sectioned at 40 µm and coverslipped. This technique has been used successfully in stomatopods earlier in combination with intracellular recordings (Kleinlogel and Marshall, 2006). Although it was not successful in these particular experiments, with Lucifer Yellow essentially spreading everywhere in the tissue and not into specific neurons, the likelihood for getting this procedure to work with a few modifications is high. New experiments are therefore planned.

Cobalt injections

Injection of cobalt chloride into nervous tissue is another procedure previously used in invertebrates to fill a few types or numbers of neurons (Strausfeld and Hausen, 1977, Davis, 1982). *Procedure:* Animals were anaesthetised on ice and decapitated. The optic nerve was dissected out and placed in distilled water for a few minutes before being placed in a drop of 200 mM cobalt chloride (232696 Sigma Aldrich) kept separated from the rest of the eye using a small ring of blue tack. The rest of the eye was immersed in artificial seawater and stored at 4°C overnight. The preparation was then washed for 10 minutes in changes of seawater to remove excess cobalt chloride before being fixed in acetic acid : ethanol (1:4) for 10 minutes. The optic lobes were then dissected out and precipitated with ammonium sulphide (3 drops in 20 ml of seawater) for 15 minutes before being washed several times in artificial seawater. Silver intensification were then carried out using the

method of Bacon and Altman (1977), the tissue was dehydrated through an ascending alcohol series and cleared in methyl salicylate. Another variation of this procedure was to inject the cobalt into the optic lobes through blunt microelectrodes, which was then allowed to diffuse for about 30 minutes before treating the tissue as described above. Some dark staining was observed in the technique involving immersion of the optic nerve, but the staining appeared diffuse and did not penetrate very far. Longer injection times with the blunt microelectrodes into specific areas of interest may improve the methodology.

Insertions of lipophilic dyes into nervous tissue

Crystals of the lipophilic dyes DIL and DIO (Molecular Probes, Life Technologies) were inserted into either whole eyes fixed in 4% or 2% paraformaldehyde, or into sections of fixed tissue (Mobbs et al., 2008). The tissue with the inserted crystals was returned to the fixative and placed in the dark at either 4°C, or 37°C for 1-2 weeks. The process of dye spreading was closely monitored using an Olympus SZX10 microscope with the appropriate fluorescent filter sets. Although both dyes spread through the nervous tissue, the spread was very diffuse and eventually covered the whole nervous tissue making it hard to make any predictions about specific nervous pathways. Smaller crystals, shorter incubation times and more specified areas (such as the hemiellipsoid body) might facilitate better results. Using iontophoresis (Sullivan and Beltz, 2001a) may also improve the specificity of the injection site and transport time of the dye.

Subchapter 6.2

The neural organisation of the stomatopod lamina

6.2 The neural organisation of the stomatopod lamina

6.2.1 Introduction

First optic neuropil

The lamina ganglionaris is the first optic neuropil in the visual processing system in arthropods and is also the best studied of the optic neuropils, especially in crustacea (Hamori and Horridge, 1966, Nässel, 1975, Nässel, 1977, Stowe et al., 1977, Strausfeld and Nässel, 1981, Sztarker et al., 2009) . The stomatopod neural architecture has been investigated in a few studies (Kleinlogel et al., 2003, Kleinlogel and Marshall, 2005), which mainly focused on the projection pattern from the photoreceptors to the lamina, and did not investigate the lamina connection patterns any further. A few studies have also focused on photoreceptor and projection patterns of the stomatopod species *Squilla mantis* (Schönenberger, 1977, Schiff et al., 1986), which has a reduced midband and does not possess the same diversity of receptors found in the superfamilies *Pseudosquilloidea*, *Hemisquilloidea*, *Gonodactyloidea*, *Lysiosquilloidea* (Marshall et al., 2007, Porter et al., 2010). The lamina cartridge is made up of the photoreceptor axons and terminals from the R1-8 cells of one ommatidium and other neuronal elements such as the monopolar cells (relay cells). The monopolar cells are usually divided into five different classes (monopolar cell 1-5), according to their morphology and synaptic connectivity (Strausfeld and Nässel, 1981). In addition there are a few other types of cells such as amacrine, tangential, centrifugal and t-cells that are involved in inhibitory feedback connections, lateral interactions and feedback loops from the medulla (Nässel, 1977, Wang-Bennett and Glantz, 1987, Glantz and Miller, 2002).

Although the projection patterns from the retina to the lamina in stomatopods were found to be retinotopic, Kleinlogel and Marshall (2005) did find differences in the shape and size of the lamina cartridges between the midband and hemispherical regions. The cartridges that receive projections from the hemispherical parts of the eye are smaller than the ones receiving projections from the midband region and the cartridges of midband row 5 and 6 are rounder and smaller compared to the rectangular and larger profile of midband row 1 to 4 cartridges. Some of these structural differences reflect the differences in shape of the overlying corneal facet lenses (Stavenga, 1979, Kleinlogel and Marshall, 2005). In the midband the facet lenses are rectangular in shape compared to the hexagonal pattern of the hemispheres, and this is reflected in the neural organisation of the lamina, where the hemispherical lamina cartridges have a more compact axonal packing compared to the midband axonal packing arrangement. The terminal endings of the short visual fibres (svfs) in the midband cartridges are also larger than the hemispherical ones, leading to bigger lamina cartridges. The differences between row 1-4 and row 5 & 6 are not, on the other hand, attributable to the facet shapes, and may be caused by variations in the position and morphology of the long visual fibre

(lvf) from the R8 cells. The LVFs of row 1-4 form many small branching processes which extend over a whole cartridge while lvfs of row 5 & 6 are spineless and smooth (Kleinlogel and Marshall, 2005). Such branching patterns have been found in other arthropods, e.g. in ants (Meyer, 1979), and dragonflies (Armett-Kibel et al., 1977) with chemical synapses identified in some species, although the branching does not necessarily mean that there are synapses present. It would be of great interest to know if these differences are also reflected in the morphology and/or size of the neurons that make up the lamina cartridges in each region, and if present, what these would tell us about the possible chromatic and polarization processing.

Our hypothesis was that there would be structural differences in the stomatopod lamina between the lamina cartridge cells in the midband row 1-4 region, the midband row 5 & 6 region and the hemispherical region that reflect the different processing requirements of chromatic, polarized and achromatic information. The first aim of this study was therefore to identify and describe the neuronal types found in the stomatopod lamina and relate these to neuronal types found in other crustaceans. The second objective was to investigate and compare the morphology of the monopolar cells within these regions when it comes to size, shape and arborisation patterns. We also wanted to know where and how other cell types such as tangential and amacrine neurons were located in the lamina and if these related to the structural layout of the different regions. What we found was that the different lamina regions, despite being larger and with slightly different shapes, appeared relatively similar when it came to neuronal types, suggesting that the processing of chromatic and polarised information does not take place in the lamina, but rather in deeper neuropils such as the medulla and lobula.

6.2.2 Results

General morphology

The lamina is positioned beneath the retina as a ~20-30 μm thick sheet (Fig. 6.2.1), with a curvature similar to that of the retina and the midband lamina cartridges visible as a swelling stretching laterally across the sheet. It is composed of a synaptic layer with stratified arrangements of processes that intersect the columnar neurons. Four main groups of neurons make up the lamina: *i*) the photoreceptor terminals from the retina which terminate in two strata, *ii*) the monopolar and the t-cells which are relay neurons carrying information from the lamina to the medulla *iii*) centrifugal cells which carry feedback information from the medulla to the lamina and *iv*) amacrine and tangential cells which carry information within the lamina cartridges. In addition there are several types of multipolar or glial cells whose function is unclear. In total these neuronal types makes up specific units, termed lamina cartridges. Each lamina cartridge consists of the terminals of

photoreceptors 1-7 (short visual fibres, svfs), the axon of the small distal photoreceptor R8 (long visual fibres, lvfs), and least 5 types of lamina monopolar cells (Monopolar cell 1-5). The amacrine cells, t-cells, tangential neurons and centrifugal neurons also make up parts of these cartridges, but are usually distributed one to several cartridges (Strausfeld and Nässel, 1981).

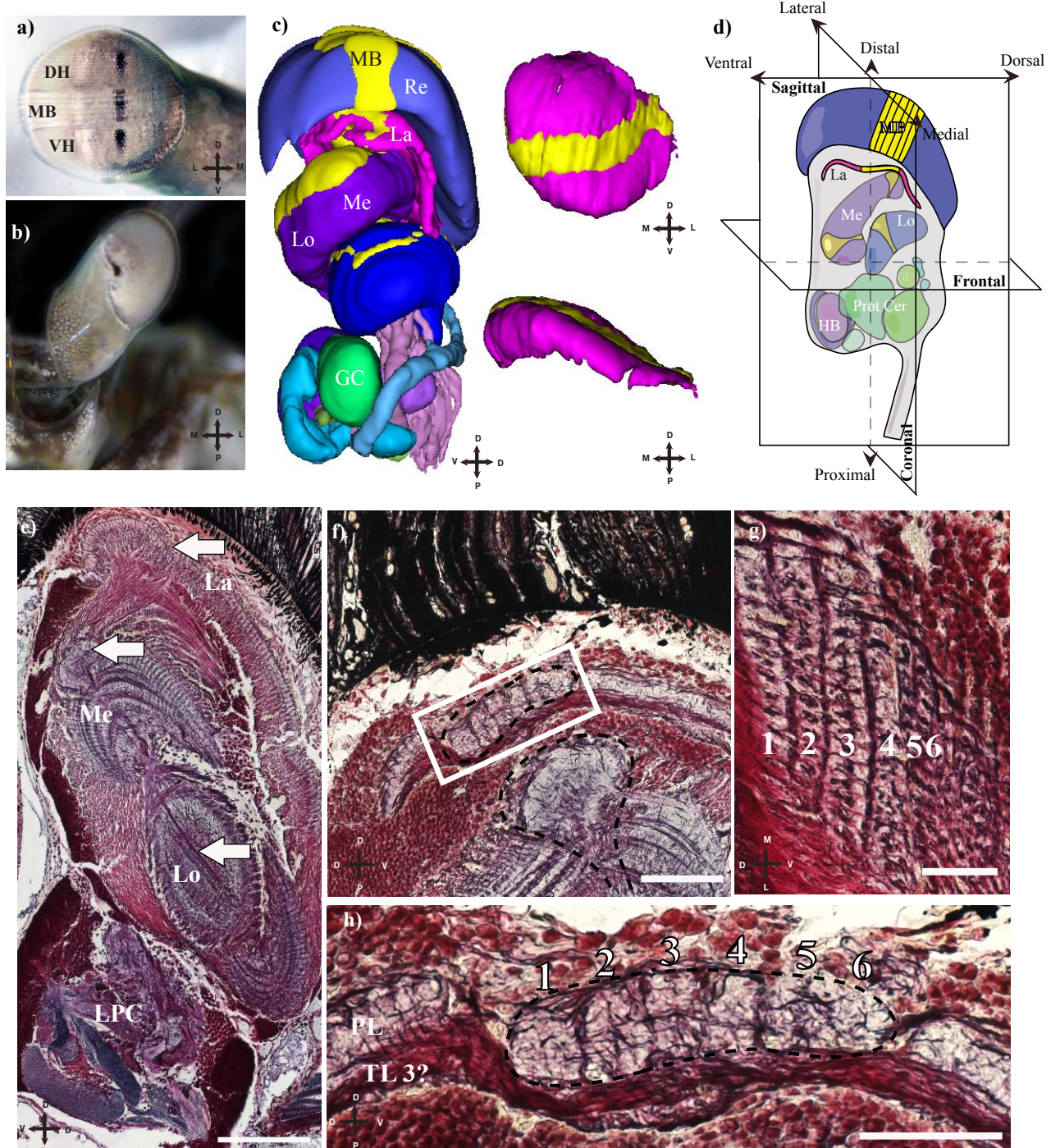


Figure 6.2.1. Overview of the eye and optic neuropils. a) Frontal view of the right eye. b) Dorsal view of the head and right eye. c) 3D-model of the eye with the retina and optic neuropils. The lamina (pink) and the midband lamina bulge (yellow) is shown next to the main model. d) Sagittal section of the eye showing the neuropils and the planes of sectioning. e) Section through the whole eye showing the midband pathway throughout the three first neuropils (arrows). f) Close up of the lamina and the midband bulge (the medulla midband bulge is also visible). g) Frontal section through the lamina showing the larger sized lamina cartridges in Row 1 to 6. h) Sagittal section through the lamina midband cartridges showing the six midband rows. Abbreviations: Ret: retina, MB: midband, La: lamina, Me: medulla, Lo: lobula, GC: glomerular complex, LPC: lateral protocerebrum. Scale bar: e) 300µm, f) 100µm, g) and h) 50µm

Photoreceptor terminals: The morphology and identity of the photoreceptor terminals were investigated by Kleinlogel and Marshall (2005) (Fig 6.2.2) and we can confirm in this study that the

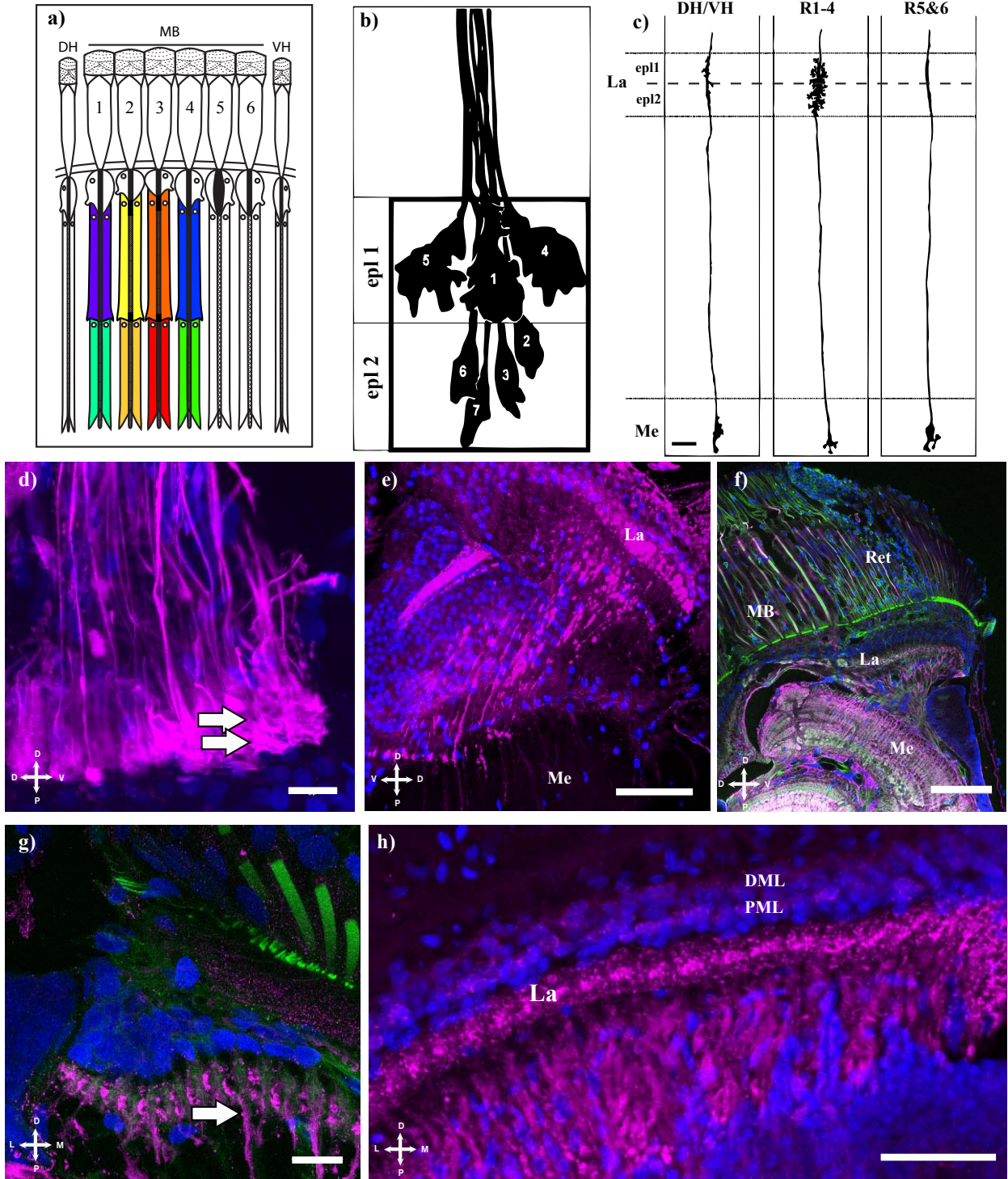


Figure 6.2.2. Lamina photoreceptor terminals. a) Illustration showing the 6 midband rows (MB), Row 1-4 with two tiers of different spectral sensitivities (indicated by colour), Row 5 and 6 which are sensitive to circular polarised light, the UV sensitive R8 cells on top of each row and the achromatic linear polarisation sensitive hemispherical receptors (DH, VH). b) Terminal endings of R1-7 from the two different tiers ending in two different strata in the lamina plexiform layer (epl₁ and epl₂) (adapted from Kleinlogel and Marshall 2005). c) Photoreceptor axons of the UV-sensitive R8 cells does not terminate in the lamina but rather project through it and terminate in the upper layers of the medulla (Me) (adapted from Kleinlogel and Marshall 2005). The R8 axons differ in their arborisation pattern within the lamina, indicating different amounts of communication between Rows 1-4, Rows 5 and 6 and the hemispheres. d) Mass fillings of the photoreceptor terminals indicating the two different lamina strata. e) Mass fillings showing axons projecting from the lamina to the medulla. f) The retina, lamina and medulla stained against synapsin (pink), f-actin (green) and cell nuclei (blue). g) Lamina cartridges stained against the same antibodies as in f), showing the synapsin stained monopolar cells (arrows). h) Same stain as in f) and g) without the stain against f-actin. The lamina monopolar cell bodies lay distal to the lamina and are divided into two different layers, the distal monopolar cell layer (DML) and the proximal monopolar cell layer (PML). Scale bars: c) 25μm. d) and g) 20μm. h) 70μm.e) 100μm. f) 200μm.

terminals end in two different strata (lamina plexiform layer 1 and 2, epl₁ and epl₂) and that the lvfs project through the lamina and terminate in small bleb like terminals in the distal layers of the

medulla (Fig 6.2.2). This configuration is present in lamina cartridges in both the midband and in the hemispheres, it even holds for midband row 2 which has an inverted cell arrangement in the two main photoreceptor tiers compared to the rest of the retina (Marshall et al., 1991a, Kleinlogel et al., 2003).

Monopolar cells: The monopolar cells in stomatopods have their cell bodies situated proximal to the lamina plexiform layers. The cell bodies are arranged in two distinct layers termed distal monoolar cell layer (DML) and proximal monopolar cell layer (PML) (Fig 6.2.1). Here we have followed Nässel's (1977) classic descriptions of the monopolar cells in the crayfish lamina, which categorises similar morphologies into single cell types. We also compared the monopolar cells found in stomatopods with the ones found in the crabs *Hemigrapsus oregonensis* and *Neohelice granulata* by Sztarker et al. (2009) and adopted some of their classifications. Monopolar cells are divided into 5 main classes (Strausfeld, 1970, Ribi, 1975) based on their arborisation patterns in the two lamina plexiform layers, the placement of their cell bodies in the DML or PML, the organisation of their processes (radial, lateral or unilateral), the width and orientation of their processes and any morphological characters of the processes. Following Sztarker (2009), we have used the terminology M for monopolar cell, with the cell number 1 to 5 for the main grouping and a letter to describe the subtype: n=narrow, b=broad, s= stratified, us=unistratified, d= diffuse, l= lateral.

M1 monopolar cells (M1): These cells are classified by having cell bodies in the PML and therefore have very short axons between the cell bodies and branching processes. In this study we found a diffuse type of M1 (M1d) (Fig 6.2.3), which had dendrites extending laterally (M1dl). Unistratified M1s (M1us) were found with sparse branching in one layer, and some were stratified into both layers (M1s).

M2 monopolar cells (M2): The M2s have cell bodies in the DML and typically have dendrites extending bilaterally through both epl₁ and epl₂. Of these, four different types were identified: M2 narrow (M2n) with tightly packed dendritic fields extending bilaterally. An M2 with laterally extending dendrites in epl₂ were found (M2lus) in addition to one that was bistratified and narrow (M2ns). Another M2 cell type was found to be narrow and diffuse (M2nd).

Monopolar cells 3 and 4 (M3 and M4): These cells are associated with the two different lamina plexiform layers (epl₁ and epl₂). Both have cell bodies originating in DML, but M3 have arborisations only in epl₁ while M4 arborizes in epl₂ (Fig. 6.2.4 and 6.2.5). Of the M3s we found a narrow type (M3n), a lateral type (M3l), and one type that had broad dendritic arborisations, which were extending laterally (M3bl). Of the M4s we found a similar arrangement, with a broad variant

(M4b), a narrow variant (M4n), and one that had quite broad lateral dendritic spread in the epl2, but also had a few minor dendrites in epl1 (M4bl).

Monopolar cell 5 (M5): The M5 cells normally branch bilaterally in spread into adjacent cartridges, sometimes with quite wide field processes. They are in general impregnated less frequently and do not occur in every cartridge. Nevertheless, a few cells were found that could be identified as possible M5s (Fig 6.2.6).

Monopolar cell 6 (M6): Sztarker et al. (2009) also identified a 6th type of monopolar cell (M6). The M6 cells have very delicate dendrites, sometimes with pinhead-like specialisations. The M6 cells have yet to be identified in the stomatopod lamina.

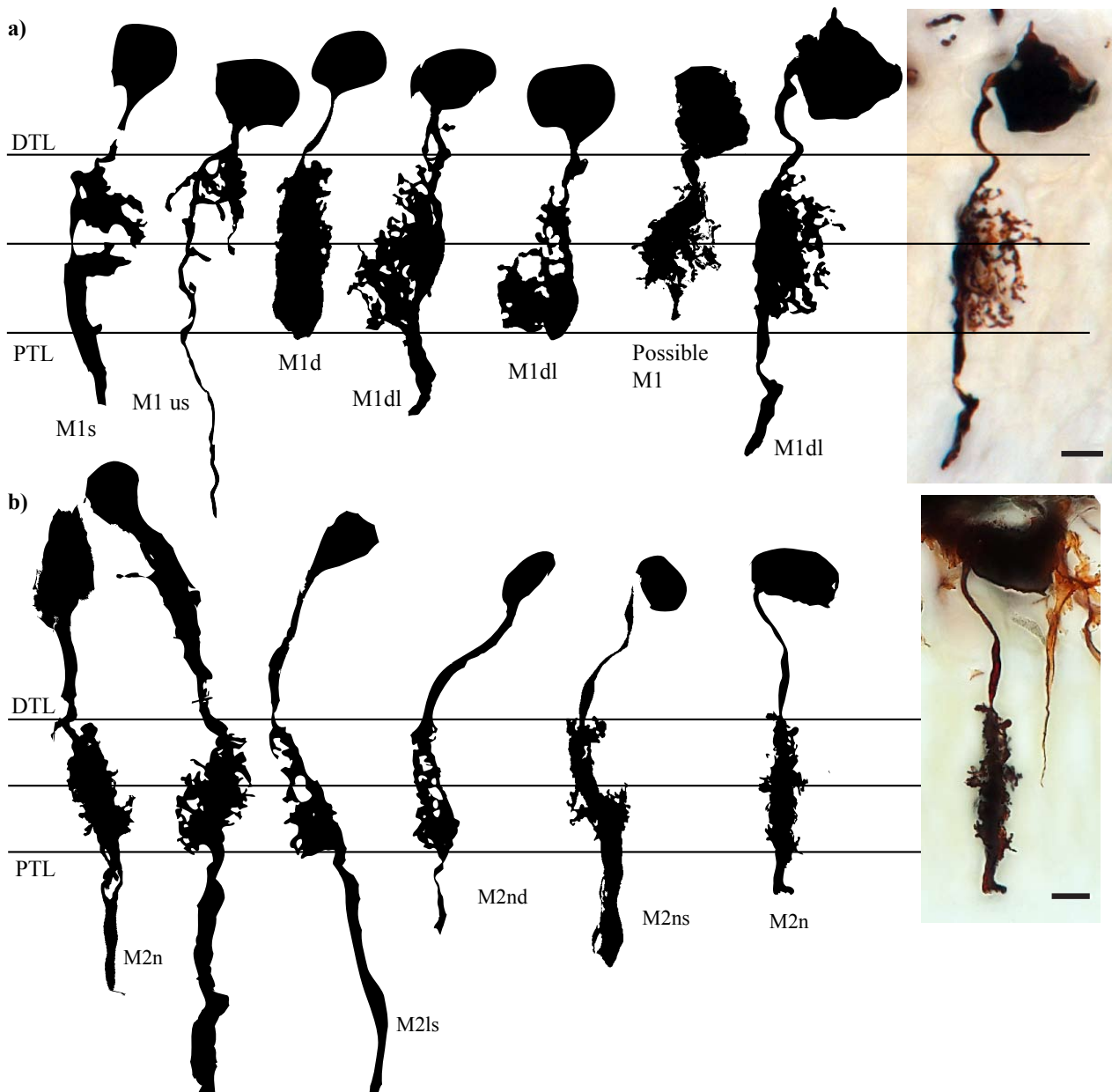


Figure 6.2.3. Lamina monopolar cell types 1 and 2. a) Monopolar cell type 1 (M1) illustrating the variation within each cell type. M1s: stratified, M1 us: unistratified, M1dl: diffuselateralised. Image shows example of traced cell b) Monopolar cell type 2 (M2) with different versions. M2n: narrow, M2ls: lateralised and stratified, M2nd: narrow diffuse, M2ns: narrow stratified. DTL: distal tangential layer, PTL: proximal tangential layer. Scale bars: 10 μ m

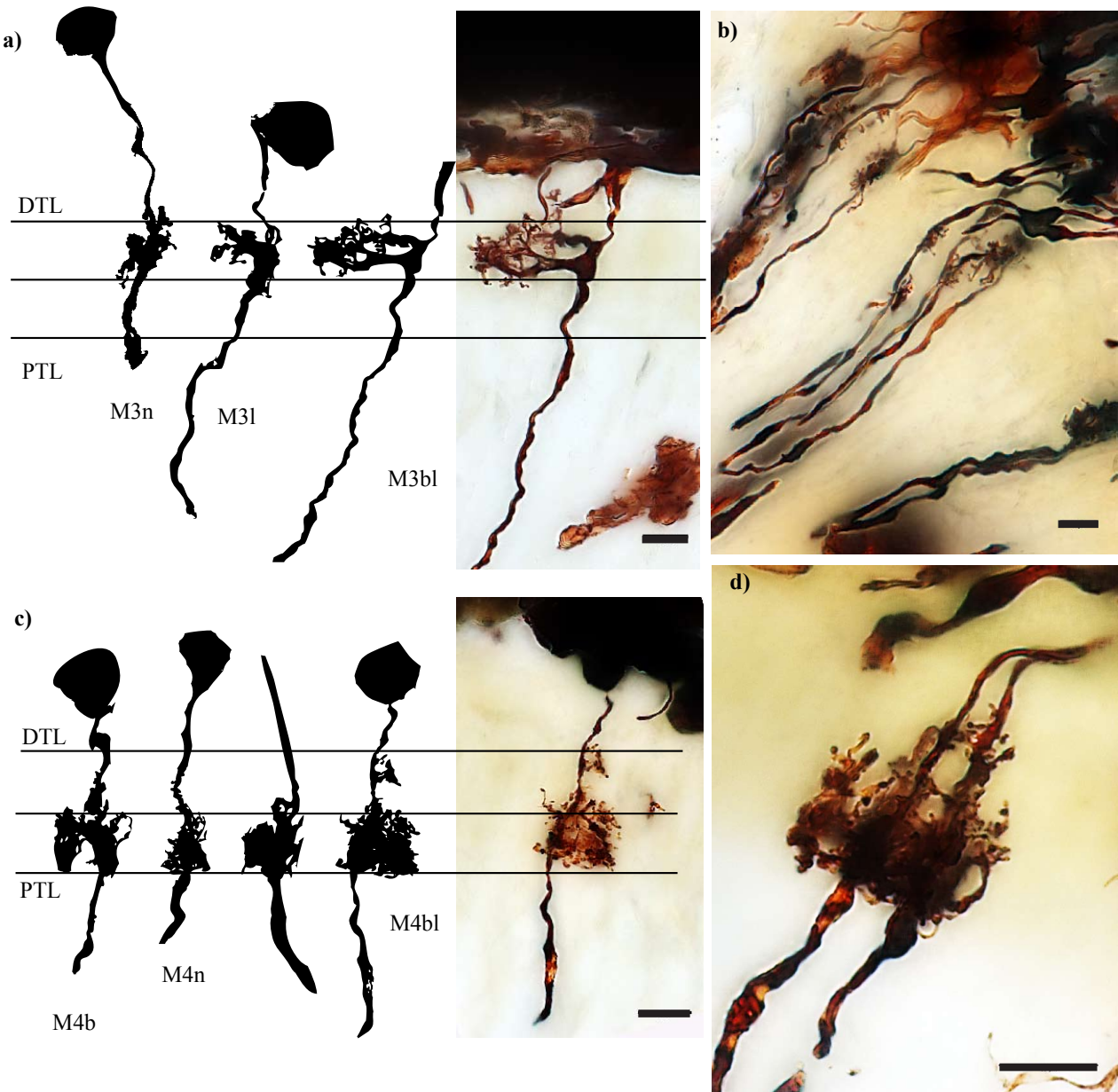


Figure 6.2.4. Stratified lamina monopolar cell type 3 and 4. a) Monopolar cell type 3 (M3) showing the typical branching pattern in lamina plexiform layer 1 (epl_1) but no branching in lamina plexiform layer 2 (epl_2). b) Examples of typical impregnations of monopolar cells 3 and 4. c) Monopolar cell type 4 (M4) which has the opposite branching pattern to M3 cells, with arborisations only in epl_2 . d) Monopolar cells type 4 with extensive arborisations in epl_1 and little arborisations in epl_1 . Scale bars: 10 μ m

Tangential cells: 3 types of tangential cells have been identified in the stomatopod lamina (Fig. 6.2.7).

Tangential cell type 1: Tan1s in other crustaceans have long arborizing processes that infiltrate the lamina in a bistratified pattern (Strausfeld and Nässel, 1981). The Tan1 found in the stomatopod lamina intersect around 6-8 cartridges with extensive branching into the epl_1 and epl_2 . It has a thick axon between the medulla and the lamina and a narrow bush like dendrite in the medulla with the cell body lying above the medullas outer surface

Tangential cell type 2: This cell type is classified as having large primary processes along the proximal part of epl_2 , with vertical branches rising orthogonally from these primary processes. The Tan 2 we found in stomatopods did not appear to have much vertical branching, they rather

appeared quite naked/bare but with very long lateral branching stretching across 10-14 cartridges. The Tan 2 neurons terminate with wide field dendrites superficially in the medulla but extend some slender branches to deeper levels.

Tangential cell type 3: A third type of tangential cell was also identified in the stomatopod lamina, with branches running along the distal part of epl₁. This one also has very thin and sparse branches coming out of the primary processes.

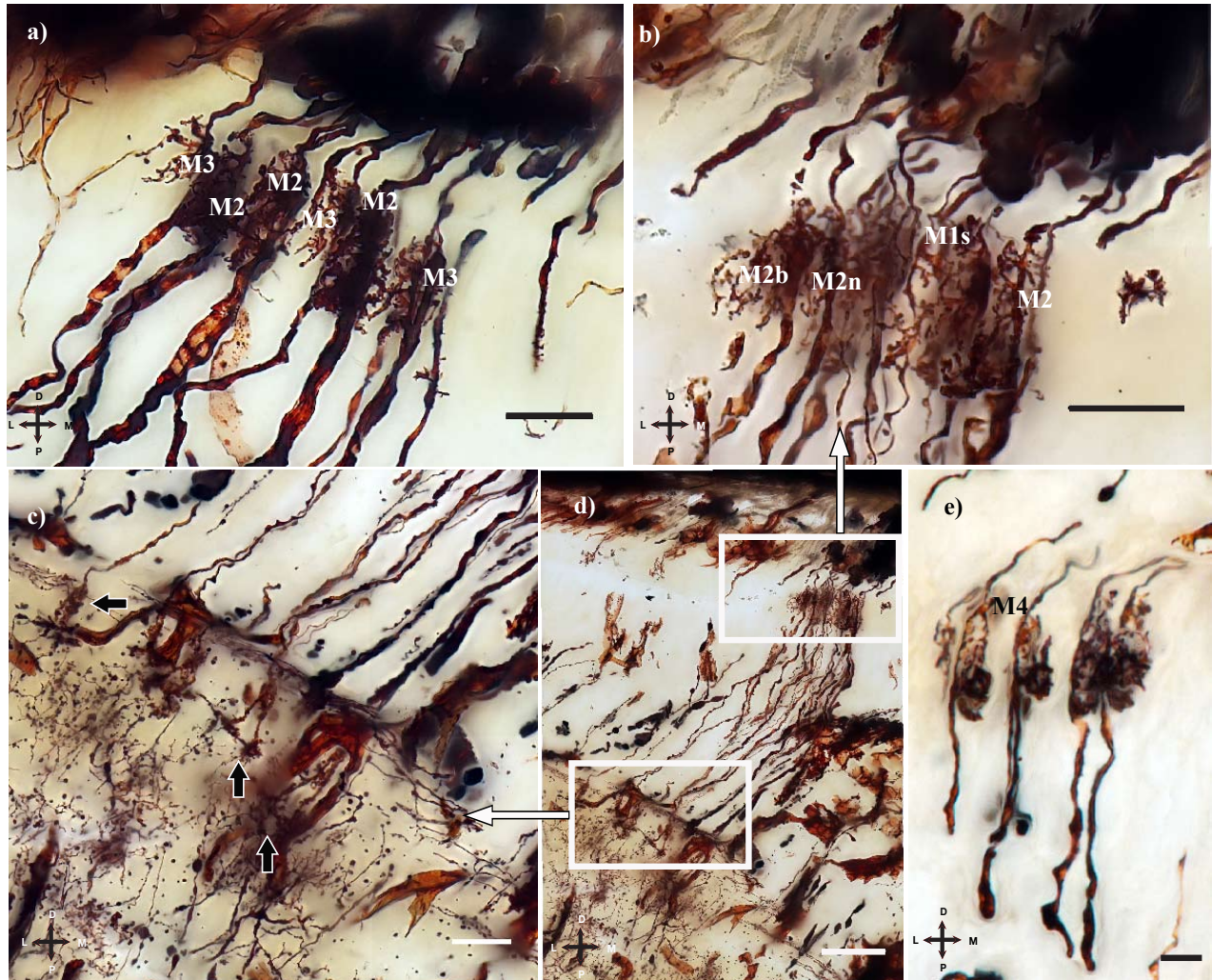


Figure 6.2.5: Examples of monopolar cells a) Cluster of monopolar cells with their terminals in the outer layers of the medulla b) A variety of different types of monopolar cells including very thin types of M1s and broad typed M2. c) and d). Unfortunately due to crossing over of axons the identity of terminals to monopolar cells were not possible to determine. e) More monopolar cells, including M4s and the flower-like possible M5. Scale bar: a) to c) 20µm, d) 300µm and e) 10µm.

T-cells: Sztarker et al. (2009) identified two types of t-cells, one small type (type 1) and one wide - field (type 2). The t-cells had small or wide-field almost parallel processes in both lamina strata, cell bodies located above the medulla and medulla components that gave rise to several small branches penetrating the outer layers of the medulla. A few cells have been identified in the stomatopod lamina with parallel processes in both strata (Fig. 6.2.8), but no medulla components have been identified so far.

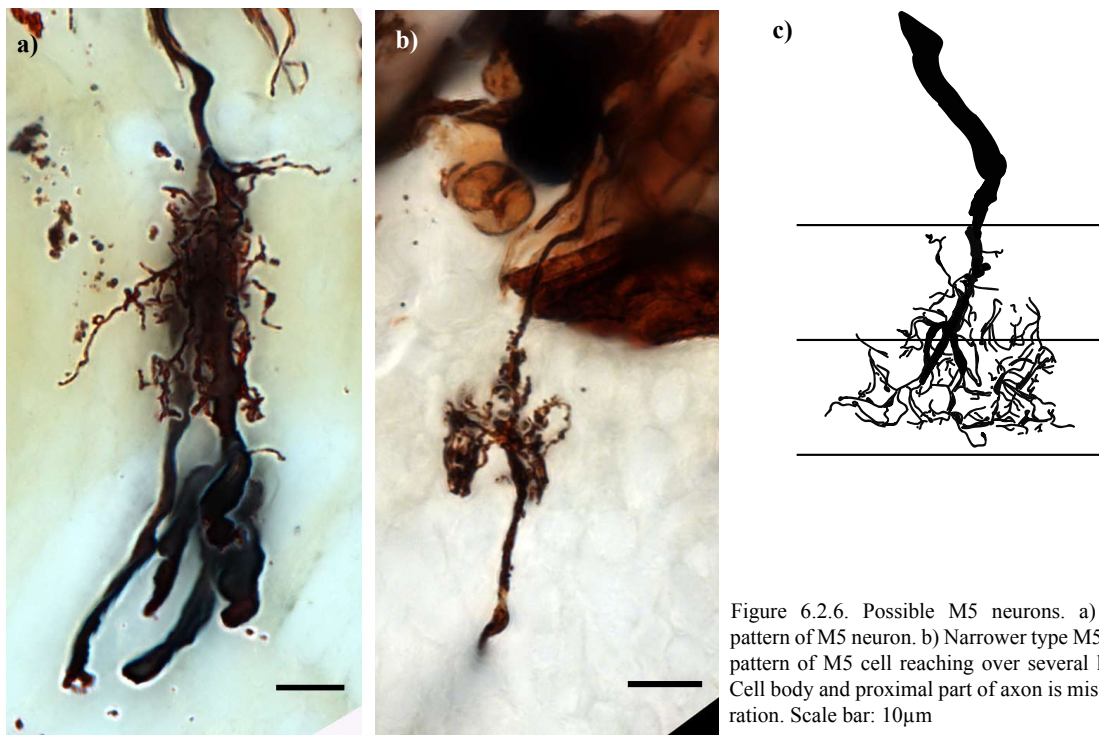


Figure 6.2.6. Possible M5 neurons. a) Wide branching pattern of M5 neuron. b) Narrower type M5 cell c) Branching pattern of M5 cell reaching over several lamina cartridges. Cell body and proximal part of axon is missing in this preparation. Scale bar: 10 μ m

Amacrine cells: Two types of amacrine cells were found in this study (Fig 6.2.8). Amacrine cells have their cell body situated below the lamina plexiform layers within the axons of the first optic chiasmata. One type had extensive arborisation throughout both lamina plexiform layers (Fig 6.2.8 a and c), and which spread across 6-8 cartridges. The other type was smaller, with fewer arborisations and thinner processes.

Centrifugal cells: Centrifugal cells originate in the medulla and terminate in the lamina. Several types of centrifugal endings have been found in the stomatopod lamina (Fig. 6.2.9). A prominent centrifugal ending with dense arborisations was identified both in the midband and in the hemispherical regions. This type is quite similar to the C2 neuron found in the crab *H. oregonensis* (Sztarker et al., 2009). Some centrifugal endings are smaller with fewer arborisations but still with the thin beaded processes appearing from the stout terminal (Fig. 6.2.9). Others have very thin beaded axonal origins which vary branching patterns in the plexiform layers.

Glial cells/multipolar cells: Several types of multipolar cells have been identified (Fig. 6.2.10), and they appear to be impregnated quite frequently in the midband region of the lamina. No classifications of these cells have been attempted, but it should be noted that they appear to have a wide range of branching patterns and arborisations.

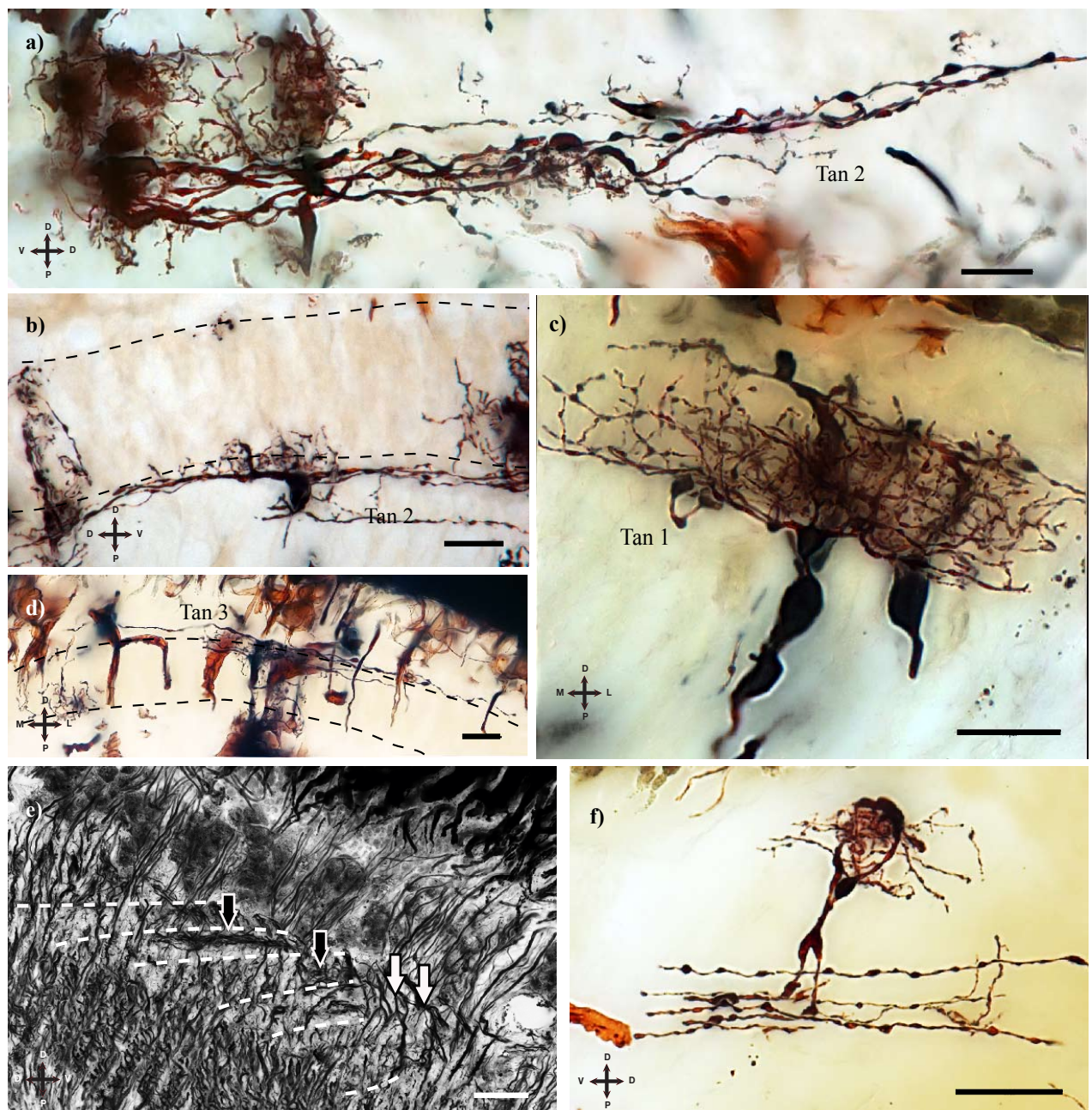


Figure 6.2.7. Tangential cells. a) Tangential cell 2 (Tan 2) with wide field main processes spreading proximally to the epl2. Few orthogonal secondary processes appear. b) Tan 2 again, with a few secondary orthogonal processes. c) Tangential cell type 1 (Tan 1) with arborisations along the vertical axis of the lamina. Processes originate from a thick vacuole axis fibre to provide a bistratified arrangement of branches that further branch off and spread laterally across several lamina cartridges. d) Tangential cell type 3 (Tan 3) with branches extending over the distal side of the lamina. e) Bodian stained section showing Tan 3 (white arrows) and Tan 1 (black arrows). f) Tan 1 or Tan 3 in the species *Haptosquilla trispinosa*. Scale bar: a) to d) plus f) 20 μ m, e) 30 μ m

Cells identified in the midband: Due to the small area of the midband cartridges in the lamina and stochastic nature of the Golgi impregnations, only a few midband lamina cells have been identified (Fig. 6.2.10). M2 and possible M3 cells have been identified and appear similar to ones found in hemispherical regions. Centrifugal endings have also been observed within the midband rows, which have been similar to centrifugal endings in hemispherical regions. Tangential cell type 2 has been

observed in several sections, projecting along the midband cartridges of each row.

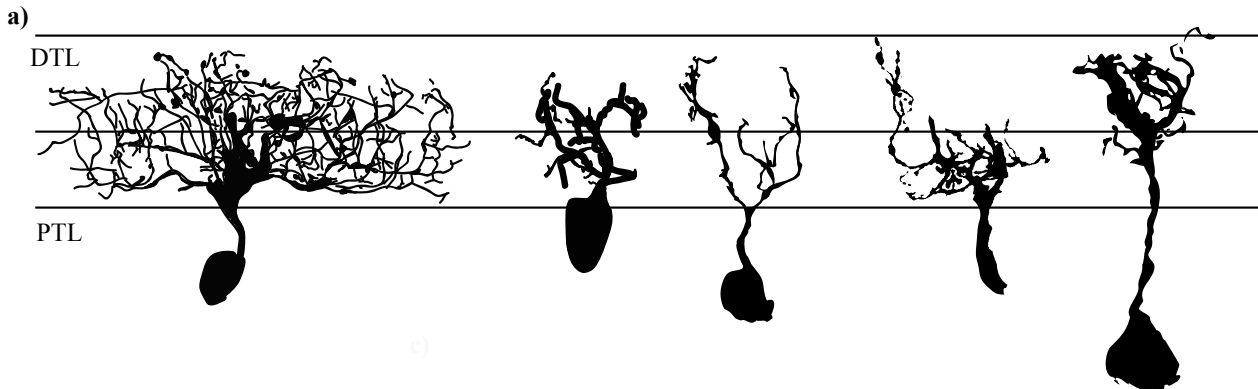


Figure 6.2.8. Amacrine and T-cells. a) At least two types of amacrine cells are found. One with large amounts of arborisations in both strata and beaded endings. A second smaller type was also identified with less branching, but as it has only been found once this needs confirming. A few different types of possible T-cells were found, one with short branches penetrating in mostly one strata and one with thinner beaded processes innervating both strata. b) Example of amacrine cell. c) Example of possible T-cell. Scale bar: b) 20 μ m, c) 10 μ m.



Figure 6.2.9. Centrifugal cells. Large variations were found among the centrifugal cells. a) Centrifugal neuron in front of M2 monopolar cell. b) Very beaded and with little branching. c) Extensive dense branching. d) Very little branching. e) and f) display the most common centrifugal endings, often seen in the midband bulge with extensive branching innervating both layers of the lamina. Scale bars: 10 μ m

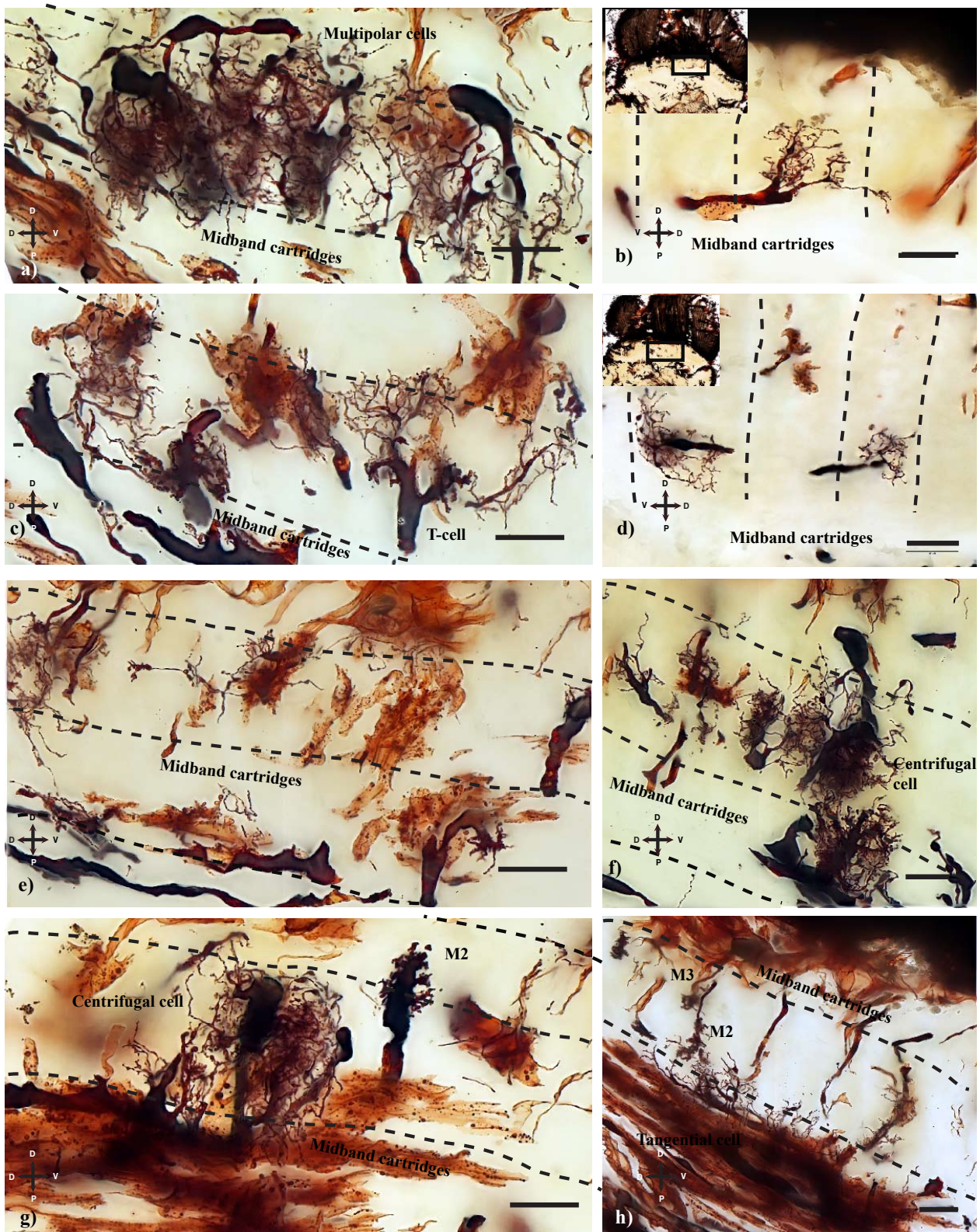


Figure 6.2.10. Cells identified in the midband lamina cartridges a) Multipolar/glia cells are often found in the midband region b) Possible part of tangential cell or t-cell in midband cartridge. c) T-cells and tangentials are evident. d) Similar to b). e) Different type of multipolar/glia cell. Also large tangentials. f) Centrifugal endings appear often in midband region. g) Centrifugal cell and normal looking M2 cell. h) Large tangential cell evident across all the midband rows. Scale bars: 20 μ m.

6.2.3 Discussion

Morphological differences between midband and hemispheres

There are distinct differences in both the size and shape of the lamina cartridges between the parts serving the midband region and also within the midband (Fig. 6.2.1) (Kleinlogel and Marshall, 2005). In the preparations investigated so far we have not seen any significant differences between the lamina cell morphology in the midband vs. the hemispherical regions. Due to a small number of impregnations and difficulties in identifying the midband row numbers, a comparison of midband rows 1-4 with rows 5 & 6 have not yet been possible. The most distinct difference we could observe was that there appeared to be more glial cells impregnated in the midband region than in the hemispherical parts. What significance this may have is not known.

Laminas in insects and crustaceans are composed of conserved cell types (Strausfeld and Nässel, 1981, Elofsson and Hagberg, 1986) and are often found to have a similar arrangement and cell morphology between species. This means that it is likely that the ecological demands of a species is not reflected in the first optic neuropil (it is, on the other hand in deeper neuropils), and that the common descent of the lamina design are of more importance. Nevertheless, some variations have been uncovered in relation to the light adaptation capabilities of the neural circuit in nocturnal versus diurnal bees (Ribi, 1975, Greiner et al., 2004). Sztarker (2009) suggest that if any ecological differences between lamina cells in different crustaceans should be found it is likely not to be in the monopolar cells but rather in the tangential neurons, which would reflect different adaptation mechanisms to a range of luminances. Although it would be of great interest to find differences in the tangential or other neurons between the midband and the hemispheres it is likely that this is not the case, as the neurons may perform very similar tasks in each area, just with a different modality (e.g. colour vs. polarization).

Communication within the lamina cartridge and its influence on colour/polarization processing

In accordance with similar studies from crayfish, (Nässel and Waterman, 1977, Nässel, 1977, Strausfeld and Nässel, 1981) the lamina cartridge is built up of two M1 cells (M1a and M1b), one M2 cell, one M3 and one M4 (Fig. 6.2.3 and 6.2.4). Within one cartridge M1a and M1b penetrate each side of the cartridge in both epl₁ and epl₂ and divide the input from the receptor terminals in each layer. M3 and M4 on the other hand only form contacts in the distal (epl₁) and the proximal (epl₂) layer respectively. The M2 forms numerous synaptic contacts with the receptor terminals in both layers. Monopolar cell M5 has wide field dendrites that form contacts within several lamina cartridges and is supraperiodic. It does not appear to form direct synaptic connections with any of the receptor terminals, and is thought to be involved in interactions with sets of relay neurons

(Strausfeld and Nässel, 1981). Although we have identified that stomatopods have all of the previously described monopolar cell forms using Golgi impregnations, there is still a need to investigate the organisation of cell types within single lamina cartridges, as there may be differences between the midband and hemispherical regions. Nonetheless, if we assume that the stomatopods have a similar layout to crayfish, and consider the differing spectral information conveyed by the receptor terminals in each lamina plexiform layer this would mean that M1a and M1b plus the M2 would receive input from receptors transferring information about two different spectral sensitivities simultaneously, while M3 and M4 would only relay the information encoded by each spectral sensitivity. Electrophysiological recordings have been made from the crayfish lamina monopolar cells (Glantz and Miller, 2002) which showed that the monopolar cells 1 to 4 exhibit a hyperpolarizing on-axis light response and are non-spiking. Due to the morphology (Nässel and Waterman, 1977) and the high response time of the M2 compared to the other monopolar cells (Wang-Bennett and Glantz, 1987, Glantz and Miller, 2002) it was suggested that the M2 cells detect high temporal frequencies while M1 detect low temporal frequencies. Further studies revealed that the M3 and M4 monopolar cells had orthogonal e-vector maxima conveying information about the angle of polarised light (Rutherford and Horridge, 1965, Nässel, 1976, Sabra, 1985, Glantz, 1996a). Although these studies did not test for wavelength discrimination, it is tempting to speculate that the stomatopods have used the same system in their colour vision pathway. In relation to the two proposed processing systems mentioned in the chapter 1, both still appear as possible solutions. A serial di- or trichromatic system could possibly involve some processing opponency between the two different receptor layers in the lamina, which could be performed by monopolar neurons such as M1 or M2. In the parallel processing scheme the M3 and M4 would likely relay the chromatic information without any further processing at this stage. It is clear that electrophysiological recordings of the lamina neurons are needed to determine which of the two is happening or, perhaps, if it is a combination of the two?

Local feedback circuits within the lamina

In addition to the monopolar cells there are also other cell types in the lamina that provide functions such as lateral inhibition and regulatory feedback control within the lamina itself. The amacrine neurons appear to form lateral inhibitory feedback connections (i.e. the ability of an excited neuron to dampen activity of neighbouring neurons) to the photoreceptor terminals, which are thought to sharpen signals and increase contrast (Glantz et al., 2000, Glantz and Miller, 2002). Studies of insect lamina cells has found communication between lamina cartridges (Souza et al., 1986, Fischbach and Dittrich, 1989) suggesting that the lamina may perform some initial colour processing which is then transferred to the medulla (Menzel, 1974, de Souza et al., 1992, Pault et

al., 2009). Whether the amacrine cells are involved in early colour processing is not known. The two types of amacrine neurons found in stomatopods resemble those found in other crustaceans and any regionalisation of the amacrine cells has not yet been identified. It is therefore not known if the amacrine cells in the midband region have any specialisations for colour processing or if they have retained the same function as in the hemispheres. The hemispheres are achromatic, but instead are sensitive to linearly polarised light. If the amacrine cells are involved in colour processing then the change between processing signals from chromatic receptors versus signals from receptors processing e-vector angle may be small enough that the cells retain a similar morphology.

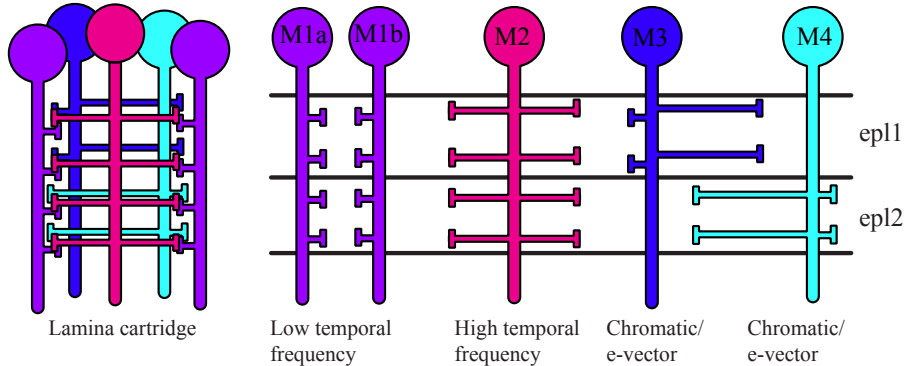


Figure 6.2.11. Summary of types and functions of monopolar cells (Adapted from Strausfeld and Nässel 1981). M5 not included as it does not appear in every cartridge. Left hand side illustrates one lamina cartridge and the monopolar cells it contains. Right side identifies the cells and their suggested function.

Tangential cells also spread across several lamina cartridges and their function is probably to regulate feedback control of lamina function and also to modulate sustaining fibres (Glantz and Miller, 2002). Stomatopods have three types of tangential neurons, similar to crabs (Stowe et al., 1977, Sztarker et al., 2005), while only two types have been found in crayfish (Nässel, 1977, Strausfeld and Nässel, 1981). The tangential neurons in stomatopods make up a rectilinear orthogonal array of processes running on the distal side of the lamina (Tan2), the proximal side of the lamina (Tan3) and throughout the lamina itself (Tan1). Together they contribute to a planar network across the columnar mosaic, which is clearly visible in the Bodian stained sections (Fig. 6.2.7e). Sztarker (2009) found that in crabs the tangential neurons supplied every optic cartridge with an axon making the tangential supply extraordinarily dense compared to insect laminas where tangential neurons are distributed one to several cartridges. It is not yet clear what this relationship is in stomatopods. Glantz (1996b) found that Tan1 neurons in the crayfish lamina were sensitive to polarised light and that this sensitivity actually exceeded that of the photoreceptors. They also found that some of these neurons exhibited opponency. At certain e-vector angles they had hyperpolarizing ON responses while depolarising OFF responses when recorded when the e-vector angle was displayed in the orthogonal direction.

6.2.4 Summary and conclusion

To summarise, there were no major differences found between the lamina cartridge of stomatopods and other crustaceans. Monopolar, tangential, amacrine, t-cells and amacrine cells had similar branching patterns and morphology to the ones found in crabs. There were a variety of centrifugal and glial/multipolar cells found, with glial/multipolar cells being more often impregnated in the midband area, but the significance of this is not yet known. The main function of the lamina in stomatopods likely follows that of other arthropods, to encode the spatiotemporal image from the photoreceptor mosaic, sharpen image contrast and establish parallel channels for colour and polarization vision (Glantz and Miller, 2002). Contrast, motion, e-vector angle and colour are encoded separately within each cartridge, and through lateral interactions and adaptation pathways this information is transferred in parallel to higher processing centres such as the medulla and lobula. Despite gross morphological differences (Kleinlogel and Marshall, 2005) no significant differences in lamina neurons were observed between hemispherical and midband lamina regions, indicating that the chromatic, achromatic and polarization information is processed using a similar set of cells and making it likely that more complex colour processing does not take place in the lamina, but rather further into the system such as in the medulla or lobula.

Subchapter 6.3

Anatomically segregated visual pathways in the
medulla of stomatopods

6.3 Anatomically segregated visual pathways in the medulla of stomatopods

6.3.1 Introduction

The complex architecture of the stomatopod retina has been the focus of many studies in recent years (Marshall, 1988, Cronin and Marshall, 1989a, Kleinlogel and Marshall, 2006, Marshall et al., 2007, Chiou et al., 2008) but we still know very little about how this plethora of visual input is processed in the optic lobes and brain. Previous studies of stomatopod optic processing have focused on the first optic neuropil, the lamina (Kleinlogel et al., 2003, Kleinlogel and Marshall, 2005 and Chapter 6.2), while investigations into higher processing centres, such as the medulla, have not yet been performed. The medulla is the second optic neuropil in the visual pathway of insects and crustaceans (Strausfeld and Nässel, 1981, Strausfeld, 2012) and is the most elaborate and intricate neuropil. It has a large number and many types of neurons (Strausfeld, 1976, Strausfeld and Nässel, 1981) receiving projections from the first optic neuropil (the lamina) and projecting information on to the third optic neuropil (the lobula). The medulla is built up in a columnar fashion, in which each column represents the information stream from one optical unit (ommatidium). Distinct horizontal elements lie across the columnar organisation, which laterally interconnect the columnar units and make up layers, or strata, in the distal-proximal direction. Intrinsic elements such as amacrine or tangential cells convey information between these layers while extrinsic elements such as transmedullary (Tm) or t-cells carry the information to other regions of the brain. The medulla necessarily encodes many different forms of visual information. Neurons in the insect medulla previously shown to be colour sensitive and display colour opponency (Hertel, 1980, Hertel and Maronde, 1987, Hertel et al., 1987, Morante and Desplan, 2008), motion sensitivity (Bausenwein and Fischbach, 1992, Douglass and Strausfeld, 2003), polarization sensitivity (Homberg and Würden, 1997) and to have spatially antagonistic receptive fields (Paulk et al., 2009). In crustaceans, modularly dimming and sustaining fibres in the medulla have been shown to be polarization sensitive in both crayfish (Glantz and McIsaac, 1998) and crabs (de Astrada et al., 2009).

A large number of neuronal types have been identified in the insect medulla. For example in the small fruit fly *Drosophila* about 45 cell types have been identified in a single column in addition to another 70 types that have been found to stretch over several columns (Gilbert, 2013). According to estimates, the medulla of the fly *Musca domestica* contains over 147,500 neurons (Strausfeld, 1976). Unfortunately, while the insect visual processing system has been scrutinised in thousands of studies, there is an absence of knowledge about crustacean medulla. The optic lobes of crayfish

(Nässel, 1977, Strausfeld and Nässel, 1981), crabs (Beron de Astrada et al., 2001, Sztarker et al., 2009, Sztarker and Tomsic, 2014), prawns (Nässel, 1975) and lobsters (Hamori and Horridge, 1966) have been examined but only a few of these focused on the medulla. Our understanding and knowledge about this complicated, but important neuropil in crustaceans is therefore limited and although comparisons with the insect medulla can give us clues to its origin and function there is still a need for further investigations.

Previous studies of stomatopod neural architecture have found that the retinotopic mosaic from the midband and hemispherical photoreceptors appear to be maintained through the three first optic lobes (Kleinlogel et al., 2003) and that the photoreceptor axons project retinotopically to the first optic lobe, the lamina (Kleinlogel and Marshall, 2005). Apart from the gross morphology of the optic lobes few other studies have been performed on the higher visual processing centres in stomatopods. Strausfeld (2005, 2012) presents images of Bodian stained sections and comments on some of the structures of the stomatopod optic lobes but does not go into any detail. Schiff et al. (1986, 1987) carried out investigations of the optic lobes of *Squilla mantis* which has a reduced midband, and did not go into details regarding the midband projections. This is therefore the first detailed study to investigate how the multipart visual system of stomatopods is processed in the medulla.

We chose to compare the optic lobes of the stomatopod to another crustacean with vision as a dominant sensory modality and active visual behaviour, namely the crab *Neohelice granulata* (until recently named *Chasmagnathus granulatus*, Sztarker et al., 2005, Sztarker and Tomsic, 2014) to disentangle any features that may be related to their visual ecology and retinal layout. Due to the different orientation in eye positioning (with the crab eye in an upright position and the stomatopod eye pointing forward) the axis have been shifted 90° (refer to Sztarker et al., 2005). Our main questions were: i) Does the stomatopod medulla have the same architectural layout as the crab? ii) Are there any special features in the region of the midband lobe that we do not see in the hemispherical parts of the stomatopod medulla or the crab medulla? iii) Is there any communication between the midband lobe and the hemispherical parts of the medulla? What we found was that the stomatopod has a strongly stratified medulla, and that the midband information is likely kept segregated from the hemispherical regions throughout the medulla.

6.3.2 Results

General morphology and stratification

The stomatopod medulla has an elongated domed shape with a lateral curve in the frontal plane (Fig. 6.3.1) and is positioned in a mediolateral position proximal to the lamina. The projections

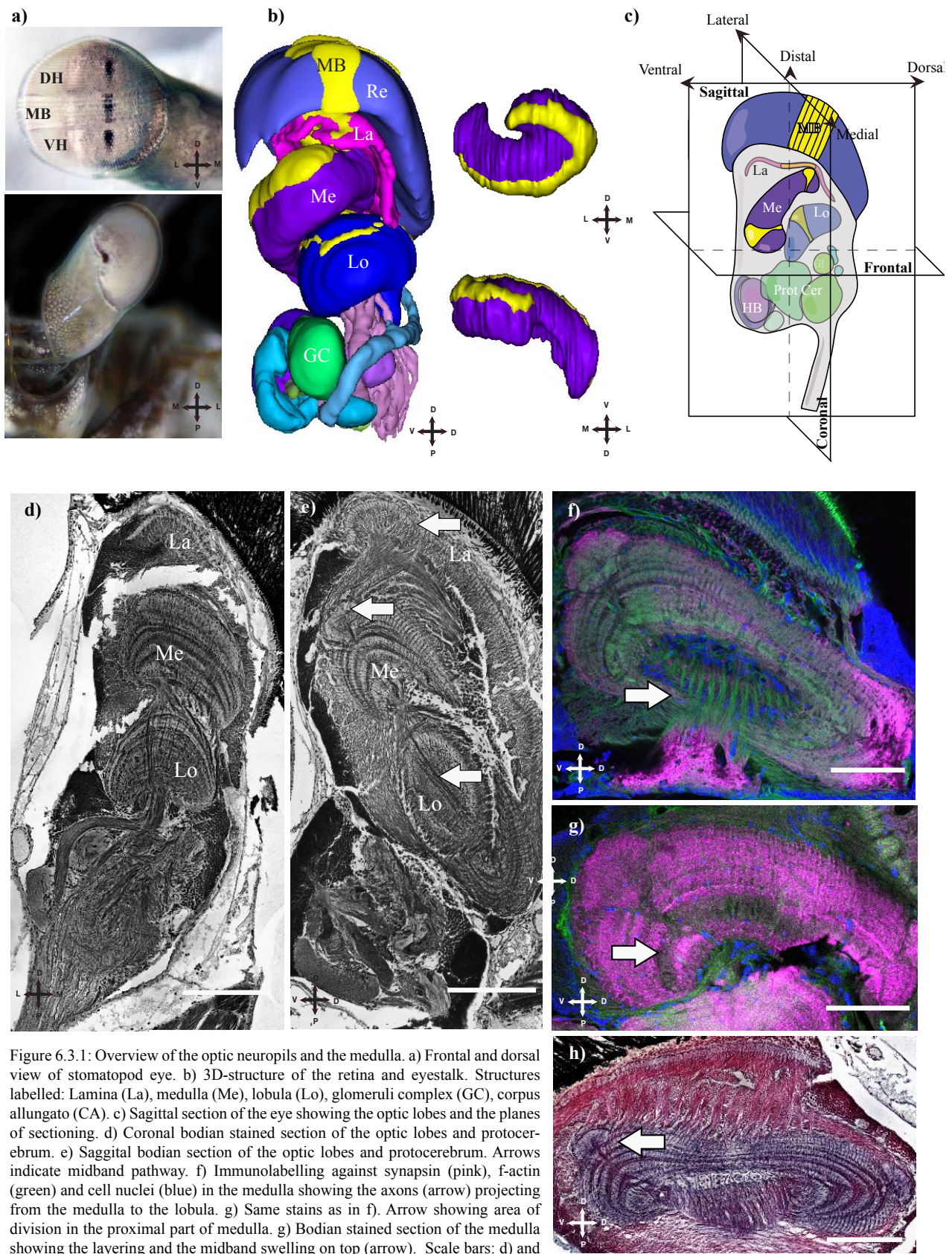


Figure 6.3.1: Overview of the optic neuropils and the medulla. a) Frontal and dorsal view of stomatopod eye. b) 3D-structure of the retina and eyestalk. Structures labelled: Lamina (La), medulla (Me), lobula (Lo), glomeruli complex (GC), corpus allungato (CA). c) Sagittal section of the eye showing the optic lobes and the planes of sectioning. d) Coronal bodian stained section of the optic lobes and protocerebrum. e) Saggital bodian section of the optic lobes and protocerebrum. Arrows indicate midband pathway. f) Immunolabelling against synapsin (pink), F-actin (green) and cell nuclei (blue) in the medulla showing the axons (arrow) projecting from the medulla to the lobula. g) Same stains as in f). Arrow showing area of division in the proximal part of medulla. g) Bodian stained section of the medulla showing the layering and the midband swelling on top (arrow). Scale bars: d) and e) 400µm, f) to h) 100µm.

from the lamina extend through the first optic chiasmata (Och_1), twist 180° and reach the outer layers of the medulla in a retinotopic fashion. Axons from the part of the retina containing the specialised midband photoreceptors project through relay neurons in the lamina down to a distinct

bulge or hernia-like swelling positioned on the distal side of the medulla (Fig 6.3.1) in a mediolateral plane, while axons from the hemispherical parts of the retina and lamina project to the corresponding regions of the medulla.

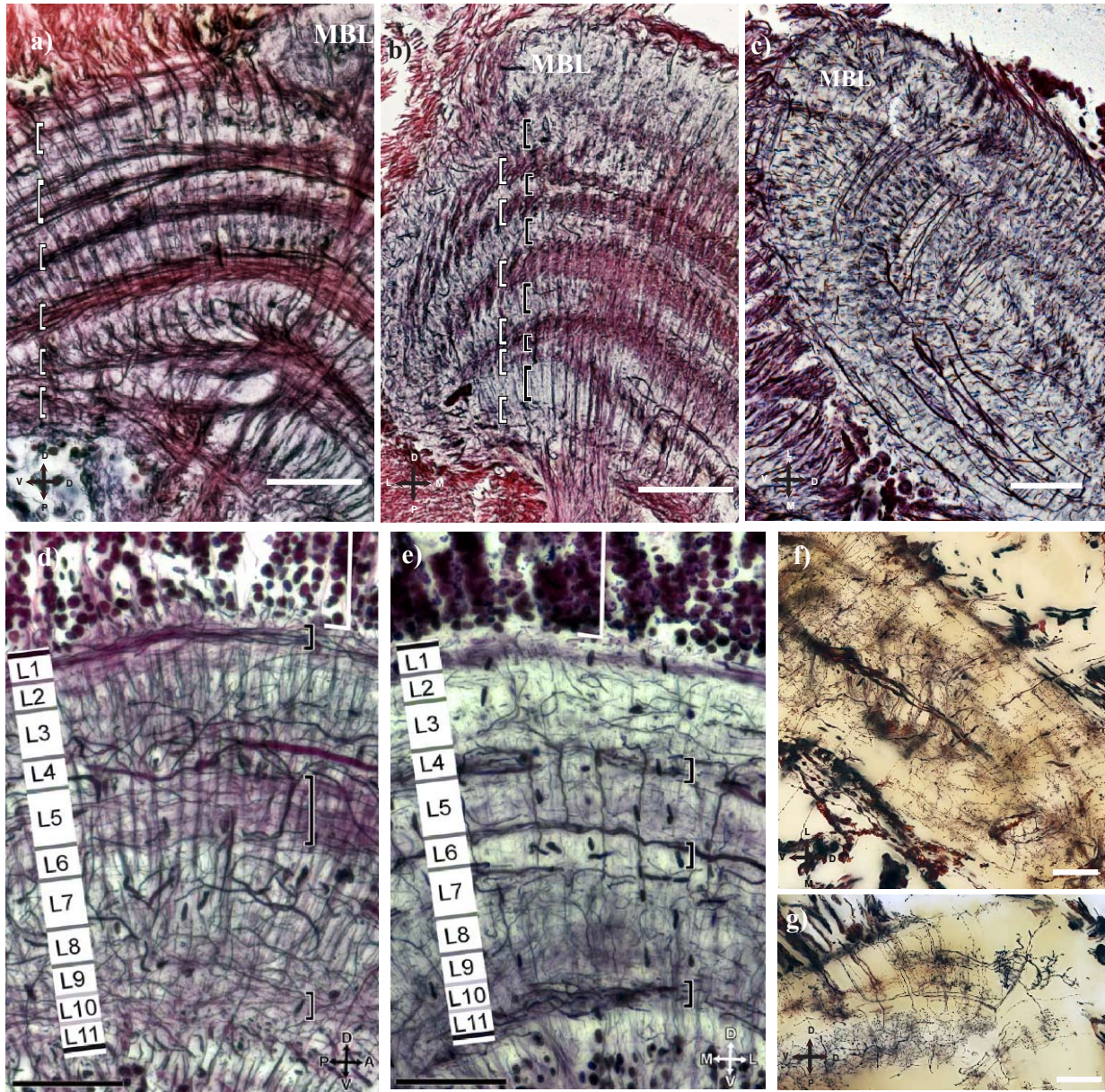


Figure 6.3.2. Medulla layers. a) Sagittal section of the medulla in *G. smithii*. The midband lobe is visible in top right corner (MBL). Tangential processes are visible as dark bands (brackets) in an dorsoventral orientation. b) Coronal section of *P. ciliata* showing the same tangential processes as in a) White brackets are indicating dorsoventrally oriented tangential processes while black brackets indicate lateromedially oriented processes. c) Oblique section of *P. ciliata* medulla showing long tangential processes extending lateromedially along the hemispherical regions of the medulla. d) Longitudinal section of *N. granulata*. Black brackets indicate anterioposterior processes (ATP1, ATP2, ATP3). From Sztaeker and Tomsic (2014). e) Transverse section of the crab *N. granulata* showing three lateromedial tangential strata (LMT1, LMT2, LMT3) in black brackets. L1 -L11 indicates layers identified by mappings of arborisations from Golgi impregnated neurons. From Sztaeker and Tomsic (2014). f) Oblique section of the medulla of *N. oerstedi* with thick neurons extrening lateromedially along the midband projections. g) Medulla of *N. oerstedi* showing examples of neurons making up tangential layers. Scale bars: 50µm

The stomatopod medulla is organised into columns and layers (Fig. 6.3.2). From Bodian stained sections it is clear that it exhibits a distal-proximal laminated architecture, consisting of at least 6 main layers made up by tangential processes oriented orthogonally to the long axis of the columns (Fig 6.3.2 a, b). These processes are oriented dorsoventrally and are interweaved into tightly bundled processes making them very distinct in the sagittal plane as dark purple layers. In addition

there are at least 6 layers of lateromedial processes visible in lightly coloured layers. Using the same stain (Bodian), Sztarker et al. (2005) divided the crab *Neohelice granulata*'s medulla into 3 strata of anterior-posterior tangential elements (APT 1-3) and 3 other strata of lateromedial tangential processes (LMT 1-3) (Fig 6.3.2). In their 2014 article Sztarker and Tomsic identified another 5 strata by the pattern of ramification of input and columnar neurons using Golgi impregnations giving the crab medulla a total of 11 layers. This work is underway for the stomatopods and will most likely divide the stomatopod medulla further.

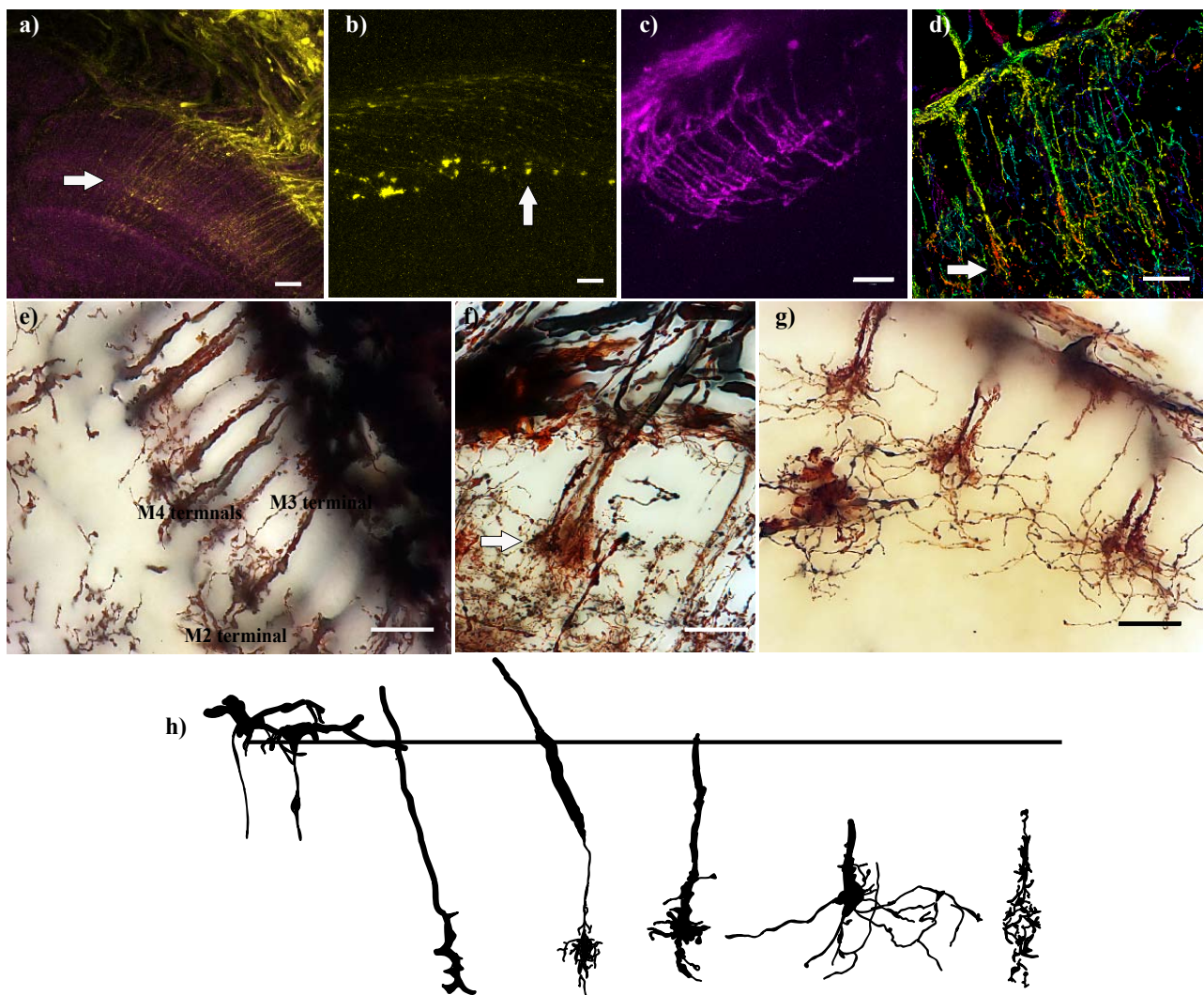


Figure 6.3.3. Termination pattern in the outer medulla layers. a) Mass fills of monopolar cells terminating deep in the outer layer of the medulla. b) Mass fill of R8 lvfs which terminate in the outermost layer of the medulla in small blobs. c) Mass fills of unidentified cell terminals in different layers. d) Golgi stained terminals in the medulla imaged with a confocal microscope and colour coded for depth. e) M3 and M4 monopolar cell terminals in the medulla. f) Other examples of monopolar cell terminals. g) Radially spreading terminal probably belonging to the M2 monopolar cell. h) Camera lucida drawings of various cell terminals. Scale bars: 20 μ m.

Termination patterns

The medulla receives axons from the lamina through the first optic chiasm, which includes lamina monopolar cell terminals, terminals from the long visual fibres (lvfs) of the R8 cells and terminals of tangential processes. The terminations are located at different layers, but they are confined to the outer two thirds of the medulla (Fig 6.3.3 and 6.3.4). The lvfs terminate in the outermost layer in small bleb-like swellings (Fig. 6.3.3). The monopolar cells terminate in the distal layers of the

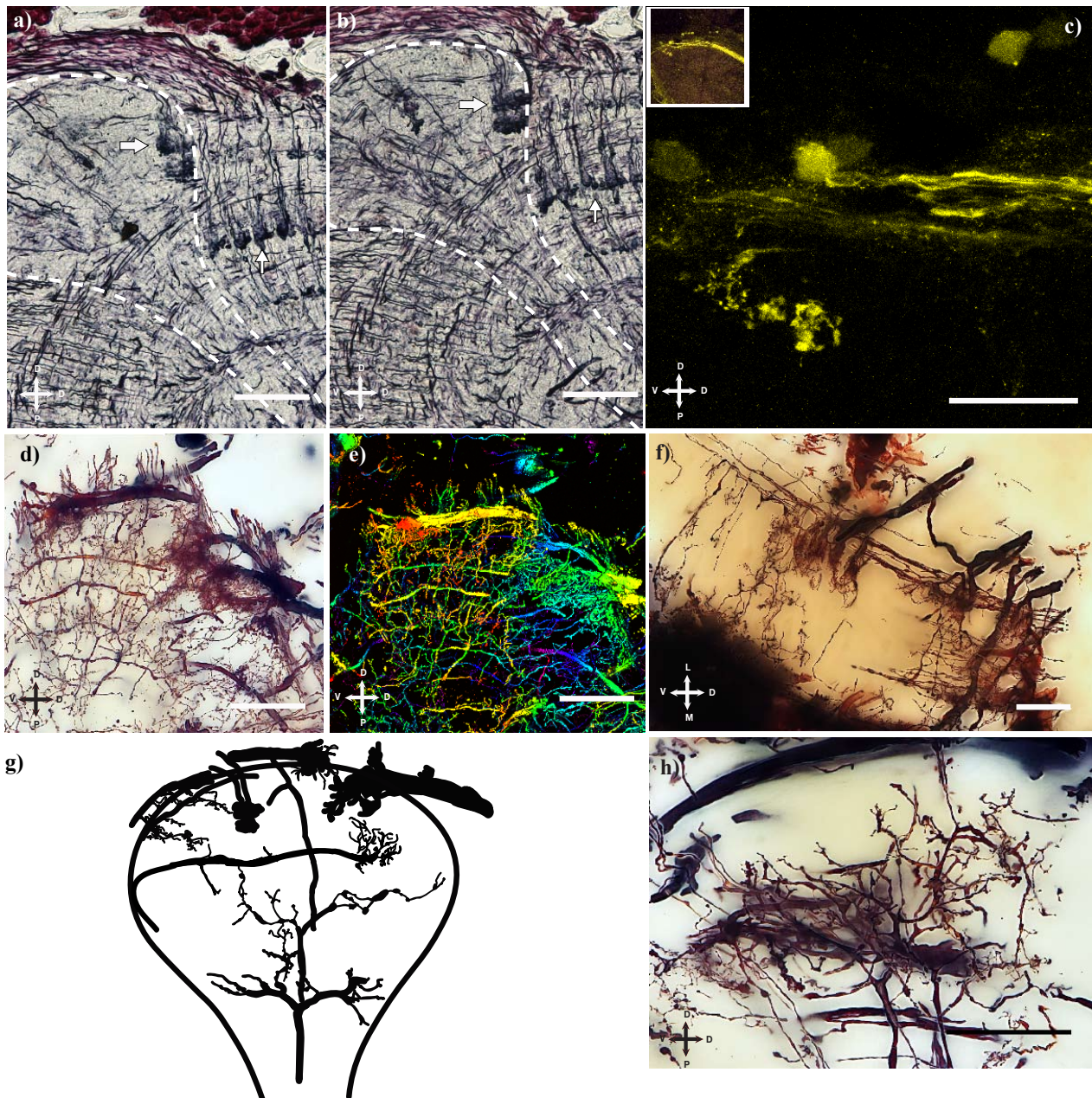


Figure 6.3.4. Termination patterns in the medulla midband lobe. a) and b) Bodian sections showing terminals in two different levels within the midband lobe. c) Mass filled neuron terminating in the midband lobe. d) Large terminals from tangential neurons in the lamina terminating on the surface of the midband lobe. e) Same as in d) but imaged with a confocal microscope. e) Large tangential terminals along the distal surface of the medulla. g) Camera lucida drawings of cells in the medulla midband lobe. h) Golgi impregnated cells in the medulla midband lobe. Thin processes entering the midband lobe and Y-shaped neurons within the lobe. Scale bar: 40 μ m.

medulla (Fig. 6.3.3) with varying degrees of arborisation patterns according to the monopolar cell identity. Because of the distance between the lamina and the medulla and the 180-degree twist in the Och₁ it is often hard to trace the axons of the monopolar cells from the lamina to the medulla. Some of the terminal identities have therefore been assumed based on similarities between these and the termination pattern of the crab (Sztarker and Tomsic, 2014). Terminals that have been identified is the M2 terminal with its radial arborisations and terminals of monopolar cell 3 (M3) and 4 (M4) was with some variations identified as M3' ad M4' according to the naming schedule in Sztarker et al. (2014). The medulla also receives axons from tangential fibres in the lamina, which terminate distally between the surface and the first layers of the medulla and have their somata

located just above the medulla. The terminal of tangential cell 1 consists of a narrow bush like ending terminating within the first few layers of the medulla, while the terminal of tangential cell 2 has a radially projecting shallow ending just penetrating the surface of the medulla.

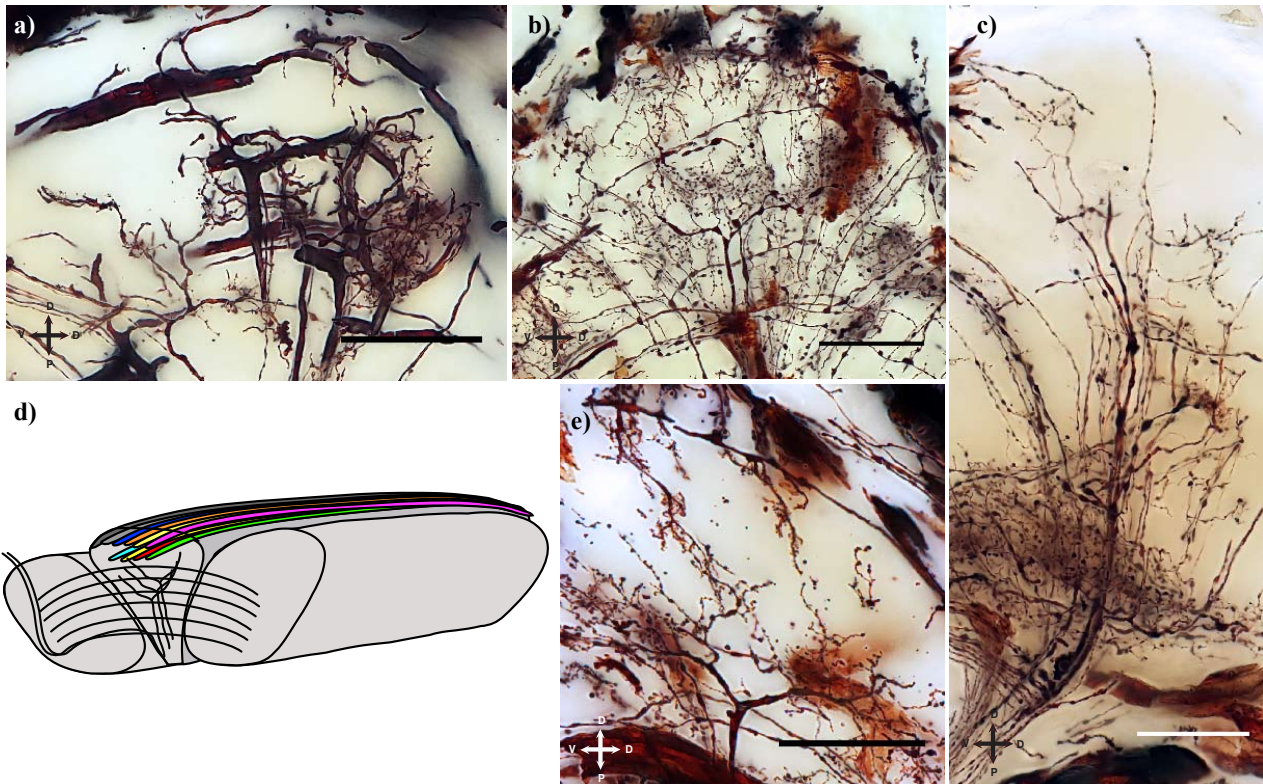


Figure 6.3.5. Neuron types within the medulla midband lobe. a) Thick Y-shaped neurons are evident in some preparations, while in others b) they are thinner and with beaded processes. c) Thin processes with little branching appear to project straight through the medulla with little interaction with other neurons. d) Illustration of the major neuronal types in and around the midband lobe. Terminal endings of lamina monopolar cells indicated in colours. e) Y-shaped beaded neuron in the stomatopod midband lobe. Scale bars: 40 μ m.

Some terminals have also been identified in the equatorial swelling (Fig. 6.3.4 to 6.3.6). The Bodian stains reveal two sets of terminals in two adjoining layers within the swelling, similar to the termination pattern of M3 and M4. At least two types of large tangential cell terminals are visible on the distal surface of the swelling likely identifiable as tangential cell 1. These terminals appear larger than the tangential terminals identified in the hemispherical parts of the medulla.

Y-shaped bifurcations

Sztarker et al. (2005, 2014) found transmedullary (Tm) cells in their longitudinal sections with prominent flattened Y-shaped bifurcations in their distal dendrites (Fig. 6.3.5). These were oriented in along the anteriorposterior axis and had retinotopic projections of their axons deep into the lobula. A similar type of neuron is found in the stomatopod medulla using Golgi impregnations, but so far it has only been discernible in the midband lobe. The Y-shaped cells in the equatorial swelling appear to project through the medulla and terminate deep in the lobula.

Large tangential neurons.

Several large tangential processes are evident in the proximal part of the medulla along the mediolateral plane (Fig. 6.3.2). These have large axons that project through the second optic chiasm down to the lobula and differ from the tangential processes that make up the layering of the medulla in their orientation (having mediolateral projections compared to the dorsoventral projections in the layers).

Projections to the lobula.

Projections from the medulla appear to converge in the medioproximal part of the medulla before becoming part of the second optic chiasm and twisting 180 degrees. There are no apparent projections circumventing the lobula.

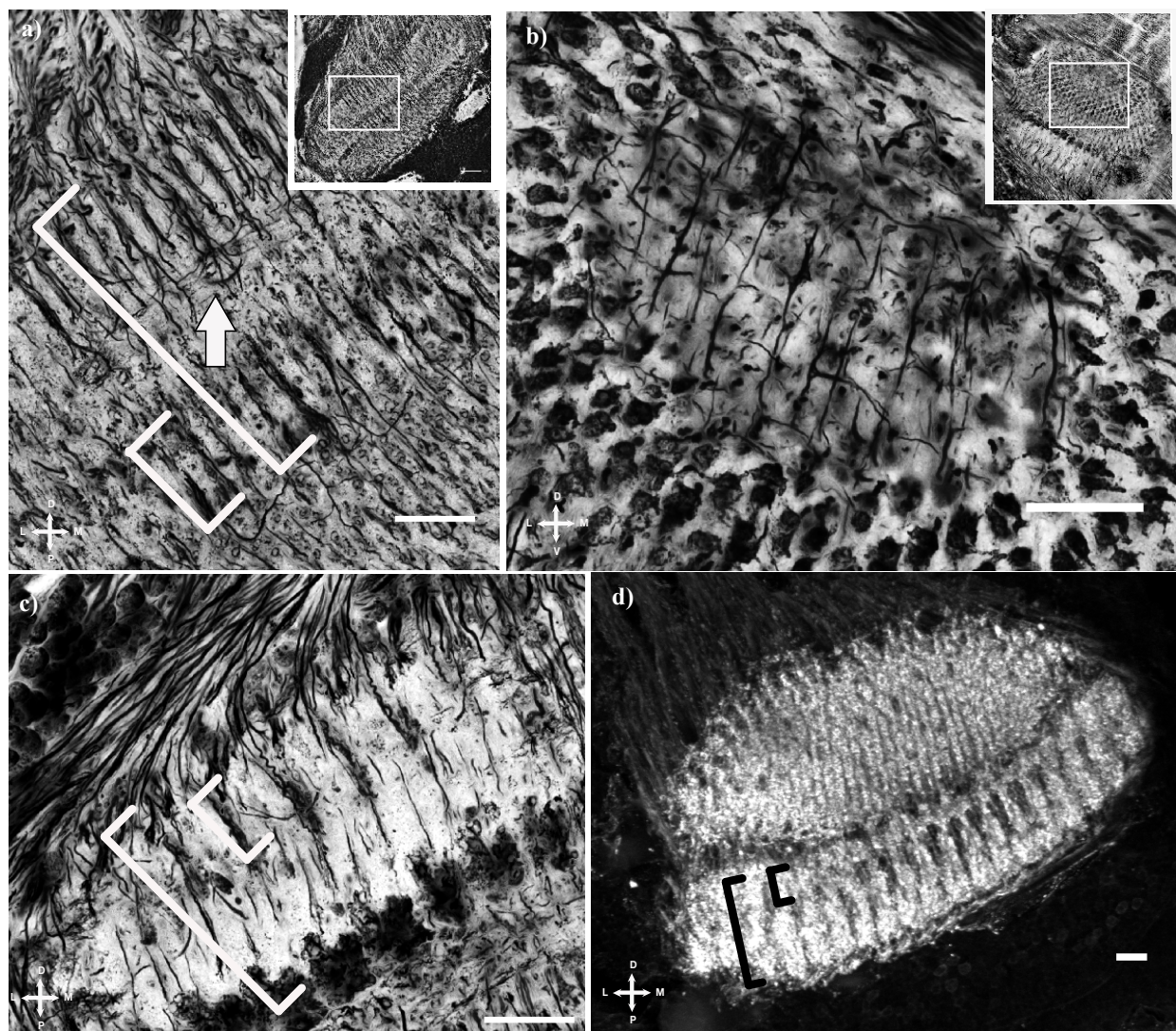


Figure 6.3.6. Medulla midband lobe. a) Arrow indicating axons from lamina celis terminating in the medulla midband lobe. Brackets indicate the midband lobe and Row 5&6 terminals. b) Tangential orthogonal processes visible on the distal surface of the medulla. c) Same as in a) with terminals from Row 5&6. d) Synapsin stained section showing the same pattern with Row 5&6 clearly visible. Scale bar: 30 μ m.

Serpentine layer

Neither in the Bodian stains or the Golgi impregnations is there obvious signs of divisions of the medulla into the outer and inner layers, such as the serpentine layer found in insects. But, as in crabs, there are apparent differences between the distal and the proximal part when it comes to the input terminal patterns, which exclusively occupy the distal two-thirds of the medulla (Fig. 6.3.3 and 6.3.4).

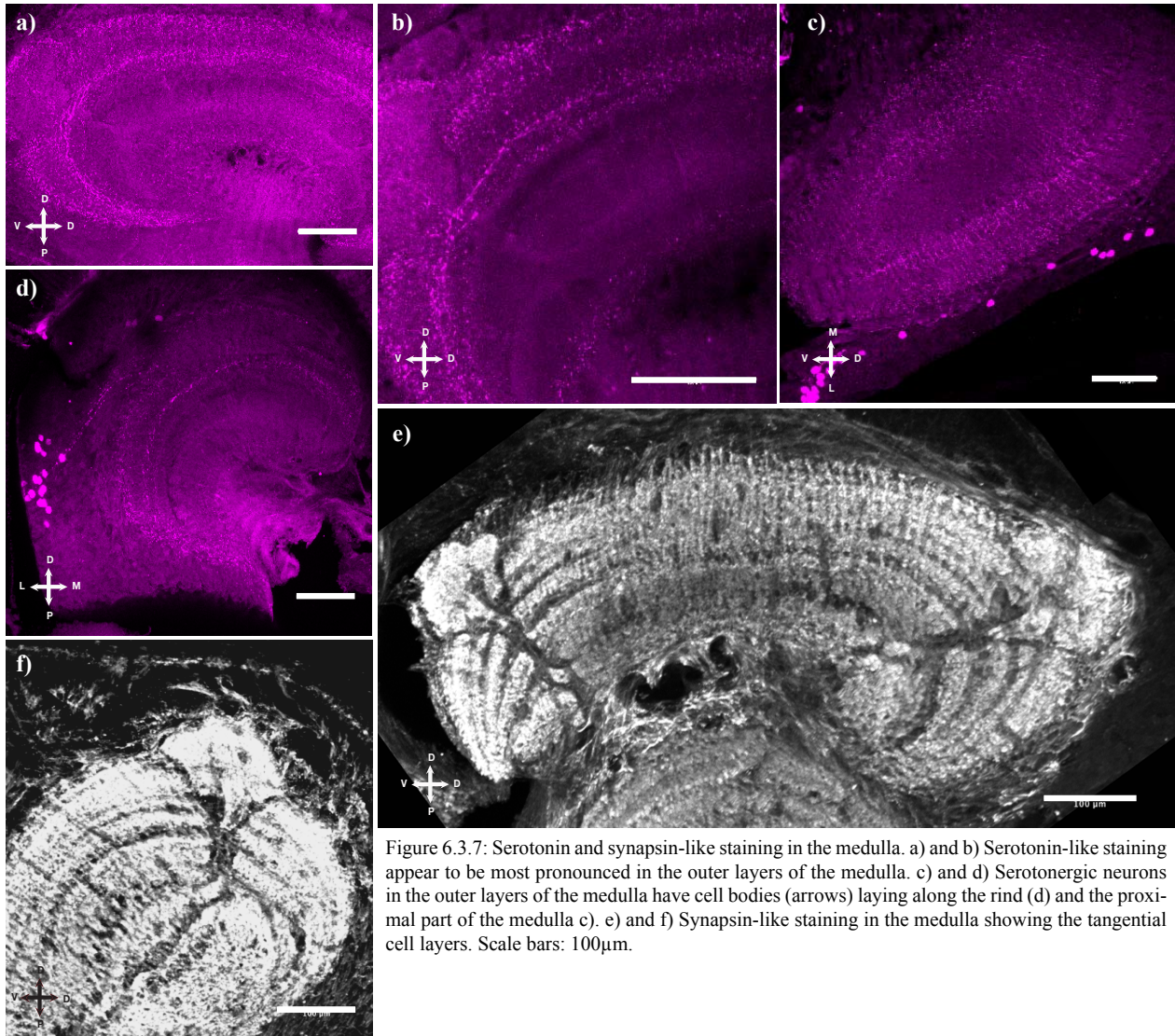


Figure 6.3.7: Serotonin and synapsin-like staining in the medulla. a) and b) Serotonin-like staining appear to be most pronounced in the outer layers of the medulla. c) and d) Serotonergic neurons in the outer layers of the medulla have cell bodies (arrows) laying along the rind (d) and the proximal part of the medulla c). e) and f) Synapsin-like staining in the medulla showing the tangential cell layers. Scale bars: 100μm.

Immunohistochemistry:

Synapsin stained sections (Fig. 6.3.7) reveal a similar layering as in the Bodian stained sections, with layers running in the lateromedial direction showing strong synapsin like staining, while the thick bundles of tangential layers running dorsoventrally have little to no synapsin-like staining. Processes in the midband lobe also appear to have strong synapsin-like staining in the distal part, but with projections running towards the lobula having little to no synapsin-like staining. Serotonin-like staining appears in the outer third of the medulla in the same layers as the axons of the lamina relay cells terminate (Fig. 6.3.7). Strong labelling appears in cell bodies positioned distally to the

medulla with axons projecting into the second layer of the lateromedially projecting processes. Some serotonergic cell bodies are also apparent on the proximal side of the medulla (Fig 6.3.7 c). These may be cell bodies of centrifugal cells, which project from the medulla and terminate in the lamina. Weak staining also appear in the most proximal layers of the medulla.

Types of neurons identified in the medulla

To best identify single neuronal types in the medulla a large number of Golgi impregnations are needed which then needs to be reconstructed using camera lucida or 3D reconstructions (in the case of confocal images). As this is very time consuming work it has not yet been carried out in a large scale, but is a planned future project.

Table 6.3.1: Similarities and differences between the stomatopod and crab medulla

	Stomatopod	Crab
Main layers	12	6
Additional layers based on the pattern of ramification (Golgi)	Not known	5
Termination patterns of lamina cells	Similar	Similar
Y-shaped cells	Only in medulla midband lobe	In the whole of medulla
Large tangential neurons in proximal medulla	Yes	No
Serpentine layer	No	No

6.3.3 Discussion

With 6 distinct layers of dorsoventrally oriented tangential elements and 6 other layers of lateromedial processes making up a total of 12 layers, the stomatopod medulla appear more stratified than the crab medulla. There are also signs of the further subdivision of the medulla, as have been seen in *N. granulata* (Sztarker and Tomsic, 2014), however these divisions await the analysis of single medullary neurons and their branching pattern. The dorsoventrally oriented processes are very sharply delineated compared to that of the crab, which only have three clearly delineated tangential layers in the dorsoventral (anterior-posterior layers 1, 2 and 3) plane. It is noted that the tangential layers of the stomatopod medulla are thicker and more distinct than those seen in the crab medulla, but what function this has is still not clear. The information from the midband is distinctly visible as a large bulge on the distal side of the medulla. As seen in the lamina, the terminals in this equatorial lobe in the medulla appear to be larger than the terminals in the hemispherical parts of the medulla, which probably account for the apparent hernia-like swelling. It could be speculated that the larger size is related to the processing requirements of the midband cells, as these would likely need to respond quickly during eye scans. Skorupski and Chittka (2010) found that the bumblebees chromatic receptors had a slower processing speed than achromatic receptors, and if this is the case for the stomatopod there may be adaptations in the midband cells to

increase processing speed. Compartmentalising parts of the optic processing system such as the stomatopod midband lobe have been recognised in other animals, such as the polarization processing pathway in locusts which project exclusively through the dorsal rim area of the medulla before innervating tangential arborisations in medulla layer with axonal processes stretching down to the ventral-most layer of the anterior lobe of the lobula (Homberg et al., 2003, Träger et al., 2008).

Branching patterns and neuron types

As the medulla is such a complex structure with numerous types of neurons belonging to each column it is a substantial task to sort these out. In general though, there are a few broad classifications that can be used to organise the main classes of neurons in the medulla such as photoreceptor and monopolar cell terminals, intrinsic transmedullary neurons, wide-field transmedullary neurons, centrifugal neurons, t-cells and amacrine neurons. Investigations are on the way to classify the different neuron types in the stomatopod medulla, but at the moment only a few types of neurons have been identified.

The terminals that have been identified are comparable with the terminals found in the medulla of the crab *N. granulata*. Within the equatorial swelling there is evidence of terminals from M3 and M4 ending in two different layers, continuing the pattern from the lamina where M3 and M4 arborize in the two lamina plexiform layers epl₁ and epl₂. Although we still don't know the synaptic connections between the photoreceptor terminals and the monopolar cells in the lamina, the branching pattern of M3 and M4 may indicate the transfer of chromatic (or polarization) information from two different sensitivities through the lamina and now possibly also through the medulla. Further connections between the terminals of M3 and M4 and other medullary cells have not yet been identified, but the work is underway.

Sztarker and Tomsic (2014) found a large number transmedullary neurons with arborisations in only the distal layers of the medulla, and this differs substantially from insects, in which only one type (Tm9 in *Drosophila*) have been found (Fischbach and Dittrich, 1989). In stomatopods it appears that some of the layering is composed of transmedullary cells (Tm cells) that have little-to-no arborisation in at least the distal layers in the medulla (Fig. 6.3.2) but which penetrate down through the outer layers of the medulla to form the dorsoventral tangential layers. Some of these cells appear to follow the tangential layers until they reach the region of the equatorial swelling, where they again project down through the rest of the medulla. These neurons have not been identified, but may have similarities with the Tm6 in *N. granulata* (Sztarker and Tomsic, 2014). It

will be interesting to investigate the branching pattern of transmedullary cells in the medulla midband lobe, as branching in only the distal layers could indicate transmission of chromatic/polarization signals from layers containing monopolar cell terminals. If these neurons are found they could be candidates for chromatic/polarization information pathways directly to the lobula without complex processing in deeper levels.

Y-shaped neurons

Another interesting neuronal type that has been identified in the stomatopod medulla is the Y-shaped transmedullary neurons. These have their Y-shaped vacariose and beaded branches in the distal layers of the medulla midband lobe and have until now been found predominantly in the medulla midband lobe. Similar neurons have been found in crabs (Sztarker and Tomsic, 2014) and insects (Strausfeld, 1970, Strausfeld, 1976, Ribi and Scheel, 1981) but in all areas of the medulla, without any regionalisation. In the crab the Y-shaped neurons coarsens the retinotopic mosaic in the medulla (several retinotopic inputs in the medulla connects to the dendritic branches of a single lobula neuron) and the lobula which contrasts the rest of the neuropil arrangement where most morphological types of through going elements can be impregnated in their neighbouring columns and gives the medulla and lobula comparable numbers of columns. The functions of these neurons are not known, but we do know that they terminate deep in the lobula with vacariose and beaded profiles indicating presynaptic swellings (Strausfeld and Bassemir, 1985).

Resemblance to insects

In insects the medulla is divided into two layers called the outer and the inner medulla (Strausfeld, 1976) by a thick layer of tangential processes termed the serpentine layer. Many neurons project from this layer via the optic commissure to regions in the midbrain and the contralateral optic lobes. This layer is not evident in crustaceans (Sinakevitch et al., 2003), nor have we been able to specifically distinguish it in this study, although there is a subdivision of the medulla seen in the termination patterns of lamina cells in the outer layers of the medulla, which is also visible in the serotonergic labelling of neurons in the outer layers. This subdivision of an outer and inner medulla is also evident in crabs, and Sztarker and Tomsic (2014) suggest a functional regionalisation in the medulla although there are not a distinct division such as the one found in insects. Differences in medulla between species and orders are most likely not due to differences in the columnar neurons but because of arrangements of local neurons such as amacrine cells. For example the motion sensitive neurons show evolutionary stability despite variations in lamina neurons termination depth in the medulla (Buschbeck and Strausfeld, 1996, Buschbeck, 2000).

Function

Previous studies (Ribi and Scheel, 1981, Douglass and Strausfeld, 1996, Glantz, 1996b, Glantz, 1998, Strausfeld, 2012) suggests that the layering in the medulla in arthropods functions like a computational device reconstructing elements of the visual scene such as edge detection, motion, centre surround fields, colour features etc. These computations may be carried out by successive networks of amacrine neurons, which together with other medulla processes, such as tangential neurons, make lateral interactions and feedback loops, modifying the signal carried by the bundled columnar neurons. Together these different medulla neurons form parallel visual pathways through the medulla with the different layers filtering out neural information and then relaying it to the lobula for further processing. Lateral processes are also evident in the stomatopod medulla midband lobe, some of which pass through both the hemispherical parts and the midband region (with unknown amounts of communication between the two), but also some that only appear within the midband lobe. As the chromatic and polarization information is already segregated into a single area, it could be that there is no need for this information to be integrated with other information pathways at this point in the processing.

Colour processing

Bumblebees exhibit an increasing complexity of colour processing in relation to the depth of the layers in the medulla (Paulk et al., 2009). The outer layers contain chromatic narrow- and broadband sensitive neurons while the inner layers demonstrate colour opponency exhibiting combination sensitive excitatory and/or inhibitory interactions by amacrine or large-field medulla neurons between two or more photoreceptor classes (Dyer et al., 2011). More work is needed to investigate if such an arrangement exists in stomatopods. The proximal layers of the stomatopod medulla does appear to have neurons with a high degree of arborisations, but detailed studies of the anatomy of single neuronal types and their activity patterns are needed to make any predictions about the function of these. Projections from the midband lobe do penetrate these layers, but it is not clear if there are any synaptic connections with the branching patterns of the previously mentioned neurons in these layers.

Subchapter 6.4

Integration and processing of chromatic and achromatic information in the stomatopod lobula and lateral protocerebrum

6.4 Integration and processing of chromatic and achromatic information in the stomatopod lobula and lateral protocerebrum

6.4.1 Introduction

The lobula (previously termed *medulla interna*) (Strausfeld and Nässel, 1981) is the third optic neuropil in the visual system of most insects and crustaceans. It is positioned in a proximally to the medulla on the lateral side of the eyestalk. In insects, a smaller tectum-like neuropil termed the lobula plate accompanies the lobula, which is characterised by large field tangential neurons and is linked to the medulla using uncrossed axons. A similar neuropil has also been found in some crustaceans such as the crab (Sztarker et al., 2005), isopod (Strausfeld, 1998) and crayfish (Strausfeld and Nässel, 1981, Strausfeld, 2005). Proximal to the lobula lies the lateral protocerebrum, which is the least studied visual region in both insects and crustaceans, and has a complex and non - columnar structure. It receives projections from the lobula, the medulla and also from the antennal lobes in the median brain, which project out into the eyestalks through the olfactory globular tract (OGT). The lateral protocerebrum consists of multiple visual and olfactory tracts or bundles, hemiellipsoid bodies, glomeruli (synaptic clusters) of varying sizes, and additional structures that have yet to be named.

Organisation

As in the medulla, the lobula consists, of columnar elements intersected by orthogonal tangential strata. In terrestrial insects (Strausfeld, 1998, Sinakevitch et al., 2003), and some crustaceans (e.g. the crayfish, Strausfeld and Nässel, 1981) the lobula is better defined as a subperiod of the medulla lattice. Spatially, a single lobula neuron receives several retinotopic inputs from the medulla, usually at around a ratio of 1:9, but unlike insects the lobula in previously studied crustaceans is densely packed with columns exhibiting the same or similar spacing as in the medulla (Sztarker et al., 2005). The columnar neurons in the lobula segregate into discrete optic glomeruli in the lateral protocerebrum, thereby loosing their retinotopic connection maintained through the three first neuropils (Strausfeld and Lee, 1991, Strausfeld and Okamura, 2007, Mu et al., 2012). One suggested function of these glomeruli is to refine noisy signals from single lobula neurons through inter-glomerulus interactions mediated by local interneurons (Mu et al., 2012). The number of glomeruli are similar to the number of columnar neurons types found in the lobula, which again relates to the number of discrete parameters that are reconstructed by the brain (Strausfeld, 2012).

Function

The lobula and protocerebrum most likely have to encode many sub modalities such as colour, motion, intensity, polarization etc. One of the main suggested purposes of the lobula complex in

both insects and crustaceans is to process motion information (O'Shea and Williams, 1974, Beron de Astrada and Tomsic, 2002, Paulk et al., 2008), with the lobula processing object motion (over a wide field) and the lobula plate processing flow field motion. Wide field motion sensitive neurons have been identified in the crab (Beron de Astrada and Tomsic, 2002), which possess dendrites extending tangentially along the lobula and relay motion information for further processing in the protocerebrum and/or brain. Recent studies of the lobula giant (LG) neurons (Beron de Astrada and Tomsic, 2002, Medan et al., 2007) have found that these are able to integrate visual information with mechanosensory information from the legs. In addition, these neurons are found to be plastic and undergo changes that assist in the formation of short- and long term visual memories (Tomsic et al., 2003, Sztarker and Tomsic, 2011, de Astrada et al., 2013) indicating that the lobula is involved in higher levels of processing than previously thought. Paulk (2008) found that the honeybee lobula contained neurons which had branching patterns in specific layers and were sensitive to either of colour, motion or stimulus timing. As the different layers project to different regions of the protocerebrum and median brain, they predicted that the lobula layers are the structural basis for segregation of visual information.

Hemiellipsoid bodies

Equivalent structures in insects, the mushroom bodies are large centres in the brain which are involved in olfaction, learning and memory formation (Heisenberg, 2003). They consist of cap- or cup-like structures called the calyces that surround a stalk termed the pedunculus. Crustaceans do not have mushroom bodies, but instead their olfactory globular tracts (OGTs) project from the olfactory lobes to prominent neuropils in the lateral protocerebrum termed, hemiellipsoid bodies. Speculations that the mushroom bodies in insects and the hemiellipsoid bodies in crustaceans are homologous structures have gained more support in later years, with evidence of similar correspondences between the morphology, structure and immunoreactivity of the two structures (Strausfeld, 2012, Wolff et al., 2012).

The lobula in insects and crustaceans have previously been shown to process chromatic and motion stimuli. Our hypothesis was therefore that the stomatopod lobula is a likely place for the processing of chromatic information from the midband. We examined the stomatopod lobula and protocerebrum to trace the optic pathway of the midband to the next level of processing and to investigate if the midband information (which appears to remain segregated from the hemispheres through the medulla) would integrate with the hemispherical parts in the lobula or remain segregated. We then investigated the trajectories of optic pathways into the protocerebrum to reveal lobula axon projection patterns and possible interactions with other neuropils in this region. We found that the

stomatopods appear to have a unique system of chromatic and achromatic channel mixing in the lobula. Also, a large neuropil containing different sized glomeruli receive projections from the lobula, suggesting this neuropil is also taking part in the processing of visual information.

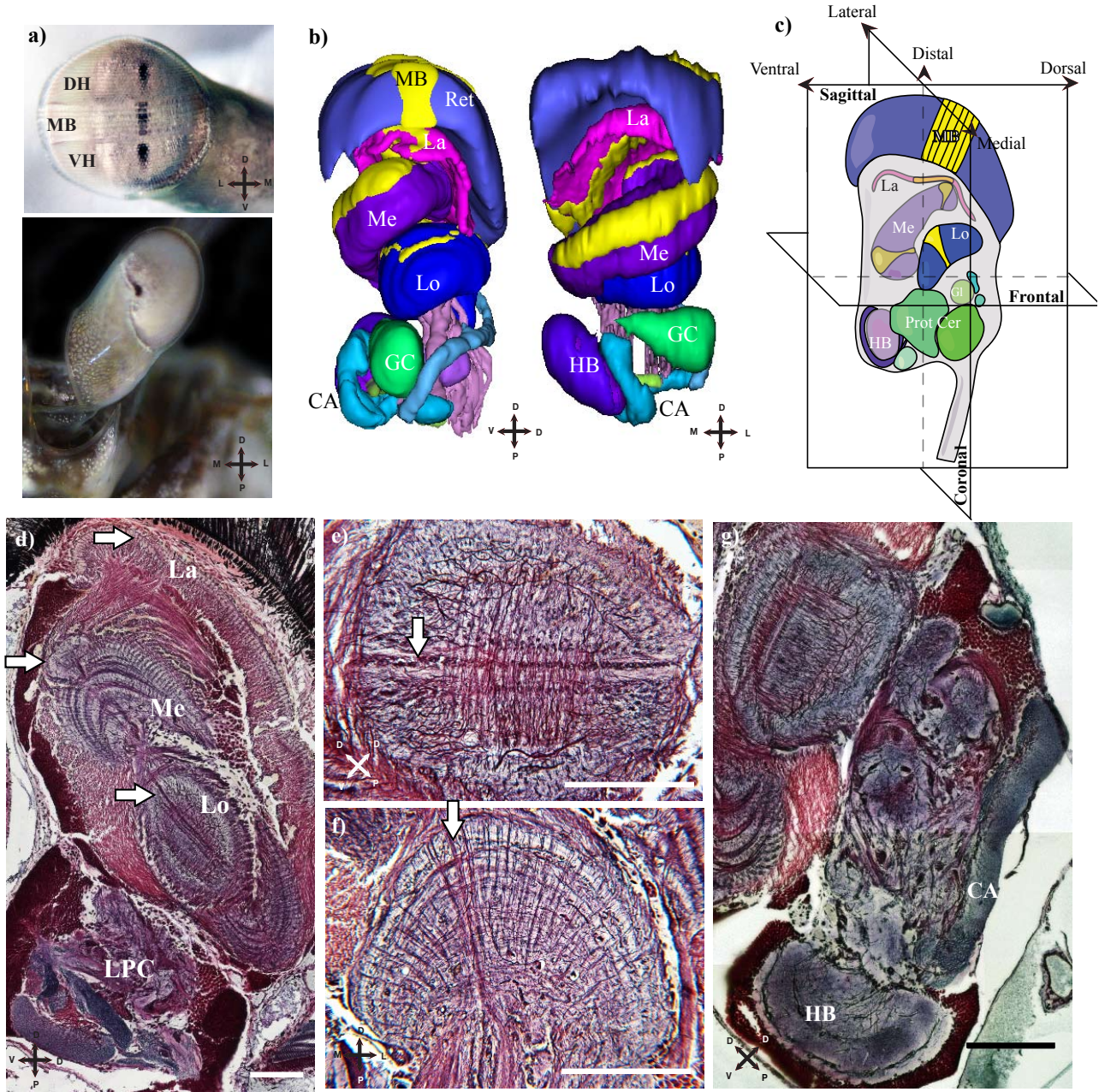


Figure 6.4.1. Overview a) Top: Frontal view of the eye showing the dorsal (DH) and ventral (VH) hemisphere with the intersecting midband (MB). Bottom: Dorsal view of both eyes. b) 3D-reconstructions of the retina and eyestalk showing the three first optic lobes (lamina, (La), medulla (Me) and lobula (Lo)), the lateral protocerebrum with the glomeruli complex (GC), hemiellipsoid body (HB) and corpus allungato (CA). The midband information pathway is highlighted in yellow. c) Sagittal section through the same parts of the eye as in b) showing the planes of sectioning. d) Bodian stained sagittal section showing the midband information pathway through the three first optic neuropils (arrows). e) Frontal section through the lobula clearly showing the midband pathway. f) Coronal section through the lobula with parts of the midband pathway still visible (arrow). g) The lateral protocerebrum with the hemiellipsoid body (HB) and the *corpo allungato* (CA). Scale

6.4.2 Results

Layering of the lobula

The lobula in stomatopods is a kidney shaped neuropil positioned in a proximal lateral position relative to the medulla (Fig 6.4.1). It is divided into distinct strata by tangentially projecting

neurons, although the layers are not as distinct as in the medulla. There are at least 5 clearly delineated tangential layers projecting lateromedially which we have termed *lateromedial tangential layer 1 to 5* (LMT1-5) (Fig. 6.4.2) following the terminology in Sztarker et al. (2005). These tangential neurons form thick bundles throughout the lobula. The LMT4 layer forms two very distinct bundles on each side of the equatorial projections that are clearly visible in the dorsoventral layer as large round shapes between DVT3 and DVT4 (see below) with increasing girth toward the medial part of the neuropil. Detailed inspections of this layer reveal thick axonal processes with extensive dendritic branching within the bundles.

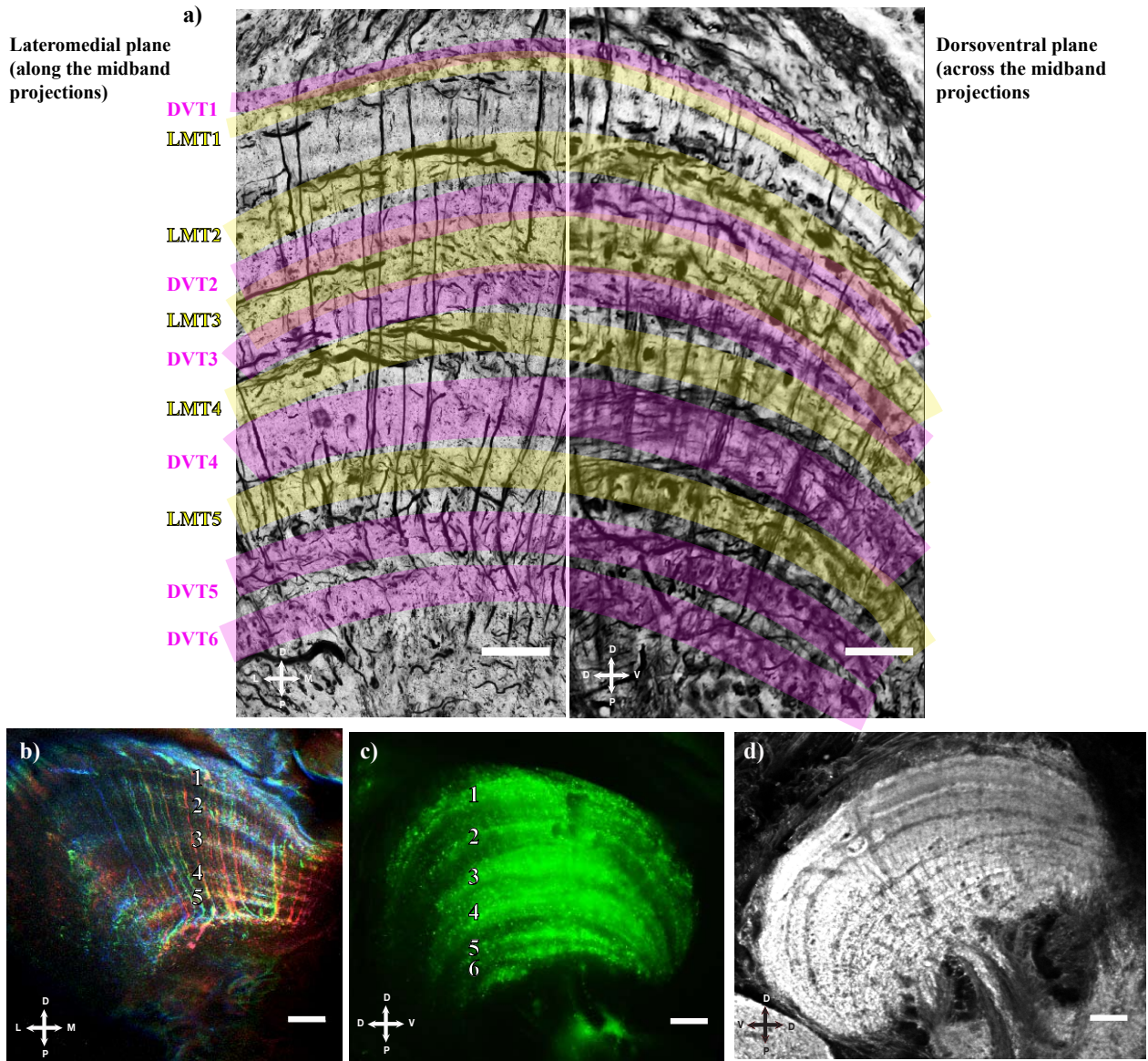


Figure 6.4.2. Lobula layers. a) Bodian stain of the lateromedial (left) and dorsoventral plane (right). The lateromedial plane is divided into 5 different layers of tangential cells, while the dorsoventral plane has at least 6 different layers. b) Insertion of dextran Texas red into medulla has spread into the columnar neurons in the lobula, and is also showing the stratification in the lateromedial plane (image colour coded for depth). c) Spreading of dextran fluorescein into the layers of medulla showing the 6 dorsoventrally oriented layers. d) Synapsin-like staining in the lobula showing stratification, especially in the outer layers. Scale bar: a) 30 μ m, b) to d) 50 μ m.

Another 6 layers of tangential processes project dorsoventrally, which we have termed *dorsoventral tangential layer 1 to 6* (DVT 1-6) (Fig. 6.4.2). This terminology differs from the anteriorposterior layer 1 to 5 in Sztarker et al. (2005) because of the altered orientation of the eye but it is essentially

the same layers. The midband information maintained from the medulla is still distinctly visible in the lobula (Fig 6.4.1), especially in transverse sections, where the equatorial projections appear as a band of two dark lines with a lighter coloured area in between (Fig. 6.4.3). There are no evident swelling on the distal surface such as the one found in the medulla.

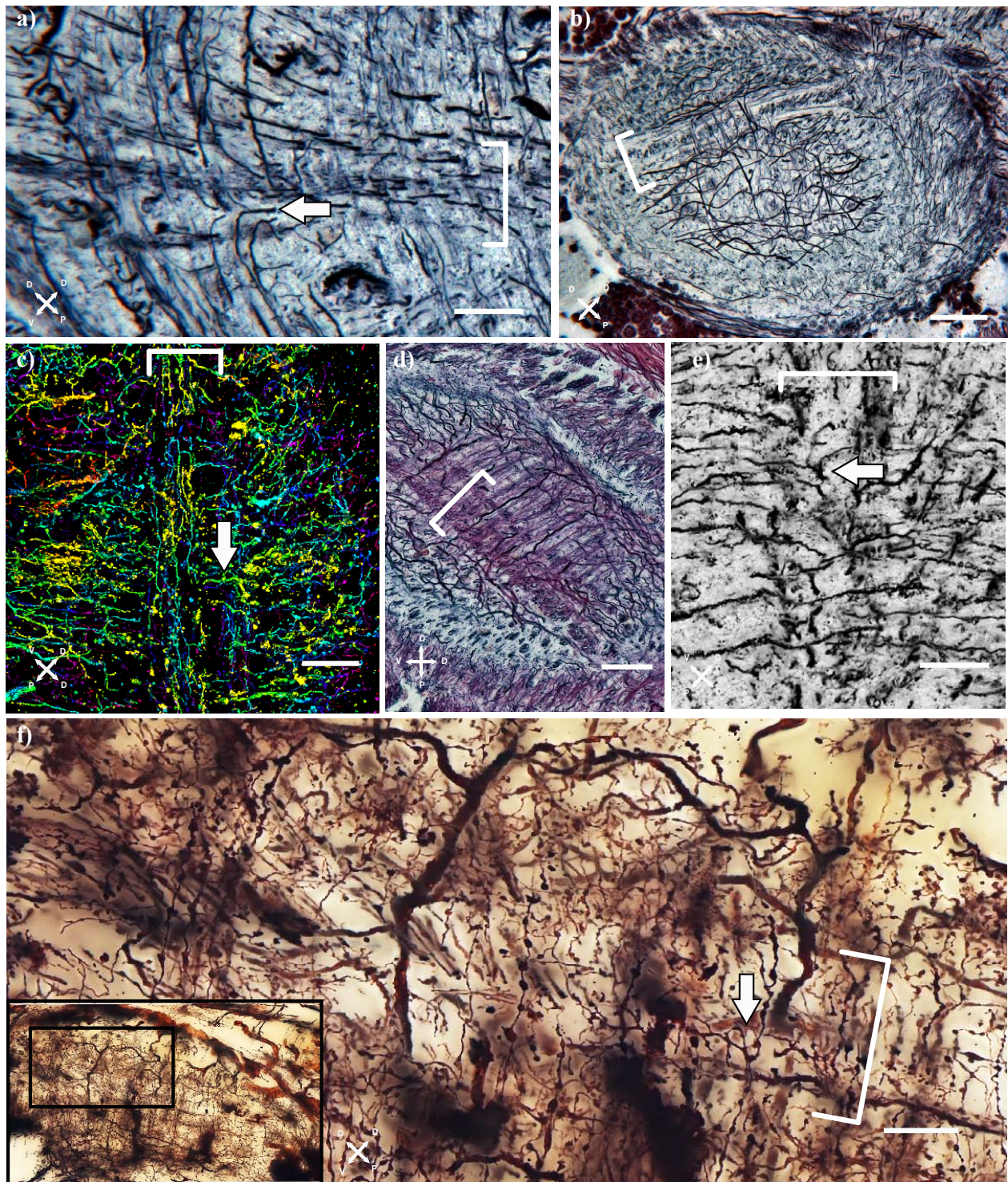


Figure 6.4.3. Midband projections through the lobula. a) Bodian staining showing the midband projections through the lobula and the hemispheres feeding into the midband. b) Section of the distal surface of the lobula with tangential processes projecting orthogonally. c) Confocally imaged (colour coded for depth) Golgi stained section showing the midband projections in the lobula (brackets and arrow). d) and e) Large t-shaped neurons projecting across the hemispherical regions and into the midband. f) Golgi stained section showing thinner t-shaped neurons projecting through the midband. White brackets in images indicate midband projections. Scale bar: a), c), e) and f) 20 μ m b) and d) 100 μ m.

Midband projections

Variation in projection patterns of the midband neurons was observed in several preparations. Lateral collaterals of the midband neurons can be seen projecting into the hemispherical parts of the lobula (Fig. 6.4.3 and 6.4.4). This mostly appears to happen in the LMT 3, but have also been detected in LMT 2 and 4. There are also medial projections from the hemispherical parts of the lobula *into* the equatorial pathway, largely in the more proximal part of the lobula in LMT 3 and 4. Many axons also appear to project straight through the lobula, continuing on to the lateral protocerebrum with what appears to be little to no interactions with other neurons.

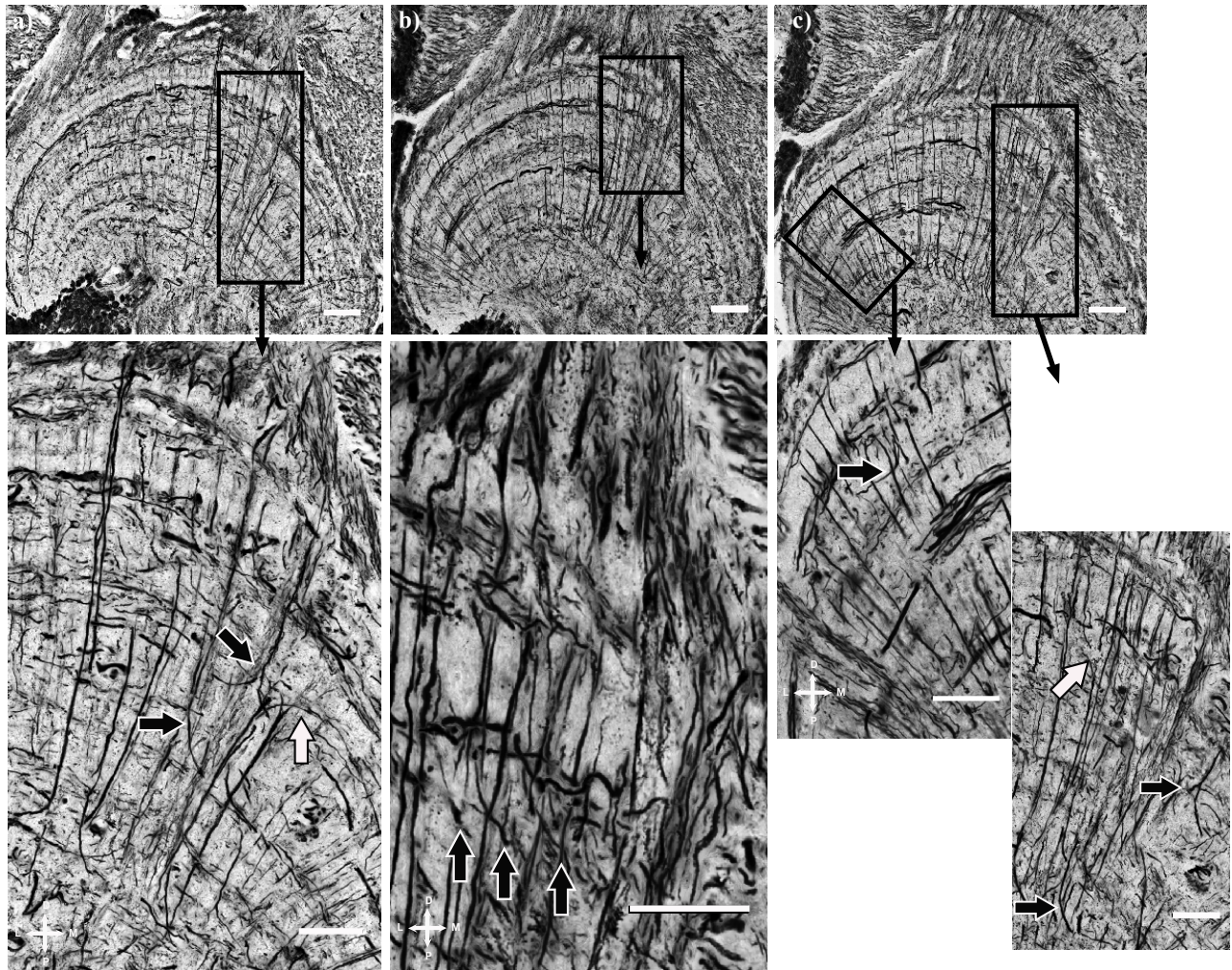


Figure 6.4.4. Lobula projections. a) Coronal section of the lobula through the midband projections. White arrow indicate projections from the hemispheres into the midband pathway, while black arrow indicate projections from the midband pathway into the hemispherical regions. b) Coronal section of the lobula with the arrows indicating the same as in a). Note that projections to and from the midband pathway appear at several layers in the lobula. c) Coronal section of the lobula with midband projections going into the outer layers of the lobula. Scale bar: Top images: 50 μ m, bottom images: 30 μ m.

Neuron types

Large T-shaped neurons: Golgi staining reveals several large T-shaped tangential neurons projecting in the lateromedial plane of the hemispherical lobula parts which then project down the same pathway as the equatorial projections (Fig. 6.4.5). These tangential neurons have a large diameter and vary from having little arborisations to bush like arborisations in the distal layers.

These T-shaped neurons contribute to the tangential layers we see in DVT 1 to DVT4. Similar T-shaped neurons were also observed by Schiff et al. (1986, 1987) in *Squilla mantis*.

Small T-shaped neurons: A smaller type of T-shaped neurons is visible in DVT2 - 4. These have thinner axons and processes, and arborize mostly in one layer (Fig. 6.4.5 e).

Large Y-shaped neurons: Several large Y-shaped neurons have also been observed, with two arms branching in the DVT layers and appearing to project down to the protocerebrum (Fig. 6.4.5 f).

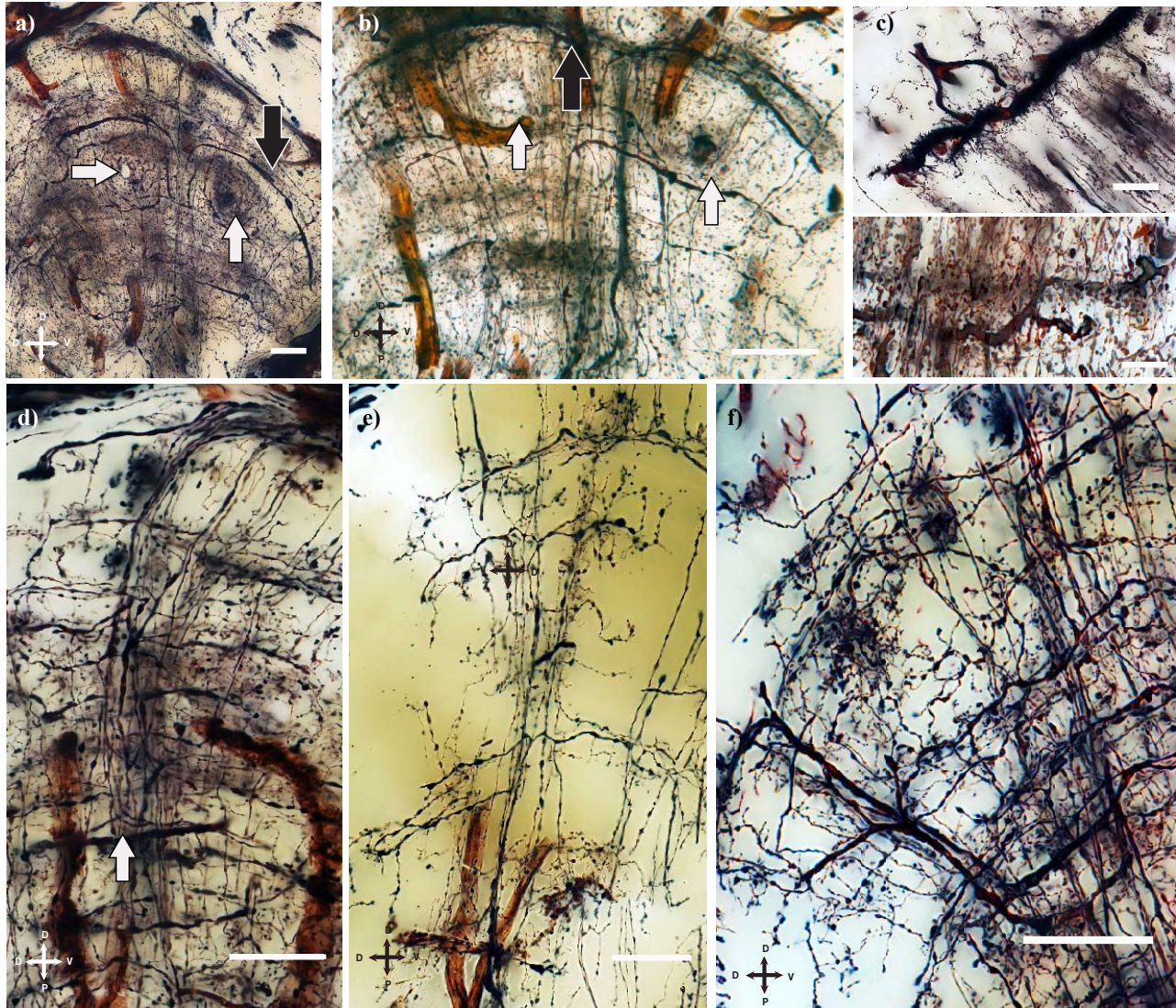


Figure 6.4.5. T-shaped and Y-shaped cells in lobula of *N. oerstedii*. a) Large T-shaped neuron in the lobula (black arrow). White arrows indicate two large neuron bundles running orthogonally to the T-shape neurons. Left neuron bundle is not impregnated but an opening is still visible. b) Different section showing the same as in a). c) Possible large neurons from the neuron bundle indicated by white arrows in a) and b). d) Midband projections extending lateral collaterals into the lobula (white arrow). e) Smaller type T-shape neurons in several layers of the lobula. f) Large Y-shaped neuron in the proximal part of the lobula. Scale bars: 30 μ m.

Terminals: A few terminals are visible that originate from medullary neurons. These appear in the layer between DVT1 and LMT1 and have small bleb like endings, with few arborisations (Fig 6.4.5 d). Other terminals have more oval shapes with radial arborisations. It is not clear what type of neurons these terminals originate form in the medulla.

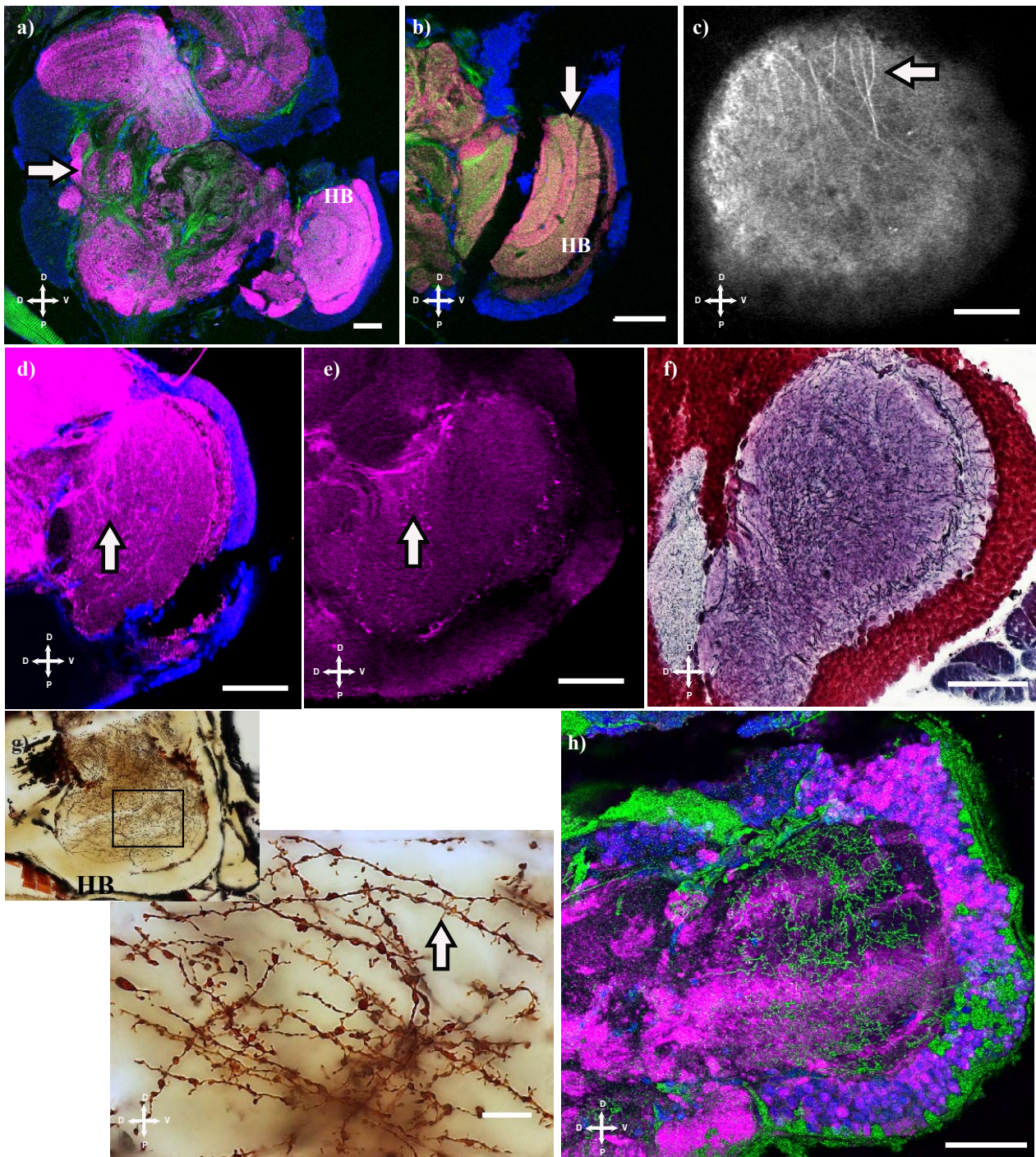


Figure 6.4.6. Hemiellioid bodies. a) Lateral protocerebrum and hemiellioid body (HB) stained against synapsin (pink), f-actin (green), and cell nuclei (blue). Note the large glomeruli indicated by white arrow. b) Same type of stains as in a), but with a clear stratification in the HB core (arrow). c) Synapsin-like staining of the thin, dendritic core neurons (arrow) in the HB. d) and e) Serotonin-like (pink) and DAPI (blue) staining in the HB cap and core. f) Bodian stain of the HB. Note the thin neurons in the core and the basophilic cell nuclei in the cap. g) Golgi impregnated neurons in the core of the HB. Notice the thin and densely dentritic neurons in the core (arrow). h) Tissue simultaneously stained with Golgi and immunohistochemistry. Golgi impregnated neurons in green, synapsin-like staining in pink and DAPI stained cell nuclei in blue. The method clearly shows how the Golgi method stains stochastically, with only a few neurons stained each time (Golgi stained cell nuclei versus the synapsin and DAPI stained nuclei). Scale bars: a) to f) plus h) 100 μ m, g) 10 μ m.

Hemiellioid body

The protocerebrum consist of several large neuropils, including the hemiellioid body. The hemiellioid body is a large neuropil consisting of a cap of basophilic cell bodies surrounding the axons and dendrites, which form the core neuropil (Fig 6.4.6). Both the cap and the core are immunoreactive to synapsin, phalloidin and serotonin. The core shows layering with different

intensities of synapsin and phalloidin reactivity (Fig. 6.4.6 b). Golgi impregnations show that the neurons in the main body display a large amount of dendritic spines, typical of hemiellipsoid body neurons (N. Strausfeld, personal communication). Possible projections from the lobula to the hemiellipsoid body were identified in the Bodian and Golgi staining, although these still have to be confirmed.

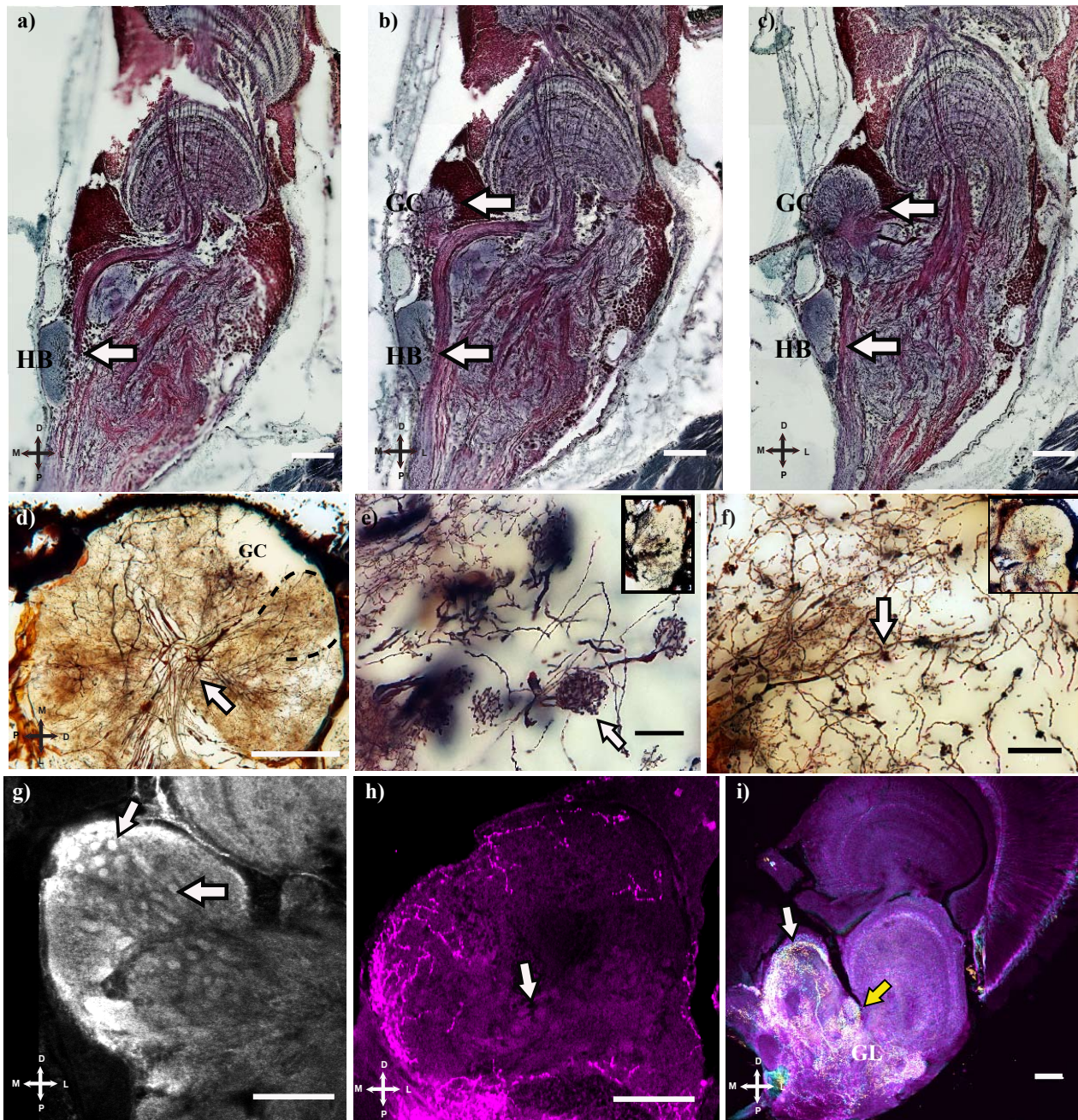


Figure 6.4.7. Glomerular complex a) to c) Bodian stained sections showing lobula projections circumventing the protocerebrum and projecting to the glomerular complex (GC). Note possible projections to the hemiellipsoid body (HB). d) Golgi staining showing interneurons (arrow) between large glomeruli (black dotted lines). e) Medium sized glomeruli (arrow) in the GC. f) Boutons, or microglomeruli (arrow) in the GC. g) Synapsin-like staining of the medium sized glomeruli (arrow) in the GC. h) Serotonin-like staining in the GC showing interneurons, but only weak staining in the glomeruli (arrow). i) Serotonin-like staining in the lateral protocerebrum. White arrow indicate serotonin-like staining along the edge of the GC while the yellow arrow indicate large sized glomeruli outside the GC. Image colour coded for depth. Scale bars: a) to d) plus g) to i) 100µm, d), e) and f) 20µm.

Glomeruli

Several types of glomeruli have been identified in the stomatopod protocerebrum (Fig. 6.4.7). Some are small oval clusters that are impregnated in batches of three or four. These are found in several areas in the protocerebrum, but most often within the boundaries of the large neuropil described below. Larger glomeruli were also identified throughout the protocerebrum, most of which appeared to receive input from lobula axons.

Glomerular complex

In addition to the hemiellipsoid body another large neuropil was located in the lateral protocerebrum (Fig. 6.4.7). It is positioned laterally, proximal to the lobula and has a similar shape and size to the hemiellipsoid body, but without the distinct cap of somata found in the hemiellipsoid body. It appears to contain many large glomeruli in a flower like arrangement with larger projection neurons crossing over in the middle of the neuropil. In the medial part there appears to be more of the smaller glomeruli mentioned above and small microglomeruli consisting of large swelling called boutons is also visible. This neuropil clearly receives projections from the lobula visualised both in the Bodian and the Golgi staining.

Corpo allungato and corpo reniforme

Two additional smaller neuropils are found in the lateral protocerebrum of stomatopods, named the *corpo allungato* and *corpo reniforme* (Bellonci, 1882). The *corpo allungato* is positioned mediolaterally, proximally to the hemiellipsoid body and has a distinctive "S" shape (Fig 6.4.1) and is associated with several small satellite neuropils. The *corpo reniforme* is a smaller, round neuropil located on the dorsal side of the lateral protocerebrum.

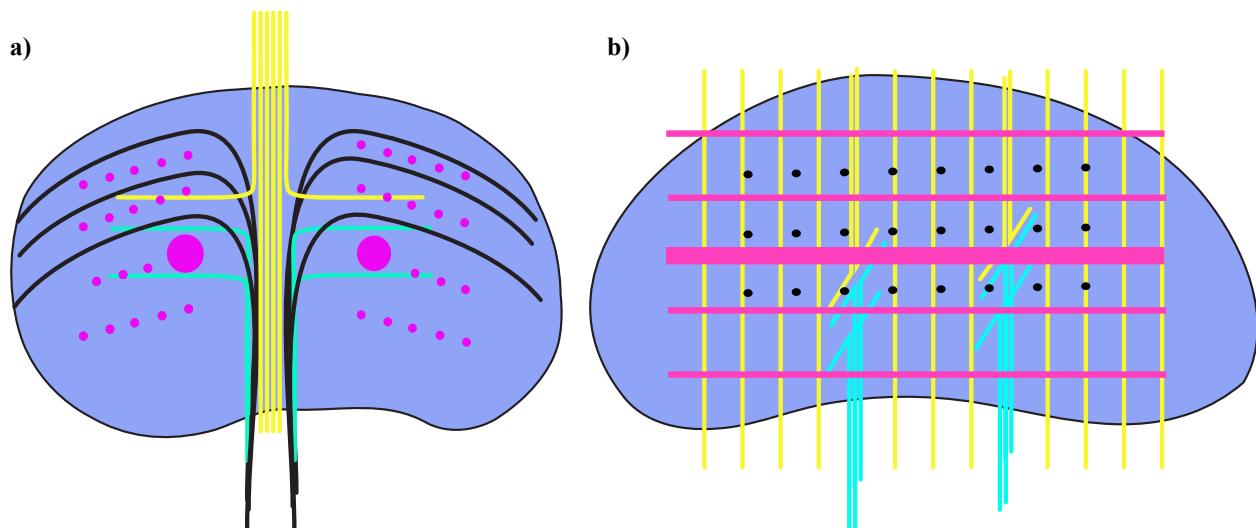


Figure 6.4.8. Model of major neuronal types and arrangements in the lobula. a) Sagittal section of the lobula showing the large T-shaped neurons in black, with orthogonally projecting neurons in pink including the two large fibre bundles indicated by large pink dots. Midband projections are shown in yellow while projections from the hemispherical parts of the lobula into the midband pathway is shown in turquoise. b) Coronal section of the lobula with the same colour coding of the neurons as described in a).

6.4.3 Discussion

Lobula structure

The lobula of the stomatopod follows a similar structure of columns and layers as found in other crustaceans (Strausfeld and Nässel, 1981, Sztarker et al., 2005, Harzsch and Hansson, 2008, Bengochea and Beron de Astrada, 2014). Comparing the number of main tangential layers to that of the crab *N. granulata* (Sztarker et al., 2005) shows that the stomatopod has one more LMT layer (LMT1-5) and at least one more DVT layer than in the crab (called *anteriorposterior tangential* (APT) layer in Sztarker et al. (2005) due to the different orientation of the eye). Bengochea and Berón de Astrada (2014) further divided the crab's layers by examining the lobula input strata. As this work has not yet been carried out in stomatopods we have stayed with the original layers as described in Sztarker et al. (2005).

In the crab *N. granulata* two of the LMT layers (LMT2 and LMT3) are formed by the bistratified branches of the movement detection neurons B-MDN (Beron de Astrada et al., 2001, Beron de Astrada and Tomsic, 2002, Sztarker et al., 2005). In addition the crab has 14 large neurons located in the APT4, which is a group of monostratified movement detection neurons (M-MDN) and are oriented orthogonally compared to the B-MDNs. These motion detection neurons have also been shown to be involved in binocular processing in crabs (Sztarker and Tomsic, 2004). Stomatopods also have large neurons running orthogonally, namely the large T-shaped neurons making up parts of the DVT layers and the large fibre bundles in the LMT layers, especially the two large bundles in LMT 3 containing thick, highly dendritic neurons (Fig. 6.4.8). Although there are some structural differences between the crab and stomatopod lobula layout, it is tempting to speculate that these orthogonally running neurons have a similar function to the movement detection neurons in crabs. Stomatopods are unusually quick crustaceans with a fast reaction time, so it would come as no surprise if they too have a well-developed movement detection circuit. The lobula plate neuropil, which has previously been identified in the crab (Sztarker et al., 2005) was not observed in these preparations. As this neuropil can be very small and easy to miss, further investigations are needed to confirm these observations.

Midband pathway

The lobula follows the same layout as the medulla in that the equatorial projections are still clearly visible throughout the neuropil, although without the distal swelling. Interestingly, it appears that some of the equatorial neurons project into the hemispherical parts of the lobula, forming lateral collaterals that spread across the achromatic mosaic. This could indicate that there is chromatic and

achromatic information integration taking place in the lobula, which would be a unique arrangement of channel mixing not seen in any other insects or crustaceans before. In addition there appear to be projections going from the hemispherical parts of the lobula into the equatorial pathway. In the bumblebee, colour and motion sensitivity are segregated by the different layers in the lobula (Paultk et al., 2008) and then projected in parallel to corresponding centres in the protocerebrum and median brain. The stomatopod midband lateral collaterals do indeed appear to project to different layers of the lobula, but it is not clear which part of the midband information project to the different layers of the lobula. Skorupski and Chittka (2010) suggested that chromatic information processing in photoreceptors may come at the cost of reduced speed compared to achromatic information processing. Could this be the reason stomatopods have segregated their chromatic system from the achromatic one? Processing the chromatic information separately from the achromatic may enable an increase in neuronal processing power in a small region and thereby saving energy in others? This may also allow the speeding up of chromatic processing speed allowing for signals to be integrated simultaneously further into the system e.g. in the lobula. Integrating the chromatic and achromatic information may also serve another purpose, relating to a feature of colour vision termed colour constancy. Colour constancy is the ability of the visual system to maintain stable colour perception under varying illumination. The proposed colour vision system in chapters 3 and 5 would necessitate achromatic input of the illuminant to later discount this factor when interpreting the perceived colour. The broadband, achromatic photoreceptors in the hemispheres would be able to provide this information, and the channel-mixing in the lobula would then initiate the colour constancy needed to ensure reliable colour perception.

Hemiellipsoid bodies

Projections from the olfactory lobes, which are the primary olfactory centres in the crustacean brain, are divided into two branches, each terminating in the hemiellipsoid body (Sullivan and Beltz, 2001b, Sullivan and Beltz, 2001a, Sullivan and Beltz, 2004). In their 2004 paper Sullivan and Beltz investigated the hemiellipsoid in stomatopods using lipophilic dyes and compared it to higher order species of decapods. They found that the olfactory pathway in stomatopods project only to the outer layers of the hemiellipsoid body in addition to having projections into other parts of the lateral protocerebrum (previously termed *medulla interna*). As found in this study, they also saw differential binding to synapsin in the hemiellipsoid body core, dividing it up into several layers. Although some decapods also have projections from accessory lobes which innervate parts of the hemiellipsoid body (Sullivan and Beltz, 2001b), Derby et al. (2003) and this study have found no sign of accessory lobes in stomatopods, suggesting that this is not the case here. An interesting aspect is the fact that in some insects the mushroom bodies have been found to process visual input,

either as part of a complete modality switch (Lin and Strausfeld, 2012) or by topographical division of the different modalities into separate areas (Kinoshita et al., 2014). The distinct projections of olfactory neurons into the outer layers of the hemiellipsoid body in stomatopods could suggest that the inner core could have a different function, perhaps processing visual information?

Glomeruli and the glomerular complex

Glomeruli complexes in flies have been shown to receive projections directly from specific types of lobula columnar neurons and also from wide-field neurons in the lobula receiving input from the medulla (Strausfeld and Bacon, 1983, Strausfeld and Lee, 1991, Otsuna and Ito, 2006, Strausfeld and Okamura, 2007). These glomeruli were shown to code noisy visual primitives from single lobula output neurons, thereby providing reliably coded information from converging sensory inputs (Mu et al., 2012). In *Drosophila*, relays from the glomeruli in the lateral protocerebrum projects to higher centres of processing such as the central complex (Liu et al., 2006, Strausfeld and Okamura, 2007) through the dorsal protocerebral lobes. But they also convey information to the rest of the body through interactions with the giant descending neurons (Mu et al., 2014), which project to the thoracic ganglia. Although we still do not know the function of the glomeruli and why they are gathered in a large glomerular complex in the stomatopod protocerebrum, it is likely that the large variety of shapes and sizes of glomeruli indicate different types of information inputs, possibly from different types of visual modalities.

6.4.4 Summary and future questions

The lobula of the stomatopod is stratified and has two more main layers than the crab. It does not appear to have the same motion detection neurons which the crab have in the proximal part of the lobula, but it does have larger T-shaped cells and fibre bundles in the distal part of the lobula that could be involved in motion detection. The stomatopod lobula appears to integrate the chromatic and achromatic information in the lobula, demonstrating a system of channel mixing not been seen before in other animals. In the lateral protocerebrum a neuropil termed the glomerular complex receive projections from the lobula. Some projections may also reach the hemiellipsoid body, which is normally involved in processing olfactory cues. These findings lead to new questions: Could the stomatopods have glomeruli that specifically process chromatic or polarization information? Clusters of glomeruli have been observed in other insects and crustaceans, but not to the extent of them forming a new neuropil. One future project worth undertaking would be to record electrophysiologically from the optic glomeruli in the stomatopods protocerebrum. As the retinotopic columnar neurons in the medulla and lobula (LCN) are very thin and consequently hard to record from it may be simpler to attempt recordings of the glomeruli responses. The glomeruli

would integrate input signals and respond to the summed response of a subset of lamina columnar neurons. Such recordings would hopefully provide some insight into how specific visual input in the retina is processed through the first three optic lobes.

Subchapter 6.5

The stomatopod central brain

6.5 The stomatopod central brain

6.5.1 Introduction

In common with other stalk-eyed crustaceans and many insects, the brain of stomatopods is divided into three different parts, with one central brain and two optic lobe clusters including the lateral protocerebrum, located within the eyestalks. The brain centres in the eyestalk are connected with the central brain through the protocerebral tracts and optic nerves. Relatively few studies of the crustacean central brain have been undertaken (Chamberlain and Wyse, 1986, Blaustein et al., 1988, Sandeman et al., 1992, Utting et al., 2000, Sullivan and Beltz, 2001a, Harzsch and Hansson, 2008, Krieger et al., 2010), and there is still a lack of knowledge, in particular when it comes to the function of the different regions. Insects on the other hand, have been investigated in numerous studies (Strausfeld, 1976, Strausfeld, 2009b, Strausfeld, 2009a, Ito et al., 2014 as a few examples), with recent advances in genetic work on *Drosophila melanogaster* providing a new method of further understanding the circuitry of the brain (Heisenberg, 2003, Olsen and Wilson, 2008). The similarities in the neural organisation between the insect and crustacean brains have been pointed out several times and suggest a shared common ancestor between the insects and crustaceans (Averof and Akam, 1995, Friedrich and Tautz, 1995, Sinakevitch et al., 2003, Strausfeld and Andrew, 2011).

One of the best studied neuropils in insects is the midline neuropil termed the central complex. In most insects this complex consists of a protocerebral bridge (PB), a central body (CB) made up by an upper division (CBU or fanshaped body), and a lower division (CBL or ellipsoid body) and a pair of small ball-like structures called the noduli (Strausfeld, 1976, Heinze and Homberg, 2008, Ito et al., 2014). In malacostracan crustaceans the central bodies are still distinctive, but a few differences compared to the insects are evident. Their protocerebral bridge is smaller than in insects, the central body is usually wider and shallower and they also lack the paired noduli (Strausfeld, 2012). The central body consists of several different modules that are connected by different types of neurons, up to around 600 have been suggested by genetic analysis in *Drosophila* (Young and Armstrong, 2010) although this number will likely vary due to the different sensory and motor demands in different animals.

Another difference between the insect and crustacean brain is the lack of mushroom bodies (Stocker et al., 1990) in the latter. The mushroom bodies in insects receive input from the antennal lobes (the first neuropil of the olfactory pathway) and are thought to be involved in learning and memory of olfactory cues (Heisenberg, 2003). In crustaceans, the olfactory globular tracts (OGT) terminate in

neuropils that arise dorsally from the lateral protocerebrum which are called hemiellipsoid bodies (Sullivan and Beltz, 2001b, Sullivan and Beltz, 2001a, Sullivan and Beltz, 2004). These hemiellipsoid bodies have been suggested to be homologues of the mushroom bodies in insects and morphology, ultrastructure and immunoreactivity advocate the same (Wolff et al., 2012). Recent studies have also revealed that the mushroom bodies are capable of modality switching, processing visual information instead of olfactory information in aquatic species which generally lack antennal lobes (Lin and Strausfeld, 2012).

A few studies have previously investigated the stomatopod brain; Derby et al. (2003) examined the antennular and olfactory pathways, while Strausfeld (2012) provide images and brief discussions regarding the stomatopods central complex, olfactory and antennal lobes in relation to their evolutionary ancestry. As the final endpoint of the optic pathway described in the previous chapters, we wanted to investigate the stomatopod central brain, and especially structures such as the central complex, which have been shown to be involved in visual processing in other arthropods. Describing the various structures and relating these to homologous structures in other crustaceans and insects we found that the stomatopods have a central complex closer to that of insects than other crustaceans. These findings could hopefully give some cues to the final processing of the signals from their complex retinal array.

6.5.2 Results

Stomatopod central complex

The central complex in stomatopods consists of the protocerebral bridge, the central body and possibly also a set of paired noduli (Fig. 6.5.1 and 6.5.2). The paired noduli are small, round neuropils located proximally to the central body, which receives projections from columnar neurons in the PB and/or the CB. Structures resembling noduli have been observed in Bodian stained preparations, but have unfortunately not been imaged during synapsin or serotonergic staining. The protocerebral bridge is positioned along the anterior medial edge of the anterior median protocerebral neuropil (AMPN) beneath a cluster of cell bodies belonging to eight bundles of fibres that connect the protocerebral bridge, central body and the lateral lobes. It consists of a tightly packed weave of thick fibres with a median depression. The central body is positioned medially in the brain, proximally to the protocerebral bridge and extends heterolaterally across three-fourths of the median protocerebrum. It has a slight medial bend with its most lateral parts extending slightly proximally. The central body is clearly divided into an upper and lower part (bilayered) with the upper and lower division being of approximately equal thickness and divided by a dark line of fibres. The central body lies ventrally to the olfactory globular tract chiasm (Fig 6.5.1d and e).

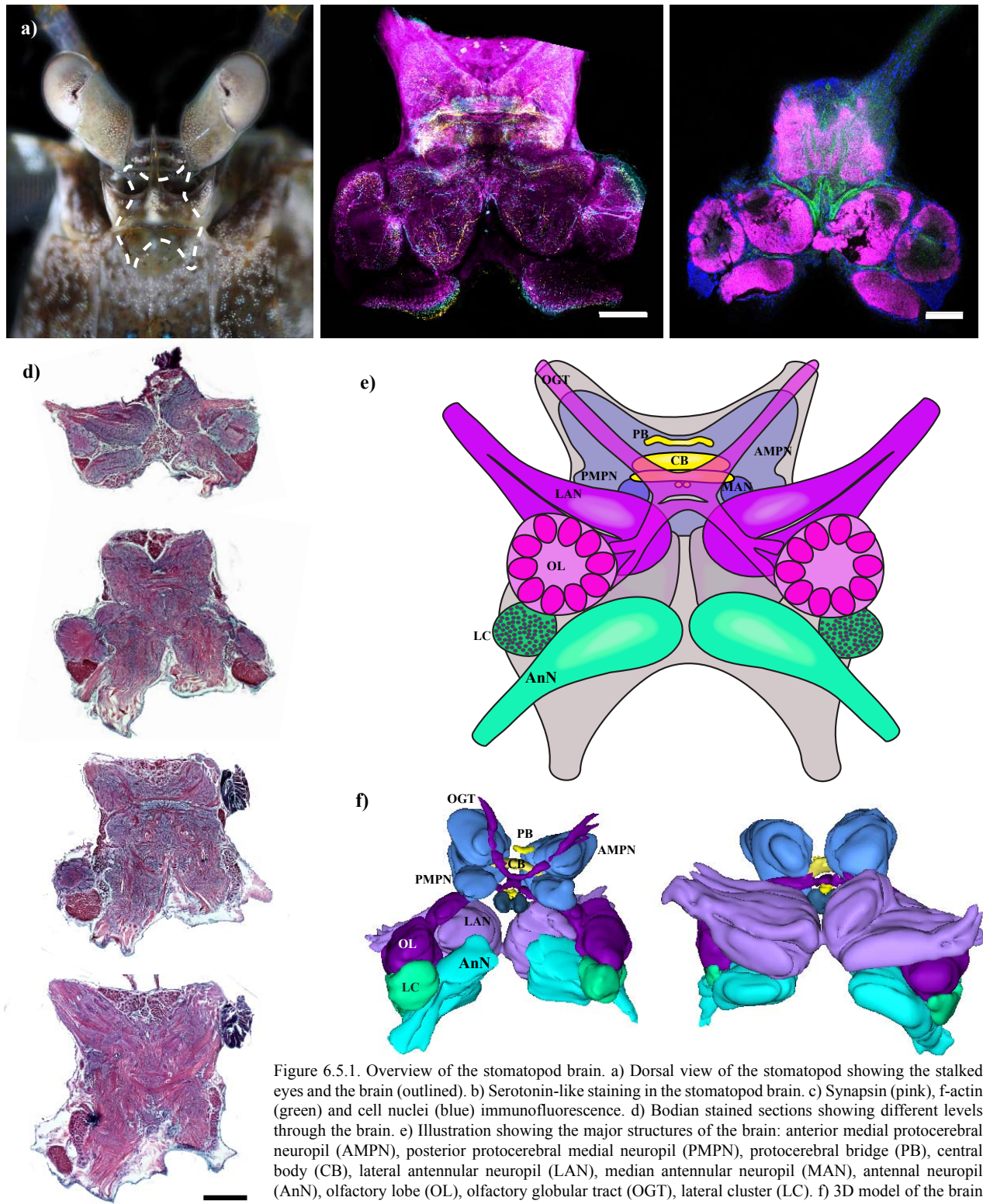


Figure 6.5.1. Overview of the stomatopod brain. a) Dorsal view of the stomatopod showing the stalked eyes and the brain (outlined). b) Serotonin-like staining in the stomatopod brain. c) Synapsin (pink), f-actin (green) and cell nuclei (blue) immunofluorescence. d) Bodian stained sections showing different levels through the brain. e) Illustration showing the major structures of the brain: anterior medial protocerebral neuropil (AMPN), posterior protocerebral medial neuropil (PMPN), protocerebral bridge (PB), central body (CB), lateral antennular neuropil (LAN), median antennular neuropil (MAN), antennal neuropil (AnN), olfactory lobe (OL), olfactory globular tract (OGT), lateral cluster (LC). f) 3D model of the brain showing the dorsal and ventral side of the brain with the same naming as in e). Scale bars: 200 μ m.

Neurons labelled by serotonin, synapsin, phalloidin and DAPI in the central complex.

Both the protocerebral bridge and the upper and lower division of the central body show serotonin-like labelling (Fig. 6.5.3). Serotonergic neurons are also visible projecting from the central body into both the AMPN and the PMPN. The synapsin strongly labelled the protocerebral bridge, but in the central body the stain was very weak. Phalloidin labelled both structures clearly. Unfortunately, the noduli were not imaged in these preparations.

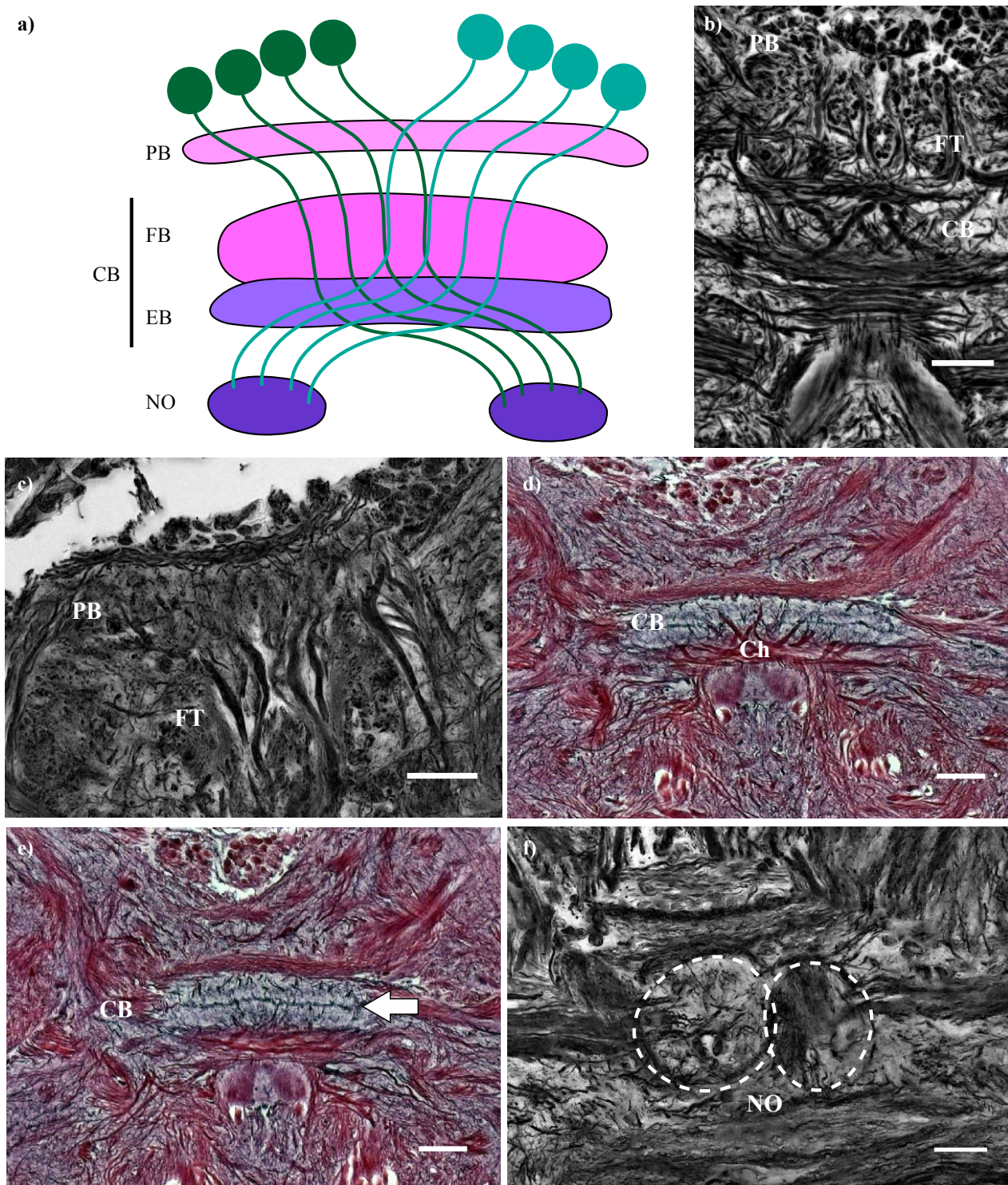


Figure 6.5.2. Stomatopod central complex: a) Illustration showing the generalised layout of the central complex (adapted from Strausfeld 2012). Protocerebral bridge (PB), central body (CB), fanshaped body (FB) ellipsoid body (EB), noduli (NO). b) Bodian stained section showing the protocerebral bridge, the central body and the large fiber tracts (FT). c) Protocerebral bridge and large fibre tracts. d) Large axons chiasma (Ch) e) Central body divided into two parts (arrow). f) Possible noduli (marked). Scale bars: b) 50µm, c) to f) 20µm.

Mass filling of neurons

Injections into lateral protocerebrum spread through the olfactory globular tract and the optic nerve into various areas of the brain. Some projections terminated in the AMPN and the PMPN (posterior protocerebral neuropil) while others filled neurons in the OGL, which reached the olfactory lobes and labelled structures there (Fig. 6.5.4). Injections that reached the PB also filled cell nuclei

positioned anterior to the PB, likely belonging to the nerve fibre bundles projecting through the PB and CB.

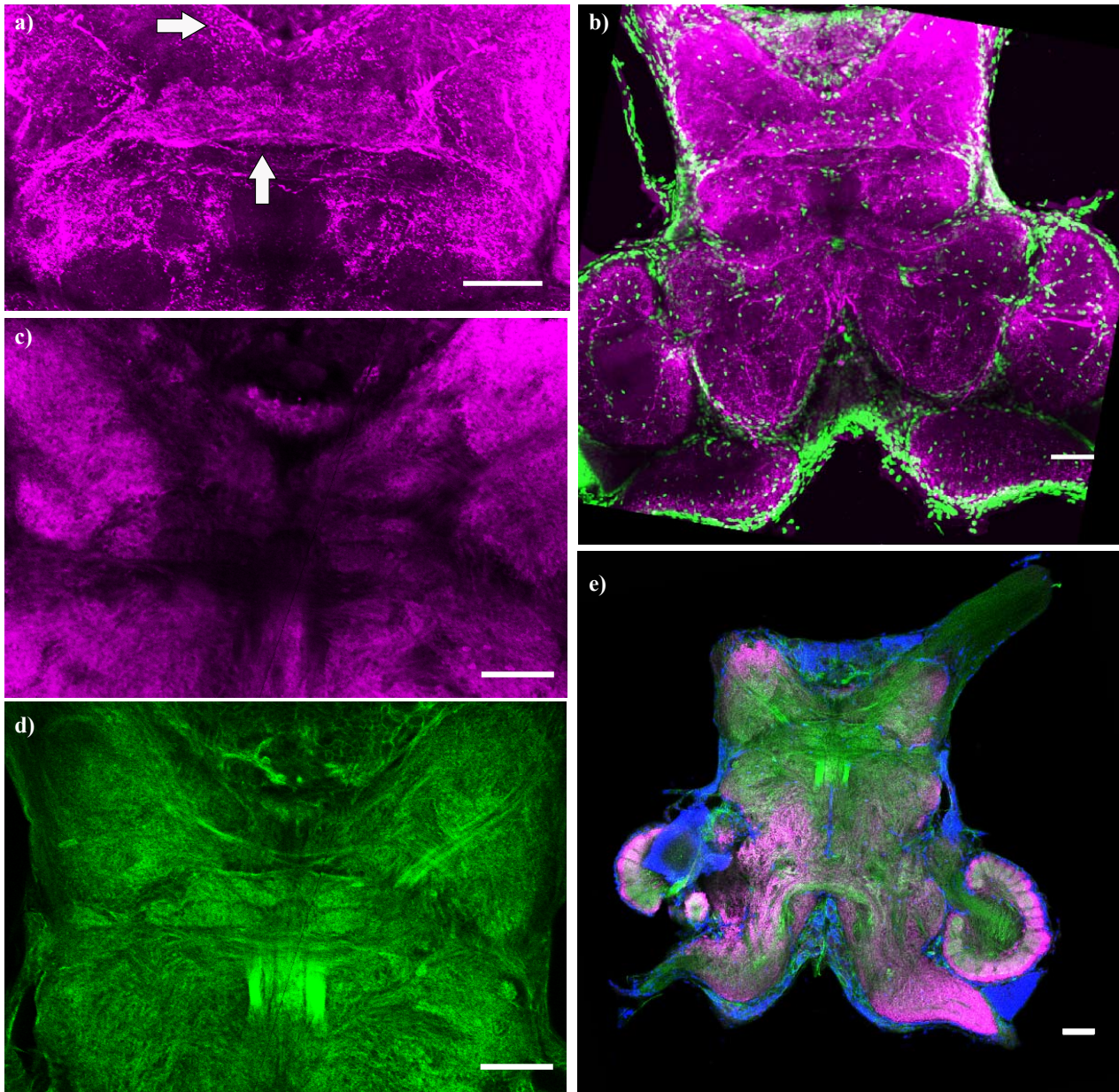


Figure 6.5.3. Immunofluorescence in the stomatopod brain. a) Serotonin-like staining of the central complex showing strong labelling in the protocerebral bridge and the central body (arrows). b) Serotonin-like staining of the whole brain showing labelling in the central complex as well as the olfactory lobes, antennal sensory neuropil, and the AMPN and LMPN. c) and d) labelling of synapsin (purple) and f-actin (green) in the central complex showing little labelling of synapsin in the central body but stronger labelling in the protocerebral bridge. e) Synapsin (pink), f-actin (green) and cell-nuclei (blue) labelled in the whole brain. Scale bars: 100 μ m.

Olfactory and antennular pathways

In stomatopods there are three sets of neuropils that receive antennular input; the olfactory lobes (OL) the lateral antennular lobes (LANs) and the median antennular neuropil (MAN). The olfactory lobes in stomatopods are positioned laterally on each side of the brain. They have a clear glomerular structure, with small round structures making up the modules within the lobe. Each glomerulus is also divided up into a clearly stratified outer cap with an inner core (Fig. 6.5.5 c and d). A cluster of nuclei, termed the lateral cluster (LC) belonging to the olfactory lobe neurons, is positioned

proximally to each olfactory lobe. The olfactory lobe is connected to higher processing centres (the protocerebrum and hemiellipsoid body) through the olfactory globular tract (OGT). No accessory lobes have been identified.

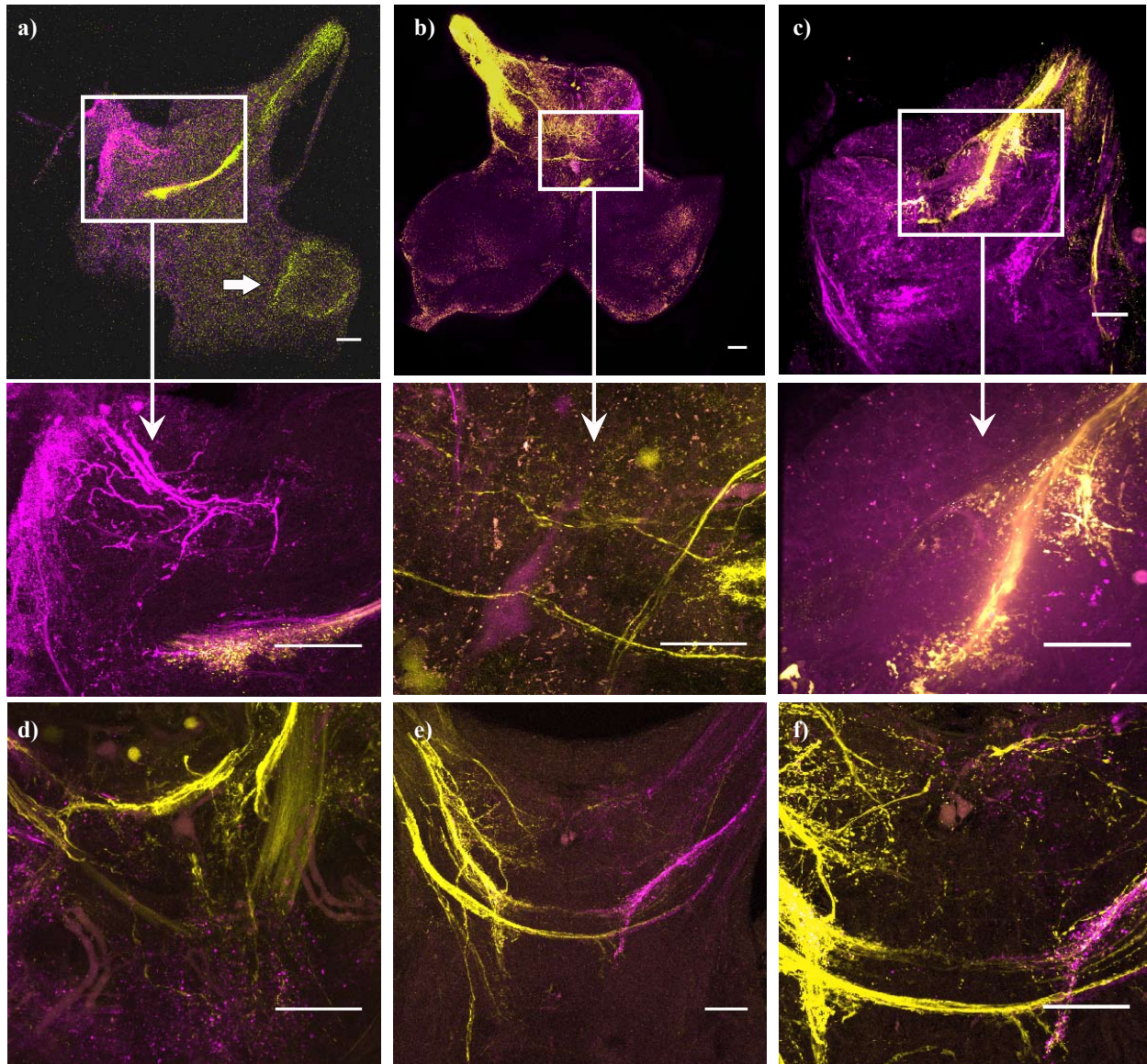


Figure 6.5.4. Mass fillings of dextran conjugated with Texas red or Fluorescein into the protocerebrum: a) Insertion into the protocerebrum and hemiellipsoid body using Texas red in the left eye (pink) and Fluorescein in the right (yellow). The Texas red has spread into the anterior median protocerebral neuropil (AMPN) while the Fluorescein has followed the olfactory globular tract (OGT). Notice the spread into the olfactory lobe through the OGT. b) Fluorescein and Texas red has both spread into the OGT. Notice the dye filled somata anteriomedially. c) Fluorescein has spread into the AMPN, while Texas red has followed the OGT. d) Fluorescein has spread into the protocerebral bridge (PB) and cell bodies anterior to the PB. Texas red did not fill successfully in this preparation. e) and f) Fluorescein and Texas red has both spread through the OGT and into parts of the AMPN. Scale bars: 100 μ m.

Serotonin-, synapsin- and phalloidin-like staining was observed in the olfactory lobes (Fig 6.5.5). Both the glomeruli-like subunits and the interneurons and relay neurons in the olfactory lobes show strong labelling to serotonin (5-HT) and synapsin. Serotonergic interneurons are clearly visible projecting between glomeruli inside the olfactory lobe (Fig. 6.5.5 e). There is a strong labelling of synapsin in the cap of each glomerulus, with weaker labelling in the core. Bundles of relay neurons sending their projections to the olfactory globular tract neuropil (OGTN) are clearly labelled using phalloidin, which binds to filamentous actin in the nerve fibres.

The LAN in stomatopods is large and bilobed, consists of layers and columns and has fibres running down the middle of the lobes with processes running perpendicularly from these. Both the Bodian and Golgi staining reveal these types of neurons (Fig. 6.5.5). The processes are axons from the chemo- and mechano- receptor neurons, which terminate as branched endings at a depth that reflects its origin along the antennule. The depth at which the branched terminals terminate in the antennal lobe determines where it originated along the antennule. A region medially to the LAN is distinguishable as the median antennule neuropil (MAN) although it is not clearly delineated. It is smaller than MANs in other decapods and has a relatively low number of serotonergic neurons. The antennal sensory neuropil (AnN) resides mediolaterally in the tritocerebrum proximal to the olfactory lobes and is primarily mechanosensory.

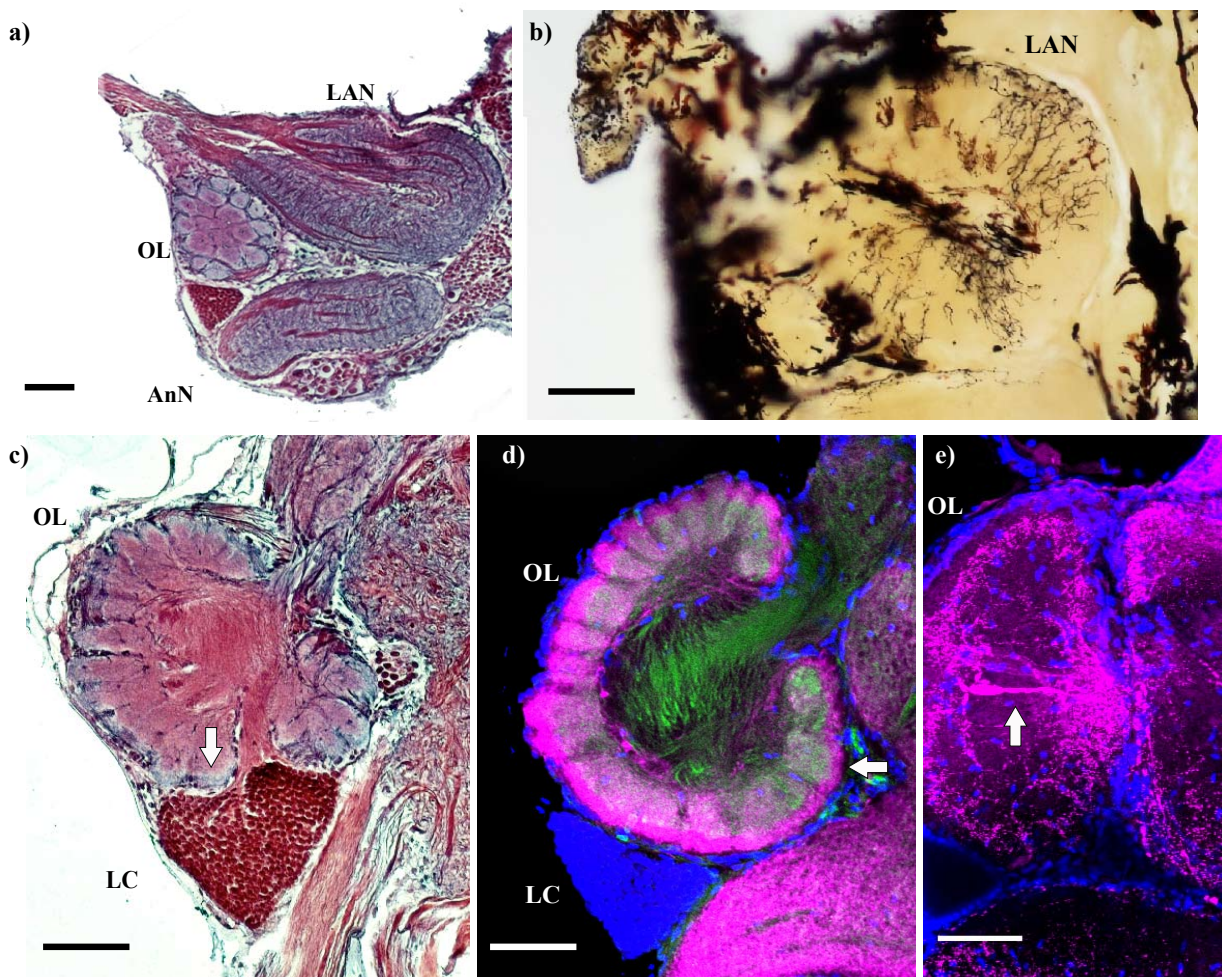


Figure 6.5.5. Olfactory lobes. a) Bodian stained section showing the olfactory lobe (OL), the lateral antennal lobe (LAN) and the antennal neuropil (AnN). b) Golgi stained LAN showing the branched terminals of the antennal neurons. c) Olfactory lobe with its cell bodies in the lateral cluster (LC). Note the cap and core structure of the glomeruli (arrow) d) Synapsin (pink), f-actin (green) and cell-nuclei (blue) stained olfactory lobe, showing the cap and core structure of each glomerulus. e) Sertolin-like staining in the olfactory lobes show the interneurons projecting between each glomerulus (arrow). Scale bars: 100μm

6.5.3 Discussion

At first glance the stomatopod central brain appears similar to other crustacean brains (Sandeman et al., 1992, Harzsch and Hansson, 2008), but a closer look reveals structures that are more

reminiscent of those found in insect brains. First, stomatopods have a pronounced protocerebral bridge, which is larger than that found in other crustaceans. Secondly, the central body is prominent, and is divided into two parts, as opposed to the singular central body found in other crustaceans such as crabs (Krieger et al., 2010) and crayfish (Upping et al., 2000). Lastly, stomatopods appear to have a pair of small neuropils called the noduli, which are present in many insects but not in any other crustacean investigated so far. The identification of these noduli is still not confirmed, but structures similar to noduli have been observed. Both the protocerebral bridge and the central body showed strong serotonin-like labelling, while only the protocerebral bridge was stained with the anti-synapsin antibody. The significance of this is not yet known but insect-like neuroanatomy has been noted before in stomatopods (Strausfeld and Nässel, 1981).

So what is the purpose of the central complex? According to research performed on locusts, the central complex seems to be involved in tasks such as spatial orientation, motor planning and goal directed behaviours (Homberg, 1994b, Homberg, 1994a, Homberg and Würden, 1997, Homberg et al., 2003, Heinze and Homberg, 2008, Homberg et al., 2011, Bech et al., 2014, Heinze, 2014). It also appears to be involved in encoding information about e-vector angles of polarized light, probably used for sky compass navigation (Heinze and Homberg, 2007). In insects, the central complex consists of three principle classes of neurons; the columnar neurons, which connect the protocerebral bridge to the central body and the lateral accessory lobes; the tangential neurons, which innervate single layers of the central body or protocerebral bridge and connect specific areas in the brain; and the pontial cells, which are intrinsic elements cells that connect specific columns and layers in the central complex (Heinze and Homberg, 2008).

The antennular and olfactory pathways in stomatopods have been investigated previously by e.g. Derby et al. (2003) and Sullivan and Beltz (2004) and we will therefore not go into any details about these structures other than to remark upon one additional similarity with the insect brain. The olfactory lobes of insects and crustaceans are composed of subunits termed glomeruli. In insects these glomeruli are round or ovoid structures, while crustaceans are known to have glomeruli that are elongated and wedge shaped. The glomeruli found in stomatopods have a round form more similar to the ones found in insects, except for the stratification into a cap and core for each glomerulus.

6.5.4 Summary and conclusion

The stomatopod central complex share more similarities with the insect central complex than that of other crustaceans. The same is also seen in the round insect like glomeruli found in the stomatopod

olfactory lobes. The similarities of the stomatopods brain to insects are fascinating, and may shed more light on the evolutionary relationships between these animal groups. The significance of these structures in relation to the processing of the complex retinal structures is still not known, and will require further investigations using electrophysiological recordings and single cell tracings. It is likely that the main portion of the processing of the spectral and polarization information have already taken place in the optic lobes and lateral protocerebrum, however it would be of great interest to find out if the stomatopods also process information regarding e-vector angles in the central complex such as found in locusts (Heinze and Homberg, 2008, Heinze and Homberg, 2009, Homberg et al., 2011), and how other visual features is represented in these structures. Does the stomatopod use neural processing paradigms similar to that of insects or has it yet again evolved a different way of doing it? Of particular interest here is recent evidence, based on stomatopod bio-inspired cameras that the underwater polarization field might be used for navigation (Powell and Gruev, 2014).

Chapter 7

Summary and future directions

7 Chapter 7. Summary and future directions

The work presented in this thesis provides new insights into how the complex colour and polarization vision of stomatopods work. Both behaviourally and neuroanatomically stomatopods appear to use a different type of colour vision than other animals (Marshall and Arikawa, 2014), which is based on simplified sampling of colours to enable quick and reliable colour judgements. For an aggressive animals like the stomatopod (Dingle and Caldwell, 1969, Adams and Caldwell, 1990), with many types of chromatic signalling displays used in complex behavioural situations (Steger and Caldwell, 1983, Caldwell, 1992, Cheroske et al., 1999, Mazel et al., 2003), having such colour vision may be beneficial and warrant the loss of fine colour discrimination. Behavioural studies carried out by How et al. (2014a, 2014b) on the stomatopods ability to discriminate different angles of polarised light indicate that their polarization vision may also function on similar simplified principles.

7.1.1 Major findings:

The electrophysiological recordings of spectral sensitivities across several species of Gonodactyloid stomatopods confirmed that they have very similar sensitivity maxima (λ -max) (Chapter 2). Similar results have been recorded previously using microspectrophotometry (MSP) (Cronin and Marshall, 1989b, Cronin and Marshall, 1989a, Cronin et al., 1993, Cronin et al., 1994e, Cronin et al., 1996, Chiao et al., 2000) but as intracellular electrophysiological recordings provide a more accurate estimate of the spectral sensitivities due to a minimal disturbance to the light path and photoreceptors themselves, we wanted to confirm the previously obtained results in this study. The positioning of their sensitivity maxima suggests that their placement may serve a specific purpose in their proposed colour-encoding scheme. The stomatopods sensitivities are evenly spread out across the spectrum, and have very narrow and steep sensitivity functions (shapes). As most other animals are able to detect and discriminate colours well across the spectrum with only three or four broadband spectral sensitivities, the stomatopods number and shape of photoreceptors implies a different type of colour vision is used (Marshall and Arikawa, 2014)

Spectral discrimination tests using peak-shaped narrowbanded spectral stimuli revealed that stomatopods have surprisingly poor discrimination throughout the spectrum (Thoen et al., 2014, Chapter 3) both compared to modelled spectral discrimination and to other animals. Modelled narrow and steep sensitivities in an opponent processing scheme produce very fine discrimination due to the large ratio differences in the signals from two sensitivities and this has previously been suggested to provide high-performance colour constancy (Osorio et al., 1997). Behavioural

discrimination testing using step-shaped spectra were carried out (Chapter 4), as a more natural shaped spectra could possibly influence their discrimination abilities. Many natural colours, especially in the longer wavelength part of the spectrum are step-shaped rather than peak-shaped, and it could be that these would be more easily discriminated by the stomatopods. But as in the experiments using peak-shaped spectra, the discrimination ability remained poor. These behavioural results coupled with their multiple spectral sensitivities lead to the hypothesis that the stomatopod may use a different form of colour vision than the conventional opponent system found in other animals (Marshall and Arikawa, 2014, Thoen et al., 2014, Chapter 3). Such a system may be based on a relatively simple interval-decoding scheme, where perceived colour corresponds to the peak sensitivity of the most responsive photoreceptor (Zaidi et al., 2014, Chapter 5). Interestingly, such a system could also work for the narrowly tuned cells found in the inferior temporal cortex (IT) in primates, which although being at a different stage in the processing pathway have surprisingly similar sensitivity functions. As the primates only have three broadband spectral sensitivities they are able to maintain good spatial resolution at the retina level, with the millions of colour-tuned cells in the IT cortex would generate narrower tuning using the stages of processing suggested in Chapter 5. Stomatopods loose the spatial resolution by only having 6 rows of colour receptors at the first level of processing and have to compensate by using scanning eye movements to sample the entire visual field. This system probably provides them with a quick and reliable colour recognition system, possibly with good colour constancy, but at the cost of good spatial resolution. These findings suggest that very similar computational strategies are used in two largely unrelated species and are an interesting example of the same robust computational strategy being used across independent evolutionary histories.

7.1.2 Summary of new neuroanatomical findings:

While the stomatopods retinal structures have been studied extensively, very little was known about their visual neural architecture and a selection of different methods was therefore used to provide a clearer image the structure of the optic lobes and the processing pathways. The following summarises the main findings from this study:

- a) The lamina have similar neuronal types to what is found in the lamina of other crustaceans and insects, and the lamina midband lobe does not appear to have specialised neurons other than being larger than the hemispherical neurons.
- b) The stomatopods medulla is strongly stratified compared to other crustaceans, and the midband projections are visible as swelling (medulla midband lobe) on the distal side, which narrows and

projects through to the proximal part of the medulla and continues on to the lobula. Y-shaped Golgi impregnated neurons appear often in the medulla midband lobe, but are not often seen in the rest of the medulla. We therefore speculate if these neurons could be involved in the chromatic processing pathway.

c) Midband neurons project from the medulla down to the lobula, where a part of the neurons form lateral collaterals that spread and integrate into the hemispherical regions of the lobula. Such a mixing of chromatic and achromatic channels have not been shown in other animals before, and it is tempting to speculate if this mixing could be involved in providing colour constancy which is needed to maintain good colour vision. Further investigations are needed however, to determine if this is the case. Large T-shaped neurons and bundles of tangential neurons were identified in the lobula, which could be involved in the processing of motion stimuli.

d) Proximal to the lobula a distinct neuropil was identified, containing various sizes of glomeruli and their interneurons. Certain projections from the lobula reach this neuropil, although it is not known which types of glomeruli they contact. In insects optic glomeruli have been shown to be involved in sharpening and refining the signal from the thin and noisy lobula neurons (Mu et al., 2012), and it is possible that this glomerular complex neuropil could be involved in similar processes in the stomatopods.

e) Another distinct structure in the lateral protocerebrum of stomatopods is the hemiellipsoid body, which process olfactory information from the antennal lobes. The hemiellipsoid body is thought to be homologous with the mushroom body in insects. Recently a modality switch between visual and olfactory input have been observed in the mushroom bodies of some insects (Lin and Strausfeld, 2012, Kinoshita et al., 2014) indicating a plasticity in the processing system. It has been shown in previous studies that the stomatopod hemiellipsoid bodies are layered, and that olfactory neurons only project to the outer layers of the hemiellipsoid body with no apparent projections to the core (Sullivan and Beltz, 2004). Results from the Bodian staining in this study indicates axonal projections from the lobula to the hemiellipsoid body, which could suggest that the stomatopod hemiellipsoid body is involved in visual in addition to olfactory processing. This, however, still needs to be confirmed with dye injections and tracings.

f) The stomatopods central complex has a similarity to an insect's central complex with a prominent protocerebral bridge, a two-part central body and possibly also two noduli. Strausfeld (2012) presented a few images of the stomatopod insect-like central complex, while this study investigated

the central complex closer using serotonergic and synapsin antibodies in addition to Bodian stained sections. A two part central body and noduli have not been seen in other crustaceans and may provide new clues to the phylogenetic relationship between crustaceans and insects. How the central complex is involved in the processing of information from the midband and hemispheres is one of the questions that will be interesting to investigate in the future.

7.1.3 Use of stomatopods as study animal

Despite the unconventional complexity demonstrated by the stomatopods visual system, this study supports the idea that stomatopods are an excellent study animal to investigate the principles of colour decoding. Unlike other crustaceans, they can relatively easily be trained to perform specific tasks relative to specific objects and their colour and polarization vision abilities can therefore be tested through various behavioural experiments. Their stalk-eyed nature is also beneficial for studying visual neuroanatomy and recording from specific neurons. While most insects have their optic lobes embedded within the brain region itself, the fact that stomatopods have their optic lobes contained within the eye stalks enables easy access to a compartmentalised system that can even be kept alive for recordings and injections after being removed from the animal itself.

Also, the compartmentalizing of the colour and part of the polarization vision system in a small region, distinctly visible through at least the three first optic lobes, means that there are very clear areas to target. Since it is likely that the retinal information within the midband is kept retinotopic at least until the second optic lobe (the distinction between row 1-4 and row 5 & 6 is still visible in the medulla midband lobe), we can even target specific areas within the medulla midband lobe as potential areas for electrophysiological recordings. Since von Frisch (1914) established that the bees indeed have true colour vision, numerous studies have used an array of techniques including behaviour, genetics, immunolabelling and electrophysiology (von Helversen, 1972, Morante and Desplan, 2008, Pault et al., 2008, Pault et al., 2009, Hamanaka et al., 2013 to mention a few) to investigate the principles of colour vision and colour decoding. Although many discoveries have been made there are still many unknowns about how colour is actually processed, especially when it comes to the location, morphology and response properties of the neurons involved in colour processing. The stomatopod could be an excellent candidate to learn more about these properties.

Inspiration from nature

Biomimicry, the concept of taking ideas from natural systems and using them as inspirations for new technology has been an emerging field in the last few decades. As mentioned in the introduction, the stomatopods have already been such an inspiration in the development of a new

type of polarised material (Jen et al., 2011) based on the structure of their R8 cells (Roberts et al., 2009) and recently a type of imaging sensor has been developed (Gruev et al., 2010, Kulkarni and Gruev, 2012) based on the stomatopods visual system which uses polarized light to perform optical neural recordings and even to detect certain types of cancer (York et al., 2014). Knowledge regarding the processing and analysis of colours could provide very valuable knowledge when it comes to technologies involving measuring chromatic spectra such as hyperspectral imaging sensors. Remote sensing has to an extent learned from, if not taken direct inspiration from the stomatopod eye (Bar - Choén, 2011, Wolpert, 2011). As the stomatopod colour vision appears to be based on a sparse signal-processing scheme (Marshall and Arikawa, 2014, Thoen et al., 2014, Chapter 3) it could again provide inspiration for artificial imaging systems that require quick and low-power processing speed.

7.1.4 Future directions:

This study has given insights into the way the stomatopods visual system work, but as with any research it has also provided many new questions. Especially in regards to the neuroanatomical side of the stomatopod visual system there are many perspectives to investigate, with some of the main ones of interest to the author listed below:

- Investigations into the synaptic connections between the arborizing R8 axons (lvfs) and the monopolar cells in the lamina are needed to further understand what information is relayed to the medulla and if there is processing of chromatic and polarization signals taking place before this information is transferred to the medulla. Ultrastructure investigations of the lamina cartridges using the novel GATAN 3view system are planned and will hopefully determine the synaptic connections between the cells within the lamina cartridge. Electrophysiological recordings of the monopolar relay cells (M3 and M4) which are postulated to relay chromatic and polarization information will hopefully reveal in what form this information is conveyed to the next processing level.
- The significance of the extensive layering of the stomatopod medulla would be interesting to investigate as previous studies in insects have suggested that medulla layers work as computational devices which reconstruct elements of the visual scene such as edge detection, motion etc. (Ribi and Scheel, 1981, Glantz, 1996b, Glantz, 1998, Strausfeld, 2012). Medulla layers have also shown to be involved in simple to more complex chromatic processing in bees (Pauk et al., 2009), and it would be of interest to examine if something similar happens within the medulla midband lobe. In addition, mapping out the neuronal types and their connections in the medulla midband lobe (and possible

connection to the hemispherical regions) would likely be very informative when it comes to understanding the transfer and processing of chromatic and polarization information in this region. Golgi impregnations of neurons in the medulla midband would probably be the best technique for such an investigation, and some of this work is already underway.

- In the lobula, one of the main questions to work out is the function of the lateral collaterals that project from the midband to the hemispheres. As lobula neurons are very thin and are known to be hard to record from this task has some challenges. Using mass fillings of neurons in the medulla midband lobe to trace their axonal trajectories into the lobula may at least provide the morphological aspect of these interactions. One solution may be to omit the lobula entirely and record directly from the optic glomeruli in the protocerebrum as these are likely involved in processing information from the lobula columnar neurons. As the number of types of lobula columnar neurons have been linked to the number of optic glomeruli in the lateral protocerebrum of insects (Strausfeld, 2012), mapping out the stomatopods optic glomeruli using immunohistochemistry and labelling them with fluorescent dye or cobalt injections which spread into the lobula columnar neurons could also provide useful information about their function.

- Finally, more detailed investigations into the central complex of stomatopods may also provide us with clues to their visual processing and perhaps also evolutionary relationships. Recordings from optic nerve would likely be useful to gain knowledge about the data being transferred from the optic processing centres to the central brain and injections into these neurons could determine the endpoint of such as data stream in the central brain. Mapping out and recording from neurons in the central complex itself would then be the next step in understanding the final endpoint of the stomatopods visual neuronal architecture.

8 References

- Adams, E. & Caldwell, R. 1990. Deceptive communication in asymmetric fights of the stomatopod crustacean *Gonodactylus bredini*. *Animal Behaviour*, 39, (4), 706-716.
- Ahyong, S. T. & Harling, C. 2000. The phylogeny of the stomatopod Crustacea. *Australian Journal of Zoology*, 48, (6), 607-642.
- Ahyong, S. T. 2001. Revision of the Australian Stomatopod Crustacea. *Records of the Australian Museum Supplement*, 26, 1-326.
- Ahyong, S. T. & Jarman, S. N. 2009. Stomatopod interrelationships: preliminary results based on analysis of three molecular loci. *Arthropod Systematics & Phylogeny*, 67, 91-98.
- Arikawa, K. 2003. Spectral organization of the eye of a butterfly, *Papilio*. *Journal of Comparative Physiology A*, 189, (11), 791-800.
- Armett-Kibel, C., Meinertzhagen, I. & Dowling, J. 1977. Cellular and synaptic organization in the lamina of the dragon-fly *Sympetrum rubicundulum*. *Proceedings of the Royal Society of London. Series B, Biological Sciences*, 196, (1125), 385-413.
- Averof, M. & Akam, M. 1995. Insect-crustacean relationships: insights from comparative developmental and molecular studies. *Philosophical Transactions of the Royal Society of London. Series B: Biological Sciences*, 347, (1321), 293-303.
- Bacon, J. P. & Altman, J. S. 1977. A silver intensification method for cobalt-filled neurones in wholemount preparations. *Brain Research*, 138, (2), 359-363.
- Bar - Choen, Y. 2011. *Biomimetics; nature based innovation.*, Boca Raton, FL, CRC press.
- Barlow, H. B. 1982. What causes trichromacy? A theoretical analysis using comb-filtered spectra. *Vision Research*, 22, (6), 635-643.
- Bausenwein, B. & Fischbach, K.-F. 1992. Activity labeling patterns in the medulla of *Drosophila melanogaster* caused by motion stimuli. *Cell and tissue research*, 270, (1), 25-35.
- Bech, M., Homberg, U. & Pfeiffer, K. 2014. Receptive fields of locust brain neurons are matched to polarization patterns of the sky. *Current Biology*, 24, (18), 2124-2129.
- Bellonci, G. 1882. *Intorno alla struttura e alle connessioni dei lobi olfattorii negli Artropodi superiori e nei Vertebrati*, coi tipi del Salviucci.
- Bengochea, M. & Beron De Astrada, M. 2014. Organization of columnar inputs in the third optic ganglion of a highly visual crab. *Journal of Physiology*, 108, (2), 61-70.
- Beron De Astrada, M., Sztarker, J. & Tomsic, D. 2001. Visual interneurons of the crab *Chasmagnathus* studied by intracellular recordings in vivo. *Journal of Comparative Physiology A: Neuroethology, Sensory, Neural, and Behavioral Physiology*, 187, (1), 37-44.
- Beron De Astrada, M. & Tomsic, D. 2002. Physiology and morphology of visual movement detector neurons in a crab (Decapoda: Brachyura). *Journal of comparative physiology. A, Neuroethology, sensory, neural, and behavioral physiology*, 188, (7), 539-551.
- Blaustein, D. N., Derby, C. D., Simmons, R. B. & Beall, A. C. 1988. Structure of the brain and medulla terminalis of the spiny lobster *Panulirus argus* and the crayfish *Procambarus clarkii*, with an emphasis on olfactory centers. *Journal of Crustacean Biology*, 8, (4), 493-519.
- Bodian, D. 1936. A new method for staining nerve fibers and nerve endings in mounted paraffin sections. *The Anatomical Record*, 65, (1), 89-97.
- Bok, M. J., Porter, M. L., Place, A. R. & Cronin, T. W. 2014. Biological sunscreens tune polychromatic ultraviolet vision in mantis shrimp. *Current Biology*, 24, (14), 1636-1642.
- Boudko, D. Y., Switzer-Dunlap, M. & Hadfield, M. G. 1999. Cellular and subcellular structure of anterior sensory pathways in *Phestilla sibogae* (Gastropoda, Nudibranchia). *Journal of Comparative Neurology*, 403, (1), 39-52.
- Buschbeck, E. K. & Strausfeld, N. J. 1996. Visual motion-detection circuits in flies: small-field retinotopic elements responding to motion are evolutionarily conserved across taxa. *The Journal of Neuroscience*, 16, (15), 4563-4578.

- Buschbeck, E. K. 2000. Neurobiological Constraints and Fly Systematics: How Different Types of Neural Characters Can Contribute to a Higher Level Dipteran Phylogeny. *Evolution*, 54, (3), 888-898.
- Caldwell, R. L. & Dingle, H. 1975. Ecology and evolution of agonistic behavior in stomatopods. *Naturwissenschaften*, 62, (5), 214-222.
- Caldwell, R. L. & Dingle, H. 1976. Stomatopods. *Scientific American*, 234, (1), 80-89.
- Caldwell, R. L. 1992. Recognition, signalling and reduced aggression between former mates in a stomatopod. *Animal Behaviour*, 44, (1), 11-19.
- Chamberlain, S. C. & Wyse, G. A. 1986. An atlas of the brain of the horseshoe crab *Limulus polyphemus*. *Journal of Morphology*, 187, (3), 363-386.
- Cheroske, A. G., Cronin, T. W., F. M. & Caldwell, R. L. 1999. Adaptive signalling behaviour in stomatopods under varying light conditions. *Marine and Freshwater Behaviour and Physiology*, 42, (4), 219-232.
- Cheroske, A. G. & Cronin, T. W. 2005. Variation in Stomatopod (*Gonodactylus smithii*) Color Signal Design Associated with Organismal Condition and Depth. *Brain, behavior and evolution*, 66, 99-113.
- Cheroske, A. G., Barber, P. H. & Cronin, T. W. 2006. Evolutionary variation in the expression of phenotypically plastic color vision in Caribbean mantis shrimps, genus *Neogonodactylus*. *Marine Biology*, 150, (2), 213-220.
- Chiao, C.-C., Cronin, T. W. & Marshall. Justin, N. 2000. Eye Design and Color Signaling in a Stomatopod Crustacean *Gonodactylus smithii*. *Brain, behavior and evolution*, 56, 107-122.
- Chiou, T.-H., Cronin, T. W., Caldwell, R. L. & Marshall, J. 2005. Biological polarized light reflectors in stomatopod crustaceans. *Optics & Photonics 2005*. International Society for Optics and Photonics.
- Chiou, T.-H., Kleinlogel, S., Cronin, T., Caldwell, R., Loeffler, B., Siddiqi, A., Goldizen, A. & Marshall, N. J. 2008. Circular Polarization Vision in a Stomatopod Crustacean. *Current Biology*, 18, (6), 429-434.
- Chiou, T.-H., Marshall, N. J., Caldwell, R. & Cronin, T. 2011. Changes in light-reflecting properties of signalling appendages alter mate choice behaviour in a stomatopod crustacean *Haptosquilla trispinosa*. *Marine and Freshwater Behaviour and Physiology*, 44, (1), 1-11.
- Chittka, L., Shmida, A., Troje, N. & Menzel, R. 1994. Ultraviolet as a component of flower reflections, and the colour perception of Hymenoptera. *Vision Research*, 34, (11), 1489-1508.
- Conway, B. R. 2014. Color signals through dorsal and ventral visual pathways. *Visual Neuroscience*, 31, (2), 197-209.
- Cronin, T. W. & Marshall, N. J. 1989a. A retina with at least ten spectral types of photoreceptors in a mantis shrimp. *Nature*, 339, (6220), 137-140.
- Cronin, T. W. & Marshall, N. J. 1989b. Multiple spectral classes of photoreceptors in the retinas of gonodactyloid stomatopod crustaceans. *Journal of Comparative Physiology A*, 166, (2), 261-275.
- Cronin, T. W., Marshall, N. J. & Caldwell, R. L. 1993. Photoreceptor spectral diversity in the retinas of squilloid and lysiosquilloid stomatopod crustaceans. *Journal Of Comparative Physiology A, Neuroethology, Sensory, Neural, and Behavioural Physiology*, 172, (3), 339-350.
- Cronin, T. W., Marshall, N. J., Caldwell, R. & Sashar, N. 1994a. Specialization of Retinal Function in the Compound Eyes of Mantis Shrimps. *Vision Research*, 34, (20), 3639-2656.
- Cronin, T. W., Marshall, N. J. & Caldwell, R. L. 1994b. The intrarhabdomal filters in the retinas of mantis shrimps. *Vision Research*, 34, (3), 279-291.
- Cronin, T. W., Marshall, N. J. & Caldwell, R. L. 1994c. The retinas of mantis shrimps from low-light environments (Crustacea; Stomatopoda; Gonodactylidae). *Journal of Comparative Physiology A*, 174, (5), 607-619.

- Cronin, T. W., Marshall, N. J., Caldwell, R. L. & Shashar, N. 1994d. Specialization of retinal function in the compound eyes of mantis shrimps. *Vision Research*, 34, 2639-2656.
- Cronin, T. W., Marshall, N. J., Quinn, C. A. & King, C. A. 1994e. Ultraviolet photoreception in mantis shrimp. *Vision Research*, 34, (11), 1443-1452.
- Cronin, T. W., Marshall, N. J. & Caldwell, R. L. 1996. Visual pigment diversity in two genera of mantis shrimps implies rapid evolution (Crustacea; Stomatopoda). *Journal of Comparative Physiology A*, 179, (3), 371-384.
- Cronin, T. W., Caldwell, R. L. & Marshall, J. 2001. Sensory adaptation: tunable colour vision in a mantis shrimp. *Nature*, 411, (6837), 547-548.
- Cronin, T. W. & Marshall, J. 2001. Parallel Processing and Image Analysis in the Eyes of Mantis Shrimps. *Biological Bulletin*, 200, (2), 177-183.
- Cronin, T. W. & Caldwell, R. 2002. Tuning of photoreceptor function in three mantis shrimp species that inhabit a range of depths. II. Filter pigments. *Journal of Comparative Physiology A: Sensory, Neural, and Behavioral Physiology*, 188, (3), 187-197.
- Cronin, T. W., Caldwell, R. & Erdmann, M. 2002. Tuning of photoreceptor function in three mantis shrimp species that inhabit a range of depths. I. Visual pigments. *Journal of Comparative Physiology A: Sensory, Neural, and Behavioral Physiology*, 188, (3), 179-186.
- Cronin, T. W. & Porter, M. L. 2008. Exceptional Variation on a Common Theme: The Evolution of Crustacean Compound Eyes. *Evolution: Education and Outreach*, 1, (4), 463-475.
- Cronin, T. W., Chiou, T.-H., Caldwell, R. L., Roberts, N. & Marshall, J. 2009. Polarization signals in mantis shrimps. In: Joseph, A., Shaw, J. & Scott, T. (eds.) *SPIE Optical Engineering + Applications*. San Diego: The International Society for Optical Engineering.
- Cronin, T. W., Porter, M., Bok, M., Wolf, J. & Robinson, P. 2010. The molecular genetics and evolution of colour and polarization vision in stomatopod crustaceans. *Ophthalmic and Physiological Optics*, 30, (5), 460-469.
- Cronin, T. W., Bok, M. J., Marshall, N. J. & Caldwell, R. L. 2014. Filtering and polychromatic vision in mantis shrimps: themes in visible and ultraviolet vision. *Philosophical Transactions of the Royal Society B: Biological Sciences*, 369, (1636), 20130032.
- Dartnall, H., Bowmaker, J. & Mollon, J. 1983. Human visual pigments: microspectrophotometric results from the eyes of seven persons. *Proceedings of the Royal Society of London. Series B. Biological Sciences*, 220, (1218), 115-130.
- Davis, N. T. 1982. Improved methods for cobalt filling and silver intensification of insect motor neurons. *Biotechnic & Histochemistry*, 57, (4), 239-244.
- De Astrada, M. B., Tuthill, J. C. & Tomsic, D. 2009. Physiology and morphology of sustaining and dimming neurons of the crab *Chasmagnathus granulatus* (Brachyura: Grapsidae). *Journal of Comparative Physiology A*, 195, (8), 791-798.
- De Astrada, M. B., Bengochea, M., Sztarker, J., Delorenzi, A. & Tomsic, D. 2013. Behaviorally related neural plasticity in the arthropod optic lobes. *Current Biology*, 23, (15), 1389-1398.
- De Souza, J., Hertel, H., Ventura, D. F. & Menzel, R. 1992. Response properties of stained monopolar cells in the honeybee lamina. *Journal of Comparative Physiology A*, 170, (3), 267-274.
- De Valois, R. L. & Jacobs, G. H. 1968. Primate color vision. *Science*, 162, (3853), 533-540.
- Derby, C. D., Fortier, J. K., Harrison, P. J. H. & Cate, H. S. 2003. The peripheral and central antennular pathway of the Caribbean stomatopod crustacean *Neogonodactylus oerstedii*. *Arthropod Structure & Development*, 32, (2-3), 175-188.
- Devoe, R. D., De Souza, J. M. & Ventura, D. F. 1997. Electrophysiological measurements of spectral sensitivities: a review. *Brazilian Journal of Medical and Biological Research*, 30, 169-177.
- Dingle, H. & Caldwell, R. L. 1969. The Aggressive and Territorial Behaviour of the Mantis Shrimp *Gonodactylus bredini* Manning (Crustacea: Stomatopoda). *Behaviour*, 33, (1), 115-136.

- Douglass, J. K. & Strausfeld, N. J. 1996. Visual motion-detection circuits in flies: parallel direction- and non-direction-sensitive pathways between the medulla and lobula plate. *Journal of Neuroscience*, 16, (15), 4551-4562.
- Douglass, J. K. & Strausfeld, N. J. 2003. Anatomical organization of retinotopic motion-sensitive pathways in the optic lobes of flies. *Microscopy research and technique*, 62, (2), 132-150.
- Dyer, A. G., Paulk, A. C. & Reser, D. H. 2011. Colour processing in complex environments: insights from the visual system of bees. *Proceedings of the Royal Society B: Biological Sciences*, 278, (1707), 952-959.
- Ehmer, B. & Gronenberg, W. 2002. Segregation of visual input to the mushroom bodies in the honeybee (*Apis mellifera*). *Journal of Comparative Neurology*, 451, (4), 362-373.
- El Jundi, B., Huetteroth, W., Kurylas, A. E. & Schachtner, J. 2009. Anisometric brain dimorphism revisited: Implementation of a volumetric 3D standard brain in *Manduca sexta*. *The Journal of comparative neurology*, 517, (2), 210-225.
- Elofsson, R. & Hagberg, M. 1986. Evolutionary aspects on the construction of the first optic neuropil (lamina) in Crustacea. *Zoomorphology*, 106, (3), 174-178.
- Fischbach, K.-F. & Dittrich, A. 1989. The optic lobe of *Drosophila melanogaster*. I. A Golgi analysis of wild-type structure. *Cell and tissue research*, 258, (3), 441-475.
- Friedrich, M. & Tautz, D. 1995. Ribosomal DNA phylogeny of the major extant arthropod classes and the evolution of myriapods. *Nature*, 376, (6536), 165-167.
- Gilbert, C. 2013. Brain connectivity: revealing the fly visual motion circuit. *Current Biology*, 23, (18), 851-853.
- Glantz, R. 1996a. Polarization sensitivity in crayfish lamina monopolar neurons. *Journal of Comparative Physiology A*, 178, (3), 413-425.
- Glantz, R. M. 1996b. Polarization sensitivity in the crayfish optic lobe: peripheral contributions to opponency and directionally selective motion detection. *Journal of Neurophysiology*, 76, (5), 3404-3414.
- Glantz, R. M. 1998. Directionality and inhibition in crayfish tangential cells. *Journal of Neurophysiology*, 79, (3), 1157-1166.
- Glantz, R. M. & Mcisaac, A. 1998. Two-channel polarization analyzer in the sustaining fiber-dimming fiber ensemble of crayfish visual system. *Journal of Neurophysiology*, 80, (5), 2571-2583.
- Glantz, R. M., Miller, C. S. & Nässel, D. R. 2000. Tachykinin-related peptide and GABA-mediated presynaptic inhibition of crayfish photoreceptors. *The Journal of Neuroscience*, 20, (5), 1780-1790.
- Glantz, R. M. & Miller, C. S. 2002. Signal processing in the crayfish optic lobe: contrast, motion and polarization vision. In: Wiese, K. (ed.) *The Crustacean Nervous System*. Berlin: Springer.
- Grant, K. A., Raible, D. W. & Piotrowski, T. 2005. Regulation of latent sensory hair cell precursors by glia in the zebrafish lateral line. *Neuron*, 45, 69-80.
- Greiner, B., Ribi, W. A., Wcislo, W. T. & Warrant, E. J. 2004. Neural organisation in the first optic ganglion of the nocturnal bee *Megalopta genalis*. *Cell and tissue research*, 318, (2), 429-437.
- Gruev, V., Perkins, R. & York, T. 2010. CCD polarization imaging sensor with aluminum nanowire optical filters. *Optics express*, 18, (18), 19087-19094.
- Hama, H., Kurokawa, H., Kawano, H., Ando, R., Shimogori, T., Noda, H., Fukami, K., Sakaue-Sawano, A. & Miyawaki, A. 2011. Scale: a chemical approach for fluorescence imaging and reconstruction of transparent mouse brain. *Nature Neuroscience*, 14, (11), 1481-1488.
- Hamanaka, Y., Shibasaki, H., Kinoshita, M. & Arikawa, K. 2013. Neurons innervating the lamina in the butterfly, *Papilio xuthus*. *Journal of comparative physiology. A, Neuroethology, sensory, neural, and behavioral physiology*, 199, (5), 341-351.
- Hamori, J. & Horridge, G. 1966. The lobster optic lamina I. General organization. *Journal of Cell Science*, 1, (2), 249-256.

- Harzsch, S. 2002. The phylogenetic significance of crustacean optic neuropils and chiasmata: A re-examination. *Journal of Comparative Neurology*, 453, (1), 10-21.
- Harzsch, S. & Hansson, B. S. 2008. Brain architecture in the terrestrial hermit crab *Coenobita clypeatus* (Anomura, Coenobitidae), a crustacean with a good aerial sense of smell. *BMC Neuroscience*, 9, (1), 58.
- Hazlett, B. A. 1979. The Meral Spot of *Gonodactylus oerstedii* Hansen as a Visual Stimulus (Stomatopoda, Gonodactylidae). *Crustaceana*, 36, (2), 196-198.
- Heinze, S. & Homberg, U. 2007. Maplike representation of celestial E-vector orientations in the brain of an insect. *Science*, 315, (5814), 995-997.
- Heinze, S. & Homberg, U. 2008. Neuroarchitecture of the central complex of the desert locust: intrinsic and columnar neurons. *Journal of Comparative Neurology*, 511, (4), 454-478.
- Heinze, S. & Homberg, U. 2009. Linking the input to the output: new sets of neurons complement the polarization vision network in the locust central complex. *The Journal of Neuroscience*, 29, (15), 4911-4921.
- Heinze, S. 2014. Polarized-Light Processing in Insect Brains: Recent Insights from the Desert Locust, the Monarch Butterfly, the Cricket, and the Fruit Fly. In: Horváth, G. (ed.) *Polarized Light and Polarization Vision in Animal Sciences*. Berlin: Springer.
- Heisenberg, M. 2003. Mushroom body memoir: from maps to models. *Nature Reviews Neuroscience*, 4, (4), 266-275.
- Helmholtz, H. 1859. Verb. des naturhist.med. Vereins zu Heidelberg. *Handbuch der physiol. Optik*. 1st ed.
- Helmholtz, H. 1896. Handbuch der physiologischen Optik 2nd edition (Hamburg: Voss).
- Hering, E. 1878. Zur Lehre vom Lichtsinne. Wien: Carl Gerold's Sohn.
- Hertel, H. 1980. Chromatic properties of identified interneurons in the optic lobes of the bee. *Journal of Comparative Physiology*, 137, (3), 215-231.
- Hertel, H. & Maronde, U. 1987. The physiology and morphology of centrally projecting visual interneurones in the honeybee brain. *Journal of Experimental Biology*, 133, (1), 301-315.
- Hertel, H., Schäfer, S. & Maronde, U. 1987. The physiology and morphology of visual commissures in the honeybee brain. *Journal of Experimental Biology*, 133, (1), 283-300.
- Homberg, U. 1994a. *Distribution of neurotransmitters in the insect brain*, Stuttgart, Gustav Fischer Verlag.
- Homberg, U. 1994b. Flight-correlated activity changes in neurons of the lateral accessory lobes in the brain of the locust *Schistocerca gregaria*. *Journal of Comparative Physiology A*, 175, (5), 597-610.
- Homberg, U. & Würden, S. 1997. Movement-sensitive, polarization-sensitive, and light-sensitive neurons of the medulla and accessory medulla of the locust, *Schistocerca gregaria*. *Journal of Comparative Neurology*, 386, (3), 329-346.
- Homberg, U., Hofer, S., Pfeiffer, K. & Gebhardt, S. 2003. Organization and neural connections of the anterior optic tubercle in the brain of the locust, *Schistocerca gregaria*. *Journal of Comparative Neurology*, 462, (4), 415-430.
- Homberg, U., Heinze, S., Pfeiffer, K., Kinoshita, M. & El Jundi, B. 2011. Central neural coding of sky polarization in insects. *Philosophical Transactions of the Royal Society of London. Series B, Biological Sciences*, 366, (1565), 680-687.
- Horridge, G. A. 1978. The Separation of Visual Axes in Apposition Compound Eyes. *Philosophical Transactions of the Royal Society of London. Series B, Biological Sciences*, 285, (1003), 1-59.
- How, M. J., Christy, J., Roberts, N. W. & Marshall, N. J. 2014a. Null point of discrimination in crustacean polarisation vision. *The Journal of experimental biology*, 217, (14), 2462-2467.
- How, M. J., Porter, M. L., Radford, A. N., Feller, K. D., Temple, S. E., Caldwell, R. L., Marshall, N. J., Cronin, T. W. & Roberts, N. W. 2014b. Out of the blue: the evolution of horizontally polarized signals in *Haplosquilla* (Crustacea, Stomatopoda, Protosquillidae). *The Journal of experimental biology*, 217, (19), 3425-3431.

- Hurvich, L. M. & Jameson, D. 1949. Helmholtz and the Three-Color Theory: An Historical Note. *The American Journal of Psychology*, 111-114.
- Hurvich, L. M. & Jameson, D. 1957. An opponent-process theory of colour vision. *Psychological Review*, 64, (6), 384-404.
- Ito, K., Shinomiya, K., Ito, M., Armstrong, J. D., Boyan, G., Hartenstein, V., Harzsch, S., Heisenberg, M., Homberg, U. & Jenett, A. 2014. A systematic nomenclature for the insect brain. *Neuron*, 81, (4), 755-765.
- Jen, Y.-J., Lakhtakia, A., Yu, C.-W., Lin, C.-F., Lin, M.-J., Wang, S.-H. & Lai, J.-R. 2011. Biologically inspired achromatic waveplates for visible light. *Nature Communications*, 2, 363.
- Jewell, S. A., Vukusic, P. & Roberts, N. W. 2007. Circularly polarized colour reflection from heliocoidal structures in the beetle *Plusiotis boucardi*. *New Journal of Physics*, 9, (4), 99.
- Kelber, A., Vorobyev, M. & Osorio, D. 2003. Animal colour vision – behavioural tests and physiological concepts. *Biological Reviews of the Cambridge Philosophical Society*, 78, (1), 81-118.
- Kelber, A. & Osorio, D. 2010. From spectral information to animal colour vision: experiments and concepts. *Proceedings of the Royal Society B: Biological Sciences*, 277, (1688), 1617-1625.
- Kinoshita, M., Shimohigashii, M., Tominaga, Y., Arikawa, K. & Homberg, U. 2014. Topographically distinct visual and olfactory inputs to the mushroom body in the swallowtail butterfly, *Papilio xuthus*. *Journal of Comparative Neurology*, 523, (1), 162-182.
- Kleinlogel, S. 2003. *Neural Connections behind the Complex Retina of the Stomatopod (Mantis shrimps)*. PhD, University of Queensland.
- Kleinlogel, S., Marshall, N. J., Horwood, J. M. & Land, M. F. 2003. Neuroarchitecture of the color and polarization vision system of the stomatopod *Haptosquilla*. *Journal of Comparative Neurology*, 467, (3), 326-342.
- Kleinlogel, S. & Marshall, N. J. 2005. Photoreceptor projection and termination pattern in the lamina of gonodactyloid stomatopods (mantis shrimp). *Cell and tissue research*, 321, (2), 273-284.
- Kleinlogel, S. & Marshall, N. J. 2006. Electrophysiological evidence for linear polarization sensitivity in the compound eyes of the stomatopod crustacean *Gonodactylus chiragra*. *Journal of Experimental Biology*, 209, (21), 4262-4272.
- Koshitaka, H., Kinoshita, M., Vorobyev, M. & Arikawa, K. 2008. Tetrachromacy in a butterfly that has eight varieties of spectral receptors. *Proceedings of the Royal Society B: Biological Sciences*, 275, (1637), 947-954.
- Krieger, J., Sandeman, R. E., Sandeman, D. C., Hansson, B. S. & Harzsch, S. 2010. Brain architecture of the largest living land arthropod, the Giant Robber Crab *Birgus latro* (Crustacea, Anomura, Coenobitidae): evidence for a prominent central olfactory pathway? *Frontiers in zoology*, 7, (1), 25.
- Kulkarni, M. & Gruev, V. 2012. Integrated spectral-polarization imaging sensor with aluminum nanowire polarization filters. *Optics express*, 20, (21), 22997-23012.
- Land, M. & Nilsson, D. 2002. *Animal eyes*, New York, Oxford University Press.
- Land, M. F., Marshall, J. N., Brownless, D. & Cronin, T. W. 1990. The eye-movements of the mantis shrimp *Odontodactylus scyllarus* (Crustacea: Stomatopoda). *Journal of Comparative Physiology*, 167, (2), 155-166.
- Leise, E. M. 1996. Selective retention of the fluorescent dye DASPEI in a larval gastropod mollusc after paraformaldehyde fixation. *Microscopy research and technique*, 33, (6), 496-500.
- Li, Y. & Strausfeld, N. 1997. Morphology and Sensory Modality of Mushroom Body Extrinsic Neurons in the Brain of the Cockroach, *Periplaneta americana*. *Journal of Comparative Neurology*, 387, (4), 631-650.
- Lin, C. & Strausfeld, N. J. 2012. Visual inputs to the mushroom body calyces of the whirligig beetle *Dineutus sublineatus*: modality switching in an insect. *Journal of Comparative Neurology*, 520, (12), 2562-2574.

- Liu, G., Seiler, H., Wen, A., Zars, T., Ito, K., Wolf, R., Heisenberg, M. & Liu, L. 2006. Distinct memory traces for two visual features in the *Drosophila* brain. *Nature*, 439, (7076), 551-556.
- Maloney, L. T. 1986. Evaluation of linear models of surface spectral reflectance with small numbers of parameters. *Journal of the Optical Society of America A*, 3, (10), 1673-1683.
- Manning, R. B. 1977. A monograph of the West African stomatopod Crustacea. Copenhagen: Scandinavian Science Press Limited.
- Manning, R. B., Schiff, H. & Abbott, B. C. 1984. Cornea Shape and Surface Structure in Some Stomatopod Crustacea. *Journal of Crustacean Biology*, 4, (3), 502-513.
- Marshall, N., Land, M. & Cronin, T. 1989. The structure and function of the mid-band in the eyes of stomatopod crustaceans. *The Journal of the Marine Biological Association of the United Kingdom*, 69, 735.
- Marshall, N. J. 1988. A unique colour and polarization vision system in mantis shrimps. *Nature*, 333, (6173), 557-560.
- Marshall, N. J., Land, M. F., King, C. A. & Cronin, T. W. 1991a. The Compound Eyes of Mantis Shrimps (Crustacea, Hoplocarida, Stomatopoda). I. Compound Eye Structure: The Detection of Polarized Light. *Philosophical Transactions of the Royal Society of London B: Biological Sciences*, 334, (1269), 33-56.
- Marshall, N. J., Land, M. F., King, C. A. & Cronin, T. W. 1991b. The Compound Eyes of Mantis Shrimps (Crustacea, Hoplocarida, Stomatopoda). II. Colour Pigments in the Eyes of Stomatopod Crustaceans: Polychromatic Vision by Serial and Lateral Filtering. *Philosophical Transactions of the Royal Society of London B: Biological Sciences*, 334, (1269), 57-84.
- Marshall, N. J., Jones, J. P. & Cronin, T. W. 1996. Behavioural evidence for colour vision in stomatopod crustaceans. *Journal of Comparative Physiology A*, 179, (4), 473-481.
- Marshall, N. J., Cronin, T. W., Shashar, N. & Land, M. 1999. Behavioural evidence for polarisation vision in stomatopods reveals a potential channel for communication. *Current Biology*, 9, (14), 755-758.
- Marshall, N. J. & Oberwinkler, J. 1999. Ultraviolet vision: The colourful world of the mantis shrimp. *Nature*, 401, (6756), 873-875.
- Marshall, N. J. 2000. The visual ecology of reef fish colours. In: Espmark, Y., Amundsen, T. & Rosenqvist, G. (eds.) *Animal signals. Adaptive significance of signalling and signal design in animal communication*. Trondheim, Norway: Tapir Publishers.
- Marshall, N. J., Cronin, T. W. & Kleinlogel, S. 2007. Stomatopod eye structure and function : A review. *Arthropod Structure & Development*, 36, (4), 420-448.
- Marshall, N. J. & Arikawa, K. 2014. Unconventional colour vision. *Current Biology*, 24, (24), R1150-R1154.
- Marshall, N. J. & Cronin, T. W. 2014. Polarization vision of Crustaceans. In: Horváth, G. (ed.) *Polarized Light and Polarization Vision in Animal Sciences*. New York: Springer.
- Marshall, N. J., Land, M. F. & Cronin, T. W. 2014. Shrimps that pay attention: saccadic eye movements in stomatopod crustaceans. *Philosophical Transactions of the Royal Society B: Biological Sciences*, 369, (1636), 20130042.
- Maxwell, J. C. 1860. On the theory of compound colours and the relations of the colours of the spectrum. *Philosophical transactions of the Royal Society of London*, 150, 57-84.
- Mazel, C. H., Cronin, T. W., Caldwell, R. L. & Marshall, N. J. 2003. Fluorescent Enhancement of Signaling in a Mantis Shrimp. *Science*, 303, (5654), 51-51.
- Medan, V., Oliva, D. & Tomsic, D. 2007. Characterization of lobula giant neurons responsive to visual stimuli that elicit escape behaviors in the crab *Chasmagnathus*. *Journal of Neurophysiology*, 98, (4), 2414-2428.
- Menzel, R. 1974. Spectral sensitivity of monopolar cells in the bee lamina. *Journal of Comparative Physiology*, 93, (4), 337-346.

- Menzel, R. 1979. Spectral Sensitivity and Color Vision in Invertebrates. In: Autrum, H. (ed.) *Comparative Physiology and Evolution of Vision in Invertebrates*. Springer Berlin Heidelberg.
- Menzel, R., Ventura, D. F., Hertel, H., De Souza, J. M. & Greggers, U. 1986. Spectral sensitivity of photoreceptors in insect compound eyes: Comparison of species and methods. *Journal of Comparative Physiology A*, 158, (2), 165-177.
- Menzel, R. & Shmida, A. 1993. The ecology of flower colours and the natural colour vision of insect pollinators: the Israeli flora as a study case. *Biological Reviews*, 68, (1), 81-120.
- Meyer, E. P. 1979. Golgi-EM-study of first and second order neurons in the visual system of *Cataglyphis bicolor* Fabricius (Hymenoptera, Formicidae). *Zoomorphologie*, 92, (2), 115-139.
- Mobbs, P., Becker, D., Williamson, R., Bate, M. & Warner, A. 2008. Techniques for dye injection and cell labelling. *The axon guide*. Sunnyvale: MDS Analytical Technologies.
- Morante, J. & Desplan, C. 2008. The color-vision circuit in the medulla of *Drosophila*. *Current Biology*, 18, (8), 553-565.
- Mu, L., Ito, K., Bacon, J. P. & Strausfeld, N. J. 2012. Optic glomeruli and their inputs in *Drosophila* share an organizational ground pattern with the antennal lobes. *The Journal of Neuroscience*, 32, (18), 6061-6071.
- Mu, L., Bacon, J. P., Ito, K. & Strausfeld, N. J. 2014. Responses of *Drosophila* giant descending neurons to visual and mechanical stimuli. *The Journal of experimental biology*, 217, 2121-2129.
- Naka, K. & Rushton, W. 1966a. An attempt to analyse colour reception by electrophysiology. *The Journal of Physiology*, 185, (3), 556-586.
- Naka, K. & Rushton, W. 1966b. S-potentials from colour units in the retina of fish (Cyprinidae). *The Journal of Physiology*, 185, (3), 536-555.
- Nässel, D. 1975. The organization of the lamina ganglionaris of the prawn, *Pandalus borealis* (Kröyer). *Cell and tissue research*, 163, (4), 445-464.
- Nässel, D. & Waterman, T. H. 1977. Golgi EM evidence for visual information channelling in the crayfish lamina ganglionaris. *Brain Research*, 130, (3), 556-563.
- Nässel, D. R. 1976. The retina and retinal projection on the lamina ganglionaris of the crayfish *Pacifastacus leniusculus* (Dana). *The Journal of comparative neurology*, 167, (3), 341-359.
- Nässel, D. R. 1977. Types and arrangements of neurons in the crayfish optic lamina. *Cell and tissue research*, 179, (1), 45-75.
- Neumeyer, C. 1991. Evolution of colour vision. In: Cronly-Dillon, J. R. (ed.) *Evolution of the Eye and Visual System*. London: The Macmillian Press LTD.
- Neville, A. & Luke, B. 1971. Form optical activity in crustacean cuticle. *Journal of Insect Physiology*, 17, (3), 519-526.
- Neville, A. C. & Caveney, S. 1969. Scarabaeid beetle exocuticle as an optical analogue of cholesteric liquid crystals. *Biological Reviews*, 44, (4), 531-562.
- O'shea, M. & Williams, J. 1974. The anatomy and output connection of a locust visual interneurone; the lobular giant movement detector (LGMD) neurone. *Journal of Comparative Physiology*, 91, (3), 257-266.
- Olsen, S. R. & Wilson, R. I. 2008. Cracking neural circuits in a tiny brain: new approaches for understanding the neural circuitry of *Drosophila*. *Trends in Neurosciences*, 31, (10), 512-520.
- Osorio, D., Marshall, N. J. & Cronin, T. W. 1997. Stomatopod photoreceptor spectral tuning as an adaptation for colour constancy in water. *Vision Research*, 37, (23), 3299-3309.
- Osorio, D. & Vorobyev, M. 2005. Photoreceptor spectral sensitivities in terrestrial animals: adaptations for luminance and colour vision. *Proceedings of the Royal Society B: Biological Sciences*, 272, (1574), 1745-1752.
- Osorio, D. & Vorobyev, M. 2008. A review of the evolution of animal colour vision and visual communication signals. *Vision Research*, 48, (20), 2042-2051.

- Otsuna, H. & Ito, K. 2006. Systematic analysis of the visual projection neurons of *Drosophila melanogaster*. I. Lobula specific pathways. *Journal of Comparative Neurology*, 497, (6), 928-958.
- Patek, S., Korff, R. & Caldwell, R. L. 2004. Biomechanics: Deadly strike mechanism of a mantis shrimp. *Nature*, 428, (6985), 819-820.
- Patek, S. N. & Caldwell, R. L. 2005. Extreme impact and cavitation forces of a biological hammer: strike forces of the peacock mantis shrimp *Odontodactylus scyllarus*. *The Journal of experimental biology*, 208, (19), 3655-3664.
- Paulk, A. C., Phillips-Portillo, J., Dacks, A. M., Fellous, J. M. & Gronenberg, W. 2008. The processing of color, motion, and stimulus timing are anatomically segregated in the bumblebee brain. *The Journal of Neuroscience*, 28, (25), 6319-6332.
- Paulk, A. C., Dacks, A. M. & Gronenberg, W. 2009. Color processing in the medulla of the bumblebee (Apidae: *Bombus impatiens*). *Journal of Comparative Neurology*, 513, (5), 441-456.
- Picaud, S., Wunderer, H. J. & Franceschini, N. 1988. 'Photo-degeneration' of neurones after extracellular dye application. *Neuroscience Letters*, 95, (1), 24-30.
- Picaud, S., W., H. & Franceschini, N. 1990. Dye-induced photopermeabilization and photodegeneration, a lesion technique useful for neuronal tracing. *Journal of Neuroscience*, 33, (2), 101-112.
- Pokorny, J. & Smith, V. C. 1970. Wavelength discrimination in the presence of added chromatic fields. *Journal of the Optical Society of America*, 60, (4), 562-569.
- Porter, M. L., Bok, M. J., Robinson, P. R. & Cronin, T. W. 2009. Molecular diversity of visual pigments in Stomatopoda (Crustacea). *Visual Neuroscience*, 26, (3), 255-265.
- Porter, M. L., Zhang, Y., Desai, S., Caldwell, R. L. & Cronin, T. W. 2010. Evolution of anatomical and physiological specialization in the compound eyes of stomatopod crustaceans. *The Journal of experimental biology*, 213, (20), 3473-3486.
- Powell, S. B. & Gruev, V. 2014. Underwater polarization camera for real-time and high definition imaging. *Proceedings of SPIE - The International Society for Optical Engineering*, In press.
- R Development Core Team 2010. R: A language and environment for statistical computing. Vienna, Austria: R foundation for Statistical Computing.
- Ribi, W. & Scheel, M. 1981. The second and third optic ganglia of the worker bee: Golgi studies of the neuronal elements in the medulla and lobula. *Cell and tissue research*, 221, (1), 17.
- Ribi, W. A. 1975. The first optic ganglion of the bee. *Cell and Tissue Research*, 165, (1), 103-111.
- Roberts, N., Chiou, T. H., Marshall, N. & Cronin, T. 2009. A biological quarter-wave retarder with excellent achromaticity in the visible wavelength region. *Nature Photonics*, 3, (11), 641-644.
- Roberts, N. W., Porter, M. L. & Cronin, T. W. 2011. The molecular basis of mechanisms underlying polarization vision. *Philosophical Transactions of the Royal Society of London. Series B, Biological Sciences*, 366, (1565), 627-637.
- Roberts, N. W., How, M. J., Porter, M. L., Temple, S. E., Caldwell, R. L., Powell, S. B., Gruev, V., Marshall, N. J. & Cronin, T. W. 2014. Animal Polarization Imaging and Implications for Optical Processing. *Proceedings of IEEE*, 102, (10).
- Rutherford, D. & Horridge, G. 1965. The rhabdom of the lobster eye. *Quarterly Journal of Microscopical Science*, 3, (74), 119-130.
- Sabra, R. 1985. Polarization sensitivity of crayfish photoreceptors is correlated with their termination sites in the lamina ganglionaris. *Zeitschrift Für Vergleichende Physiologie*, 156, (3), 315-318.
- Sandeman, D., Sandeman, R., Derby, C. & Schmidt, M. 1992. Morphology of the brain of crayfish, crabs, and spiny lobsters: a common nomenclature for homologous structures. *The Biological Bulletin*, 183, (2), 304-326.

- Schiff, H., Abbott, B. C. & Manning, R. B. 1986. Optics, Range-Finding, and Neuroanatomy of the Eye of a Mantis Shrimp, *Squilla mantis* Linnaeus. *Smithsonian Contributions to Zoology*, 440.
- Schiff, H. 1987. Optical and neural pooling in visual processing in crustacea. *Comparative Biochemistry and Physiology Part A: Physiology*, 88, (1), 1-13.
- Schindelin, J., Arganda-Carreras, I., Frise, E., Kaynig, V., Longair, M., Pietzsch, T., Preibisch, S., Rueden, C., Saalfeld, S. & Schmid, B. 2012. Fiji: an open-source platform for biological-image analysis. *Nature Methods*, 9, (7), 676-682.
- Schönenberger, N. 1977. The fine structure of the compound eye of *Squilla mantis* (Crustacea, Stomatopoda). *Cell and tissue research*, 176, (2), 205-233.
- Schram, F. R. 1969. Polyphyly in the Eumalacostraca? *Crustaceana*, 16, (3), 243-250.
- Schram, F. R., Ahyong, S. T., Patek, S. N., Green, P. A., Rosario, M. V., Bok, M. J., Cronin, T. W., Vetter, K. S. M., Caldwell, R. L. & Scholtz, G. 2013. Subclass Hoplocarida Calman, 1904: Order Stomatopoda Latreille, 1817. *Treatise on Zoology-Anatomy, Taxonomy, Biology. The Crustacea, Volume 4*. Brill.
- Sinakevitch, I., Douglass, J. K., Scholtz, G., Loesel, R. & Strausfeld, N. J. 2003. Conserved and convergent organization in the optic lobes of insects and isopods, with reference to other crustacean taxa. *The Journal of comparative neurology*, 467, (2), 150-172.
- Skorupski, P. & Chittka, L. 2010. Differences in photoreceptor processing speed for chromatic and achromatic vision in the bumblebee, *Bombus terrestris*. *The Journal of Neuroscience*, 30, (11), 3896-3903.
- Smith, V. C. & Pokorny, J. 1972. Spectral sensitivity of color-blind observers and the cone photopigments. *Vision Research*, 12, (12), 2059-2071.
- Souza, J., Hertel, H., Menzel, R. & Ventura, D. 1986. Marking and recording of monopolar cells in the bee lamina. *Brazilian Journal of Medical and Biological Research*, 20, (6), 851-855.
- Spiga, S., Acquas, E., Puddu, M. C., Mulas, G., Lintas, A. & Diana, M. 2011. Simultaneous Golgi-Cox and immunofluorescence using confocal microscopy. *Brain Structure and Function*, 216, (3), 171-182.
- Stavenga, D. G. 1979. Pseudopupils of compound eyes. *Comparative Physiology and Evolution of Vision in Invertebrates*. Berlin: Springer.
- Steger, R. & Caldwell, R. L. 1983. Intraspecific deception by bluffing: a defense strategy of newly molted stomatopods (Arthropoda: Crustacea). *Science*, 221, (4610), 558.
- Stocker, R., Lienhard, M., Borst, A. & Fischbach, K. 1990. Neuronal architecture of the antennal lobe in *Drosophila melanogaster*. *Cell and tissue research*, 262, (1), 9-34.
- Stockman, A., Macleod, D. I. & Johnson, N. E. 1993. Spectral sensitivities of the human cones. *Journal of the Optical Society of America A*, 10, (12), 2491-2521.
- Stowe, S., Ribi, W. & Sandeman, D. 1977. The organisation of the lamina ganglionaris of the crabs *Scylla serrata* and *Leptograpsus variegatus*. *Cell and tissue research*, 178, (4), 517-532.
- Strausfeld, N. & Hausen, K. 1977. The resolution of neuronal assemblies after cobalt injection into neuropil. *Proceedings of the Royal Society of London. Series B. Biological Sciences*, 199, (1136), 463-476.
- Strausfeld, N. & Nässel, D. 1981. Neuroarchitectures serving compound eyes of Crustacea and insects. In: Atrum, H. (ed.) *Comparative Physiology and Evolution of Vision in Invertebrates. B Invertebrate Visual Centres and Behavior I*. Springer Berlin Heidelberg New York.
- Strausfeld, N. & Bacon, J. 1983. Multimodal convergence in the central nervous system of dipterous insects. *Fortschritte der Zoologie*, 28, 47-76.
- Strausfeld, N. & Bassemir, U. 1985. Lobula plate and ocellar interneurons converge onto a cluster of descending neurons leading to neck and leg motor neuropil in *Calliphora erythrocephala*. *Cell and tissue research*, 240, (3), 617-640.
- Strausfeld, N. J. 1970. The Optic Lobes of Diptera. *Philosophical Transactions of the Royal Society of London. Series B, Biological Sciences*, 258, (820), 135-223.

- Strausfeld, N. J. 1976. *Atlas of an insect brain*, Springer-Verlag Berlin, Heidelberg, New York.
- Strausfeld, N. J. & Lee, J. K. 1991. Neuronal basis for parallel visual processing in the fly. *Visual Neuroscience*, 7, (1), 13-33.
- Strausfeld, N. J. 1998. Crustacean-insect relationships: the use of brain characters to derive phylogeny amongst segmented invertebrates. *Brain, behavior and evolution*, 52, (4-5), 186-206.
- Strausfeld, N. J. 2005. The evolution of crustacean and insect optic lobes and the origins of chiasmata. *Arthropod Structure & Development*, 34, (3), 235-256.
- Strausfeld, N. J. & Okamura, J.-Y. 2007. Visual system of calliphorid flies: Organization of optic glomeruli and their lobula complex efferents. *Journal of Comparative Neurology*, 500, (1), 166-188.
- Strausfeld, N. J. 2009a. Brain organization and the origin of insects: an assessment. *Proceedings of the Royal Society B: Biological Sciences*, 276, (1664), 1929-1937.
- Strausfeld, N. J. 2009b. Brain and Optic Lobes. In: Resh, V. H. & Cardé, R. (eds.) *Encyclopedia of Insects (Second Edition)*. San Diego: Academic Press.
- Strausfeld, N. J. & Andrew, D. R. 2011. A new view of insect-crustacean relationships I. Inferences from neural cladistics and comparative neuroanatomy. *Arthropod Structure & Development*, 40, (3), 276-288.
- Strausfeld, N. J. 2012. *Arthropod brains: evolution, functional elegance, and historical significance*, Cambridge, MA, Belknap Press of Harvard University Press
- Sullivan, J. M. & Beltz, B. S. 2001a. Development and connectivity of olfactory pathways in the brain of the lobster *Homarus americanus*. *Journal of Comparative Neurology*, 441, (1), 23-43.
- Sullivan, J. M. & Beltz, B. S. 2001b. Neural pathways connecting the deutocerebrum and lateral protocerebrum in the brains of decapod crustaceans. *Journal of Comparative Neurology*, 441, (1), 9-22.
- Sullivan, J. M. & Beltz, B. S. 2004. Evolutionary changes in the olfactory projection neuron pathways of eumalacostracan crustaceans. *Journal of Comparative Neurology*, 470, (1), 25-38.
- Sztarker, J. & Tomsic, D. 2004. Binocular visual integration in the crustacean nervous system. *Journal of comparative physiology. A, Neuroethology, sensory, neural, and behavioral physiology*, 190, (11), 951-962.
- Sztarker, J., Strausfeld, N. J. & Tomsic, D. 2005. Organization of optic lobes that support motion detection in a semiterrestrial crab. *Journal of Comparative Neurology*, 493, (3), 396-411.
- Sztarker, J., Strausfeld, N., Andrew, D. & Tomsic, D. 2009. Neural organization of first optic neuropils in the littoral crab *Hemigrapsus oregonensis* and the semiterrestrial species *Chasmagnathus granulatus*. *Journal of Comparative Neurology*, 513, (2), 129-150.
- Sztarker, J. & Tomsic, D. 2011. Brain modularity in arthropods: individual neurons that support "what" but not "where" memories. *The Journal of Neuroscience*, 31, (22), 8175-8180.
- Sztarker, J. & Tomsic, D. 2014. Neural organization of the second optic neuropil, the medulla, in the highly visual semiterrestrial crab *Neohelice granulata*. *Journal of Comparative Neurology*, 522, (14), 3177-3193.
- Thoen, H. H., How, M. J., Chiou, T.-H. & Marshall, J. 2014. A Different Form of Color Vision in Mantis Shrimp. *Science*, 343, (6169), 411-413.
- Tomsic, D., De Astrada, M. B. & Sztarker, J. 2003. Identification of individual neurons reflecting short-and long-term visual memory in an arthropod. *The Journal of Neuroscience*, 23, (24), 8539-8546.
- Träger, U., Wagner, R., Bausenwein, B. & Homberg, U. 2008. A novel type of microglomerular synaptic complex in the polarization vision pathway of the locust brain. *Journal of Comparative Neurology*, 506, (2), 288-300.

- Utting, M., Agricola, H. J., Sandeman, R. & Sandeman, D. 2000. Central complex in the brain of crayfish and its possible homology with that of insects. *Journal of Comparative Neurology*, 416, (2), 245-261.
- Van Hateren, J. 1993. Spatial, temporal and spectral pre-processing for colour vision. *Proceedings of the Royal Society of London. Series B: Biological Sciences*, 251, (1330), 61-68.
- Von Frisch, K. 1914. *Der Farbensinn und Formensinn der Biene*, Abteilung für allgemeine Zoologie und Physiologie der Tiere.
- Von Helversen, O. 1972. Zur spektralen Unterschiedsempfindlichkeit der honigbiene. *Journal of Comparative Physiology*, 80, (4), 439-472.
- Vorobyev, M. 1997. Discrimination of natural colours and receptor spectral sensitivity functions. In: Tadei-Ferretti, C. (ed.) *Biophysics of photoreception: Molecular and phototransductive events*. Singapore: World Scientific.
- Vorobyev, M. & Osorio, D. 1998. Receptor noise as a determinant of colour thresholds. *Proceedings of the Royal Society of London Series B: Biological Sciences*, 265, (1394), 351-358.
- Wang-Bennett, L. T. & Glantz, R. M. 1987. The functional organization of the crayfish lamina ganglionaris. *Journal of Comparative Physiology A*, 161, (1), 131-145.
- Watanabe, A., Obara, S. & Akiyama, T. 1967. Pacemaker potentials for the periodic burst discharge in the heart ganglion of a stomatopod, *Squilla oratoria*. *The Journal of General Physiology*, 50, (4), 839.
- Wolff, G., Harzsch, S., Hansson, B. S., Brown, S. & Strausfeld, N. 2012. Neuronal organization of the hemiellipsoid body of the land hermit crab, *Coenobita clypeatus*: correspondence with the mushroom body ground pattern. *Journal of Comparative Neurology*, 520, (13), 2824-2846.
- Wolpert, H. D. 2011. An eye toward multispectral imaging. *Optics & photonics news*, 22, (April 2011), 16-19.
- York, T., Powell, S., Gao, S., Kahan, L., Charanya, T., Saha, D., Roberts, N., Cronin, T., Marshall, J. & Achilefu, S. 2014. Bioinspired Polarization Imaging Sensors: From Circuits and Optics to Signal Processing Algorithms and Biomedical Applications. *Proceedings of IEEE*, 102, (10), 1450-1469.
- Young, J. & Armstrong, J. 2010. Structure of the adult central complex in *Drosophila*: organization of distinct neuronal subsets. *Journal of Comparative Neurology*, 518, (9), 1500-1524.
- Young, T. 1802. The Bakerian lecture: On the theory of light and colours. *Philosophical transactions of the Royal Society of London*, 12-48.
- Zaidi, Q., Marshall, J., Thoen, H. & Conway, B. R. 2014. Evolution of neural computations: Mantis shrimp and human color decoding. *i-Perception*, 5, (6), 492-496.

Appendix I

9 Appendix I

Supplementary Materials for

A new form of colour vision in Mantis shrimps

Authors: Hanne H. Thoen¹, Martin J. How¹, Tsyr-Huei Chiou², Justin Marshall¹

Affiliations:

¹Queensland Brain Institute, University of Queensland, Brisbane, Qld 4072, Australia.

²Department of Life Sciences, National Cheng Kung University, Tainan city 70101 Taiwan R.O.C.

*Correspondence to Hanne H. Thoen: h.thoen@uq.edu.au

This PDF file includes:

Materials and Methods

Supplementary Text

Figs. S1 to S2

Tables S1 to S3

Material and Methods

Animal capture and handling

Stomatopods of the species *Haptosquilla trispinosa* were collected at Lizard Island Research Station, Australia (GBRMPA Permit no. G12/35005.1, Fisheries Act no. 140763) and transported to our aquarium facility at The University of Queensland. Animals were kept in saltwater aquaria in a 12h/12h-dark/light cycle with UV enhanced full-spectrum lighting. Some experiments were also conducted under natural light conditions at Lizard Island Research Station. Experiments were performed according to the ethical considerations of the University of Queensland.

Intracellular electrophysiology

Intracellular electrophysiological recordings from the photoreceptors of *H. trispinosa* were performed to determine the spectral sensitivities of this species. Recordings were made using the spectral scan method (Menzel et al., 1986, Marshall and Oberwinkler, 1999, Kleinlogel and Marshall, 2006) and were, in brief, as follows: At least half an hour before each experiment the animal was placed in total darkness to dark-adapt the photoreceptors. The following steps were then all performed in dim red light. The animal was killed by chilling and decapitation and the eyestalk was removed. A small hole was cut through the cornea in the dorsal or ventral hemisphere using a sharp razorblade, taking care not to disturb the underlying photoreceptor cells. The location of recorded cells was identified by injecting a fluorescent dye (Alexa Fluor 568, Molecular probes) through the microelectrode. The results from the electrophysiological recordings are shown in figure 1 and Supplementary Table 1.

Model calculations

The spectral sensitivities (Fig 1) were used to model expected discrimination ability based on analogue comparison. UV-sensitive photoreceptors were not included in this modelling or in the following behavioural experiments due to the uncertain connections between the UV- sensitive R8 cells and the R1-7 cells and to simplify both modelling and behavioural methods. We used the Vorobyev-Osorio receptor noise-limited colour opponent model (Vorobyev and Osorio, 1998) for a simplified serial di-chromatic system, using the spectral sensitivities obtained from electrophysiological recordings for each row in the midband. The comparison of within-row spectral sensitivities is based on previous hypotheses detailed in Neumeyer (Neumeyer, 1991) and later reviewed in Marshall et al. (Marshall et al., 2007). From this model we get the ΔS^t , which is an estimated perceptual distance between the two stimuli. This distance can then be used to predict the $\Delta\lambda$ function by setting a threshold distance for ΔS . In this instance we set the threshold distance to be 1 according to Koshitaka et al. (Koshitaka et al., 2008). See Supplementary Text for details of the visual modelling.

Behavioural determination of spectral discrimination ($\Delta\lambda$).

Small burrows were constructed from small plastic screw-top vials covered with black electrical tape to darken the interior (Caldwell and Dingle, 1975) (Fig 1). The burrow was placed in a container filled with sediment and one animal was added per container. The animal was allowed to habituate for around 2 days before the experiment. Colour stimuli were produced using a pair of high-pass and low-pass linear variable filters (LVF-H, LVF-L, Ocean-optics) mounted together to create a nearly monochromatic light with a FWHM of ~ 20 nm (Supplementary figure 1). The filters were placed in an adjustable filter holder (Ocean optics, FHS-LVF) with a micromanipulator (Mitutoyo 151-223) placed on one end to enable the fine-tuning of the correct wavelengths. A halogen light source (AmScope Haloid 150w) was connected to a pair of adjustable filter holders via a collimating lens using a split light guide. On the other side of the filters another collimating lens guided the monochromatic light into an outgoing optical fibre (1000 µm, Ocean Optics). Prior to stimulus presentation, the animal's burrow was temporarily blocked with a small piece of white plastic sheet while the stimuli were placed in the correct position to ensure standardised placement

for each animal. When the plastic sheet was removed the animal was therefore presented with two different light stimuli from the end of each optical fibre. The natural foraging behaviour of this species involves smashing or grabbing objects in front of the burrow, a behaviour which was exploited in the current experiment, where a choice was determined by the animal swimming out and grabbing the end of the optical fibre. The optical fibres were placed as close to each other as possible (~1cm). This allowed animals to make and demonstrate a positive choice by grabbing the stimulus while having both stimuli simultaneously in view.

Brightness control

Earlier calculations of the relative size and lengths of various parts of the ommatidia in stomatopods (such as aperture widths, filter lengths and rhabdoms dimensions) (Cronin et al., 1994d) have led to the conclusion that the photon absorption rates of the different photoreceptor types are very similar, enabling the eye to operate at similar levels of stimulation. We therefore kept the brightness of the presented stimuli as similar as possible using a variety of neutral density (ND) filters, providing an absolute irradiance of around $2.16E15$ photons/cm²/sec. In addition to this we performed several brightness control experiments in which the intensity of light was varied randomly between choice stimuli over three log units using ND filters, in order to make sure that the trained stomatopods did not use brightness as a cue when making choices. We found no significant differences in response rate between light and the dark stimuli (Supplementary figure 2) implying that the trained animals made choices based only on colour information.

Training:

The animals were primed for about two weeks before testing using small pieces of food attached to the end of a single optical fibre displaying the correct training colour. We used 10 different training wavelengths, 400, 425, 450, 470, 500, 525, 570, 578, 628 and 650 nm. After about 1 - 1½ week most of the animals were actively choosing, and the priming continued with the trained colour. During priming the food reward was placed directly on the target to allow the association between the training wavelength and food. During testing, two cleaned or fresh fibres were used, one of which displayed a wavelength 50 nm away from the trained wavelength either towards longer wavelengths or towards shorter wavelengths. The position of the trained and the test stimuli (left – right) was varied in a semi-randomised order.

Testing:

Testing was carried out approximately 4-6 times per day for 4-5 days each week. During testing, re-enforcement was provided using a food-stick immediately after a correct choice was made. An animal was therefore always rewarded if it made a correct choice, thus avoiding any loss of motivation due to the loss of association between the correct choice and the reward. Between 4 and 7 animals were successfully trained to each of the ten training wavelengths. Wavelengths of the test stimuli were 5, 8, 12, 25, 50 and 100 nm longer or shorter than the trained wavelengths.

Statistical analysis

As the target choice was a binary response variable (correct or incorrect) we used a binomial test to determine whether the choice frequencies were significantly different from chance ($P_0 = 0.5$, $\alpha = 0.05$). All analyses were carried out using the open source software R (R development Core Team, 2010). The results from these tests are displayed in Supplementary Table 2 and 3.

Supplementary Text

Supplementary formulas 1

Visual modelling of a simplified serial di-chromatic system

For a dichromatic system the distance between stimuli will be:

$$(\Delta S')^2 = \frac{(\Delta q_1 - \Delta q_2)^2}{e_1^2 + e_2^2} \quad (1)$$

with

$$q_i = k_i \int R_i(\lambda) I(\lambda) d\lambda \quad (2)$$

where $i = 1, 2, \dots, n$; q_i is the quantum catch of receptor i ; e_i is the noise level of a particular group of receptors; λ is wavelength, R_i is the spectral sensitivity of receptor i , $I(\lambda)$ is the spectrum of the stimuli, k_i is an arbitrary scaling factor and the integration is over the visible spectrum. k_i is set so that the quantum catches for the background is equal to 1:

$$k_i = 1 / \int_{\lambda} R_i(\lambda) I^b(\lambda) d\lambda \quad (3)$$

where $I^b(\lambda)$ is the background spectrum.

Noise is estimated using the following model:

$$e_i = v_i / \sqrt{\eta_i} \quad (4)$$

where v_i is the noise level of a single photoreceptor and η_i is the number of receptors of a type i .

Here we assumed that noise in different photoreceptors were similar and set the noise to 0.05 (Weber fraction), which is a value that has been used in previous studies of animal colour vision (Vorobyev and Osorio, 1998, Koshitaka et al., 2008).

Using the threshold distance of 1 together with the data from equation 1) we can predict the $\Delta\lambda$ function using:

$$\Delta\lambda = 1 / (\Delta S') C_i \quad (5)$$

where C_i is the interval between the stimulus colours.

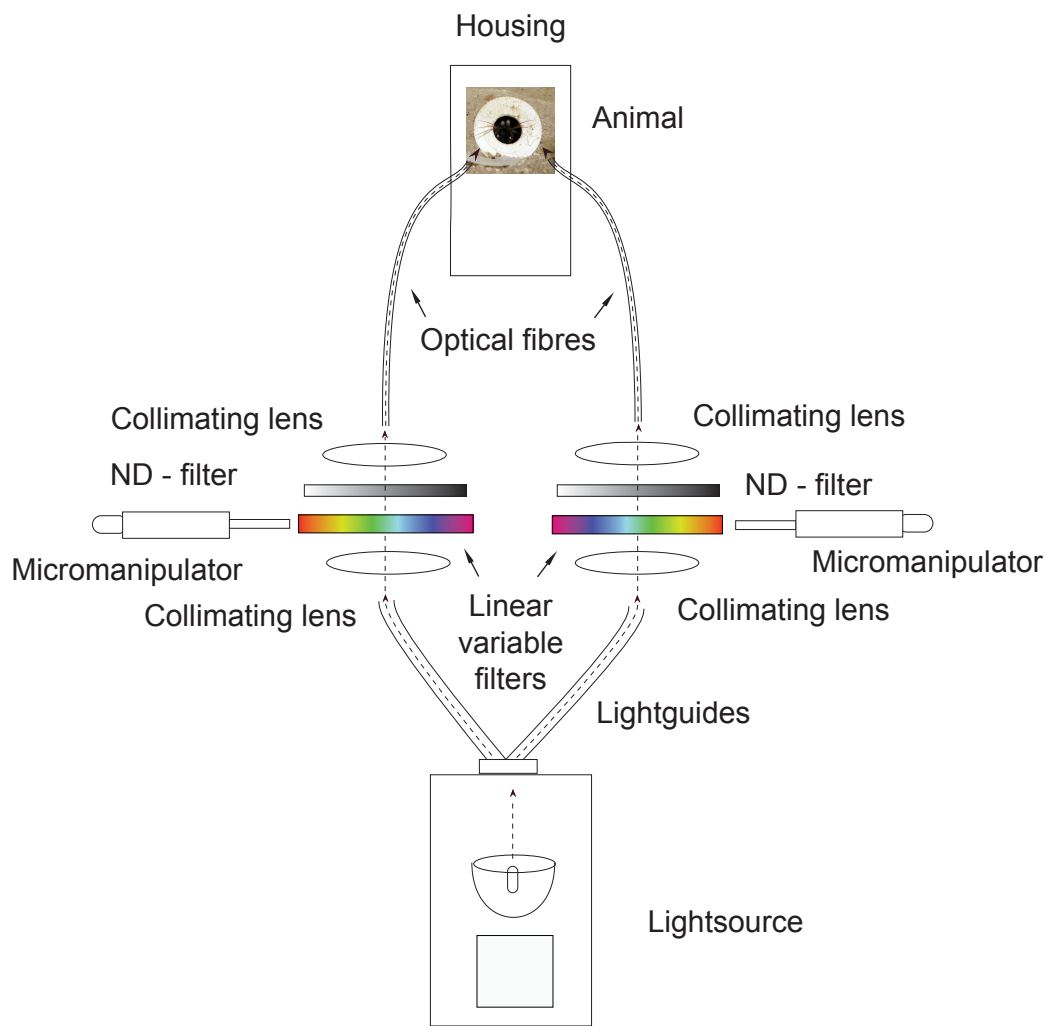


Fig. S1.

Test setup: Experimental setup for presentation of monochromatic light in front of stomatopod. The light from a 150w halogen lamp was directed through adjustable linear variable filters using light guides and collimating lenses. The light was attenuated using neutral density filters before it was led through two optical fibres (1000 µm), which were positioned in front of the animal.

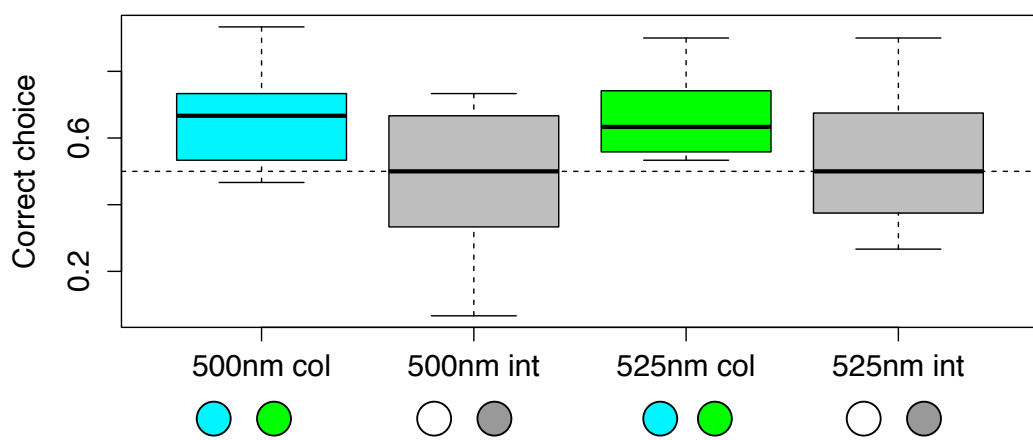


Fig. S2

Brightness control: Animals trained to reward stimuli at 500 nm (left) and 525 nm (right) were tested using the coloured stimuli presented at different light intensities, high vs. low. Results show that animal continued to choose the reward colour significantly above chance (turquoise and green boxes; t-test with Bonferroni adjustment for 500 nm, $p = 0.009$, $n = 4$ and for 525 nm, $p = 0.008$, $n = 4$), while ignoring the effect of intensity (grey boxes; t-test with Bonferroni adjustment for 500 nm, $p = 0.62$, $n = 4$ and for 525 nm, $p = 0.67$, $n=4$). Dots underneath each boxplot indicate the type of presented stimuli.

Table S1

Electrophysiological recordings: For each spectral sensitivity maximum (λ_{\max}): number of cells recorded, range of times each cell was recorded from, total number of recordings from all cells, the identified midband row and the position (distal/proximal) in the midband row.

<i>Sensitivity max</i> (<i>)</i>	<i>No of</i> <i>cells</i>	<i>Range of</i> <i>recordings per</i> <i>cell</i>	<i>Total no of</i> <i>recordings</i>	<i>Identified</i> <i>row</i>	<i>Distal/</i> <i>proximal</i> <i>position</i>
315	1	4	4	-	R8
325	3	3	9	-	R8
370	5	3	15	-	R8
420	6	3-4	20	1	D
445	7	2-4	21	4	D
470	4	3	12	1	P
490	5	3-4	16	4	P
555	5	3-4	18	2	D
585	2	3	6	2	P
610	2	3	6	3	D
665	5	4-5	21	3	P

Table S2

Choice numbers: Number of choices (n) made by (N) number of animals for each trained wavelength and at each test interval.

<i>No of choices made per test point (n)</i>						
<i>Trained wl (nm)</i>	<i>N</i>	<i>100 nm</i>	<i>50 nm</i>	<i>25 nm</i>	<i>12 nm</i>	<i>8 nm</i>
400	5	-	113	98	104	-
425	4	-	-	154	76	-
450	6	-	106	103	118	-
470	7	133	77	76	140	-
500	5	-	174	236	182	170
525	4	-	116	187	137	132
570	4	82	51	48	99	-
578	5	-	138	166	155	127
628	6	-	209	215	181	236
650	5	-	84	92	88	-

Table S3

P-values: Exact p-values for each test and training wavelength using a binomial test ($P_0 = 0.5$, $\alpha = 0.05$).

<i>Trained wl (nm)</i>	<i>100 nm</i>	<i>50 nm</i>	<i>25 nm</i>	<i>12 nm</i>	<i>8 nm</i>	<i>5 nm</i>
400	-	5.73e-06	8.00 e-04	0.461	-	-
425	-	-	1.69e-05	0.211	-	-
450	-	4.55e -06	3.30e-05	0.463	-	-
470	1.46e-12	1.53e-06	7.72E-03	0.336	-	-
500	-	1.70e-04	5.68e-05	0.011	0.351	0.682
525	-	2.70e-05	1.67e-03	0.500	0.060	0.765
570	1.616e-05	3.11e-04	2.97e-02	0.843	-	-
578	-	2.69e-05	1.97e-03	0.012	0.239	-
628	-	5.11e-07	1.31e-03	0.117	0.892	-
650	-	7.93e-07	2.47e-06	0.375	-	-